ELECTRICAL ANALOGUE COMPUTATION OF PERIODIC HEAT FLOW THROUGH BUILDINGS

THESIS SUBMITTED FOR THE AWARD OF THE DEGREE
OF DOCTOR OF PHILOSOPHY
IN APPLIED PHYSICS

BY

K. RAMAMOHAN RAO, M.Sc.

UNIVERSITY OF ROORKEE
ROORKEE

1963

ELECTRICAL ANALOGUE COMPUTATION OF PERIODIC HEAT FLOW THROUGH BUILDINGS

Thesis submitted for the award of the Degree of Doctor of Philosophy in Applied Physics

by

K. [illegible] RAO, M.Sc.

UNIVERSITY OF ROORKEE
ROORKEE

1963

CERTIFICATE

Certified that the Thesis entitled " Electrical Analogue Computation of Heat Flow through Buildings " which is being submitted by Shri K. Ramamohan Rao for the award of the Degree of Doctor of Philosophy in Applied Physics, of the University of Roorkee, is his own work carried out under my supervision and guidance. The matter embodied in this Thesis has not been submitted for the award of any other Degree or Diploma of any University.

This is to further certify that he has worked for a period of two and a half years (from June 1961 to December 1963) on this problem.

P.V. Indiresan

(P.V. Indiresan)
Associate Professor,
Electrical Engineering Deptt.,
University of Roorkee.

ROORKEE

Date : 25.12.1963

A B S T R A C T

O F

T H E T H E S I S

A B S T R A C T

This thesis contains a record of research work carried out on periodic heat flow characteristics of building elements and the prediction of indoor air temperatures of buildings by Electrical Analogue method. Such a study was found essential for evolving building designs to suit diverse climatic conditions of India.

A building element is represented on this analogue by a suitable combination of resistance - capacitance network. The type and the number of lumps required to represent a building fabric is decided by the thickness and physical properties of the material. The surface heat transfer coefficients are represented by suitable resistances.

A steady state sinusoidal excitation has been adopted to simulate the diurnal sol-air temperature variations. The main advantages of this approach over other simulation techniques are (i) it eliminates the need of complicated electronic equipment like function generators and recording devices, (ii) makes possible to separate the effects of climatic factors from the thermal characteristics of the building fabric and (iii) only two quantities viz., amplitude decrement and phase lag angle are sufficient to measure on the analogue network.

To facilitate phase measurements, a direct reading audio phase meter capable of reading upto ± 1° has been specially designed and fabricated.

The number of lumps required to represent any building element adequately on the analogue has been established both theoretically and experimentally. Computed data, on the transfer matrix coefficients, for lumped and distributed systems, required for evaluating the lumping errors in the estimation of temperatures and heat fluxes, are also included.

To define completely the transient behaviour of a building component a set of three analogous system functions (one transfer and two driving point) are required. Relationships between these functions and the transfer matrix coefficients, for commonly occuring boundary conditions have been derived in this thesis.

A detailed study of the type and thickness of each layer and the effect of the order of arrangement on the overall thermal functions of the composite construction, has also been made.

A simple and flexible computational method for the prediction of the indoor air temperatures, in terms of thermal system functions, 'U' values and sol-air temperatures, has been evolved. As this method utilises the pretabulated thermal system function data, it eliminates the necessity of representing a full room or a building with all its structural elements and input generators, on the analogue, for each specific study.

This method, when used with the data presented in this thesis, leads to a quantitative evaluation of the relative thermal efficiencies of the various possible structural combinations and other design factors. A few applications of the data are also illustrated.

ACKNOWLEDGEMENTS

The author gratefully thanks Prof. C.S. Ghosh Head of the Department of Electrical Engineering, University of Roorkee, for the keen interest shown in the present work, and DR. P.V. Indiresan, Associate Professor Electrical Engineering Department, University of Roorkee, for his able guidance.

He is also indebted to Shri Dinesh Mohan, Deputy Director Incharge, and Shri N.K.D. Choudri, Assistant Director, Central Building Research Institute for the encouragement given by providing the facilities to carry out this work.

The author further wishes to express his thanks to DR. V. Narasimhan, Senior Scientific Officer, Central Building Research Institute, Roorkee, for several helpful discussions in the preparation of this thesis.

C O N T E N T S

NOMENCLATURE IS GIVEN
AT THE END.

C O N T E N T S

CHAPTER 1

INTRODUCTION

CHAPTER 1

INTRODUCTION

Accurate prediction, of the thermal behaviour of building under periodic variations of temperatures and heat flow, is of considerable practical importance in building design. Although a good deal of work has been done in this direction and new methods and techniques evolved, several problems of practical interest, still await solutions. This owes mainly to the multiplicity of the variables involved and the lack of a simple and flexible method for studying the transient heat flow, through building fabrics.

A purely analytical solution of this problem is not impossible, but it is very laborious and time consuming, even with the availability of such efficient methods, as matrix analysis, and symbolic calculus. If more than a few variables are to be investigated simultaneously, field measurements are not practicable. This imposes a serious limitation on those results which do not lead to any generalised conclusions. Further, to determine the influence of each of the several variables that one normally comes across in heat transfer problems, a large number of test houses have to be built in different climatic zones and the results analysed statistically. Such a procedure is time consuming and uneconomical.

Electrical analogue methods have been found to be more suitable for such problems and yield quick and economical results.

The electrical analogue simulates thermal problems in terms of electrical quantities. Within the limits set by the accuracy of the analogue and the basic assumptions made in the theory, the analogue method may be regarded as a means of carrying out controlled experiments on a variety of building elements, under identical conditions.

Most of the investigations employing electrical analogue methods were mainly restricted to the estimation of fabric cooling loads for air conditioning purposes. Though these techniques can be extended to unconditioned buildings, these will have only a limited application. The simulation of a room or a building with all its structural components, and the associated input generators, make the network too complex for experimental work. Even the initial cost of the equipment becomes exhorbitant. Moreover the efforts involved in simulating the several variables (climatic and design) and their possible combinations on such an analogue make the method cumbersome and unsuitable for design problems.

It is, therefore, apparent that there is a genuine need for the development of a simple and flexible method to obtain a quick evaluation of thermal efficiencies of buildings and building elements. The primary requisite of such a method is that it should be capable of taking into account the influence of various factors, other than the constructional variations, viz., ventilation, orientation, surface treatments, internal heat sources and sinks, regional and seasonal variations of temperatures and solar radiation etc.

A very profitable line of approach would be i) to obtain the basic reference data on transient thermal characteristics of a large number of building sections, that one might come across in practice, by the electrical analogue method, and ii) to devise a simple computational method to predict the indoor air temperatures, utilising the above pretabulated data, for any combination of building sections under any climatic conditions.

This thesis is mainly directed towards the development of such a method and the data.

In addition several other problems of interest such as i) the analogue representation of the building sections by lumped cascaded networks, ii) influence of surface heat transfer coefficients on the lumping errors and thermal system functions, iii) the effect of different combinations of layers of materials on the thermal behaviour of the individual layers and on the composite section as a whole, have also been studied in this thesis.

Such a study will lead to a better understanding of the transient behaviour of composite constructions and will finally result in the appropriate design of composite constructional elements, best suited to the climatic conditions of a given place.

CHAPTER 2

PERIODIC HEAT FLOW THROUGH BUILDINGS

CHAPTER 2

PERIODIC HEAT FLOW THROUGH BUILDINGS

2.1 Introduction

In the steady state heat flow analysis the heat storage capacity of the structure does not come into the picture. In climates where, there are large periodic variations of air temperature and solar radiation, the thermal capacity of external and internal building elements play a great role in modifying the temperature distribution and the rate of heat flow, with respect to both space and time.

The mechanism, of heat flow through a building element, say a wall, under transient conditions may be visualised in the following manner. An elementary thickness of wall just beneath the outside surface, receives a net heat gain by convection and radiation. A portion of this energy is spent in heating up the element (in question) while the balance is conducted on to the next elementary thickness of the wall and so on. As a definite interval of time is required for the incident heat to raise the temperature of the element (in question) there is a phase difference between the temperature or heat waves at the outer and the inner surfaces. Further, as some of the input energy is used up in heating the wall, the amplitude of the wave at the inner surface is considerably reduced.

The main object of the investigations on periodic heat flow through the building elements is to establish a relationship between the thermal conditions of the outdoor and indoor environments and the properties of the intervening structure. This necessitated a development of the theory of non-steady state heat flow, and solutions to the Fourier heat conduction equation under natural boundary conditions. The differential equation of heat flow in solids which gives the temperature distribution with time was given by Fourier as

$$\frac{\partial t}{\partial T} = a\left(\frac{\partial^2 t}{\partial x^2} + \frac{\partial^2 t}{\partial y^2} + \frac{\partial^2 t}{\partial z^2}\right) \qquad \ldots(1)$$

where t = temperature at the point (X,Y,Z) at time T.

a = K/ρs - thermal diffusivity in Ft^2/Hr.

K = thermal conductivity in Btu/Ft/Hr/°F.

s = specific heat Btu/Lb/°F

ρ = density Lb/Ft^3.

In special conditions (parallel bounding surfaces with large area compared to the thickness) the heat flow can be considered as one dimensional. Then the above equation reduces to

$$\frac{\partial t}{\partial T} = a\frac{\partial^2 t}{\partial x^2} \qquad \ldots(2)$$

For all practical purposes the building components such as walls, roof, floor etc., satisfy the condition of unidirectional heat flow. Hence this equation (2) is to be solved, for a given building element, with the appropriate external and internal boundary conditions, which of course vary from situation to situation. The heat exchange taking place at the outer and inner surfaces form the outside and inside boundary conditions respectively. Hence the expressions for these heat exchanges are of fundamental importance and should be expressed in the simplest possible form consistent with the requirements, to a satisfactory degree of accuracy.

2.2 Heat Exchange at the Outside Surface of a Building Element

The phenomena of heat exchange at the outside surface of a building element as illustrated in Fig. (2.1) can be resolved into the following components :-

i) Heat transfer by convection between the surface and the outdoor air.

ii) Total solar radiation (Direct + Diffuse) absorbed by the surface.

iii) Heat transfer by low temperature radiation exchange between the surface and the outdoor environment.

and iv) The rate of heat transfer by conduction into the building element.

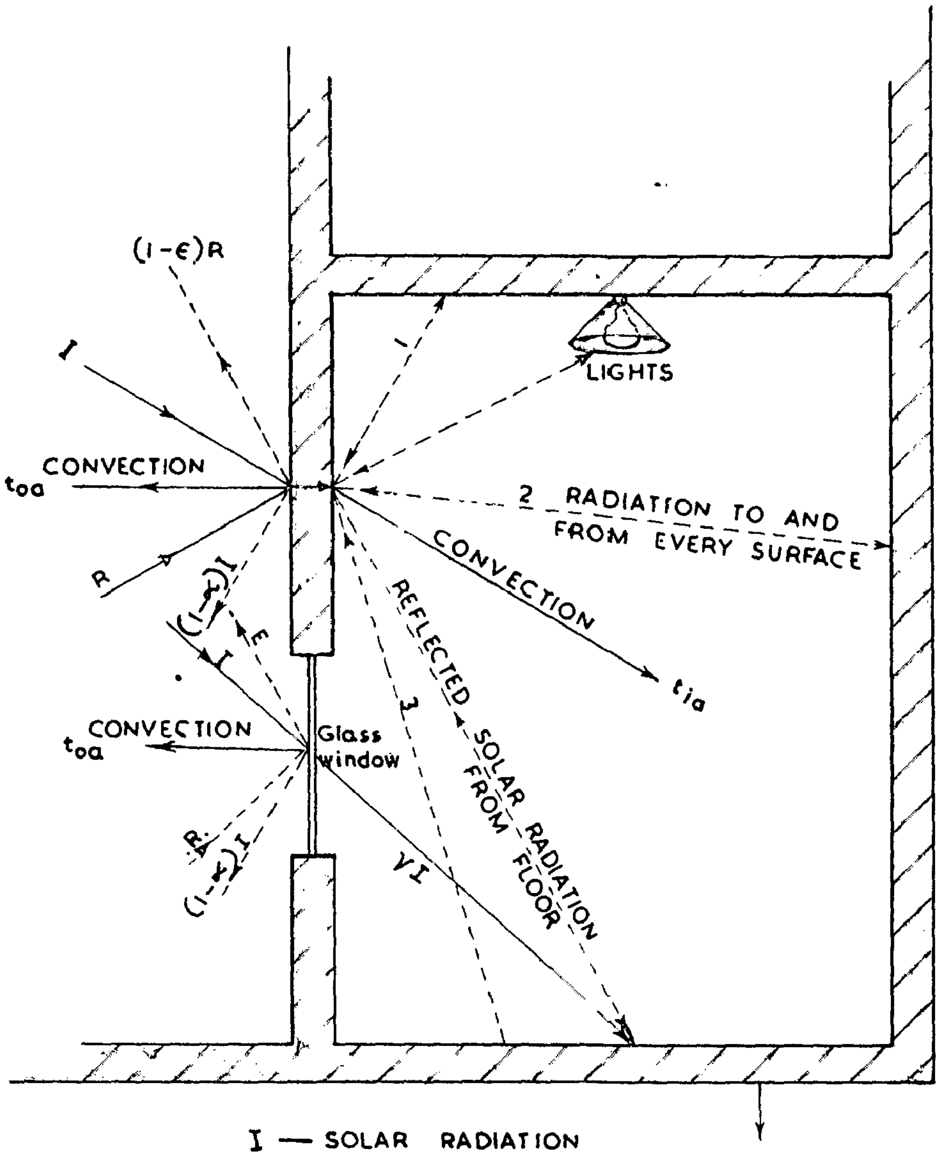

I — SOLAR RADIATION

γ — SOLAR TRANSMISSIVITY OF WINDOW

t_{os} — OUTSIDE SURFACE TEMP.

t_{is} — INSIDE SURFACE TEMP.

q — HEAT FLOW FROM OUTSIDE SURFACE TO INSIDE

t_{oa} — AMBIENT TEMPERATURE

t_{ia} — ROOM AIR TEMPERATURE

α — SOLAR ABSORPTIVITY OF THE SURFACE

R — LONG WAVE RADIATION FROM THE SURROUNDINGS

E — RADIATION EMITTED FROM THE SURFACE

∈ — EMISSIVITY OF SURFACE

2·1 HEAT BALANCE AT THE OUTSIDE AND INSIDE SURFACES OF AN EXPOSED WALL OF AN ENCLOSURE

The heat balance equation at the outside surface is given by

$$q_{os} + h_{oc}\,(t_{oa} - t_{os}) + \alpha I_T \pm I_L = 0 \qquad \ldots (3)$$

where

q_{os} = instantaneous heat flux entering the building element at the outside surface per unit area.

h_{oc} = outside surface convection heat transfer coefficient.

t_{oa} = outside air temperature.

t_{os} = outside surface temperature.

I_T = intensity of the total solar radiation incident on the surface (Direct + Diffuse).

α = absorptivity of surface for solar radiation.

I_L = net long wave radiation exchange between the surface and its surroundings.

All these component parts of the equation (3) depend upon the weather elements and the surface properties. Seasonal and diurnal variations of these climatic factors will have to be taken into consideration. Combining all these factors into a single parameter will simplify the computations to a great extent.

2.3 Sol-Air Temperature

Mackey and Wright (1) have introduced the concept of sol-air temperature, which combines the air temperature and solar radiation into a single equivalent temperature. As per the definition of the sol-air temperature, the external boundary condition is given by

$$q_{os} = h_{oc} (t_{sa} - t_{os}) \quad \ldots (4)$$

where t_{sa} is the sol-air temperature. In their original work, these authors have not taken the low temperature radiation, into account and the sol-air temperature is given by the equation

$$t_{sa} = t_{oa} + \frac{\alpha I_T}{h_{oc}} \quad \ldots (5)$$

Neglecting the low temperature radiation is not justifiable and the above formula for sol-air temperature requires modification. The modified equation according to Roux (2) may be written as

$$t_{sa} = t_{oa} + \frac{\alpha I_T \pm I_{LT}}{h_{oc}} \quad \ldots (6)$$

To compute the sol-air temperature, a knowledge of the incident solar radiation intensity, surface absorption coefficient, low temperature radiation surface convection heat transfer coefficient, are required, apart from the outdoor air temperatures data. The intensity of solar radiation incident upon a surface, depends upon many factors such as orientation, latitude, day and time, atmospheric conditions etc. Hence for a given locality, though all the surfaces of a building are subjected to the same ambient air temperature, the sol-air temperatures will be different for differently oriented surfaces. The solar radiation intensity data (measured as well as computed) for a number of places and differently oriented surfaces is available in the literature (3). Preparation of design curves of diurnal variations of sol-air temperature for summer and winter seasons for various places, facilitate the calculations of heat transfer through building elements and the design of buildings to suit a given climate.

The surface absorption coefficient for solar radiation depends upon the surface colour and the angle of incidence. Considerable work has been done on this aspect (4, 5) and large amount of reference data is available in the literature (6, 7).

3.4 Low Temperature Radiation

The low temperature radiation received by a building element, depends upon the mean radiant temperature of the surroundings, ground and atmosphere. It is usually assumed that the outdoor surroundings emit long wave radiation as a black body at air temperature (8). Hence the net radiation exchange between the surface and its surroundings is expressed as

$$I_L = \epsilon \sigma (T_{os}^4 - T_{oa}^4) \qquad \ldots (7)$$

where

ϵ = absorptivity and emissivity of the surface for long-wave thermal radiation.

σ = Stephan Boltzman constant.

T_{os} = absolute surface temperature, and

T_{oa} = absolute air temperature.

Burnt (9) has pointed out that the outdoor surroundings by no means radiate as a black body at air temperature and correlated the long wave radiation emitted by cloudless atmosphere with water vapour pressure present in the atmosphere based on Dines and Dines measurements (10). The correlation is given by

$$R = R_b \left(a + b\sqrt{P_w} \right) \qquad \ldots (8)$$

where

R_b = low temperature radiation emitted by a blackbody at outdoor air temperature (i.e., σT_{oa}^4)

R = low temperature radiation emitted by the atmosphere.

P_w = the water vapour pressure in inches of mercury.

'a' and 'b' are constants and given as 0.55 and 0.33 respectively for horizontal surfaces and as 0.3 and 0.165 for vertical surfaces.

Roux (2) pointed out, that while the Burnt's equation (8) gives an accurate estimate of low temperature radiation during night times, is not strictly valid for conditions for day times when solar radiation intensity is high. However, the equation (8) is very useful as a working formula in the absence of more reliable data. Under cloudy conditions the low temperature radiation of the atmosphere increases and approaches the black body radiation at air temperature for an overcast sky condition. Substituting the value of I_L in the sol-air temperature equation (5) we get

$$t_{sa} = t_{oa} + \frac{\alpha I_T + (\sigma T_{oa}^4 (a + b\sqrt{p_w}) - \epsilon \sigma T_{os}^4)}{h_{oc}} \quad \text{.. (9)}$$

This expression includes a term of surface temperature, which is a function of the physical properties of the building element as well. As the sol-air temperature is to be computed exclusively from the weather data, the term t_{os} from the above expression is to be eliminated. For this purpose a new term "artificial surface radiative heat transfer coefficient" has been defined (2) as

$$h_{or} = \frac{\epsilon \sigma (T_{os}^4 - T_{oa}^4)}{(t_{os} - t_{oa})} \quad \text{... (10)}$$

With the help of the equation (10) we obtain the sol-air temperature as

$$t_{sa} = t_{oa} + \frac{\alpha I_T - (\epsilon \sigma T_{oa}^4 - R)}{(h_{oc} \pm h_{or})} \quad \text{... (11)}$$

The terms $(h_{oc} \pm h_{or})$ are combined into a single term which is called, the outside surface heat transfer coefficient (h_o)

2.5 Outside Surface Heat Transfer Coefficient (h_o)

As seen from the above equation 'h_o' consists of two parts, namely, convective and radiative coefficients. The convective coefficient is made up of two components, namely the forced convection (h_{ofc}) and natural convection (h_{onc}). Several investigators (11 - 15) have studied the nature of the forced and natural convective heat transfer and given empirical equations relating several factors involved in the phenomena. Both the convective and radiative coefficients have been found to vary considerably during day and night, as they are dependent on the air temperature and wind velocity (16, 17).

However, it is combined value of h_{oc} and h_{or} rather than their separate individual values that is of interest. Fortunately, this combined value h_o (i.e., $h_{oc} + h_{or}$) appears to remain fairly constant (13), although the individual variations of h_{oc} and h_{or} are large. This approximation of taking the combined heat transfer coefficient (h_o), as constant, greatly simplifies the computations of heat transfer through building elements. Errors due to this approximation are found to be small (18).

With these simplifications the boundary condition at the outside surface may be written as

$$- K \left(\frac{\partial t}{\partial x}\right)_o = h_o (t_{sa} - t_{os}) \qquad \text{... (12)}$$

where

$$- K \left(\frac{\partial t}{\partial x}\right)_o = q_{os}$$

3.6 Heat Exchange at the Inside Surface

Various heat transfer processes that take place at the inside surface, are illustrated in Fig.(3.1). At this surface the heat transfer takes place to the inside air by convection and by radiative exchange between all the interior surfaces. The heat balance equation for an inside surface can be expressed as

$$q_{is} + h_{ic} (t_{ia} - t_{is}) + \sum_{n=1}^{n=M} {}_sF_n \, \sigma \, (T_n^4 - T_s^4) = 0 \qquad \text{... (13)}$$

where

q_{is} = the heat flow through the wall at the inside surface.

h_{ic} = convective heat transfer coefficient at the inside surface.

t_{ia} = inside air temperature.

t_{is} = inside surface temperature.

n = subscript indicating one of the surfaces enclosing.

M = number of surfaces forming the enclosure.

${}_sF_n$ = overall interchange factor for radiant energy exchange between surfaces.

As in the case of outside surface coefficient, if the inside surface, convective (h_{ic}) and radiative (h_{ir}) heat transfer coefficients are combined into a single term (h_i) and assumed constant, the expression for the internal boundary condition simply becomes

$$- K \left(\frac{\partial t}{\partial x} \right)_i = h_i \; (t_{is} - t_{ia}) \qquad \ldots (14)$$

where

$$- K \left(\frac{\partial t}{\partial x} \right)_i = q_{is}$$

and

$$h_i = (h_{ic} \pm h_{ir})$$

The major advantage of combining the convection and radiation heat exchange at the inside surface, is that the overall radiation interchange factors need not be known. This saves the difficulty of finding the geometric view factors between the surfaces. Another significant simplification achieved by this assumption is that the heat flow paths to the room air, can be considered separately, without reference to any other surface.

2.7 Types of Problems met with in Practice

The types of non-steady state heat flow problems related to buildings can be broadly divided into the following three categories :-

1) Air conditioned buildings - where the indoor

air temperature is maintained constant by artificial cooling or heating. For this class of buildings the periodic heat flow through all the components of the fabric, due to external air temperature and solar radiation variations, are to be precisely calculated.

ii) Air conditioned buildings with insufficient plant capacity - where the indoor air temperatures, which vary to a certain extent, are to be calculated.

and iii) Un-conditioned buildings - where the calculation of indoor air temperatures under various climatic conditions is the main objective.

Once these outside and inside boundary conditions are established, for any given situation the solution for the Fourier heat conduction equation can be obtained by several established methods such as Analytical (19,20), Numerical (21,22), Matrix (23,24,25), Symbolic Calculus (26,27), Influence and Weighting functions (28,29,30), Direct Analogues (31 - 40) and (Electronic Analogue and Digital) Computers (41 - 45) etc. The relative merits of the various methods employed for calculating heat conduction for the determination of cooling loads for Air conditioned buildings, have been discussed by Stephenson (46).

2.8 <u>Assumptions made in the Theory</u>

In all the methods, certain simplifying assumptions are made for obtaining solutions of the practical design problems. The usual ones are :-

i) Heat flow through the building element is unidirectional.

ii) The differential equation describing the heat flow is linear, which implies that the physical properties of the materials (K, ρ, and c) are independent of temperature.

iii) Heat exchange phenomena at the external surface of a building element can be expressed by a single parameter (Sol-air temperature).

iv) The heat transfer by convection and radiation at the inside and outside surface can be represented by a combined film conductance which does not vary with time and temperature.

v) The absorptivity of the outside surface of building elements, to solar radiation is independent of the angle of incidence.

vi) The variations of the outdoor air temperature and solar radiation intensity with time are identical on successive days.

Most of the methods enumerated above were developed for estimating the fabric cooling loads, for air conditioning purposes. However, some of them are extended for the unconditioned buildings too. As pointed out earlier (Chapter 1) though these methods provide solutions for any specific situation with good accuracy, the complexity and the effort involved is so great, that for generalised design problems of buildings, for various climates, these become rather unsuitable. Simpler methods, utilizing maximum amount of pretabulated, thermal characteristic data, are to be evolved.

C H A P T E R 3

ANALOGUE SETUP AND MEASUREMENTS

CHAPTER 3

ANALOGUE SETUP AND MEASUREMENTS

3.1 Introduction

Electrical Analogue techniques for the study of transient heat flow problems in different fields are well established. Although the thermal electrical analogy is based on the similarity of mathematical formulation of heat flow through a material with that of the electric current flow in a transmission line

$$\frac{\partial t}{\partial \tau} = a \frac{\partial^2 t}{\partial x^2}$$

$$\frac{\partial E}{\partial \tau} = \frac{1}{RC} \frac{\partial^2 E}{\partial x^2}$$

in practice the analogue networks may be of different designes (31,34,36,47). The main difference between the earlier R-C models and the recent ones contres round the choice of the time scale, which has a direct bearing on the size of the components and the methods of generating and recording the input and output wave forms.

Paschkis (31) and Bowkon (33) who are the poineers of the direct analogue method have used "slow time" scale and studied the thermal transients over long durations, of the order of several minutes, with ordinary galvonometers and potentiometric type recorders. The major drawback in such "slow time" analogues is the requirement of large time constants which are obtained by the use of capacitors of several hundreds of Microfarads and resistors of several Megohms. Cost of these components of the necessary quality is prohibitive, while leakage current present in the large capacitors, constitute serious source of error.

Burnand (43) has shown that for the study of periodic heat flow problems "fast time" analogues can be employed with advantage. A repitition frequency of 50 c/s was successfully used by them. Later Lawson and McGuire (33) described a device, for the study of transients of only a few milliseconds duration. Robertson and Gross (34) have used much faster time analogues with a time compression of the order of 10^6 (1 sec of electrical is equal to 10^6 sec of thermal) in their study of fire resistance characteristics of building elements. The fast time scaling has the advantage of requiring circuits of smaller time constants, permitting thereby the use of capacitors and resistors of smaller value and size. The leakage current problem is almost absent in this case. Securing precision capacitors and resistors in these ranges is neither difficult nor expensive. However, the use of fast time analogue calls for more complicated electronic devices for the generation and recording of the special wave forms. The use of cathode ray oscillographs for measuring and recording the wave forms has become a common feature in such studies.

In all these studies, an electrical signal representing the outside temperature variation with time is to be generated. This is done electronically in several ways. Robertson and Gross (34) have used a photoformer type function generator (40) whereas Burnand employed special wave shaping devices (43). Input devices like diode function generators commonly used in analogue computers, can also be used with these direct analogues. In this study a fast time scale (a frequency of 100 c/s) is used. A brief description of the analogue setup and the experimental procedure adopted is given below.

3.2 Resistance - Capacitance Models

A building element, whose transient thermal characteristics are to be studied, is often represented on the Electrical Analogue model as a Resistance - Capacitance lumped system consisting of a cascaded T, L π networks. The actual value of the electrical resistance and capacitance of each section of the network lump depends on the thermal conductivity, specific heat, density of the material and the thickness of the building element, the choice of the scaling factor and the number of lumps used to represent the element.

In order to make the analogue representation more flexible, so that any material or combination of materials (with their usual thicknesses), can be represented as an R-C network, panels of resistances and capacitances to provide any desired value of R and C, are to be constructed. Sufficient number of such panels should be available in order that an analogue lumped representation, of dense as well as thick materials is feasible. For this study, twelve panels, each consisting of fixed resistors permanently connected on proper insulating supports having values from 100 ohms to 1 Megohm, and capacitors having values from 10 pF to 20,000 pF, were constructed. The resistors and capacitors were so connected that any desired resistance between 100 ohms to 2.1111 Megohms and any capacitor between 10 pF to 61,110 pF, can easily be selected in a short time by a suitable plugging arrangement.

If the required resistance and capacitor values fall beyond the range provided by the panels, either the resistance scaling factor or the capacitance scaling factor may be suitably altered without affecting the time scaling factor (frequency) or the time scaling factor itself may be varied, thus automatically affecting both the resistance and capacitance scaling factors.

The ease with which the selection of the resistance capacitance values, is one of the salient features of the panel design. This arrangement not only facilitates the construction of analogue models on the panels, but also permits the use of a given model to simulate a whole range of structural thicknesses, simply by a suitable change of the time scale (i.e., frequency).

All the resistors used were of precision cracked carbon type with 1 % tolerance and 1 watt rating. All the capacitors are precision polysterene type with 2 % tolerance.

All the individual resistors and capacitors were checked for their rated values with a precision G.R. type 1650 A impedance bridge before their installation in the panels. The front and back views of the panels are shown in plates 1 and 2 respectively.

The arrangement of the resistors and capacitors in a single unit is diagramatically shown in Fig. (3.1). As all the resistances in this unit are

RESISTANCE CAPACITANCE PANELS

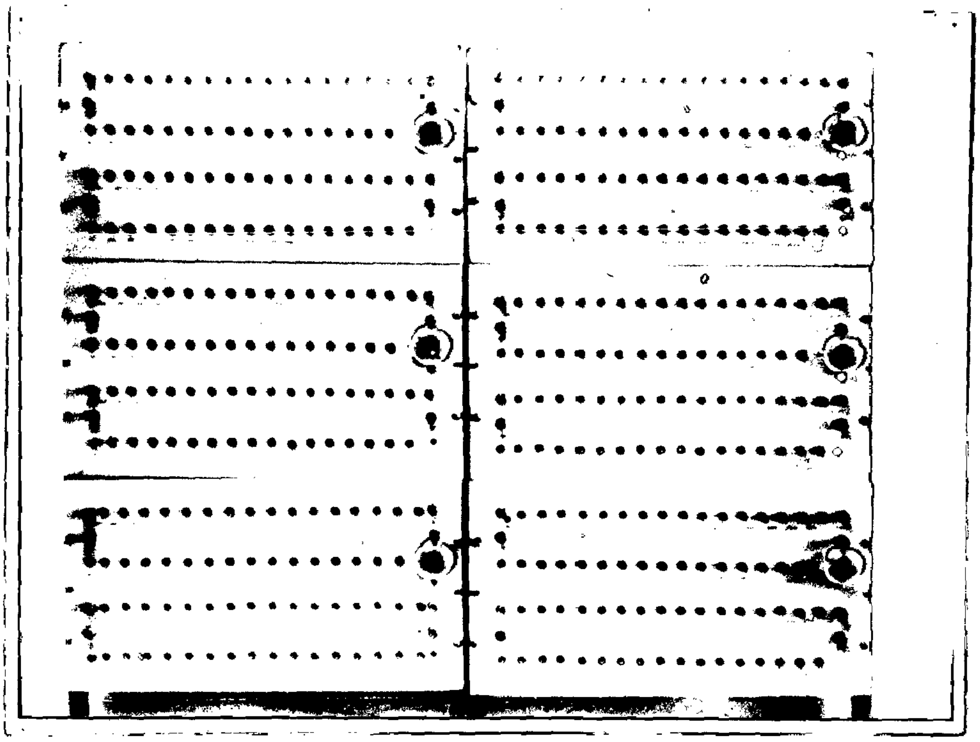

PLATE 1 Front View

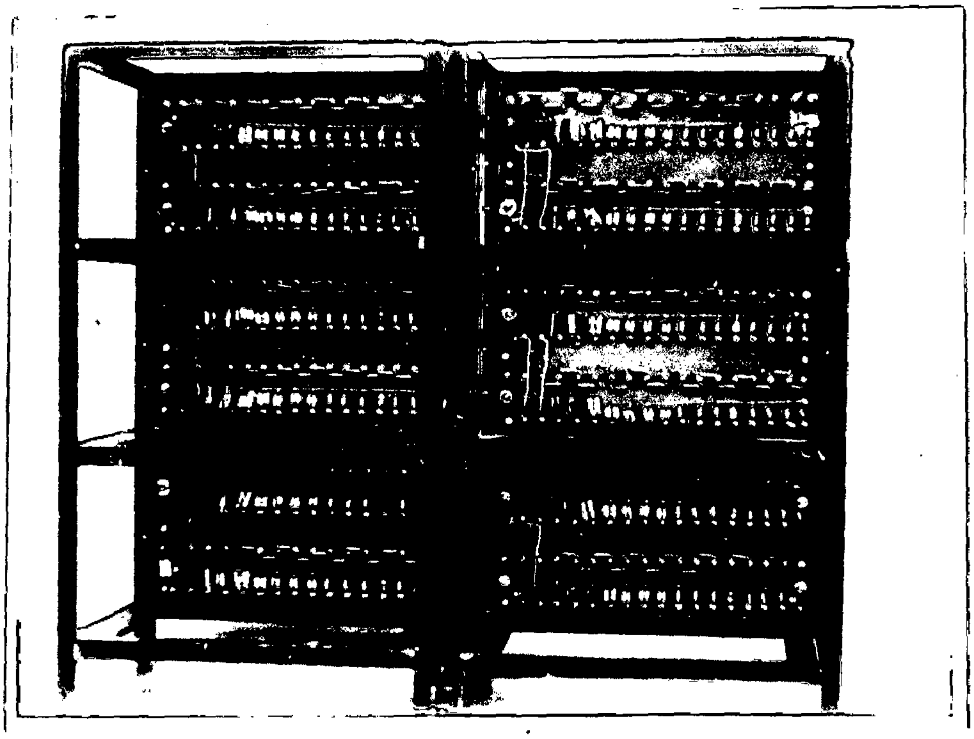

PLATE 2 Back View

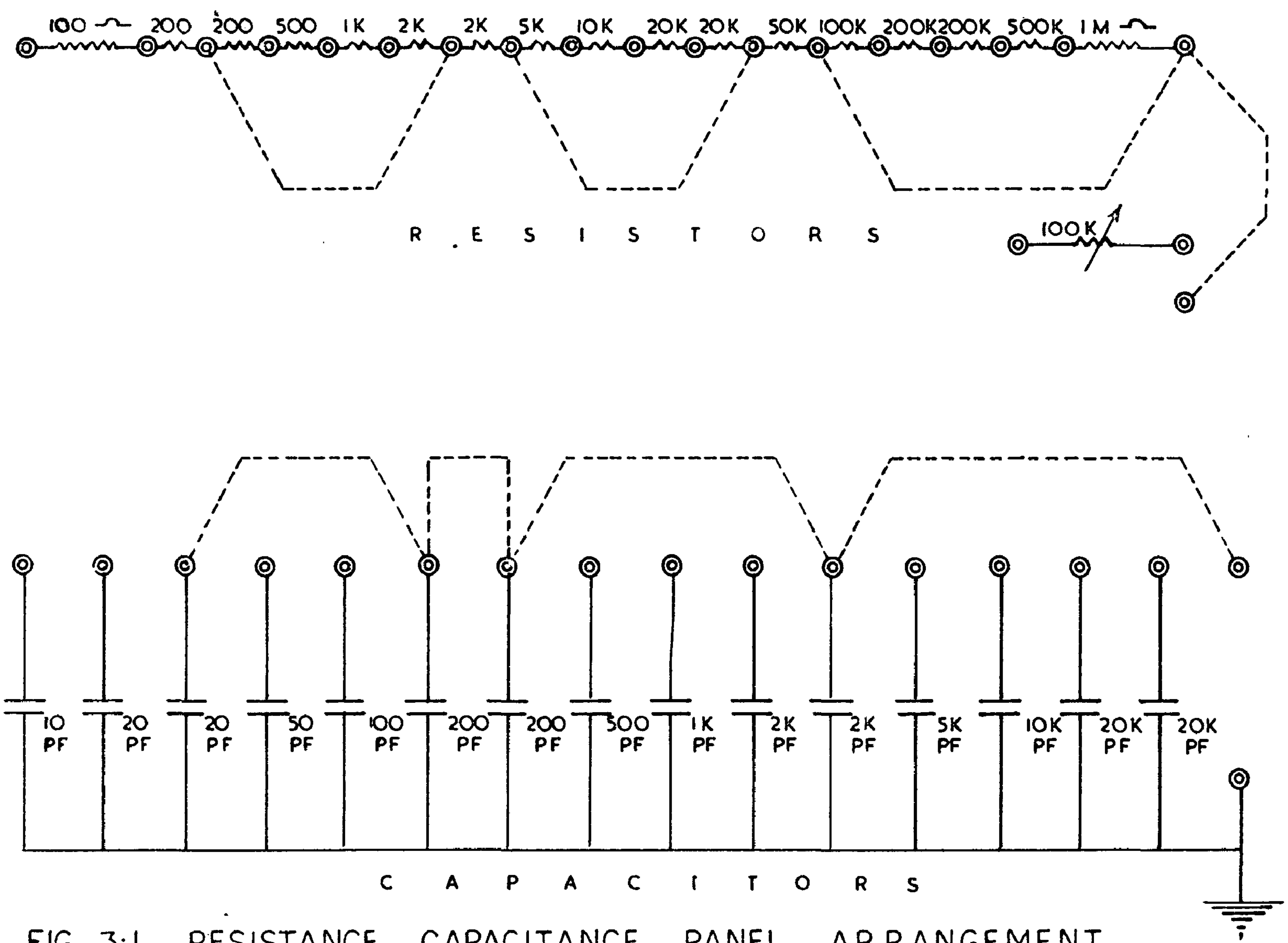

FIG. 3·1. RESISTANCE CAPACITANCE PANEL ARRANGEMENT permanently connected in series, those resistances between the plugged points are shorted. The plugged in terminals of the capacitor units, come in parallel and the total capacitance of the circuit will be additive. Finally at the output terminals the required resistance and capacitance values are obtained. As an example, the dotted lines indicate the external plugging connectors to obtain a value of 52.3 Kilo ohms resistance and 2420 pF capacitance. In this manner any desired value of 'R' and 'C' can easily be selected from each unit quickly.

Apart from these twelve units of fixed resistors, six units of linear ten turn helical potentiometers (Helipots) each of 100 K ohms resistance, are also installed on the panels to represent purely resistive circuit elements like surface film resistances and enclosed "Air spaces".

3.3 Scaling Factors

The relevant thermal quantities of a building element that are to be determined and converted into equivalent electrical quantities, (in order to represent it on the Electrical Analogue) are its Thermal resistance and Thermal capacity.

The thermal resistance and the thermal

capacity per unit area depend upon the thickness (l) of the material and the thermal conductivity (K) specific heat (s) and density (ρ).

Thermal resistance R_T is given by $\frac{L}{K}$

Thermal capacity C_T is given by $L \rho s$.

where

L = thickness in Ft.

K = thermal conductivity in Btu/(Ft.)(Hr)(°F).

s = specific heat in Btu/(Lb)(°F).

ρ = density in Lb/Ft^3.

Once the thermal resistance and thermal capacity are calculated from the properties of the material, their corresponding electrical resistance and capacitance can be determined with use of suitable scaling factors. Scaling factors actually correlate the thermal quantities to electrical quantities. There are three independent scaling factors, namely :

1) Potential scaling factor

$$N_p = \frac{\text{Unit of potential in the thermal}}{\text{Unit of potential in the electrical}} = \frac{{}^\circ F}{\text{Volt}}$$

2) Time scaling factor

$$N_T = \frac{\text{Unit of time in thermal}}{\text{Unit of time in electrical}} = \frac{\text{Hr.}}{\text{Sec.}}$$

3) Resistance scaling factor

$$N_R = \frac{\text{Unit of resistance in thermal}}{\text{Unit of resistance in electrical}}$$

$$= \frac{(^{\circ}F)(Hr)(Ft)/Btu}{\text{ohms}}$$

Other scaling factors, for capacitance and current are interrelated with the above three independent factors. The product of resistance and capacitance is called time constant of the circuit and is of dimensions of time. Hence the relation between the time scaling factor and the resistance and capacitance scaling factors is given by

$$N_T = N_R \times N_C$$

Similarly the relation between the Flux scaling factor and the potential and resistance scaling factors is given by

$$N_Q = \frac{N_P}{N_R}$$

In the present study a thermal cycle of 24 hour period has been represented by an electrical generator with a frequency of 100 c/s. This gives a time scaling factor of 1/2400 sec of electrical time i.e., one hour of thermal time corresponds to factor N_T of 1/2400 of electrical time. By this a time compression of 8.64 x 10^6 is obtained.

Once the time scaling factor has been fixed thor is a choice in fixing either the capacitance or the resistance scaling factor. The capacitance scaling factor was chosen as $N_C = 10^{-8}$ so that 1 Btu/°F corresponded to 10000 pF. This automatically fixed the resistance scaling factor as $N_R = 41.66 \times 10^3$ i.e., one unit of thermal resistance corresponds to 41.66×10^3 ohms.

3.4 Representation of Electrical Model

Using these scaling factors the total equivalent electrical resistance and capacity of the building element to be represented on the Analogue model are easily obtained. As mentioned earlier, to represent the building component accurately on the analogue as a lumped R.C. network, the number of lumps necessary have to be known. This problem of lumping is dealt in Chapter (4) in detail. Let us suppose that it is required to use 'N' lumps of 'T' circuit elements. The resistance value of each arm of the 'T' network will be equal to R/2N and the shunt capacitance will be equal to C/N. These values of R/2N and C/N are to be selected from each unit in the manner described earlier. As an example of the manner in which an electrical model may be constructed, a brick wall, 9" thick, is considered below. It is assumed that the model is to have 8 sections of 'T' type cascaded circuit. This is shown in Fig. (3.2). The thermal properties of the brick wall considered are :-

Thermal conductivity K = 6.3 $Btu/Ft^2/Hr/^oF$ per inch.

Specific heat 's' = 0.200 $Btu/Lb/^oF$

Density 'ρ' = 120 Lb/Cu.Ft.

The total thermal resistance of the wall (R_T)

$$= \frac{9}{6.3} = 1.423(^oF)(Hr)(Ft)^2/Btu.$$

Thermal resistance per lump (R/N) $= \frac{1.423}{8} = 0.1785$

Thermal resistance for each arm of the 'T' circuit

$$R/2N = 0.08925$$

The total thermal capacity $= \frac{9 \times 0.200 \times 120}{12}$

$$C_T = 18\ Btu/^oF$$

Thermal capacity per lump = $(C/N) = \frac{18}{8} = 2.25\ Btu/^oF$

The electrical equivalents are obtained as

$$R_e/2N = 0.08925 \times 41.66 \times 10^3 \text{ ohms}$$

$$C_e/N = 2.25 \times 10^4 = 22.5 \times 10^3 \text{ pF}.$$

These can be easily represented on the panels. Then the equivalent resistance values of the exterior and interior wall surface heat transfer coefficients are to be calculated and added on either side of the lumped RC network. This completes the representation of the wall panel with its boundary conditions on the analogue.

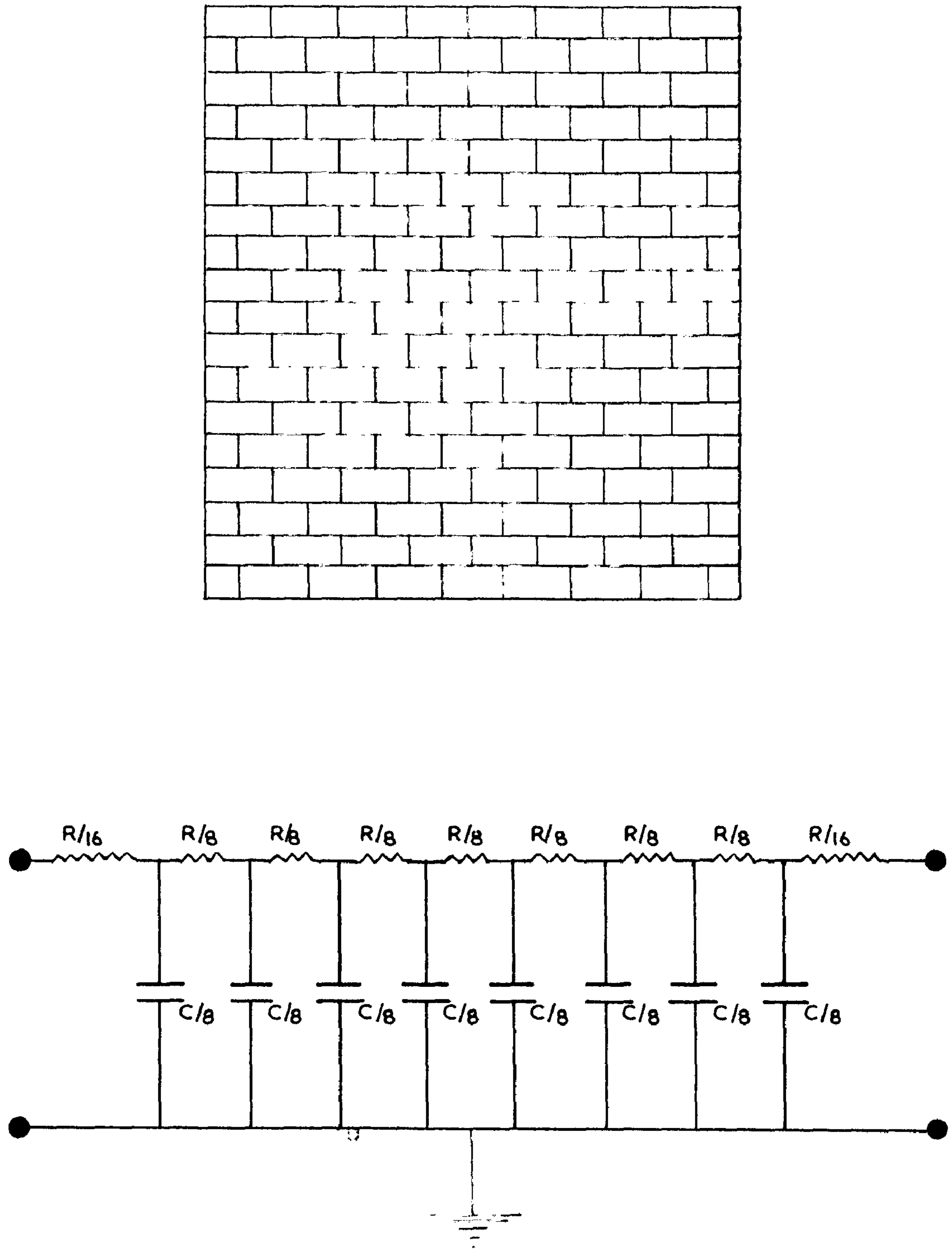

FIG. 3·2. R – C LUMPED T NETWORK REPRESENTATION OF A BRICK WALL

3.5 Signal Generation

The next requirement is to generate an electrical signal to simulate (a) the external air temperature variation, (b) the solar radiation, and (c) the low temperature radiation exchange at the external surface. Mackey (1) has introduced the concept of sol-air temperature, which combines all the above phenomena into a single temperature variation. This approach has the advantage of requiring only one potential generator instead of three separate ones representing each of these three phenomena. The sol-air temperature depends on many factors, such as, latitude, time of the year, orientation of the surface, surface colour, wind speed, outdoor air temperature, dust content and precipitable water vapour present in the atmosphere etc. All these quantities are either available from Meteorological data or can be computed to a fair degree of accuracy. The sol-air temperature variation with time is then computed for any given situation. An electrical wave form representing the sol-air temperature is to be generated. As mentioned earlier, special function generators which demand complicated electronic equipment are to be employed for this purpose.

3.6 Steady State Sinusoidal Method

An alternative approach is to analyse the sol-air temperature wave form and represent as a fourier trigonometric series of harmonic waves of different amplitudes and phases, super imposed over a steady level.

$$t_{sa}\ (\tau) = t_{sa}\ (\text{mean}) + \sum_{n=0}^{\infty} t_{sa\ n}\ \cos\ (\omega_n \tau - \gamma_n)$$

For all practical purposes, three or four harmonics are sufficient for a good representation of any periodic wave form. This approach makes the problem of input signal generation very simple. Any stable commercially available Audio Oscillator which can generate 100 c/s to 1000 c/s will do the job. This obviously eliminates the need for complicated expensive equipment. The amplitude decrement (λ) and phase lag (φ) characteristics of the network model for the fundamental and three or more higher harmonics have to be determined once only. Then the inside surface temperature equation can readily be obtained as

$$t_{is}\ (\tau) = t_{is}\ (\text{mean}) + \sum_{n=0}^{\infty} \lambda_n t_{sa\ n}\ \cos\ (\omega_n \tau - \gamma_n - \varphi_n)$$

Another major advantage of this approach is apparent. The amplitude decrement and phase lag characteristics of a given R-C network depend only on the frequency but not on the amplitude of the input wave form. Hence, the inside surface temperature variation under any external climatic conditions can easily be obtained once λ and φ are determined. This is possible because even though the sol-air temperature profile is influenced by the variations of external climatic factors, (which in turn depend upon latitude, time of the year, orientation etc.), it can still be represented by the same Fourier series, with variations only in amplitude and inital phase angles. Instead, when the sol-air time temperature variations are impressed to the model directly, in its complex form, as for example by a photoform function generator, the output wave form will be true only for that condition. Hence, for each variation in the climatic factor, and the consequent variation in sol-air temperature, a new wave form should be generated and the output wave form recorded. This makes the material behaviour and the climatic factors inseparable. Another disadvantage with this method is that for measuring the amplitude variations and phase lag characteristics of such complex wave forms, cathode ray oscillographic recording has to be employed. This method of recording will not yield accurate measurements.

For sinusoidal excitation, there is no need to record the wave forms, since for linear networks with such excitation, the response will also be sinusoidal with a lesser amplitude and a phase shift. Hence, only the amplitude of the output wave form and the phase shift introduced by the network have to be measured. Precise measurements of amplitude may be made with inexpensive equipment, like a Vacuum-tube Voltmeter. Accurate phase shift measurements, however, need special consideration.

3.7 Input Signal Generation

In the light of above advantages, the steady state sinusoidal method has been adopted in these studies. The only drawback of this approach is that it involves a little extra mathematical operation in carrying out the Fourier analysis of the sol-air temperature wave form. However, the advantages of this method over weigh this drawback.

A Hewlet Packard (Hp) type 201 C Audio Oscillator having a frequency range of 100 c/s to 10 Kc/s has been used as an input signal source. The fundamental frequency used is 100 c/s. The frequency calibration and stability of the oscillator was checked against a precision electronic frequency counter, (Hp type 523 B) which can read upto 0.1 c/s. The oscillator was found to be highly stable, the frequency drift was only of the order of a cycle over a prolonged period of several hours. It was also found, that the voltage output was also constant over long periods and had a flat response within the full frequency range. The output impedance of the oscillator was quite low (600 ohms) and hence the voltage output was not affected to any significant extent by the network.

3.8 Measuring Equipment

The amplitude (peak to peak) of the voltages of the input and output wave forms of the networks were measured by an R.C.A. Senior Voltohmyst vacuum tube voltmeter type WV 98 A. This V.T.V.M. had an input impedance of 0.33 Megohms shunted by 70 pF for A.C. measurements. Though this is a high input impedance compared to the most of the network simulations, in certain cases, especially while studying the insulating materials, the network output impedances were of the order a few hundred kilo ohms when the loading of the network by the measuring meter became noticeable. To prevent this loading effect a cathode follower unit was designed and employed as a low impedance matching unit. This unit has an input impedance of greater than 60 Meg-ohms and the output impedance of 600 ohms. The cathode follower will have gain of less than unity and for this unit it was found to be 0.9, and was very stable in operation. In order to get the correct output of the network the actual measured amplitude at the cathode follower terminals is to be multiplied by a factor (10/9). The amplitude decrement factor (λ) is defined as a ratio of the output to input amplitude. As the attenuation of the amplitude for some networks and especially for higher harmonics is sufficiently high, if an input voltage of unit amplitude is fed to the network the output may be of the order of few millivolts. The lowest voltage that can be read in the V.T.V.M. was 0.1 V (peak to peak). Hence, in determining the amplitude decrement factors, an input amplitude of 60 V (peak to peak) was applied and the output amplitudes are mostly within the measurable range. By dividing the output voltage (after correcting for the Cathode follower) by the input voltage (60 V) the amplitude decrement factor is obtained.

Inspite of this procedure, in a few cases the output was found to be below 0.1 V. For such measurements a commercially available Electronic Millivoltmeter reading upto 0.1 mv was used after calibration.

3.9 Phase Measurement

Accurate measurement of phase lag angles posed a problem. Commercially made equipment were not readily available. Initially it was measured on a double Beam oscilloscope. Solartron type CD 711 S, by simultaneously displaying the input and output wave forms and the phase shift was noted on the calibrated expanded time base. Though this method enabled one to make quantitative measurements, the accuracy was not high, especially for small phase shifts. The other disadvantage was that the measuring procedure was time consuming and tedious.

To facilitate phase measurements, a direct reading Audio phasemeter was designed and fabricated. The instrument reads with an accuracy of $\pm 1^{o}$, throughout the audio frequency range, over a wide range of input amplitudes 0.3 to 100 V and irrespective of the audio signal frequency under measurement. Photographs of the phase meter are shown in plates 3 and 4.

.10 Design Principles of Phase Meter

Various techniques have been developed for the phase angle measurements of periodic signals. These employed cathode ray tube method (50), vector addition of voltages (51) and null methods (52). But these techniques lack in precision and are not capable of measuring phase angles directly in degrees. In some methods the amplitudes of the two signals must be made equal and the calibration is frequency-sensitive.

AUDIO PHASE METER

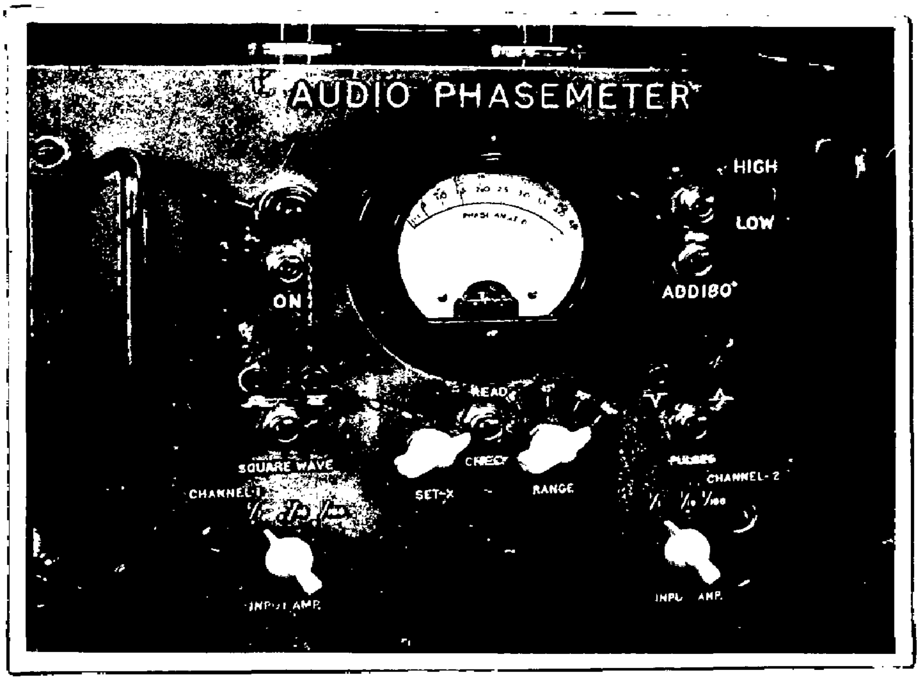

PLATE 3 Front View

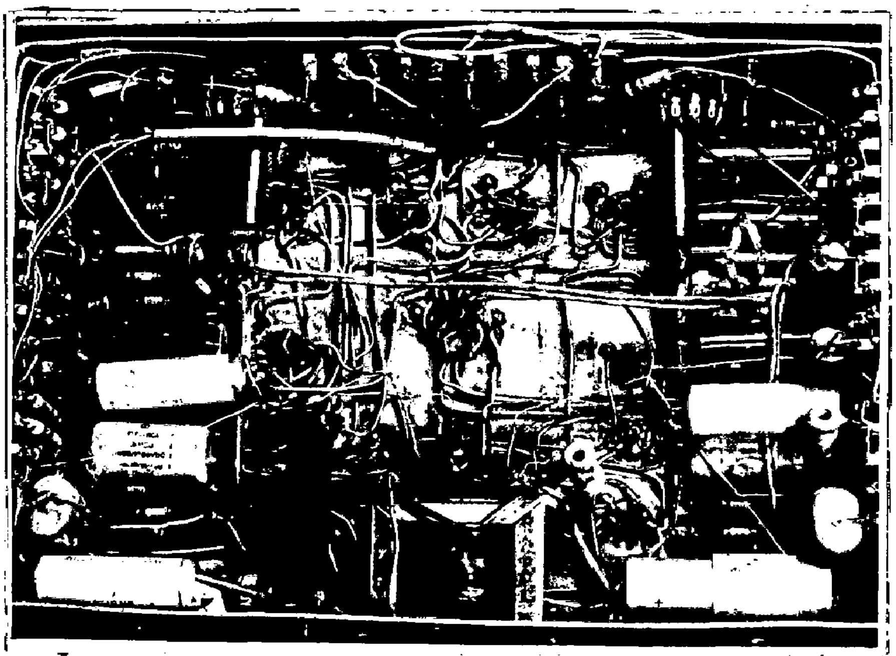

PLATE 4 Bottom View

AUDIO PHASE METER

PLATE 3 Front View

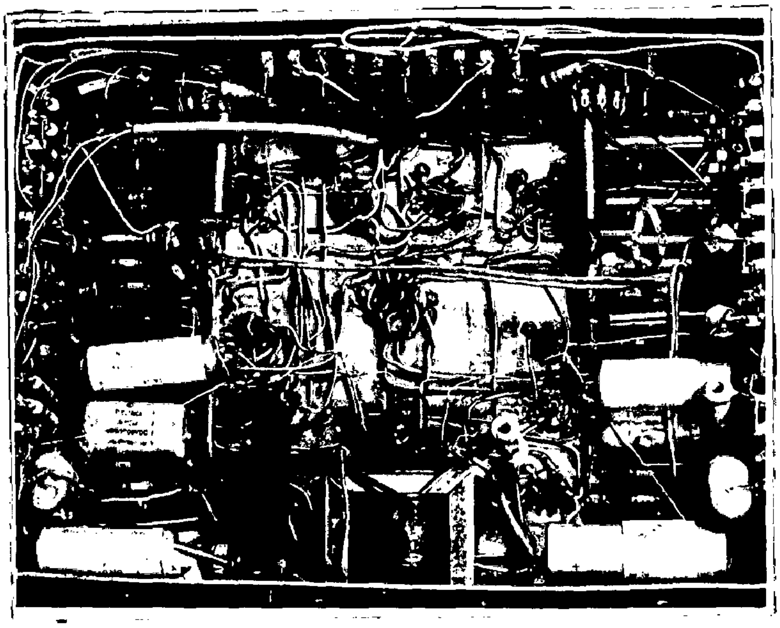

PLATE 4 Bottom View

Use of the foregoing methods have been superseded by direct reading phasemeters (53, 54). The basic principle of this type of phase meter is sensing the phase shifts as a relative time delay between the zero-axis crossings of the reference and phase delayed wave forms.

The direct phase measuring techniques consist of two operations namely conversion of input sine waves into square waves, preserving their times of zero-axis crossings, and an electronic device whose indications are linear functions of zero crossing-time intervals. Though the principle appears to be simple, complexities of circuit design are encountered in maintaining zero-axis crossings of input and output waves, throughout and in reducing the instrumental errors. The block diagram of the phase meter is shown in Fig.(3.3).

The instrument consists of two identical channels. The first stage of each channel is a cathode follower with a high input impedance (about 70 megohms) and prevents the loading of the network under study. The output of the cathode follower is clipped symmetrically at 1.5 volts before it is fed to the grid of the next high gain amplifier. Signal amplitudes whose peak value exceeds 1.5 volts are clipped off at this level, while smaller signals were clipped in the subsequent stages of the amplifier. With the aid of an attenuator,

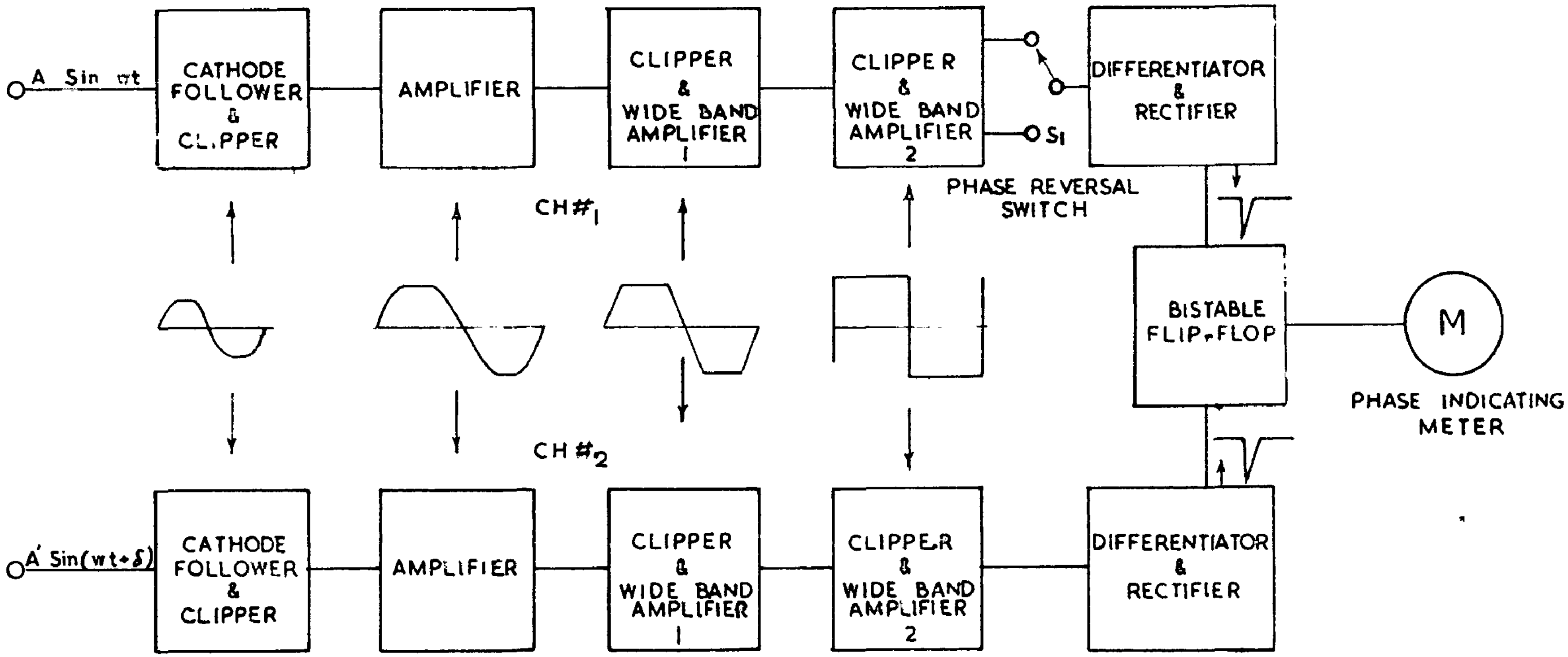

FIG.3·3 BLOCK DIAGRAM OF PHASE METER

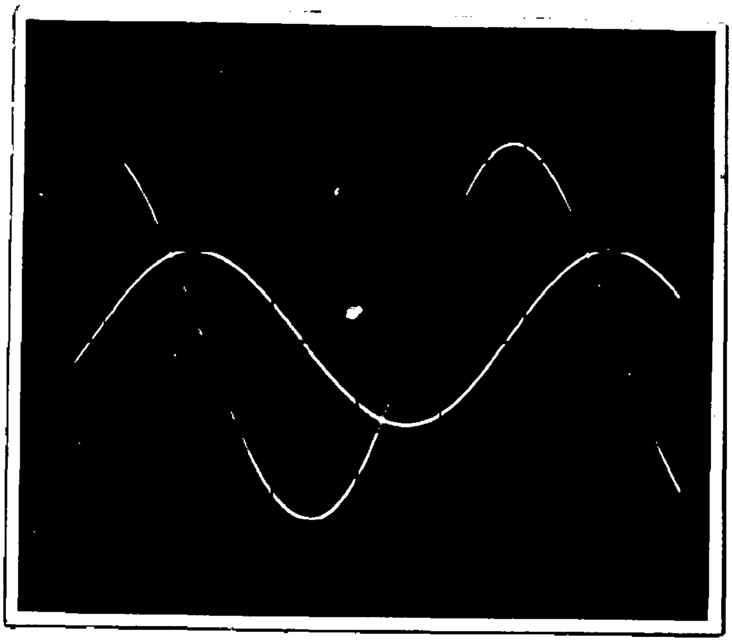

PLATE 5
Input to the two channels (excitatiom & response of the R.C. Network)

PLATE 6
Symmetrical Squarewave output of the two channels.

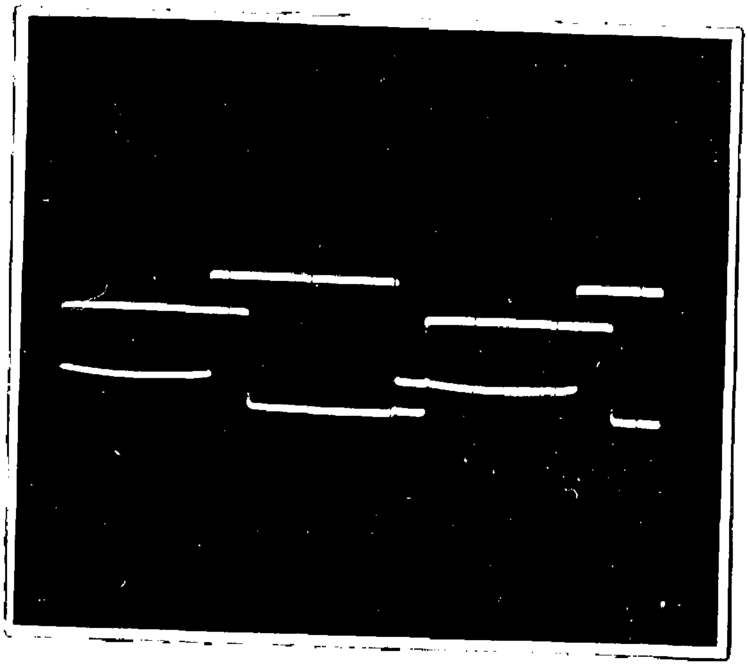

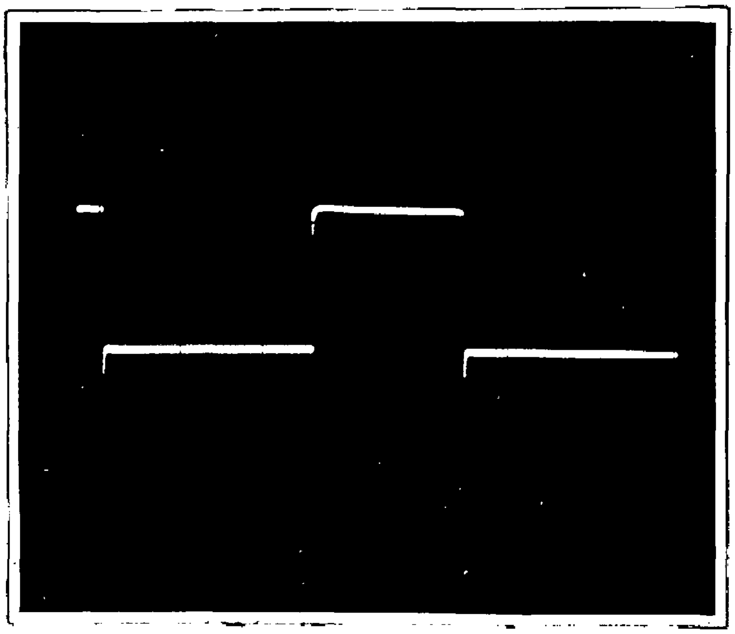

PLATE 7
Bistable output corresponding to the phase difference

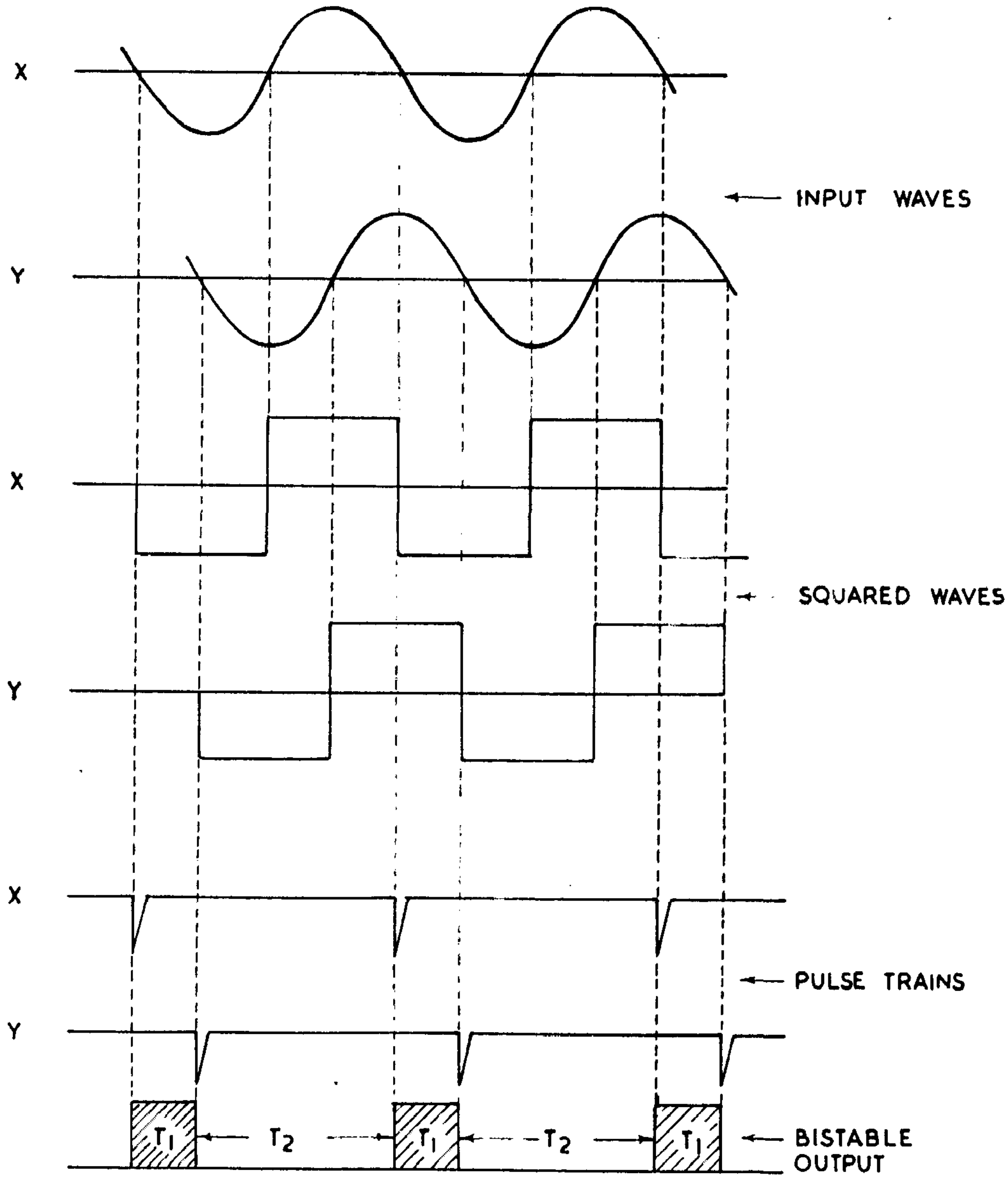

FIG. 3·4 PRINCIPLE OF PHASE MEASURMENTS

again restoring (the conduction to A) the initial conditions and maintains it for a time interval T_2. The action is repetitive. It is obvious that greater the phase lag between the reference and the test signals, the larger is the fraction of a cycle for which B conducts and hence will be higher in the D.C. average indicated by the microammeter put in series with its anode. The phase difference is directly proportional to the fraction T_1 $(T_1 + T_2)$ and hence to the average current through the anode circuit of B. A typical bistable output with phase delayed signals is shown in plate 7.

$$\text{Phase angle} \quad \varphi \propto \frac{T_1}{(T_1 + T_2)}$$

$$\varphi = c \quad \frac{T_1}{T_1 + T_2} \quad = c\ I_b$$

where c is a constant and I_b is the average current through the anode circuit of B indicated by the meter. The meter dial was calibrated directly in terms of phase angles (degrees) linearly. The phase angles from $0-360^\circ$ degrees in six ranges $0-45^\circ$, $0-90^\circ$, $0-180^\circ$, $180-225^\circ$, $180-270^\circ$ and $180-360^\circ$ were obtained with suitable shunts to the microammeter.

The phase inverter incorporated in channel 1 was used to produce 180° phase shift. This arrangement enables measurement of phase angles beyond 180° (180-360°) by transposing them into the lower ranges and hence without loss of measuring accuracy. The circuit diagram of the phasemeter is shown in Fig. (3.8).

With this specially designed Audio phase meter, the problem of accurate determination of phase lag angles has been simplified considerably and being a direct reading type, quick measurements are made possible, compared to the cathode ray oscillographic method.

The complete experimental setup for the determination of thermal system functions of building elements by the Electrical Analogue method is shown in plate 8 and illustrated by the block diagram Fig.(3.6). With this setup it is possible to simulate any type of building component, wall, roof or floor, etc. homogeneous or composite (multi layer), with little effort. This system is particularly suitable for the study of the effect of various parameters, especially, the influence of surface heat transfer coefficients on the overall thermal behaviour under periodic heat flow conditions.

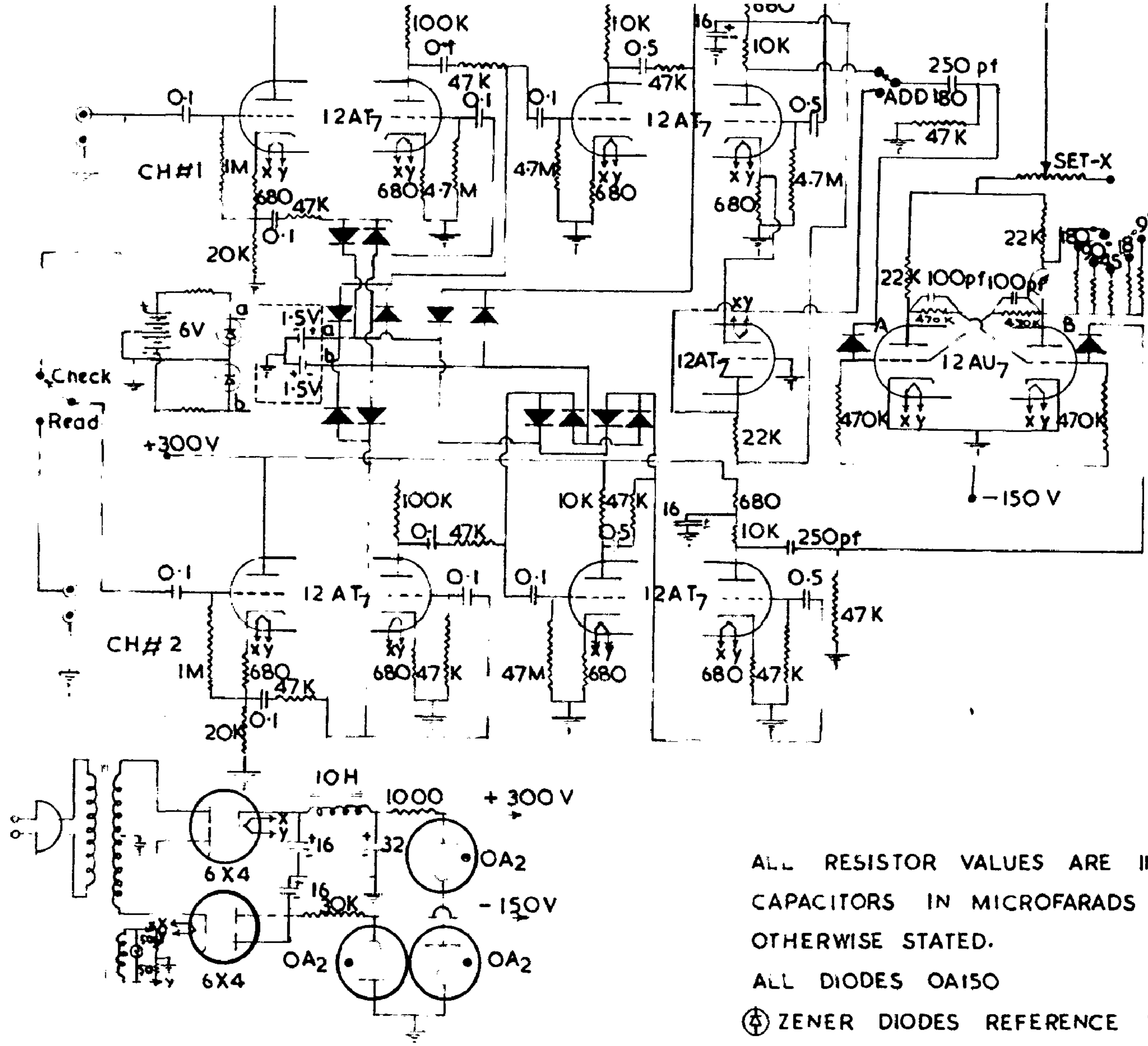

ALL RESISTOR VALUES ARE IN OHMS CAPACITORS IN MICROFARADS UNLESS OTHERWISE STATED.

ALL DIODES OA150

(Z) ZENER DIODES REFERENCE VOLTAGE 1·5V

FIG. 3·5 SCHEMATIC CIRCUIT DIAGRAM OF THE AUDIO PHASE METER

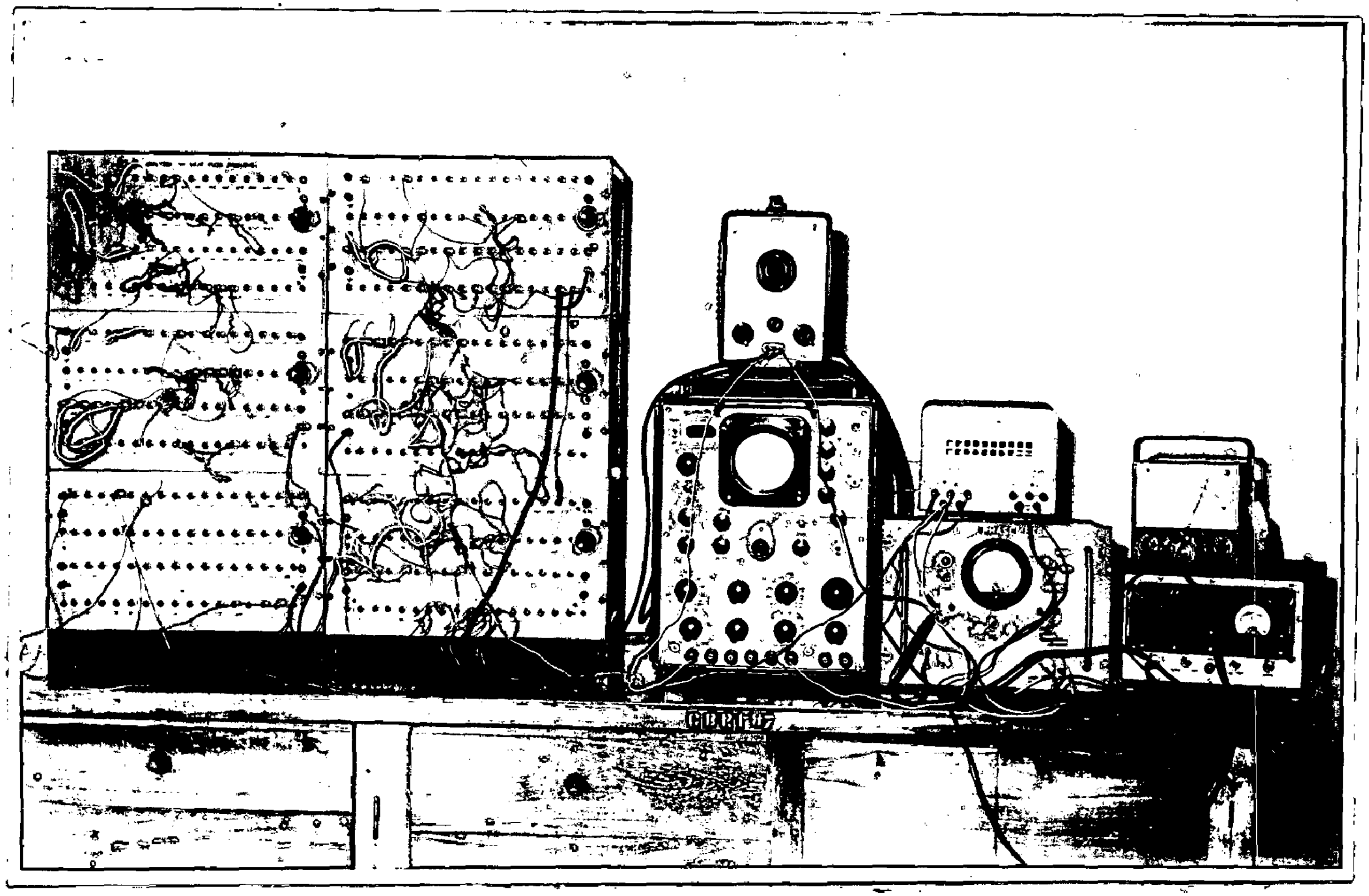

PLATE 8 Photograph of the Experimental Setup

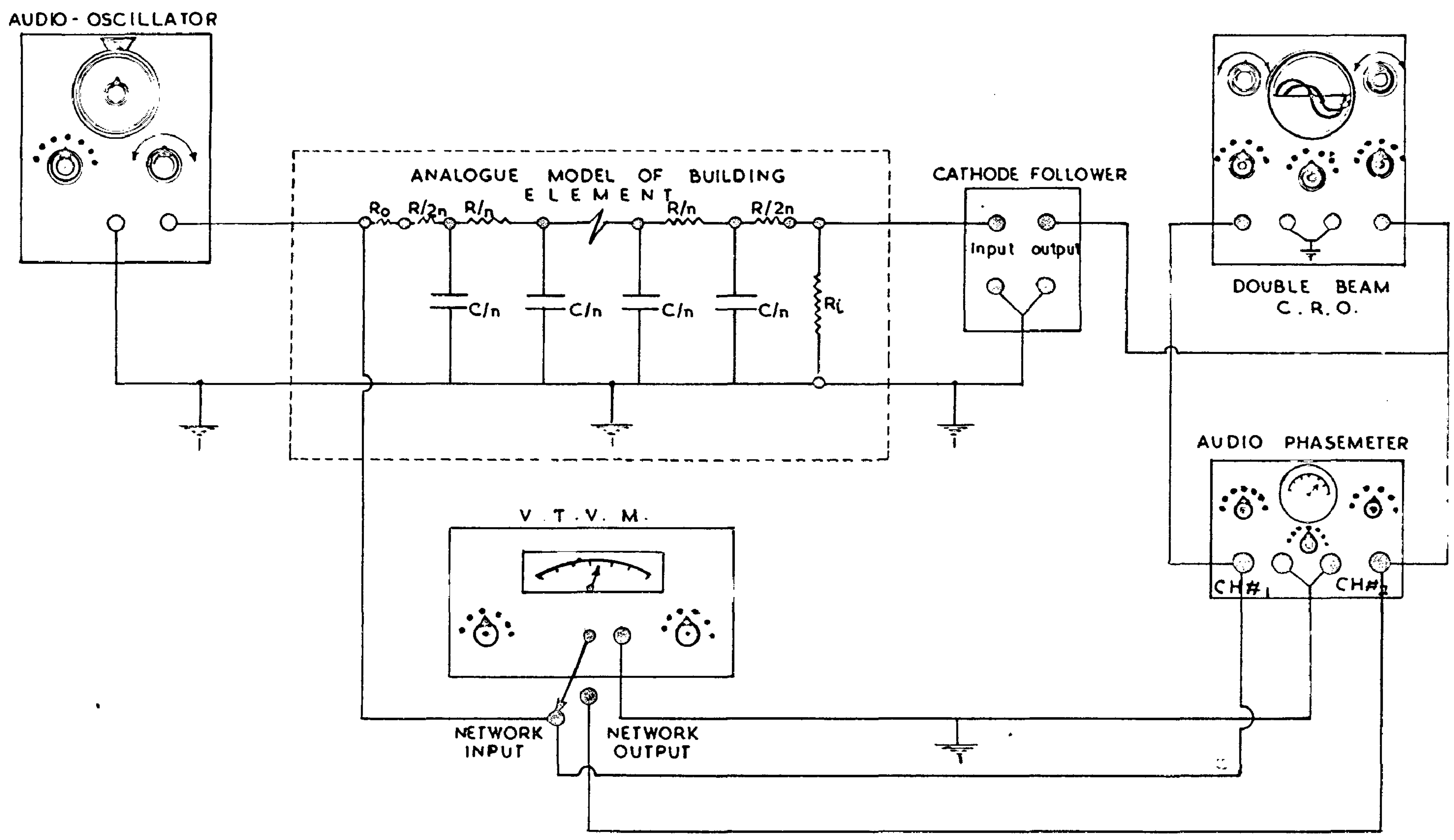

FIG. 3·6 BLOCK DIAGRAM OF THE EXPERIMENTAL SET UP

C H A P T E R 4

LUMPING ERRORS

C H A P T E R 4

LUMPING ERRORS

4.1 Introduction

The heat flow through a body is analogous to the current flow through a non-inductive transmission line with distributed resistance and capacitances. To represent a building element in the electrical model by a transmission line of reasonable length is difficult. Hence, in the study of the problems of heat transfer through building elements, approximate representations by lumped circuits are used. Mathematically "lumping" is the representation of a partial differential equation by an approximate finite difference equation. The behaviour of the lumped circuit approaches the distributed system as the number of lumps are increased. However, there are certain practical limitations due to the component qualities and cost, which restrict the number of lumps used in the network. So the first problem is to determine the optimum number of lumps required to represent a thermal system for obtaining reasonably accurate results. The errors introduced due to lumping depend on many factors such as thickness and properties of the material, the type of lumped circuit (T, L or Π networks), number of lumps used, boundary conditions, surface film resistances, frequency of the input wave form and the location of the point of interest in the network.

Several investigators have studied this problem under specified boundary conditions. Paschkis and Heisler (55) have investigated the inaccuracies of RC lumped circuits at different depths and time intervals using a step function excitation. The influence of film resistances on the errors were also studied. In their studies, 12 lumps were taken to be the equivalent of the distributed value. The voltage variations (which corresponds to the temperature rise) with time at the junction points of the various lumped circuit elements were compared with those of the 12 lump values. Their results indicated that (i) five lumps gave sufficient accuracy except for relatively small values of t/RC (ratio of the time at which measurements were taken to the time constant of the circuit), (ii) for high ratios of the film resistance to the circuit resistance the number of lumps used had no significant influence, (iii) inside film resistance had smaller influence than the external film resistance, and (iv) lumped circuit representation of the building element without the inclusion of film resistances, would present maximum errors. Lawson and McGuire (33) have shown that for a semi infinite slab, with a step function excitation, the responses are identical after the first section for T, L and π sections. Klein, et.al. (56) have analysed the distribution errors in a finite bar, subjected to a step function excitation at one end, the other maintained at constant potential. They have found that the errors, at the centre of the bar have shown a high positive departure during the early part of the transient and reduced to negative errors - 6 per cent for 5 lumps and - 2 per cent for 11 lumps. Clarke (57) has analysed the error in a finite bar represented by different number of L sections one end of which is supplied w with a constant heat flux, the other end being perfectly insulated. It was found that the deviation of the lumped system behaviour from that of the distributed one, at the insulated end of the bar was always positive but decreased with time. Friedman (58) has estimated an upper limit of the error between the exact solution and its lumped parameter analogue for the case examined by Klein et.al. The solution for the lumped system of 'T' sections was given by Jaeger (59) and the exact analytical solution was provided by Carslaw and Jaeger (60). The errors were greatest at the first section and decreased rapidly for points farther off from the source. Robertson and Gross (34) have compared the percentage errors for open and short circuit terminations for step function excitation, and concluded that the changes in the circuit termination do not result in appreciable changes in the errors within the lumped circuit.

Most of the above investigators have considered the transient response for step function excitation. However, as mentioned earlier, the external boundary conditions for a building element can be represented by the sol-air temperature which can be expressed with sufficient accuracy as a Fourier series with three or four harmonic components. Hence, it is sufficient to consider the lumping errors for the fundamental and two or three higher harmonic sinusoidal inputs. Designing of lumped circuits for a limited frequency range leads to lesser number of sections than are needed for a transient response for a step function. Burnand (43) has suggested that division of a commonly used wall or roof element into 3 or 4 sections would be a sufficient approximation to the true analogy.

Mason (61) presented an approximate method of selecting the number of lumps, based on filter network analysis in terms of the wave length of the temperature wave through the medium. He has shown that if the length of each lumped section 'L' is $\delta/8$, the errors would be within 8 per cent of the distributed one. Mattage and Parmelee (33) have applied this one-eighth wave length representation to the periodic heat conduction through building elements and have derived an expression between the thickness of the material representing each lump and the thermal diffusivity of the material (a), and the frequency of the thermal cycle (f) as

$$L = 0.44 \sqrt{\frac{a}{f}} \qquad \ldots(1)$$

Drake et.al. (62) had pointed out that the above criterion may be useful for homogeneous structures, but do not hold good for composite constructions. They have also shown that the fraction of wave length needed for 5 % accuracy varied between 1/25 to 1/12 for composite constructions. This indicates that in a composite construction the manner in which a given material is located in relation to other materials, influences the size of lump to be used for obtaining a specified accuracy. Stephenson and Mitalas (63) have compared the theoretical frequency responses of distributed and lumped networks employing Matrix method. They have attempted to present a rational method of designing active as well as passive networks to represent homogeneous slabs, to any desired degree of accuracy. Recently Murray and Landis (64) have derived matrix equations for estimating the lumping errors of any parameter.

The determination of errors introduced due to lumping requires a comparision of the network solution with an exact analytical solution for the distributed system. The analytical solution is a difficult one particularly for composite constructions. Instead Drake et.al. (62) have adopted an experimental procedure in which the number of lumps are increased to an extent, where further increase of lumps does not significantly alter the transfer functions.

Though a good deal of theoretical as well as experimental studies were carried out on this problem of lumping, no definite generalisations regarding the choice of the numbers of lumps based on the knowledge of the thermal properties (Resistance and Capacitance) are available. Hence, a systematic study of the effect of various parameters on the lumping errors was carried out theoretically (Matrix method) and experimentally. The total errors in analogue studies are, due to lumping, component tolerances and measurements. In order to separate the lumping errors from other errors, theoretical calculation of lumping errors have to be made. The procedure followed here was to calculate the transfer functions for both the distributed and lumped circuit representations, starting with one lump and increasing to 10 lumps, for different thermal time constants (RC) ranging from 0.5 to 200 and then to compare their moduli and arguments.

The following aspects were included in the study :-

1. Selection of the type of network (T, L or π) configuration, for obtaining a specified accuracy with minimum number of sections.
2. Determination of the variation of percentage errors in transfer function (amplitude decrements and phase lags) as a function of the thermal time constants (RC) and the number of lumps, for the best type of network (obtained from the results of (1).
3. Evaluation of the influence of film resistances on the lumping errors of transfer functions.
4. Determination of the effect of input frequency on the lumping errors.

4.2 Choice of the Network

To determine which type of network (T, L or π) will yield best results with lesser number of lumps for any building element of a given thermal time constant (RC), the transmission matrices of the lumped and distributed systems were computed and compared.

For a lumped circuit of 'N' network elements, the overall transfer matrix is obtained by matrix multiplication of the transfer matrix of each lump 'N' times. The overall transmission matrices for 1, 2, 4, 6, 8, and 10 lumps, for all the three network configurations are calculated. The calculated lumped matrix elements are for RC values ranging from 0.1 to 200 and the distributed matrix elements are included in Appendix (I). This data will enable a quick estimation of the lumping errors, in the determination of the surface temperatures, heat fluxes and the thermal system functions.

For surface to surface transmission with open circuit termination (considering the material alone without surface heat transfer coefficients the transfer function is given by the reciprocal of the element 'A' of the transmission matrix i.e., $\frac{1}{A}$. Where A is a complex number. In order to estimate the lumping errors, the modulus and arguments of the transfer functions for distributed and the lumped T and L networks of 1, 2, 4 and 8 lumps for RC values from 0.5 to 50, have been determined and compared in Figs. (4.1 and 4.2). The matrix element 'A' is the same for T and π networks.

The results have shown that the lumped T and π circuit configurations give less deviation

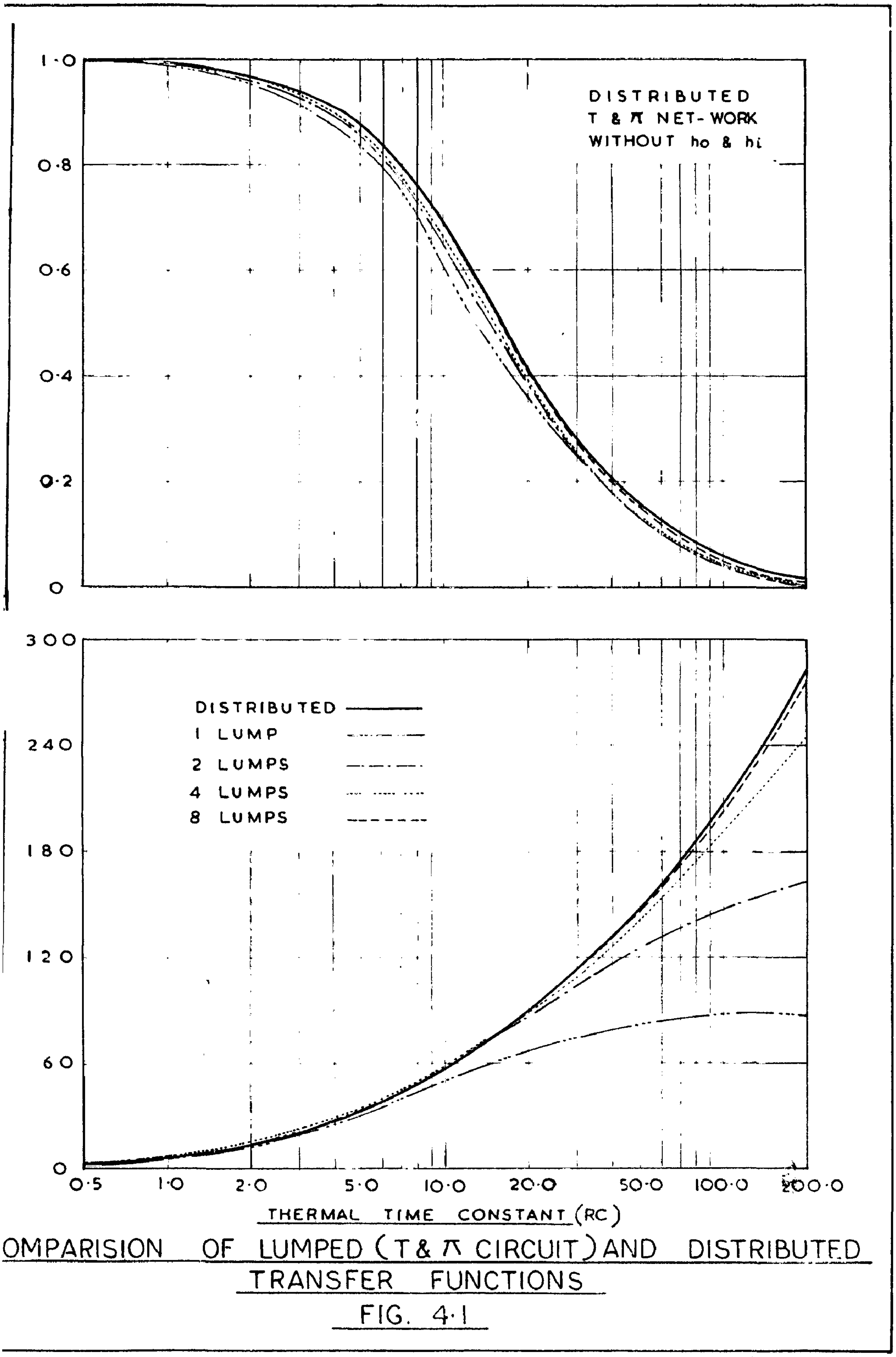

OMPARISION OF LUMPED (T & π CIRCUIT) AND DISTRIBUTED TRANSFER FUNCTIONS

FIG. 4·1

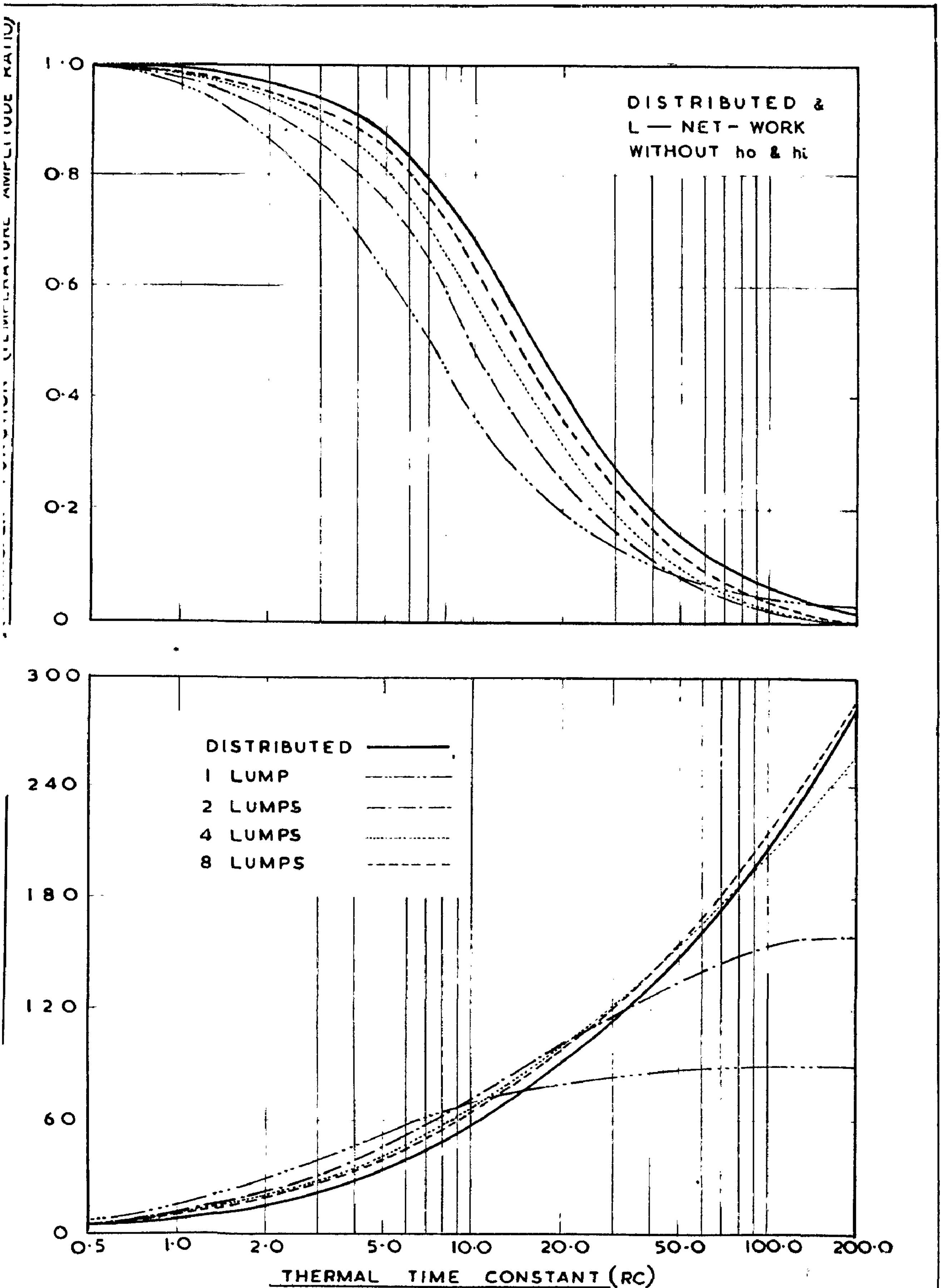

OMPARISION OF LUMPED (L-CIRCUIT) AND DISTRIBUTED TRANSFER FUNCTIONS

FIG. 4·2

from the distributed values than the L type. In both the errors in amplitude as well as phase decreased with increasing number of lumps for any given RC value. For large RC values less than 4 lumps are totally inadequate. Based on these results, the 'T' type of network was finally chosen for further studies on the effect of various factors on the lumping errors.

4.3 Thermal Time Constant Versus Lumping Errors

The transfer functions are computed, for distributed and lumped 'T' circuits of 1, 2, 4, 6, 8 and 10 lumps for RC values from 0.1 to 200 are given in Table (4.1). The percentage errors due to lumping and its reduction with the number of lumps were determined for matrix elements A, B and C (both modulus and argument) and are presented in Figs. (4.3, 4.4 & 4.5 respectively). These comparisions were made for the fundamental frequency which is most significant. The results of these studies are broadly summarised in Table (4.2)

TABLE (4.2)

Thermal time constant RC	No. of lumps required
Upto 1	1 lump
Between 1 and 5	2 lumps
" 5 and 20	4 lumps
" 20 and 50	8 lumps
" 50 and 100	10 lumps
Above 100	more than 10 lumps

COMPARISON OF LUMPED 'T' NETWORK AND DISTRIBUTED SYSTEM TRANSFER FUNCTIONS FOR RC VALUES 0.1 to 200
(Independent of Surface Coefficients)

S. No.	RC	TRANSFER FUNCTION $\lambda_i \angle -\phi_i$													
		Distributed		LUMPED 'T' NETWORK											
				1 Lump		2 Lumps		4 Lumps		6 Lumps		8 Lumps		10 Lumps	
		Modulus	Arg. in deg.	Modulus	Arg in deg.	Modulus	Arg in deg	Modulus	Arg in deg	Modulus	Arg in deg	Modulus	Arg in deg	Modulus	Arg in deg.
1.	0.1	1.000	0.7	1.000	0.8	1.000	0.8	1.000	0.8	1.000	0.8	1.000	0.8	1.000	0.8
2.	0.5	0.993	3.9	0.993	3.7	0.993	3.7	0.993	3.7	0.993	3.7	0.998	3.7	0.993	3.7
3.	1.0	0.994	7.4	0.991	7.5	0.994	7.5	0.994	7.5	0.994	7.5	0.994	7.5	0.994	7.5
4.	5.0	0.831	35.1	0.837	33.3	0.869	34.7	0.873	35.0	0.880	35.0	0.831	35.0	0.831	35.0
5.	10.0	0.632	60.6	0.607	52.6	0.655	59.0	0.673	60.3	0.677	60.7	0.679	60.7	0.631	60.7
6.	20.0	0.412	93.0	0.357	60.0	0.381	87.0	0.400	91.5	0.409	92.3	0.410	92.6	0.411	92.6
7.	50.0	0.154	147.0	0.151	81.3	0.137	124.0	0.142	141.0	0.149	144.0	0.153	146.0	0.153	147.0
8.	100.0	0.055	206.0	0.076	85.6	0.041	147.0	0.044	191.0	0.048	201.0	0.051	204.0	0.052	206.7
9.	200.0	0.012	292.0	0.038	83.0	0.011	162.8	0.003	225.9	0.009	274.0	0.010	282.0	0.011	283.4

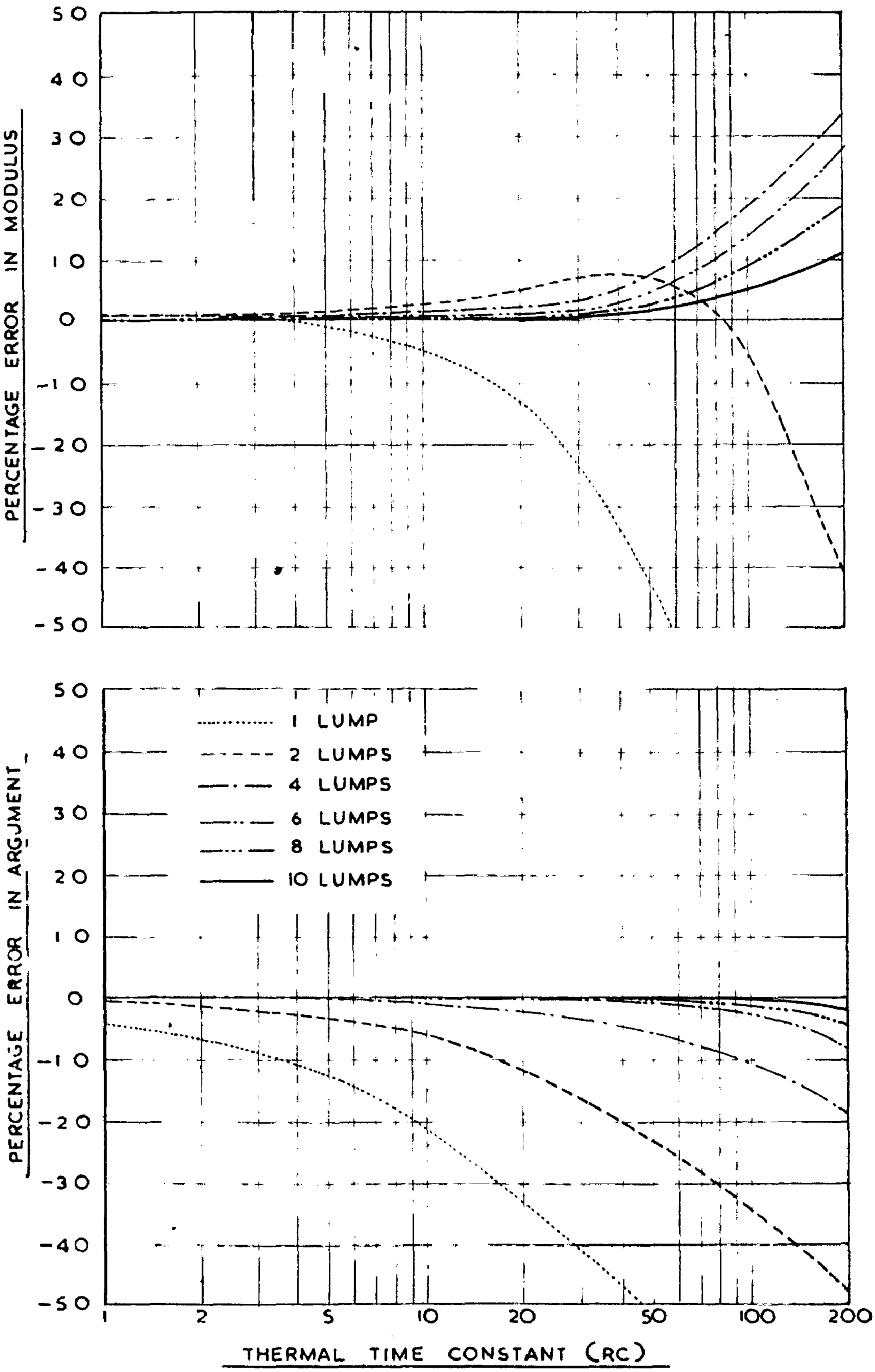

FIG.4·5. LUMPING ERRORS OF TRANSMISSION MATRIX

ELEMENT - C

(T - NETWORK)

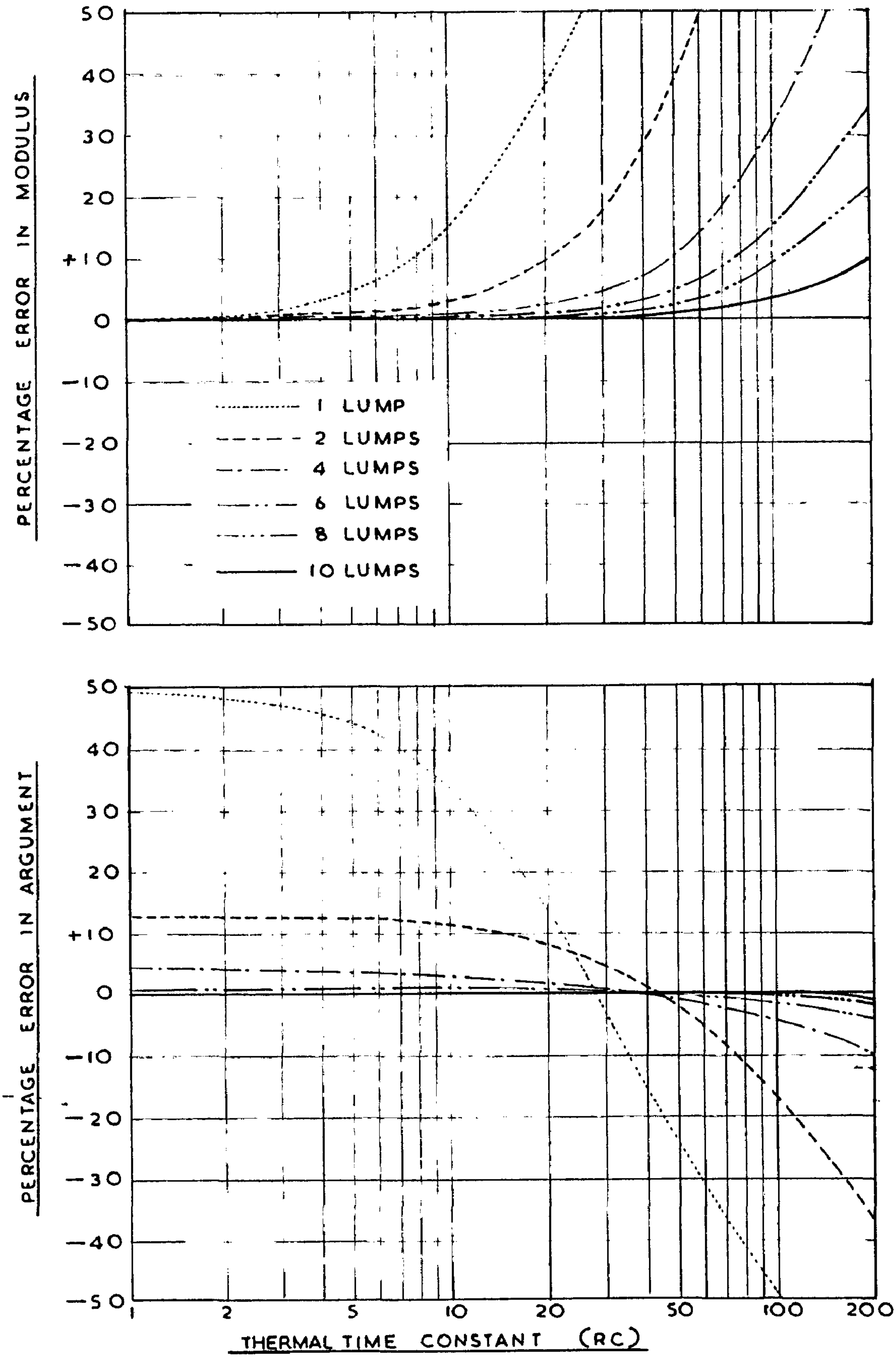

FIG. 4·4 LUMPING ERRORS OF TRANSMISSION MATRIX

ELEMENT – B

(T - NETWORK)

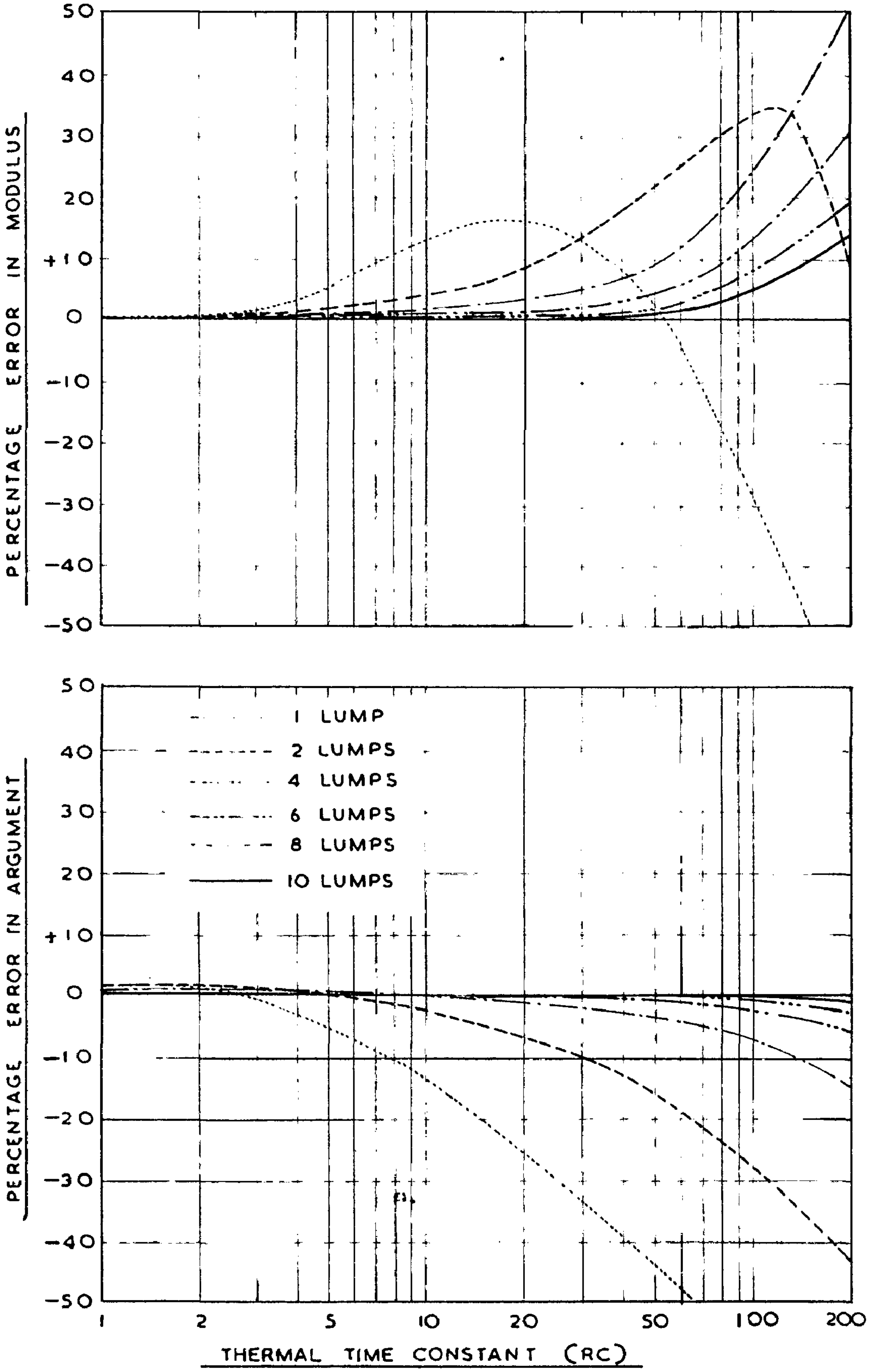

FIG.4·3. LUMPING ERRORS OF TRANSMISSION MATRIX ELEMENT – A (T-NETWORK)

This indicates that the number of lumps are proportional to the square root of RC. This provides a basis for the direct selection of the number of lumps required to represent any building element of known thermal time constant (RC), ensuring an accuracy of 2 to 3 % in the transfer functions. The above criterion of lumping was employed for further studies by the Analogue method. The transfer functions were determined, by the Analogue method, for building elements having different time constants, for the fundamental and three higher harmonics. These are compared with the corresponding distributed system transfer functions (computed) in Fig. (4.6). Since experimental errors were of the order of 2 to 3 %, any attempt to obtain better precision by increasing the number of lumps than those recommended here is not justifiable.

4.4 Effect of Film Resistances on Lumping Errors

It has been pointed out (48, 55) that the boundary conditions influence the lumping errors but quantitative variation of these errors with surface film resistances have not so far been fully evaluated for sinusoidal inputs.

Inclusion of the surface film resistances on either side of the building element will alter the overall transmission matrix. This transfer matrix is

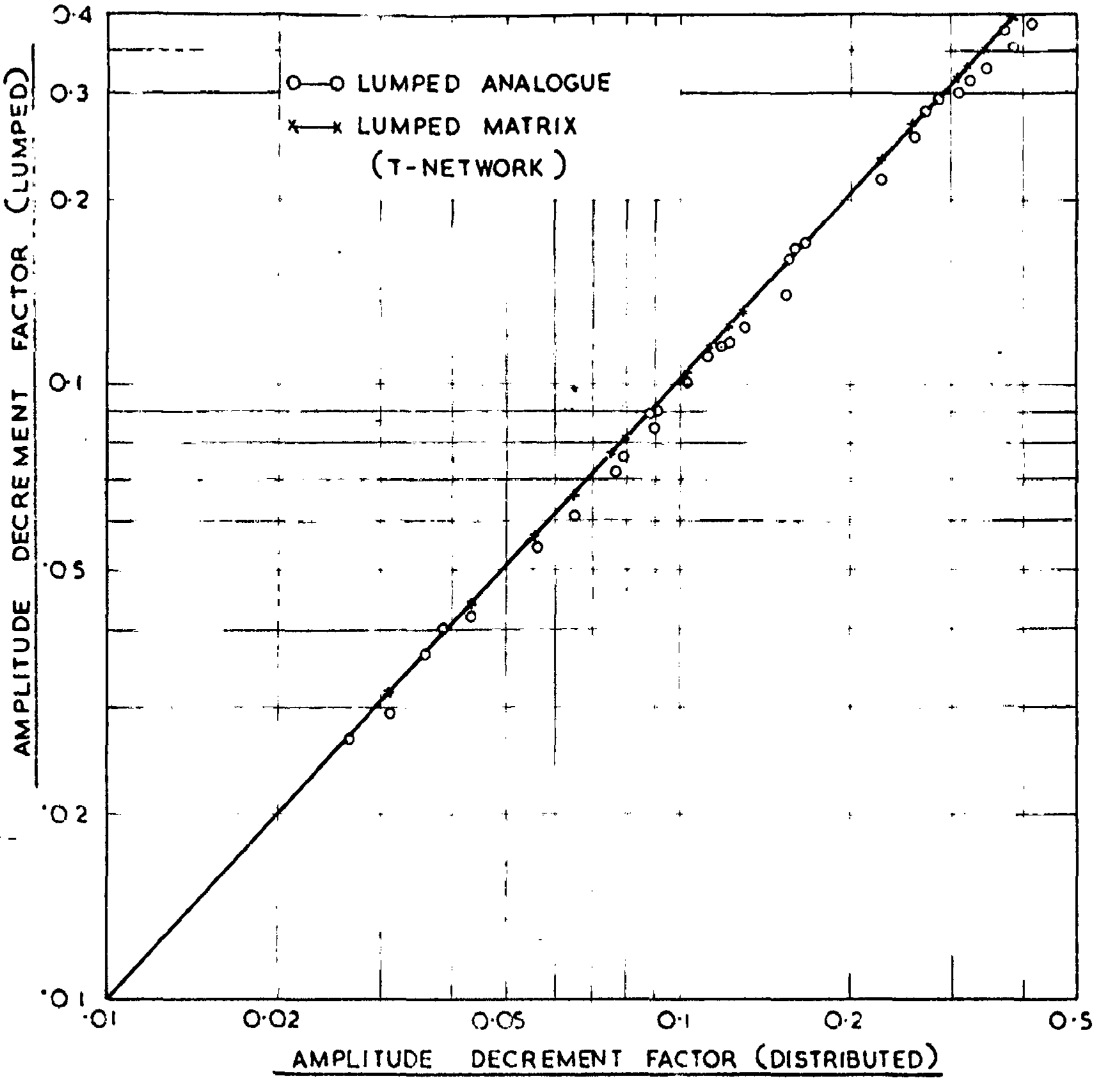

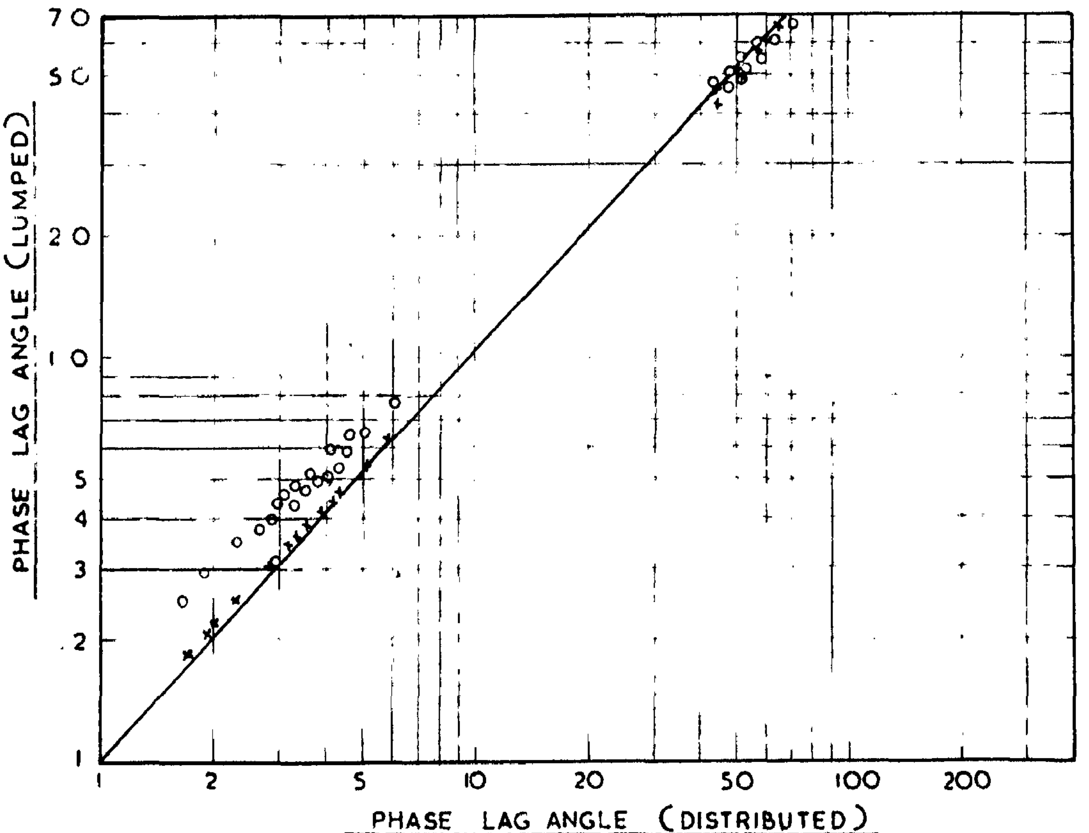

FIG. 4·6 DISTRIBUTED VERSUS LUMPED (THEORETICAL & ANALOGUE) TRANSFER FUNCTIONS given by

$$\begin{bmatrix} A' & B' \\ C' & D' \end{bmatrix} = \begin{bmatrix} 1 & 1/h_o \\ 0 & 1 \end{bmatrix} \begin{bmatrix} A & B \\ C & D \end{bmatrix} \begin{bmatrix} 1 & 1/h_i \\ 0 & 1 \end{bmatrix} \qquad \cdots(2)$$

For such a case the overall transfer function, $(\lambda_i \angle -\varphi_i)$ is given by $1/A'$

where

$$A' = A + Bh_i + C/h_o + D \; h_i/h_o \qquad \cdots(3)$$

The elements A and D of the matrix of the building component, depend only on the thermal time constant (RC) for a given frequency, while elements B and C will depend both on the thermal time constant and the thermal resistance (R). Hence, the overall transfer function will not only depend on 'RC' but also on the ratios of R/R_i, R_o/R and R_o/R_i where R_o and R_i are the reciprocals of the surface heat transfer coefficients h_o and h_i respectively. This implies that building components having the same thermal time constant (RC) but different thermal resistances will give different transfer functions. Hence for evaluating the effect of film resistances or lumping errors, four specific values of RC with fixed resistances, each representing a class of materials commonly used in practice, were chosen. These are :-

i) RC = 0.1 and R = 0.1 which represents highly conducting sections like Asbestos cement and Galvonised Iron sheets, glass panes etc.

ii) RC = 1.0 R = 5.0 which represents high resistive low capacity insulating materials like, slag wool, Thermocole etc.

iii) RC = 10; R = 1.0 - Medium resistance and medium capacity type representing a range of light weight concretes.

and iv) RC = 50, R = 2.0 - High capacity and high density type of heavy materials like Dense concrete, Brick, stone etc.

The number of lumps required for each case was fixed according to Table (4.2) and were 1, 2, 4 and 8 respectively for these four cases considered. These RC and R values chosen would provide a fairly representative idea of the lumping errors as influenced by the surface resistances for most of the commonly used building materials in their usual thicknesses.

For each case the transfer functions (amplitude decrement and phase lag) were computed for external surface heat transfer coefficient (h_o) of values 1.0, 2.03, 3.5, 6.0, 8.0 and 10.0 with a fixed inside film conductance (h_i) of 1.5, and also for internal surface heat transfer coefficient (h_i) of values 0.5, 1.0, 1.5, 2.0 and 5.0 with a fixed h_o of 3.5. Experimental and theoretical values of transfer functions for distributed and lumped systems, are compared in Tables (4.3 and 4.4).

The analogue and computed (Matrix calculated) lumped circuit transfer functions were plotted against the distributed transfer functions, and shown in Fig. (4.6). The ideal correlation curve would be a straight line passing through the origin making 45° with the axes. The deviations in the amplitude decrement factor from the ideal line were only 2 to 3 percent, irrespective of the 'N' value and the surface coefficient variation, when the above recommended number of lumps were used. The deviations of the phase lag angles from the ideal curve appear to be larger for low phase lag angles than for higher phase lags, in Fig. (4.6) but when plotted linearly this deviation is the same (within 3°) all over. In all practical problems, such deviations are minute and are insignificant.

By a close examination of the equation (3) giving the overall transfer function in terms of the matrix coefficients for the building component and surface resistances, the following comments are

TABLE 4.3

EFFECT OF OUTSIDE SURFACE HEAT TRANSFER COEFFICIENT (h_o) ON LUMPING RATIOS OF TRANSFER FUNCTIONS

(Inside Surface Coefficient $h_i = 1.6$)

S. No.	Outside surface coefficient h_o	D, T_M, T_A	RC = 0.1, R = 0.1 Trans. Function Modulus λ_i	RC = 0.1, R = 0.1 Arg. $-\varphi_i$ in deg	RC = 1.0, R = 5.0 Trans. Function Modulus λ_i	RC = 1.0, R = 5.0 Arg $-\varphi_i$ in deg	RC = 10.0, R = 1.0 Trans. Function Modulus λ_i	RC = 10.0, R = 1.0 Arg $-\varphi_i$ in deg	RC = 50.0, R = 2.0 Trans. Function Modulus λ_i	RC = 50.0, R = 2.0 Arg $-\varphi_i$ in deg
1.	1.0	D	0.375	5.9	0.100	4.0	0.151	71.5	0.035	155.7
		T_M	0.374	6.3	0.099	4.1	0.143	71.4	0.034	155.3
		T_A	0.378	7.0	0.100	7.0	0.144	70.0	0.033	153.0
2.	2.0	D	0.525	4.3	0.103	3.6	0.217	62.7	0.052	149.8
		T_M	0.525	4.7	0.103	3.7	0.212	62.9	0.051	147.4
		T_A	0.533	6.0	0.109	6.0	0.211	60.0	0.049	144.0
3.	3.5	D	0.633	3.0	0.112	3.4	0.262	55.0	0.065	141.5
		T_M	0.632	3.0	0.112	3.4	0.253	56.3	0.064	140.6
		T_A	0.640	5.0	0.111	5.0	0.256	54.0	0.061	140.0
4.	6.0	D	0.714	2.3	0.114	3.2	0.294	51.2	0.074	137.0
		T_M	0.714	2.5	0.114	3.3	0.290	51.6	0.073	136.0
		T_A	0.711	4.0	0.113	4.0	0.286	50.0	0.070	134.0
5.	8.0	D	0.747	1.9	0.115	3.2	0.307	49.2	0.078	134.3
		T_M	0.746	2.1	0.115	3.3	0.300	49.7	0.077	133.3
		T_A	0.744	3.0	0.115	4.0	0.300	48.0	0.073	132.0
6.	10.0	D	0.769	1.7	0.116	3.2	0.315	47.9	0.081	133.0
		T_M	0.760	1.8	0.116	3.2	0.310	48.3	0.079	132.5
		T_A	0.763	2.0	0.114	4.0	0.307	46.0	0.076	130.0

D = Distributed, T_M = Lumped T Circuit Matrix, T_A = Lumped T Circuit Analogue.

TABLE 4.4

EFFECT OF INSIDE SURFACE HEAT TRANSFER COEFFICIENT (h_i) ON LUMPING ERRORS OF TRANSFER FUNCTIONS

(Outside Surface Coefficient h_o = 3.5)

S. No.	Inside surface coefficient h_i	D, T_M, T_A	RC = 0.1, R = 0.1 Trans. Function Modulus λ_i	RC = 0.1, R = 0.1 Trans. Function Arg-ϕ_i in deg	RC = 1.0, R = 5.0 Trans. Function Modulus λ_i	RC = 1.0, R = 5.0 Trans. Function Arg-ϕ_i in deg	RC = 10.0, R = 1.0 Trans. Function Modulus λ_i	RC = 10.0, R = 1.0 Trans. Function -ϕ_i arg in deg	RC = 50.0, R = 2.0 Trans. Function Modulus λ_i	RC = 50.0, R = 2.0 Trans. Function Arg-ϕ_i in deg
1.	0.5	D	0.836	4.0	0.274	4.2	0.390	67.7	0.090	152.5
		T_M	0.840	4.1	0.274	4.3	0.332	67.6	0.039	152.0
		T_A	0.844	5.0	0.278	5.0	0.376	65.0	0.085	149.0
2.	1.0	D	0.721	3.5	0.159	3.6	0.315	60.7	0.076	146.0
		T_M	0.719	3.8	0.159	3.7	0.309	60.8	0.075	146.0
		T_A	0.722	4.0	0.168	5.0	0.300	58.0	0.071	142.0
3.	1.5	D	0.633	3.2	0.112	3.4	0.262	55.9	0.065	141.5
		T_M	0.632	3.5	0.112	3.4	0.253	56.3	0.064	140.6
		T_A	0.634	4.0	0.116	5.0	0.256	54.0	0.061	133.0
4.	2.0	D	0.564	3.9	0.033	3.2	0.224	52.9	0.056	137.9
		T_M	0.567	3.1	0.086	3.3	0.219	53.3	0.053	135.6
		T_A	0.567	4.0	0.039	4.0	0.216	51.0	0.054	133.0
5.	5.0	D	0.341	2.0	0.036	3.0	0.117	44.0	0.031	123.2
		T_M	0.341	2.2	0.036	3.0	0.114	44.0	0.030	123.0
		T_A	0.333	3.0	0.035	4.0	0.116	42.0	0.023	124.0

D = Distributed, T_M = Lumped T Circuit Matrix, T_A = Lumped T Circuit Analogue.

made :-

i) The matrix element 'A' is not affected by the inclusion of surface resistances, whereas the coefficient 'B' is affected by inside surface film resistance by the ratio of R/R_1. Coefficient 'C' is affected by the external surface film resistance by the ratio R_o/R while the coefficient D is affected by both the surface resistances by the ratio R_o/R_1.

ii) If A_N, B_N, C_N and D_N be the elements of the transmission matrix of an 'N' lumped circuit, the errors due to lumping in individual matrix elements will be $(A - A_N)$; $(B - B_N)\ R/R_1$; $(C - C_N)\ R_o/R$ and $(D - D_N)\ R_o/R_1$ respectively. The total lumping error will then be cummulative.

iii) For a given RC and surface resistances R_o and R_1, the error $(B - B_N)\ R/R_1$ will increase with the increase of R while the error $(C - C_N)\ R_o/R$ will decrease.

iv) For a given RC and R, increase in R_o will increase the error in $(C - C_N)\ R_o/R$ and $(D - D_N)\ R_o/R_1$ value.

While an increase in R_1 will decrease $(B - B_N)\ R/R_1$ and $(D - D_N)\ R_0/R_1$ the error in $(A - A_N)$ will be unaltered. For a given number of lumps the error in all the four elements will increase with increasing RC and frequency.

As seen from the above, for any particular condition, the overall error in a lumped circuit will depend on the relative increase or decrease of the errors due to $(B - B_N)\ R/R_1$ and $(C - C_N)\ R_0/R$ and $(D - D_N)\ R_0/R_1$ as these errors oppose each other. Under natural conditions the external surface resistance will be usually less than that of the internal surface resistance. Hence, the net effect of surface resistances is to reduce the errors due to lumping. These conclusions can also be verified from the data given in Tables (4.3 and 4.4).

4.5 Effect of Frequency on Lumping Errors

For a given thermal time constant (RC) and fixed number of lumps used, the error between the lumped and distributed transfer functions will increase with the increase of frequency. With the increase of frequency, the transfer constant θ which is given by $\sqrt{\frac{\omega CR}{2}}$ will also increase. For higher values of θ larger number of lumps are to be employed.

The effect of higher harmonics can be treated as if the 'RC' value is increased in harmonic steps and the frequency itself is unaltered. The advantage of this approach is that the curves already drawn between RC and transfer functions and errors for the fundamental frequency, may be utilised for the higher harmonics as well, to obtain the above mentioned quantities.

It follows that if the number of lumps to be used are selected on the basis of the fundamental frequency, increased errors are likely to occur for higher harmonic inputs. However, for practical case of a periodic sol-air temperature excitation, the overall errors will not be increased to any significant extent, as the higher harmonic components in the sol-air temperature will usually be of lower amplitudes than the fundamental and the attenuation in the amplitude for higher harmonics will be quite high.

4.6 Composite Constructions

Evaluation of lumping error in composite constructions, theoretically is highly involved. In order to estimate the overall errors of the Analogue method for composite constructions, the Matrix calculated distributed system transfer functions were compared with Analogue results for some typical composite wall panels in Table (4.5). In setting up the Analogue model, each homogenous section of the composite panel was represented by the number of lumps as recommended in Table (4.8). The comparisions indicate, that such a method of representation is permissible to obtain reasonably accurate results.

COMPARISON OF THE MATRIX AND ANALOGUE TRANSFER AND DRIVING POINT FUNCTIONS OF COMPOSITE CONSTRUCTIONS

$h_o = 3.5$
$h_i = 1.5$

S. No.	Construction	M / A	External Driving point Function: Modulus λ_o	External Driving point Function: Argument in deg. $-\phi_o$	Transfer Function: Modulus λ_i	Transfer Function: Argument in deg. $-\phi_i$	Internal Driving point Function: Modulus λ_i'	Internal Driving point Function: Argument in deg. $-\phi_i$
1.	½" p + 13½" brick + ½"p	M	0.719	14.0	0.065	156.0	0.496	24.0
		A	0.734	15.0	0.062	160.0	0.493	25.0
2.	½" p + 4½" brick + 8" air space + 4½" brick + ½" p	M	0.726	17.0	0.033	128.0	0.432	31.0
		A	0.744	19.0	0.033	123.0	0.437	33.0
3.	3" marble + 9" brick + ½" p	M	0.633	36.0	0.090	143.0	0.434	31.0
		A	0.696	34.0	0.092	140.0	0.439	32.0
4.	½" p + 2" foamed conc. + 4" dense conc. + ½" p	M	0.900	12.0	0.030	90.0	0.563	34.0
		A	0.912	14.0	0.033	94.0	0.573	36.0
5.	½" p + 4½" brick + 1" thermocole + 1" p	M	0.719	26.0	0.050	85.0	0.800	18.0
		A	0.734	24.0	0.055	87.0	0.822	13.0
6.	3" lime conc. + 6" R.B. + ½" p	M	0.720	11.0	0.130	90.0	0.448	27.0
		A	0.733	13.0	0.133	92.0	0.456	30.0
7.	3" lime conc. + 4" mud phuska + 4½" R.B. + ½" p	M	0.723	13.0	0.054	140.0	0.476	22.0
		A	0.730	13.0	0.050	144.0	0.484	24.0
8.	½" hardboard + 1" thermocole + ½" hardboard	M	0.900	4.0	0.034	23.0	0.370	10.0
		A	0.913	5.0	0.039	30.0	0.878	11.0

p = plaster, R.B. = Reinforced brick,

C H A P T E R 5

EXPERIMENTAL CHECK OF THE ANALOGUE BEHAVIOUR

CHAPTER 5

EXPERIMENTAL CHECK OF THE ANALOGUE BEHAVIOUR

5.1. Introduction

Before taking up a study of new problems on a large scale by the analogue method, it is necessary to check the analogue performance with experimental results, under different boundary conditions. It was therefore proposed to verify the R-C network analogue behaviour by comparing the analogue predicted diurnal temperature variations of inside surfaces with those actually measured ones on full scale experimental houses. For this purpose four cases, for which thermal data and the boundary conditions were available, have been chosen. These are given in Table (5.1).

TABLE (5.1)

Sl. No.	Building Element	Construction	External Boundary Condition	Internal Boundary Condition
1.	Homogeneous Roof Slab	4.26 inch concrete	Surface input	Inside air temperature constant.
2.	Homogeneous Wall	9.25 inch Brick	"	"
3.	Homogeneous Wall	"	Sol-air input	"
4.	Composite Wall	1" plaster + 1" Thermocole + 4½" Brick + ½" plaster	Surface input	Indoor air temperature

5.2 Concrete Roof Slab with Surface Input

Raychoudhuri (65) has studied the heat flow variations through a concrete slab 4.26 inch thick which formed the roof of a well insulated enclosure. The external surface was exposed to natural weather conditions, while the inside air temperature of the enclosure maintained nearly constant. The surface temperatures were measured continuously over 36 hours with thermocouples.

The physical properties of the concrete slab are given in Table (5.2).

Thickness (L)	= 4.26 inches
Thermal resistance of the slab R	= 0.39
Thermal capacity of the slab C	=10.3

This concrete slab (with an 'RC' value of 4.0) can be adequately represented on the Analogue by 4 lumped 'T' circuit network.

As the external surface temperature forms the external boundary condition, the outside surface coefficient (h_o) need not be included in the analogue circuit. The inside surface coefficient (h_i) is assumed to be constant, of value 1.5 Btu/Ft.^{2}/Hr/^{o}F. The concrete slab was simulated on the Analogue with the given boundary conditions and the transfer

TABLE 5.2

PHYSICAL PROPERTIES OF THE MATERIALS USED IN EXPERIMENTAL WALLS

S. No.	Material	K	ρ	s
1.	Concrete	10.8	132	0.22
2.	Brick	6.4	117	0.20
3.	Plaster	12.0	120	0.22
4.	Thermocole	0.2	1	0.32
5.	Brick	6.0	100	0.21

K = Thermal conductivity in $Btu.in/Ft^2.Hr.^{o}F$

ρ = Density in Lb/Ft^3

s = Specific heat in $Btu/Lb.^{o}F$

functions $\lambda_i \angle -\phi_i (t_{is}/t_{os})$ is constant for the fundamental and two higher harmonics were determined. These are given in Table (5.3).

The measured external surface temperatures were harmonically analysed and its Fourier representation is given by equation (1)

$$
\begin{aligned}
t_{os}(\tau) = 65.30 &+ 18.67 \operatorname{Cos}(15\,t - 54^\circ 48') \\
&+ 6.7 \operatorname{Cos}(30\,t - 54^\circ 54') \quad ..(1) \\
&+ 1.53 \operatorname{Cos}(45\,t - 47^\circ 30')
\end{aligned}
$$

Fundamental and two harmonic terms are found to be sufficient for a fairly accurate representation of the actual wave form.

The corresponding Fourier representation of the inside surface temperature variation, can be obtained with a knowledge of the 'U' value and transfer functions of the slab, by using Mowgten et.al. (63) method. The Fourier equation of the inside surface temperature is obtained as

$$
\begin{aligned}
t_{is}(\tau) = 66.20 &+ 13.6 \operatorname{Cos}(15\,t - 82^\circ 43') \\
&+ 3.3 \operatorname{Cos}(30\,t - 106^\circ 54') \quad ..(2) \\
&+ 0.6 \operatorname{Cos}(45\,t - 121^\circ 30')
\end{aligned}
$$

The diurnal variation of inside surface temperatures were obtained by synthesising the equation (2) and are compared with the measured temperatures in

TABLE 5.3

THERMAL TRANSFER AND DRIVING POINT FUNCTIONS OF EXPERIMENTAL WALLS

S. No.	Construction	h_o	h_i	Thermal Function	M A' A	Fundamental Z Mod.	Fundamental Z Arg. in deg	Second Harmonic H_2 Mod.	Second Harmonic H_2 Arg in deg	Third Harmonic H_3 Mod.	Third Harmonic H_3 Arg in deg	Fourth Harmonic H_4 Mod.	Fourth Harmonic H_4 Arg in deg
1.	4.26" concrete slab	--	1.5	Transfer	M	0.726	26	0.482	49	0.358	70	...	..
					A	0.734	28	0.483	52	0.386	74	...	..
2.	9.25" brick wall	..	1.4	-do-	A'	0.197	87	0.104	135	0.031	171	0.038	201
					A	0.190	90	0.099	140	0.058	176	0.037	200
3.	9.25" brick wall	1.6	1.7	-do-	M	0.091	106	0.039	159	0.021	193	0.012	229
					A'	0.089	103	0.039	160	0.020	198	0.012	229
					A	0.084	110	0.036	158	0.019	202	0.011	234
				Ext.Driv. point	M	0.482	22	0.403	29	0.356	30	0.316	30
					A	0.494	24	0.400	30	0.344	32	0.311	32
4.	1" p + 1" thermocole + 4½" brick + ½" p	..	1.5	Transfer	M	0.046	87	0.026	106	0.015	151	0.011	198
					A	0.043	90	0.024	110	0.014	154	0.009	202
				Int.Driv. point	M	0.581	21	0.390	34	0.329	35	0.299	36
					A	0.570	24	0.378	36	0.322	38	0.296	39

p = plaster. M = Matrix A' = Analytical A = Analogue

Fig. (5.1). From Fig. (5.1) it can be seen, that the agreement, between the measured and analogue predicted temperature, is good (within 3 per cent) throughout the daily cycle except at the initial hours.

5.3 Brick Wall with Surface Input

Roux (67) had investigated, how far the use of the analytical solutions developed, by Houghton et.al. (66) and Mackey and Wright (30) for non-steady state heat flow through materials with all their simplifying assumptions are justified for practical building problems. In his investigations a room with all the four sides made up of walls of brick whose physical properties, are given in Table (5.2).

Thickness (L) = 9.25 inches
Thermal resistance of the wall R = 1.44
Thermal capacity of the wall C = 18.0

The inside air temperature was kept constant by an air-conditioning system and outside and inside surface temperatures were measured. The inside surface co-efficient was taken 1.4 Btu/sq.ft/Hr/°F and assumed constant. This brick wall of 9.25 inches thickness, having an 'RC' value of 25.9 can be represented on the analogue by 8 lumps of 'T' network with sufficient accuracy. The transfer functions (amplitude decrement

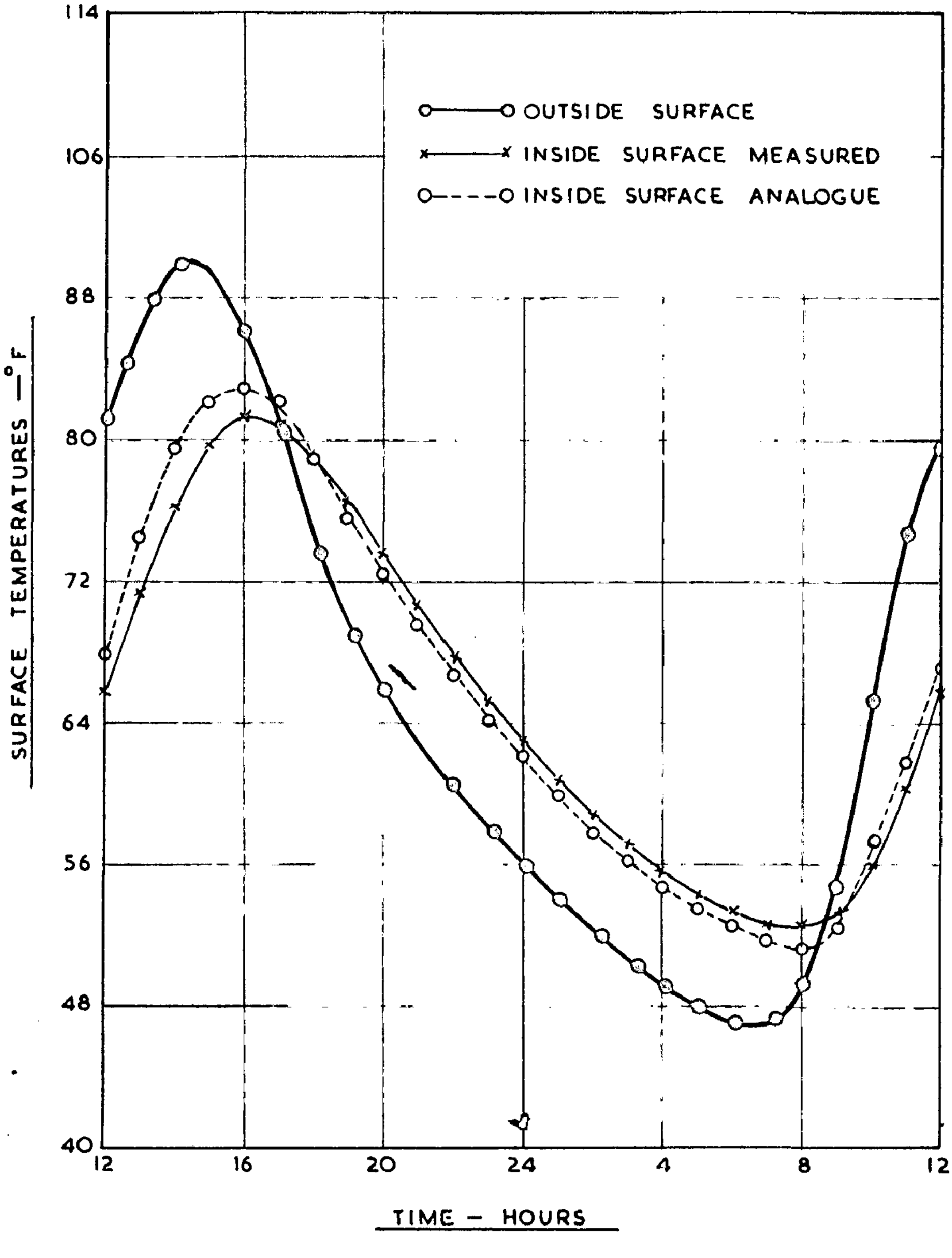

COMPARISION OF INSIDE SURFACE TEMPERATURES FOR A 4·26" THICK CONCRETE SLAB

FIG. 5·1

factor and phase lag) of the brick wall were determined by the analogue method, for the fundamental and three higher harmonics. These are given in Table (6.3) alongwith the computed values by the analytical methods.

The Fourier analysis of the outside surface temperatures for a north wall on a summer test day is given by

$$\begin{aligned} t_{os}\,(\tau) = 78.73 &+ 15.80 \sin (15\,t - 133^{\circ}10') \\ &+ 4.63 \sin (30\,t - 303^{\circ}53') \\ &+ 1.47 \sin (45\,t - 123^{\circ}57') \\ &+ 0.14 \sin (60\,t - 61^{\circ}41') \end{aligned} \qquad ..(3)$$

steady state component of the inside surface temperature is obtained from the equation

$$t_{is}\,(\text{mean}) = t_{ia} + U/h_i \left\{ t_{os}\,(\text{mean}) - t_{ia} \right\} \qquad ..(4)$$

The harmonic components of the inside surface temperature are obtained with the help of transfer functions previously determined.

The Fourier equation for the inside surface temperatures corresponding to the input (equation - 3) is then obtained as

$$\begin{aligned} t_{is}\,(\tau) = 72.32 &+ 2.53 \sin (15\,t - 233^{\circ}) \\ &+ 36.00 \sin (30\,t - 93^{\circ}) \\ &+ 0.066 \sin (45\,t - 309^{\circ}) \\ &+ 0.004 \sin (60\,t - 276^{\circ}) \end{aligned} \qquad ..(5)$$

The hourly variation of inside surface temperatures obtained by synthesising the equation (5) are compared with the measured and the theoretically computed temperatures in Fig. (5.2). It can be seen from the Fig. (5.2) that the agreement between the analogue and theoretically computed results is excellent throughout daily cycle, while the deviations between the analogue and measured values, are more in the initial hours.

5.4 Brick Wall with Sol-air Temperature Input

The above two comparisions are for a particular external boundary condition, viz., outside surface temperature as the input. For this purpose, the outside surface temperature variations are to be known. These are not readily available. In order to make theoretical and Analogue methods, practicable the external boundary conditions should be computable from the available weather data. Mackey and Wright (1) have introduced sol-air temperature concept, which can be computed from the known weather data. They have also provided theoretical solutions taking sol-air temperature as the external boundary condition. Roux (63) had made use of the same room (9.25 in. brick walls) for the verification of the theoretical solutions, with this sol-air temperature input. In

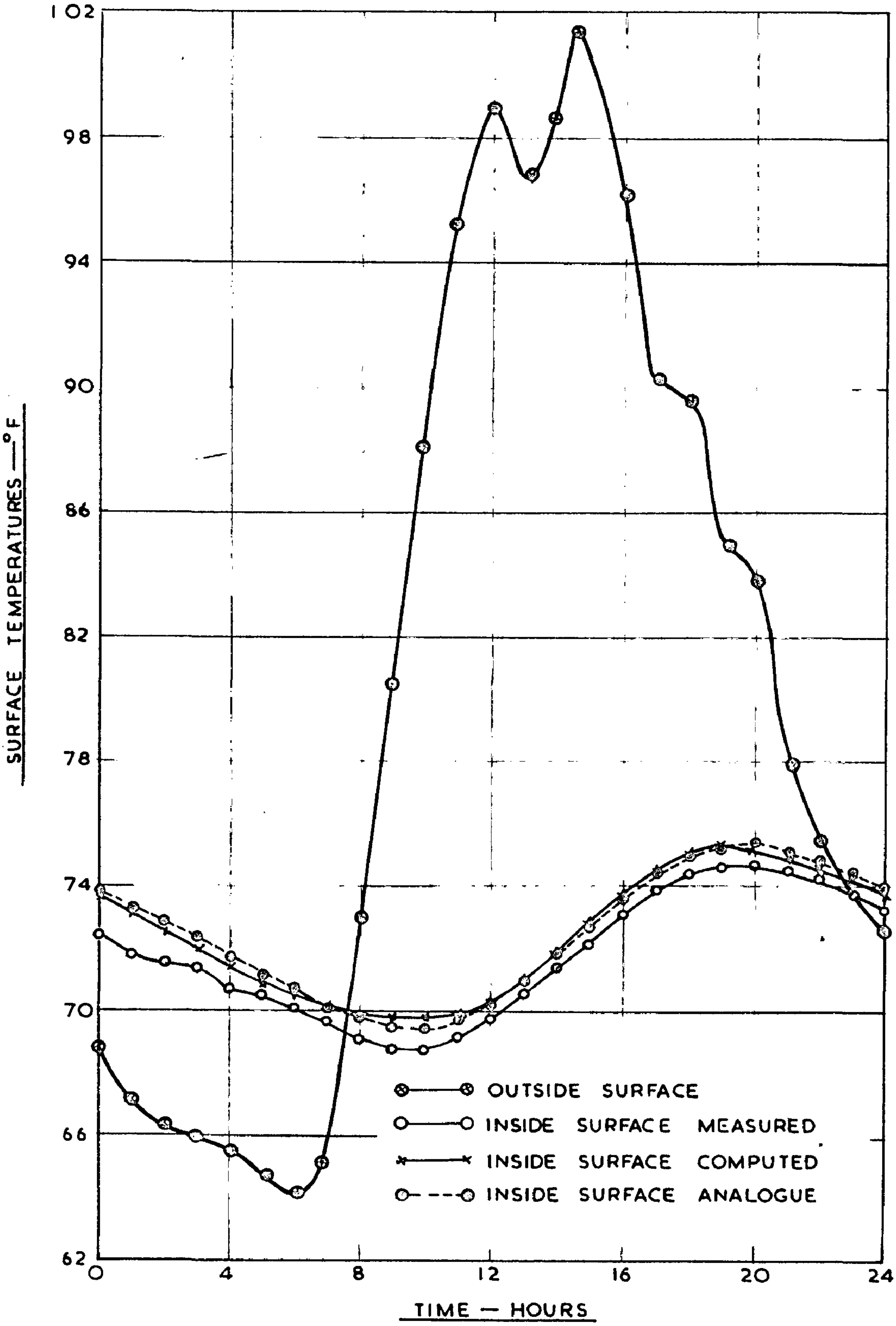

COMPARISION OF INSIDE SURFACE TEMPERATURES FOR A 9·25" THICK BRICK WALL

FIG. 5·2

this case the outside surface coefficient (h_o) is to be included in the analogue circuit. The outside and inside surface coefficients were taken as 1.6 and 1.7 Btu/sq.ft./Hr/^oF respectively. The transfer functions $\lambda_i \angle \phi_i (t_{is} / t_{sa})$ for this input boundary conditions will be different from the previous ones. These transfer functions determined by the analogue alongwith those theoretically computed are also given in table (5.3). The Fourier equation of the sol-air temperature for the experimental conditions is given by

$$\begin{aligned} t_{sa}(\tau) = 66.27 &+ 61.48 \;\; \text{Cos}\,(15\,t - 183^o31') \\ &+ 35.00 \;\; \text{Cos}\,(30\,t - 1^o8') \\ &+ 5.75 \;\; \text{Cos}\,(45\,t - 165^o30') \\ &+ 4.67 \;\; \text{Cos}\,(60\,t - 199^o25') \end{aligned} \quad ..(6)$$

The corresponding inside surface temperatures obtained, from the known 'U' value and the transfer functions, is given by equation (7)

$$\begin{aligned} t_{is}(\tau) = 68.70 &+ 4.9 \;\; \text{Cos}\,(15\,t - 293^o) \\ &+ 1.12 \;\; \text{Cos}\,(30\,t - 159^o) \\ &+ 0.098 \;\; \text{Cos}\,(45\,t - 7^o) \\ &+ 0.047 \;\; \text{Cos}\,(60\,t - 69^o) \end{aligned} \quad ..(7)$$

The time temperature variations obtained by the analogue method and experimentally measured ones are compared in Fig. (5.3).

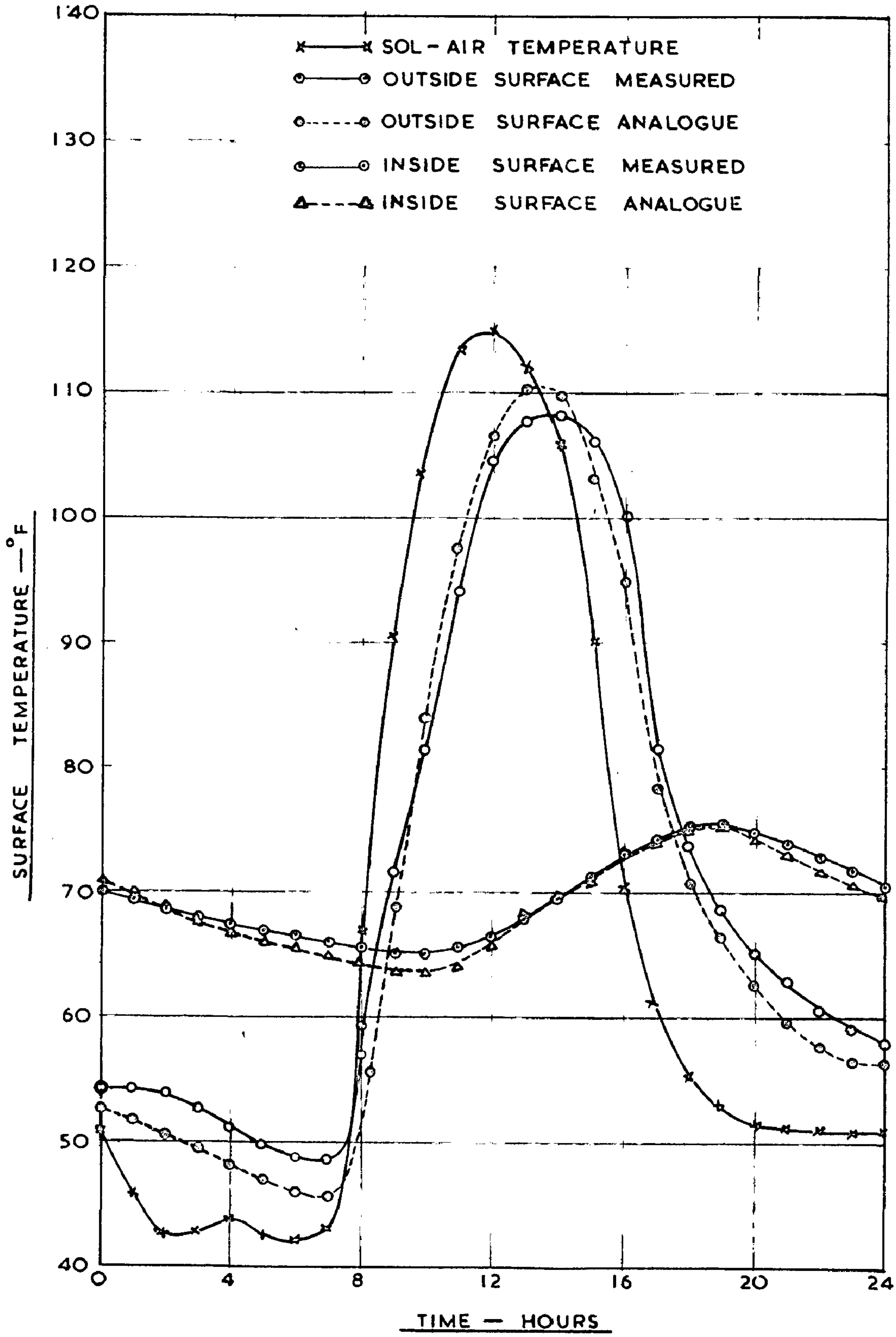

COMPARISION OF OUTSIDE AND INSIDE SURFACE TEMPERATURES FOR A 9·25" THICK BRICK WALL WITH SOL-AIR INPUT

FIG. 5·3

It is also possible to determine analogically the outside surface temperatures of a building surface for a given sol-air temperature and outside surface coefficient (h_o). For this purpose, external driving point transfer functions t_{os}/t_{sa} i.e., $\lambda_o \angle \phi_o$ are to be determined for the fundamental and higher harmonics. The mean outside surface temperature is obtained by the equation

$$t_{os}\ (\text{mean}) = t_{sa}\ (\text{mean}) - U/h_o \left\{ t_{sa}\ (\text{mean}) - t_{ia} \right\} \qquad ..(8)$$

The external driving point transfer functions determined by the analogue are given in Table (5.5). The fourier representation of the outside surface temperatures corresponding to the given sol-air temperature (equation - 6) for the brick wall is obtained as

$$\begin{aligned} t_{os}\ (\tau) = 67.10 &+ 27.6\ \text{Cos}\ (15\ t - 207^\circ) \\ &+ 13.3\ \text{Cos}\ (30\ t - 31^\circ) \\ &+ 1.9\ \text{Cos}\ (45\ t - 197^\circ) \\ &+ 1.46\ \text{Cos}\ (60\ t - 231^\circ) \end{aligned} \qquad ..(9)$$

The comparision of the analogically determined and experimentally measured outside surface temperatures are also made in the above Fig. (5.3).

The deviations between the measured and analogue temperatures for the outside surface are greater than those for the inside surface. This may be attributed to two factors, namely (i) as 'h_o' is directly dependent on the outside weather conditions, is liable to larger variations with time, than 'h_i', and (ii) the sol-air temperatures as suggested by Mackey and Wright need correction for low temperature radiation exchange taking place between the external surface and its surroundings. The computational methods employed (1) for low temperature radiation estimation are empirical and need improvement.

Inspite of these drawbacks the overall agreement between the measured and analogue predicted outside surface temperatures may be considered as quite satisfactory, in dealing with problems of day to day engineering practice.

5.8 Composite Wall with External Surface Input and Indoor Air Temperature Variable

The above three instances are for homogeneous constructions. In practice many building elements are made of composite sections. The internal boundary condition, of constant indoor air temperature, is true for air conditioned enclosures only. But the main bulk of buildings are unconditioned and the indoor air temperatures fluctuate periodically. Hence a more general case of a composite construction with variable indoor air temperature is also included for the verification of the Analogue.

Raychoudhri et. al. (69) have reported experimental studies on the effect of walls and roofs (composite) on the indoor air temperatures for unconditioned rooms. The wall chosen for the present study has the following constructional details :-

1" plaster, 1" thermocole, 4½" brick, ½" plaster.

The order of the layers being from outside to inside. The physical properties of the materials of each layer are given in Table (5.3). The equations of the external surface temperatures and the indoor air temperatures which form the boundary conditions, are given as

i) outside surface temperatures

$$t_{os}(\tau) = 105.5 + 21.33 \cos(15t - 52^\circ 31') + 8.41 \cos(30t - 100^\circ 42') + 4.10 \cos(15t - 185^\circ 24') + 2.12 \cos(60t - 247^\circ 24') \qquad ..(10)$$

ii) indoor air temperatures

$$t_{ia}(\tau) = 83.88 + 3.67 \cos(15t - 125^\circ) + 0.43 \cos(30t - 169^\circ 12') + 0.003 \cos(45t - 247^\circ) + 0.14 \cos(60t - 260^\circ) \qquad ..(11)$$

In representing the composite wall on the Analogue, each homogeneous layer, is represented by the number of lumps (based on their RC values) as per earlier recommendations. Inside surface coefficient is taken as 1.5 Btu/Sq.ft./Hr/^{o}F and assumed to be constant.

For a boundary condition where air temperatures on either side vary, the problem can be treated as consisting of two superposed parts, namely (i) outside air or surface temperature is variable, with a constant indoor air temperature, and (ii) indoor air temperature is variable with constant outside temperature. The actual inside surface temperature variation is then obtained by the super position of the solutions of the two parts. Hence not only the usual transfer functions $\lambda_i \angle -\phi_i$ i.e., (t_{is}/t_{os}) but also the internal driving point transfer function $\lambda'_i \angle -\phi'_i$ i.e., (t_{is}/t_{ia}) is required. These two sets of transfer functions are determined on the Analogue and given in Table (5.3). The equation for the inside surface temperature in terms of the boundary variations and transfer functions can be expressed as

$$t_{is}\,(\tau) = t_{is}\,(\text{mean}) + \sum_{n=0}^{\infty} \lambda_{in} t_{os\,n} \cos\,(\omega_n t - \gamma_n - \phi_{in}) + \lambda'_{in}\; t_{ia\,n} \cos\,(\omega_n t - \xi_n - \phi'_{in}) \quad \ldots(12)$$

where $t_{is}\,(\text{mean}) = t_{ia}\,(\text{mean}) + U/h_i \left\{ t_{os}(\text{mean}) - t_{ia}(\text{mean}) \right\}$

Substituting the numerical values for this present example, the inside surface temperature equation is

$$t_{is}(\tau) = 97.80 + \begin{array}{l} 0.79 \cos(15t - 123^{\circ}) \\ +0.23 \cos(30t - 209^{\circ}) \\ +0.075 \cos(45t - 310^{\circ}) \\ +0.025 \cos(60t - 58^{\circ}) \\ \\ +2.18 \cos(15t - 144^{\circ}) \\ +0.31 \cos(30t - 203^{\circ}) \\ +0.09 \cos(45t - 302^{\circ}) \\ +0.056 \cos(60t - 200^{\circ}) \end{array} \quad ..(13)$$

The hourly variations of the inside surface temperatures as obtained by synthesising the equation (13) and compared with the measured values in Fig. (5.4). It can be seen from Fig. (5.4) that the analogue predictions agree closely with the measured temperatures as in the previous cases within 3 to 4 per cent. In the above comparisions it is expected that the deviations between the analogue predicted and theoretically computed values to be minimum as all the simplifying assumptions made in theoretical computations, apply to the analogue also. The deviations between the measured and the theoretical values may be attributed to the following assumptions made in the theoretical solution :-

i) The surface coefficients are taken as of a constant value, though in practice they vary to a certain extent.

ii) The radiation exchange at the inside surface has not been separately treated, but the inside surface coefficient is taken as the combined radiation and convection coefficient.

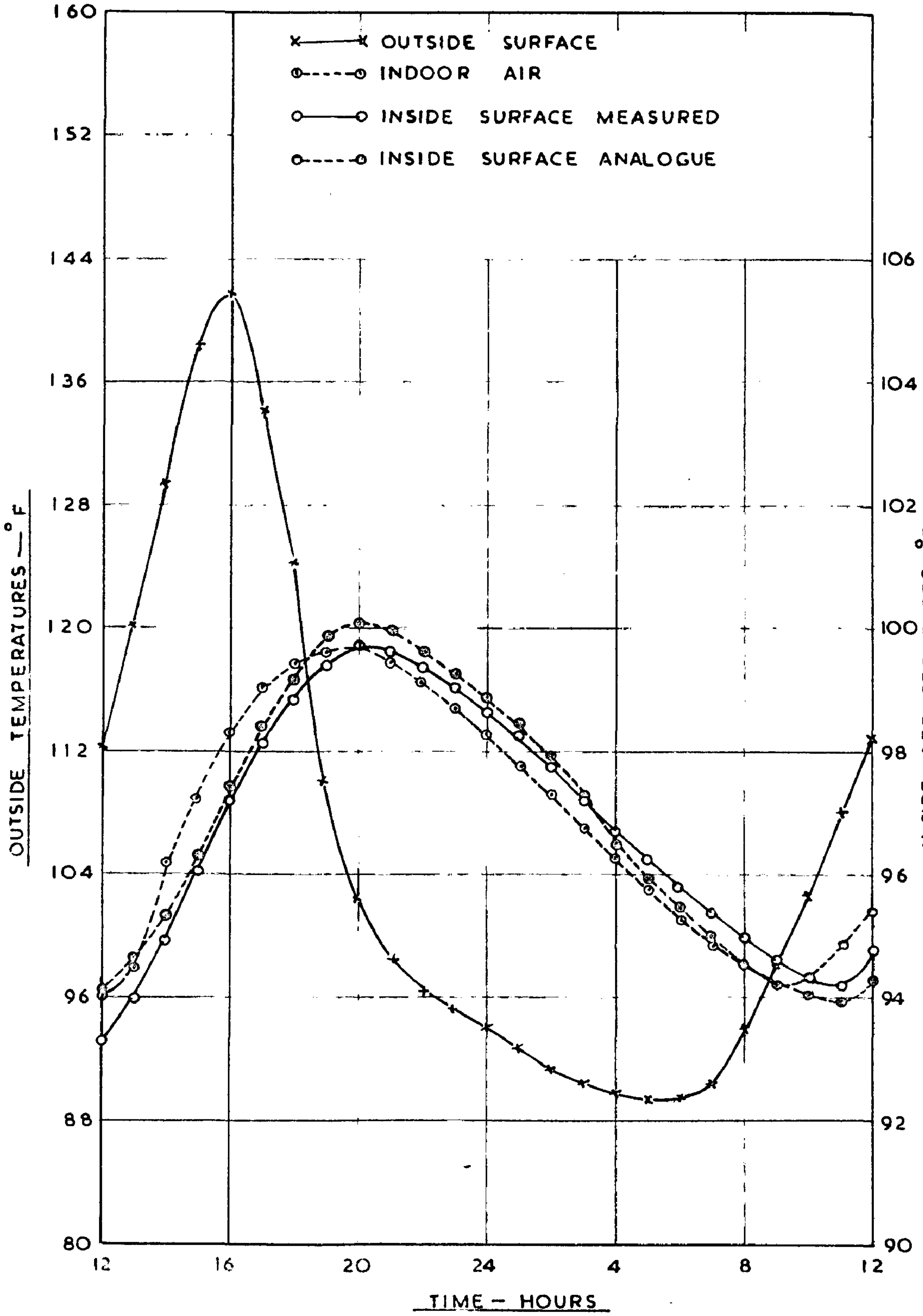

COMPARISION OF INSIDE SURFACE TEMPERATURES FOR A COMPOSITE WALL WITH VARIABLE INDOOR AIR TEMPERATURES

FIG. 5·4

In other words all the heat transfer from the inside surface to the indoor air is taking place directly through the film conductance, duly corrected for radiation transfer.

iii) The sol-air or outside surface temperature wave forms, are identical on two successive days. This assumption is not strictly true. Non-conformity of this assumption is expected to introduce increased deviations in the first few hours corresponding to the time lag period.

However, all the above simplifying assumptions made in the theory and the analogue errors dealt in Chapter (4), combinedly do not exceed 3 to 4 per cent for all practical problems. The predictions of periodic temperatures within 5 per cent of the actual conditions can be considered as more than sufficient for engineering accuracies.

The above comparisions, which cover the commonly occurring boundary conditions and types of constructions, amply justify the validity of adopting the analogue method in the proposed form, for studying the periodic heat flow through building elements of different constructions and under different climatic conditions.

C H A P T E R 6

THERMAL SYSTEM (TRANSFER AND DRIVING POINT) FUNCTIONS OF HOMOGENEOUS BUILDING ELEMENTS

C H A P T E R 6

THERMAL SYSTEM (TRANSFER AND DRIVING POINT) FUNCTIONS OF HOMOGENEOUS BUILDING ELEMENTS

6.1 Introduction

Comprehensive data on the thermal characteristics which completely define the thermal behaviour of building elements, under periodic heat flow and natural boundary conditions, are not as yet available. It has been shown (70) that a set of three system functions, i.e., one transfer and two driving point functions will completely characterise a four terminal network. Von Gorcum (23) and later Marmot (27) Muncey (25) Pipes (26) have shown that a homogeneous slab can be treated as a passive four terminal (two pair) two element (R and C) network and the same mathematical methods employed for solving such electrical network problems can also be applied to solve the problems of periodic heat flow through building elements. The network system functions, developed for electrical problems can profitably be used for the analogous thermal system functions. The computation of these functions for sinusoidal excitations, employing the well established mathematical methods used in electrical problems (Laplace transforms, Symbolic Calculus, Matrix) are hardly any simpler than analytical methods used for thermal problems. The most promising approach lies in the possibility of determining those system functions experimentally by the electrical analogue method which obviates complex calculations.

6.2 Thermal System Functions

The system functions depend not only on the network elements but also on its nature of termination. For a building element the surface heat transfer coefficients which are represented by pure resistances, form the termination on both ends. The boundary conditions, that are encountered in periodic heat flow problems of buildings and the corresponding system functions are derived in terms of general circuit parameters and given in Appendix (II). The three thermal functions determined by the analogue method are :-

i) Transfer temperature amplitude ratio

$$\lambda_i \angle -\phi_i \ i.e \left(\frac{t_{io}}{t_{oa}}\right) \quad t_{ia} = 0$$

ii) External driving point temperature amplitude ratio

$$\lambda_o \angle -\phi_o \ i.e \left(\frac{t_{oo}}{t_{oa}}\right) \quad t_{ia} = 0$$

and iii) Internal driving point temperature amplitude ratio

$$\lambda_i' \angle -\phi_i' \ i.e \left(\frac{t_{io}}{t_{ia}}\right) \quad t_{oa} = 0$$

As these functions are vector quantities, for each function two quantities viz., the amplitude decrement and phase lag angle have to be measured. The procedure followed for the determination of these quantities have been described in Chapter 3.

Though the transfer and internal driving point admittance functions are of direct significance, in the heat flow calculations, the temperature amplitude ratios were chosen for the analogue determination, because these are easily measured. However, the admittance functions can be obtained from the following relationships between them.

i) Transfer admittance function

$$Y_i \angle -\psi i = \frac{q_{ia}}{t_{oa}} \qquad t_{ia} = 0$$

$$Y_i \angle -\psi i = h_i \lambda i \angle -\phi i \qquad .. (1)$$

ii) Internal driving point admittance function

$$Y_i' \angle \psi' i = \frac{q_{ia}}{t_{ia}} \qquad t_{oa} = 0$$

$$Y_i' \angle \psi' i = h_i (1 - \lambda' i \angle -\phi' i) \qquad .. (2)$$

The relation between these transfer and driving point thermal system functions and the generalised transfer matrix parameters have also been derived and presented in Appendix (II).

Once these thermal functions are determined all other desired thermal quantities for a building element, such as the surface temperatures ($\overrightarrow{t_{os}}$ and $\overrightarrow{t_{is}}$) and the heat fluxes entering and leaving ($\overrightarrow{q_{os}}$ and $\overrightarrow{q_{is}}$) can be obtained. In practice the periodic driving temperatures are not simple sinusoidals, but can be expressed as a Fourier series. However, these can be adequately described by the fundamental and a few harmonics.

Thermal system functions of different types of materials commonly used in building practice, were determined for the fundamental and the first three harmonics on the electrical network analogue. As this data is of considerable practical utility, these along with their 'U' values are presented in Tabular form (Table 2) for reference purposes in Appendix (III). The physical properties, the characteristic thermal impedances and the propagation constants of these materials are also given therein (Table 1).

An inspection of Table (1) of Appendix (III) indicates that i) dense materials have lower characteristic impedance (Z_c) and constants of propagation, and their variation from material to material is not significant; and ii) light weight materials have higher characteristic impedance and these vary considerably from material to material.

The following inferences are made from an analysis of the thermal system function data given in Table (2) of Appendix (III).

6.3 $\lambda_o \angle -\phi_o$ - External Driving Point Function

This function enables one to estimate the outside surface temperatures attained by different materials for a known sol-air temperature excitation. The magnitude of λo depends upon the coefficient of thermal absorption 'p' $\left(\sqrt{\frac{\omega C}{R}}\right)$ of the material. Materials with high 'p' value, will have lower λo and larger ϕo for a given thickness and vice versa. For a given material and frequency, 'p' is independent of thickness, whereas λo and ϕo depend on the thickness as well. With the increase of thickness both R and C will increase in the same proportion and the ratio C/R and hence 'p' is unaltered, for a given frequency. λo and ϕo depend on R and C and also on the ratio of the material resistance (R) to the surface resistances (R_o and R_i). Hence λo and ϕo depend on the thickness of the material. For higher harmonics the magnitude of λo decreases while ϕo increases, slightly. Light weight materials having high characteristic impedance (Z_c) will have higher λo and lower ϕo than for dense materials.

6.4 $\lambda_i \angle -\phi_i$ - Transfer Function

i) The magnitude of λi will depend not only upon 'RC' but also on the ratios of R/R_i, R_o/R and R_o/R_i.

ii) For a given thickness materials having large 'p' will have high phase lags and vice versa.

iii) The decrease of λi and increase of ϕi are more marked with the increase of thickness for dense materials than for light materials.

iv) The effect of harmonics on λi and ϕi is more pronounced than on λo and ϕo. Higher harmonics have no significant effect on λi and ϕi for very thin sections, such as glass panes, plasters, G.I. and A.C. sheets. (These have small C and R values).

6.5 $\lambda'_i \angle -\phi'_i$ - Internal Driving Point Function

i) The variation of $\lambda' i$ and $\phi' i$ with 'p' and thickness are similar to that of λo and ϕo.

ii) For a given material and thickness λi will be lower than the corresponding λo. This is because 'h_i' is less than 'h_o'.

iii) When both the surface coefficients (h_o and h_i) are equal, λo and ϕo will also be equal to $\lambda' i$ and $\phi' i$ respectively.

The over all decrement factor (λi) is the product of decrement factors of the outside surface resistance (λo) and the decrement factor of the material (λm).

$$i.e\ \lambda_i \angle{-\phi_i} = \lambda_o \angle{-\phi_o} \times \lambda_m \angle{-\phi_m} \quad .. (3)$$

Hence the decrement factor of the material or for the external surface input (i.e., without considering the outside surface coefficient) is obtained from the above equation as

$$\lambda m \ \angle{-\phi m} = \frac{\lambda i}{\lambda o} \ \angle{-(\phi i - \phi o)} \quad .. (4)$$

6.6 <u>Thermal Time Constant (RC) Versus Transfer Function</u>

Some investigators (71) (73) have attempted to correlate the ratio of thermal capacity (C) and the thermal conductance (K/L) i.e., (RC) of a building element with the amplitude decrement factor (λi) and phase lag angle (ϕi) and suggest that the thermal time constant (RC) can be taken as a single parameter to characterise the non-steady state behaviour of a homogeneous building element. This is true only when the material without surface resistances is considered, as shown in Fig. (6.1). In order to find out how far this relationship holds good with the inclusion of surface resistances (which is necessary and essential when one considers the behaviour of a material under natural conditions) a graph is plotted between transfer function (fundamental) $\lambda_1 \angle -\phi_1$ with surface resistance heat transfer coefficients h_o and h_1 as 3.6 and 1.5 Btu/Sq.ft./Hr/°F and 'RC' in Fig. (6.2). This set of curves clearly indicate that such a correlation does not hold good, for these boundary conditions. There is a great scatter between points representing different materials and no single curve could be drawn. It can further be seen that each material forms a separate curve by itself and the curves of dense materials are far separated from those of the insulating materials. Thus two materials having same RC value but widely different R may very well have λ_1 values differing from one another by a factor of even 3 or more. These large variations are due to the fact that λ_1 depends not only on RC but also on the ratios of R/R_1, R_o/R and R_o/R_1. This is evident from the equation 14 of Appendix II.

6.7 Effect of Thickness on Transfer and Driving Point Functions

A graph of the fundamental transfer function ($\lambda_1 \angle -\phi_1$) versus thickness; plotted for different

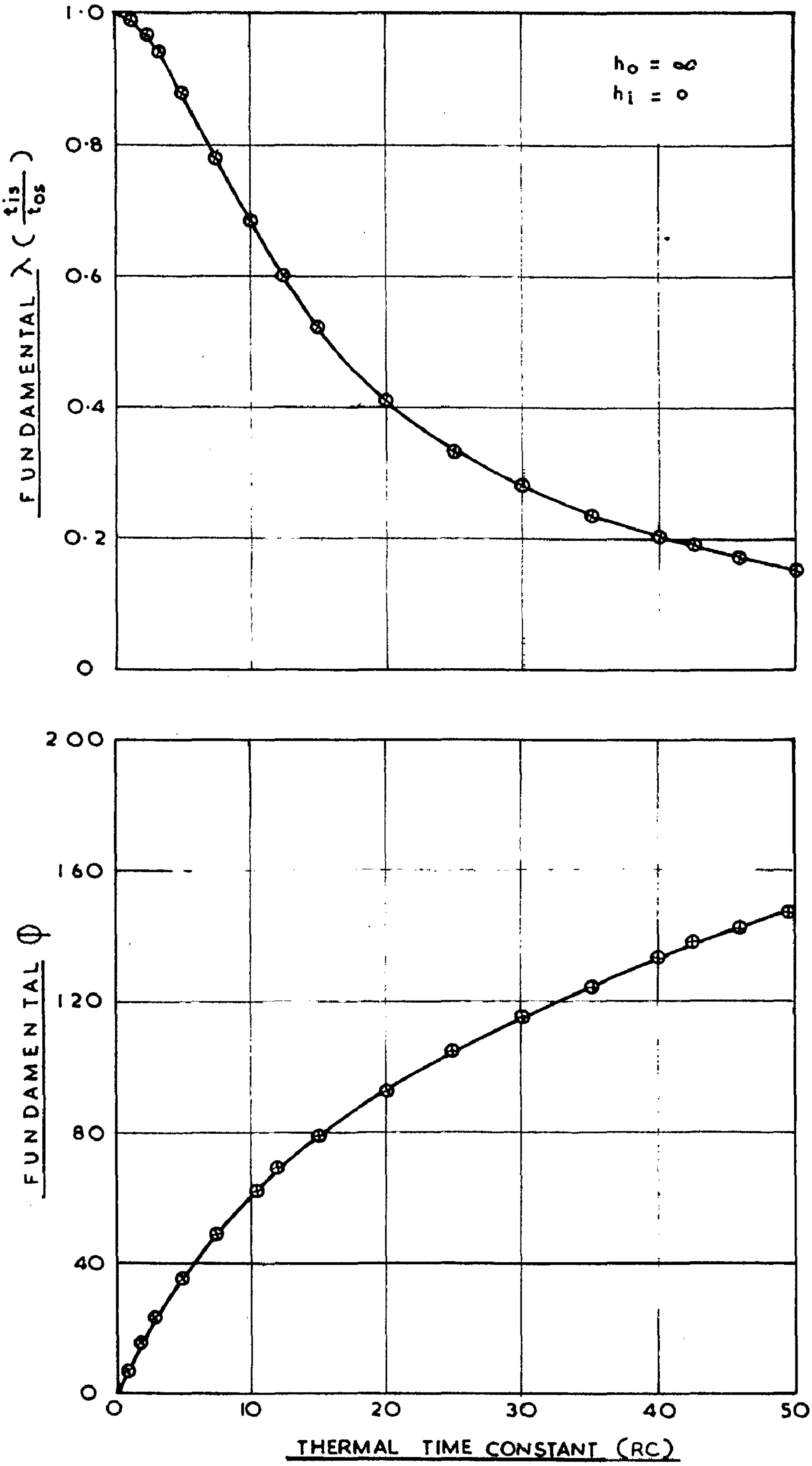

FIG 6·1. THERMAL TIME CONSTANT VERSUS λ AND ϕ

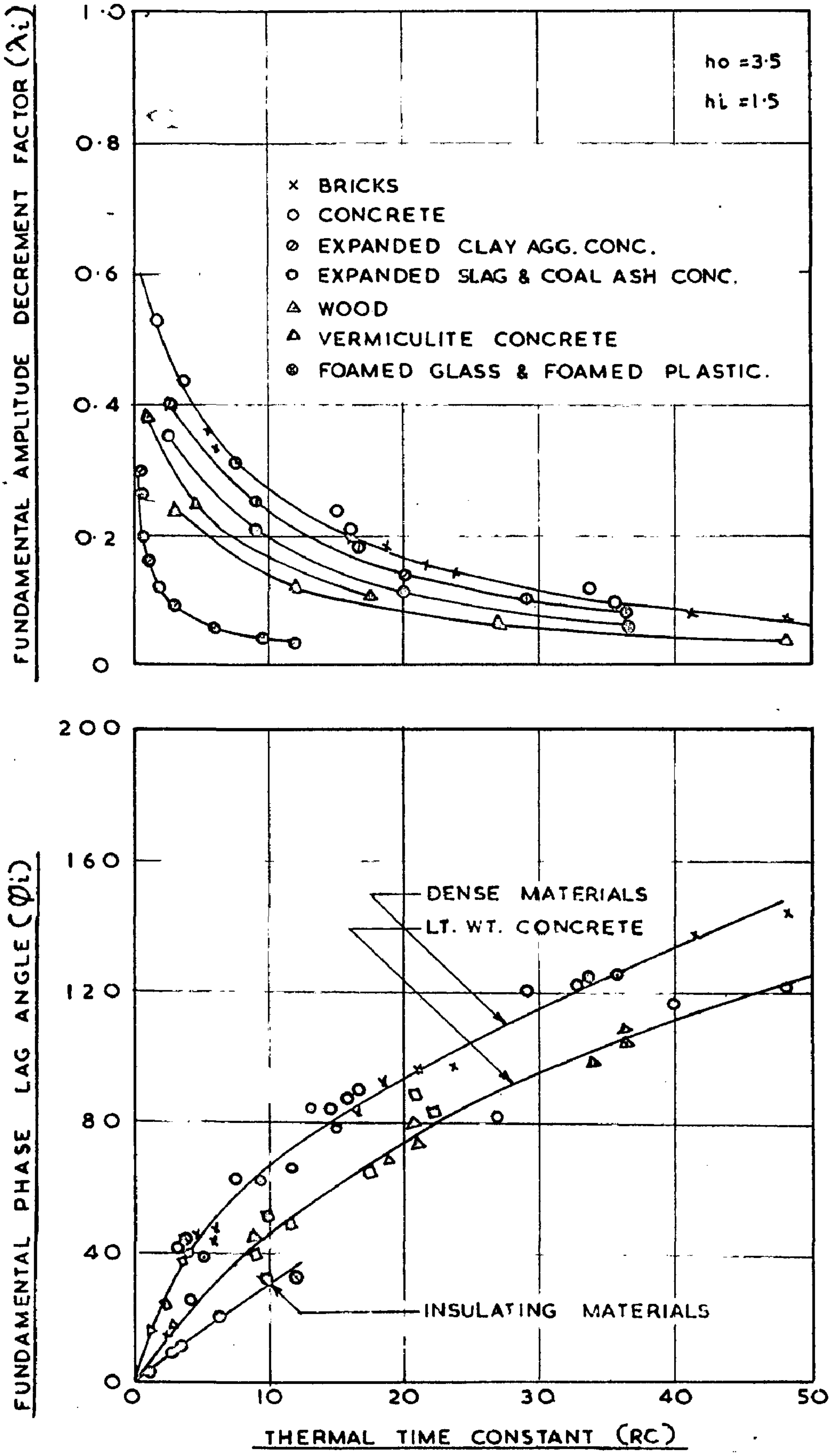

FIG.6·2. THERMAL TIME CONSTANT VERSUS λ_i AND φ_i

materials is shown in Fig. (6.3). Here also each material behaves uniquely and no single curve will satisfy all the materials. For any one material the relation between thickness and phase lag is practically a straight line. The slope of these lines are different for different materials. For any material an increase of thickness will result in an increase of RC and R/R_i and R/R_o. As this increase is different for different materials the variation in λi and ϕi with thickness will also be widely different.

Danter (73) has shown that the ratio of alternative heat transmittance (which is identical with the transfer admittance function $Y i$) and the steady state heat transmittance (U) i.e. $Y i/U$, versus thickness, provide a good single correlation curve. In his studies Danter considered only five materials with densities ranging from 43 to 155 Lb/Cu.ft. and thermal conductivities ranging from 1.11 to 11.1 Btu in/Sq.ft./Hr/^{o}F. The validity of these conclusions were checked for a wider range of materials. For this purpose about twenty materials covering almost all possible values of density, thermal capacity (C) and thermal resistance (R) were included in this study. The transfer admittance functions $Y_i \angle \psi i$ were obtained by multiplying the analogically determined transfer function $\lambda i \angle \phi i$ with h_i.

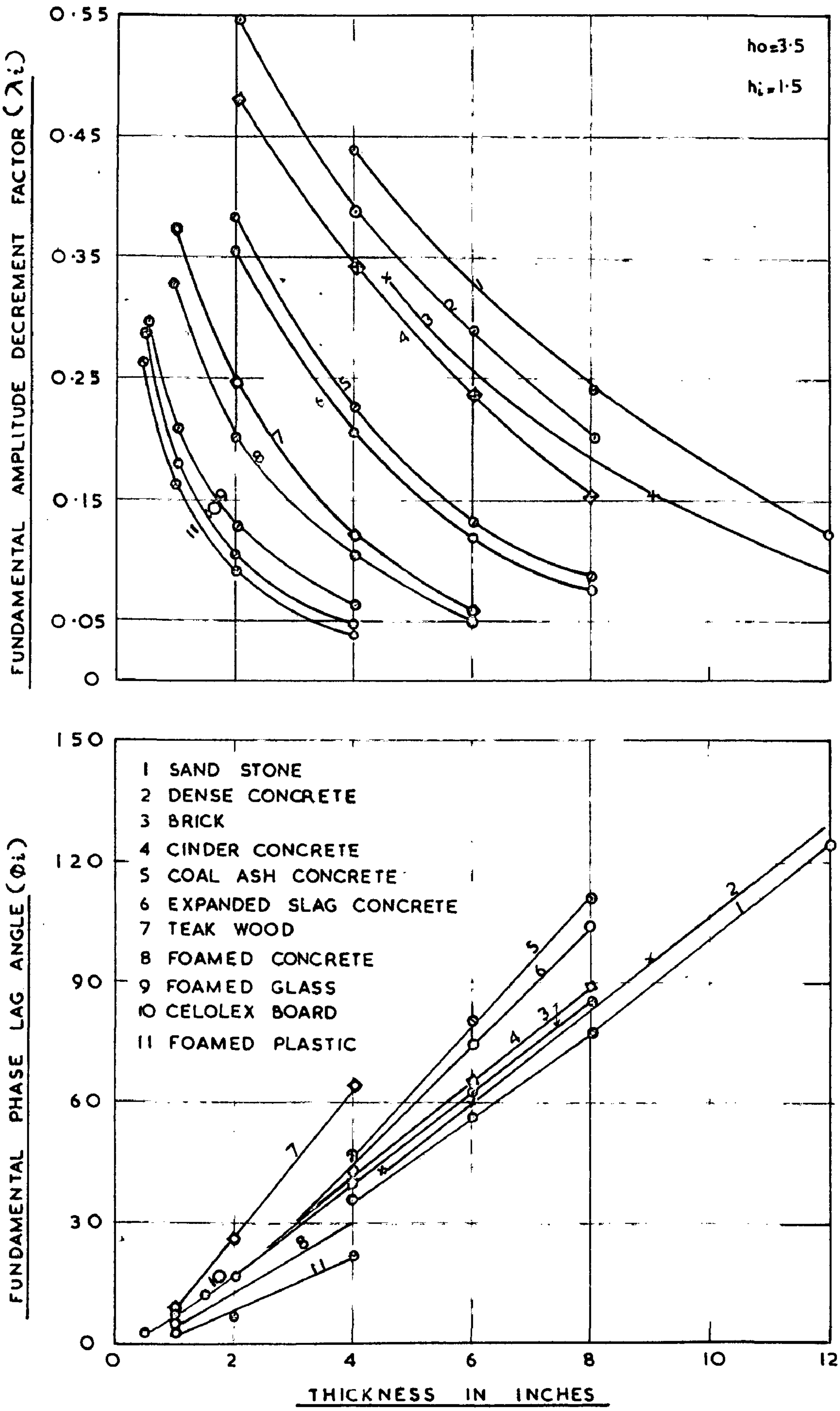

FIG.6·3 THICKNESS VERSUS λi AND φi

Taking the values of fundamental Y_1/U and ϕ_1 as ordinates and thickness as abscissa, graphs were plotted and shown in Fig. (6.4). All the materials irrespective of their physical properties fairly fit in one single curve, although the deviations of individual points are larger than those of Dantor. The main advantage of this relationship is from a knowledge of steady state 'U' value and thickness of a material, the periodic transfer admittance functions are directly obtained. These correlations were checked for three higher harmonics and the shape of the curves are found to be similar, to those of the fundamental.

It will be of interest to find out whether similar relationships could be obtained for driving point admittance functions as well. The external and internal driving point admittance functions i.e., $Y_o \angle \psi_o$ and $Y_i' \angle \psi_i'$ were obtained from the analogically determined driving point temperature amplitude ratio functions ($\lambda_o \angle -\phi_o$ and $\lambda_i' \angle -\phi_i'$) from the equations (5) and (6) respectively.

$$Y_o \angle \psi_o = h_o (1 - \lambda_o \angle -\phi_o) \qquad \text{.. (5)}$$

and $$Y_i' \angle \psi_i' = h_i (1 - \lambda_i' \angle -\phi_i') \qquad \text{.. (6)}$$

The relation between Y_o/U and Y_i'/U and thickness is shown in Figs. (6.5 and 6.6). It can be seen that

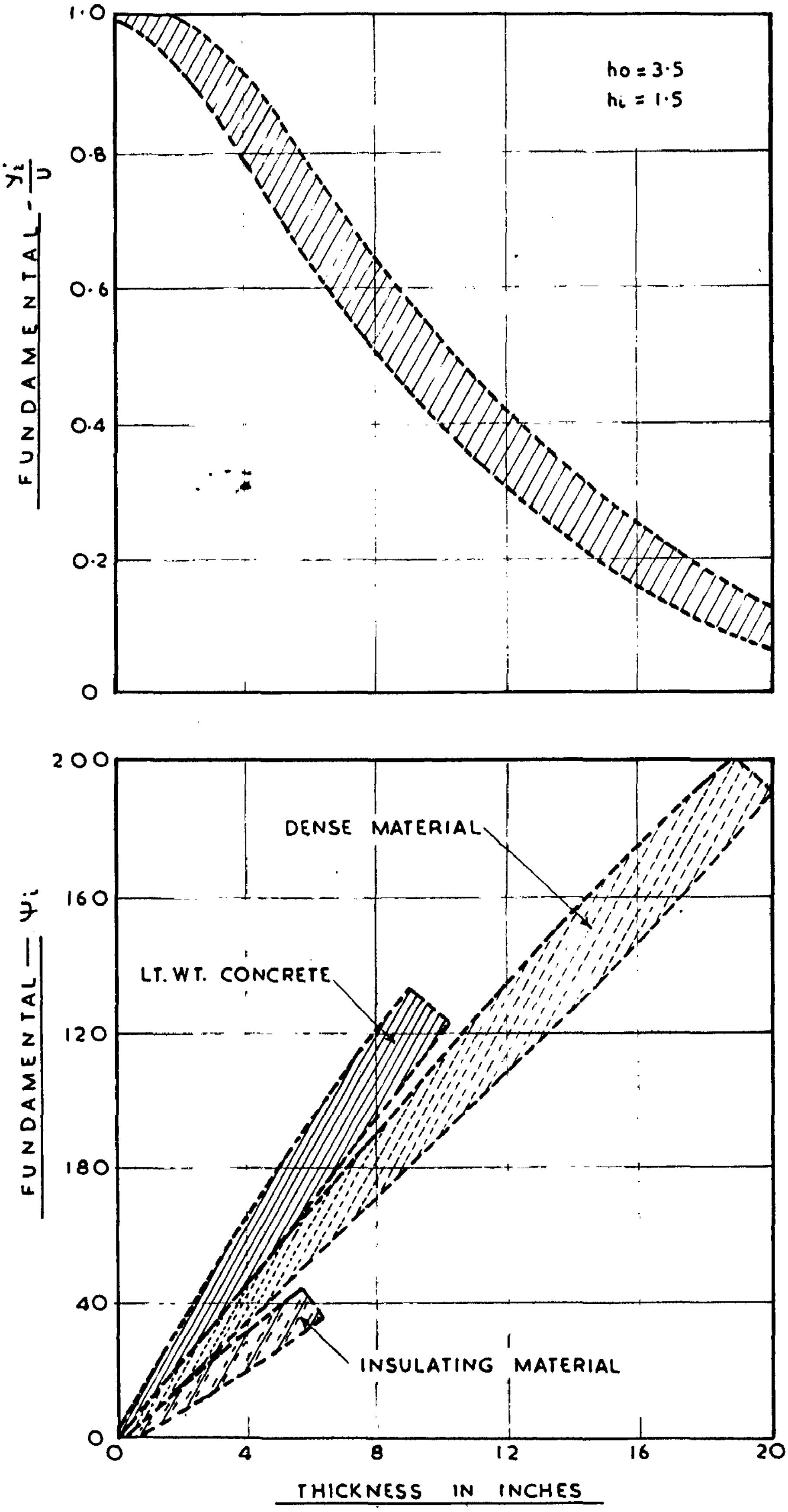

FIG.6·4 THICKNESS VERSUS $\frac{y_i}{u}$ AND ψ_i

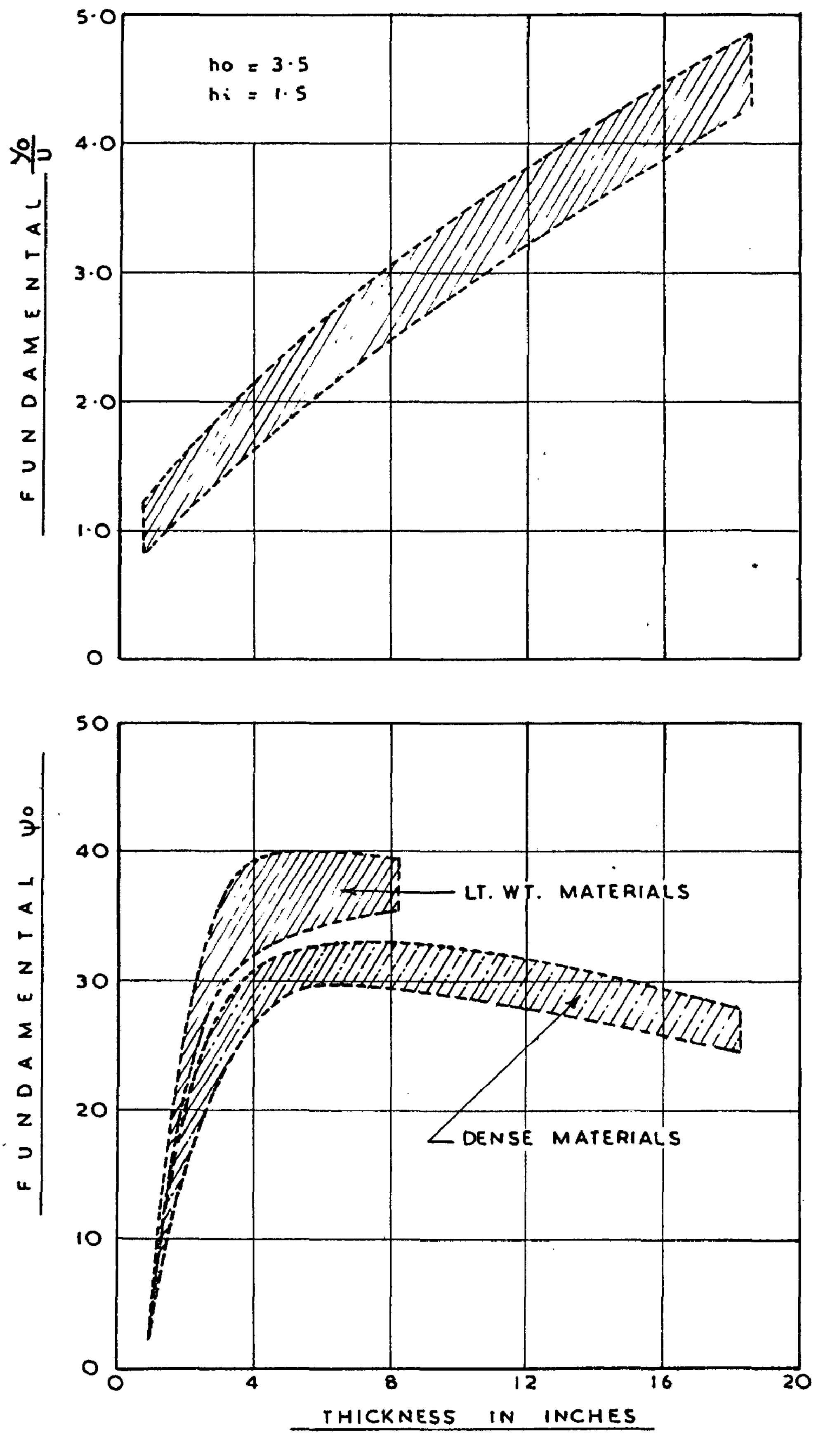

FIG. 6·5 THICKNESS VERSUS $\frac{y_o}{U}$ AND ψ_o

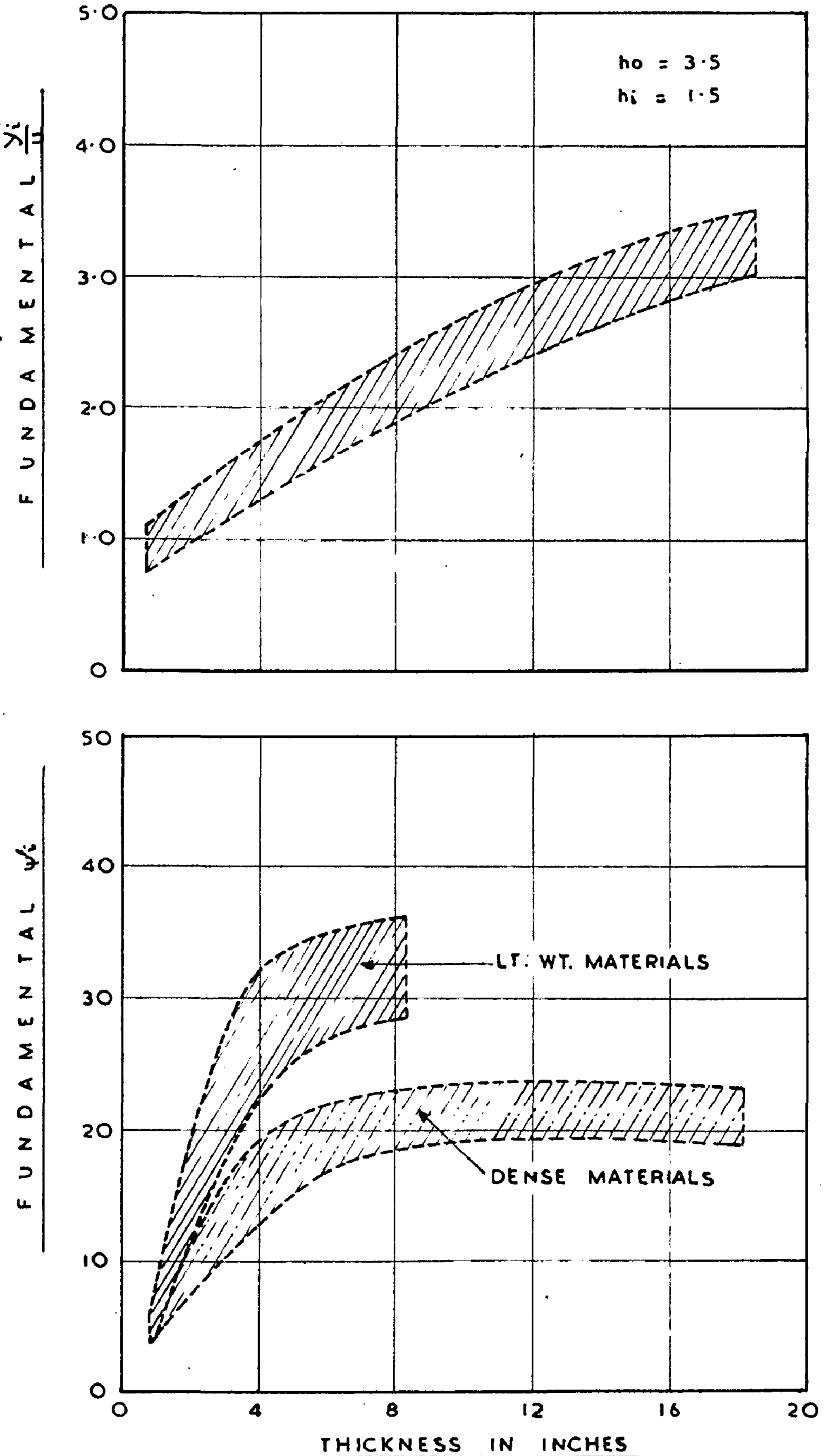

FIG. 6·6 THICKNESS VERSUS $\frac{y_i'}{U}$ AND Ψ_i'

these also give a similar correlation (i.e., all the materials represented by a single mean curve) but deviations of the individual points from the mean curve are much larger. It can further be noted that the trend of these curves is ascending i.e., Y_0/U and Y_1'/U increase with the increase of thickness, in contrast to that of the curve in Fig. (6.4) where the curve is a descending one i.e., Y_1/U decreases with the increase of thickness.

In all the three cases the phase angle versus thickness did not yield a single curve correction. Each class of materials give one line.

6.8 Variation of Amplitude Decrement and Phase Inside the Material

The progressive damping and phase shift of a temperature wave, while it advances through a homogeneous material depends on the characteristics of the material. These can be obtained by determining the amplitude decrement factors and phase lag angles at different points inside the material. The analogue is convenient for this purpose as the lumping points are accessible for making these measurements. The amplitude decrement factors and phase lag angles were measured for different types of materials for the fundamental and higher harmonics. The fundamental values shown in Fig. (6.7) is a typical representation.

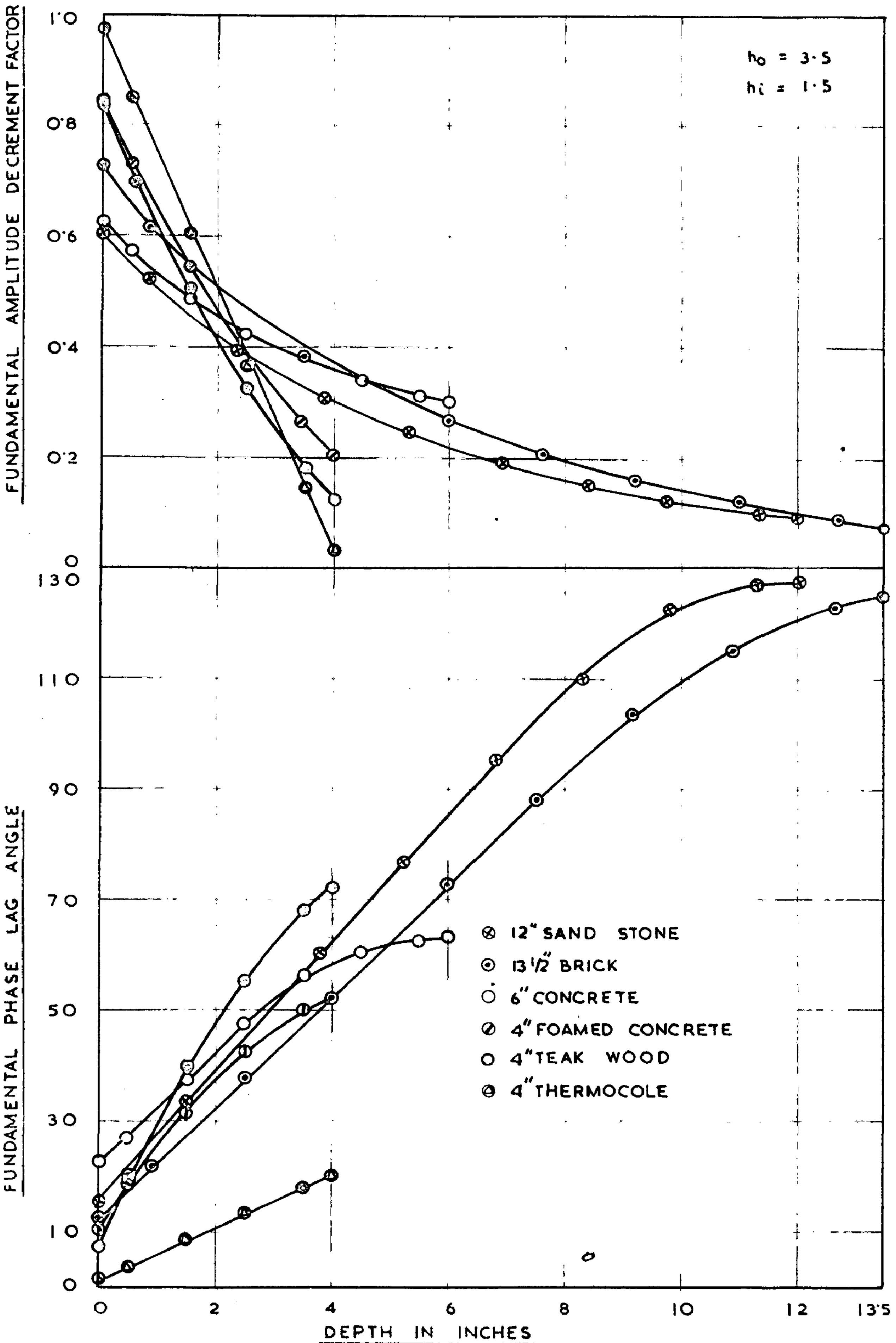

G. 6·7 VARIATION OF AMPLITUDE DECREMENT AND PHASE LAG WITH DEPTH

The general nature of the curves are similar for higher harmonics though the actual values are different. The decrease in λi for higher harmonics is not appreciable for insulating materials as compared to dense materials.

The drop in λi with depth is exponential for dense materials except at the boundaries whereas for insulating materials this tends to be a straight line with a steep slope. The increase in phase angle (ϕ) with depth is practically a straight line throughout except for the points approaching the other boundary.

6.9 Generalised Charts for Transfer and Driving Point Functions

In the Table (3) of Appendix III the thermal function data are given for most of the commonly used homogeneous building materials with different thicknesses. For these studies, the thermal capacity (C) and thermal resistance (R) were obtained from the average value of the physical properties of the materials listed in Table (1) of the same Appendix. As these depend upon many factors, wide variations of these properties (for the same type of material) are to be expected in practice. These will impose limitations on the use, the data presented. They may be taken only as indicative average values, but for any specific material the precise transfer and driving point functions have to be determined every time experimentally. If generalised charts, relating those thermal functions and the physical properties of materials, are available, the above limitations will be overcome and the data will be of greater utility.

Mackey and Wright had presented one such set of charts for λi and ϕi as functions of thermal conductance (K/L) and the specific thermal absorption coefficient ($K\rho s$). These were drawn for a fixed values of h_o and h_i, of 4.0 and 1.5 Btu/sq.ft./Hr/^{o}F respectively. These charts are useful only for the estimation of fabric cooling loads of air conditioned buildings. However, for a complete description of the thermal behaviour of a building element, three thermal system functions namely one transfer function and two driving point (external and internal) functions, are required. Further, the surface heat transfer coefficients for internal walls and intermediate floors will be different from those of the external building elements. As the overall thermal system functions are affected by the surface coefficients, the above charts of Mackey and Wright will not be applicable for internal building elements like partitions.

Roux had found (63) that the most suitable values for the outside and inside surface heat transfer coefficients for South African climatic conditions were 3.5 and 1.5 Btu/sq.ft./Hr/°F respectively. These values are more appropriate for India, because South African conditions are close to Indian climatic conditions.

Five sets of such generalised thermal function charts are shown in Figs. (6.8 .. through 6.12). In each chart a family of curves one for each ..ω value ranging from 0.1 to 250, with thermal resistance (R) as the abscissa (from 0.1 to 10) and the appropriate fundamental thermal function as the ordinate are drawn. Though 'ω' values greater than '50' are not likely to be met with in practice, ω values even upto '250' have been included as the same set of curves are intended to provide the thermal functions for higher harmonics as well. The transfer and driving point functions given in these charts are :

1) $\lambda_i \angle -\phi_i$

2) $\lambda_o \angle -\phi_o$ for $h_o = 3.5$ and $h_i = 1.5$

3) $\lambda'_i \angle -\phi'_i$

4) $\lambda_i \angle -\phi_i$

for $h_o = h_i = 1.5$

and 5) $\lambda'_i \angle -\phi'_i$

With these five sets of the charts, the thermal characteristics for periodic heat flow of any material

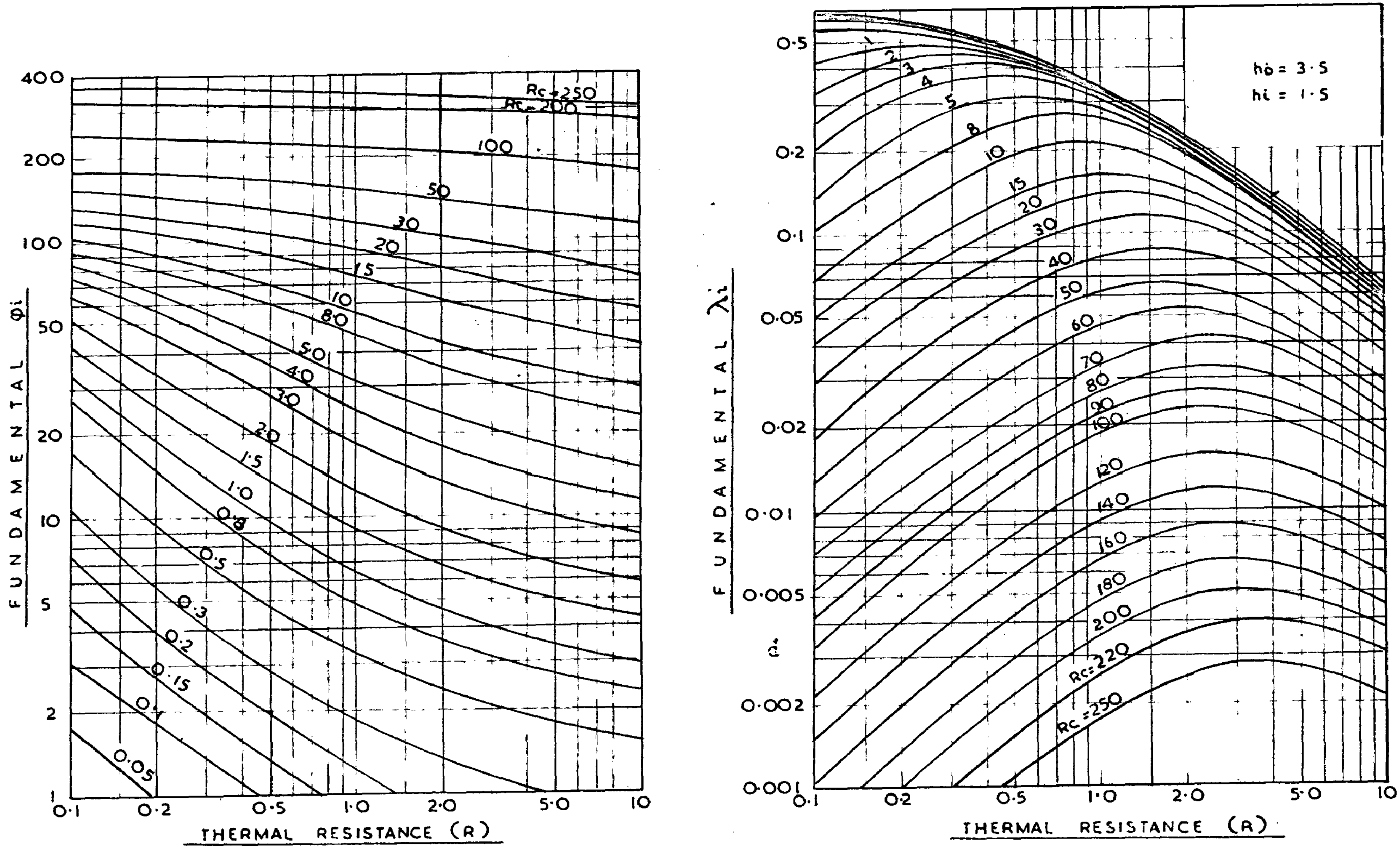

FIG.6·8. R Vs TRANSFER FUNCTION ($\lambda_i \angle -\phi_i$) FOR RC VALUES 0·1 TO 250

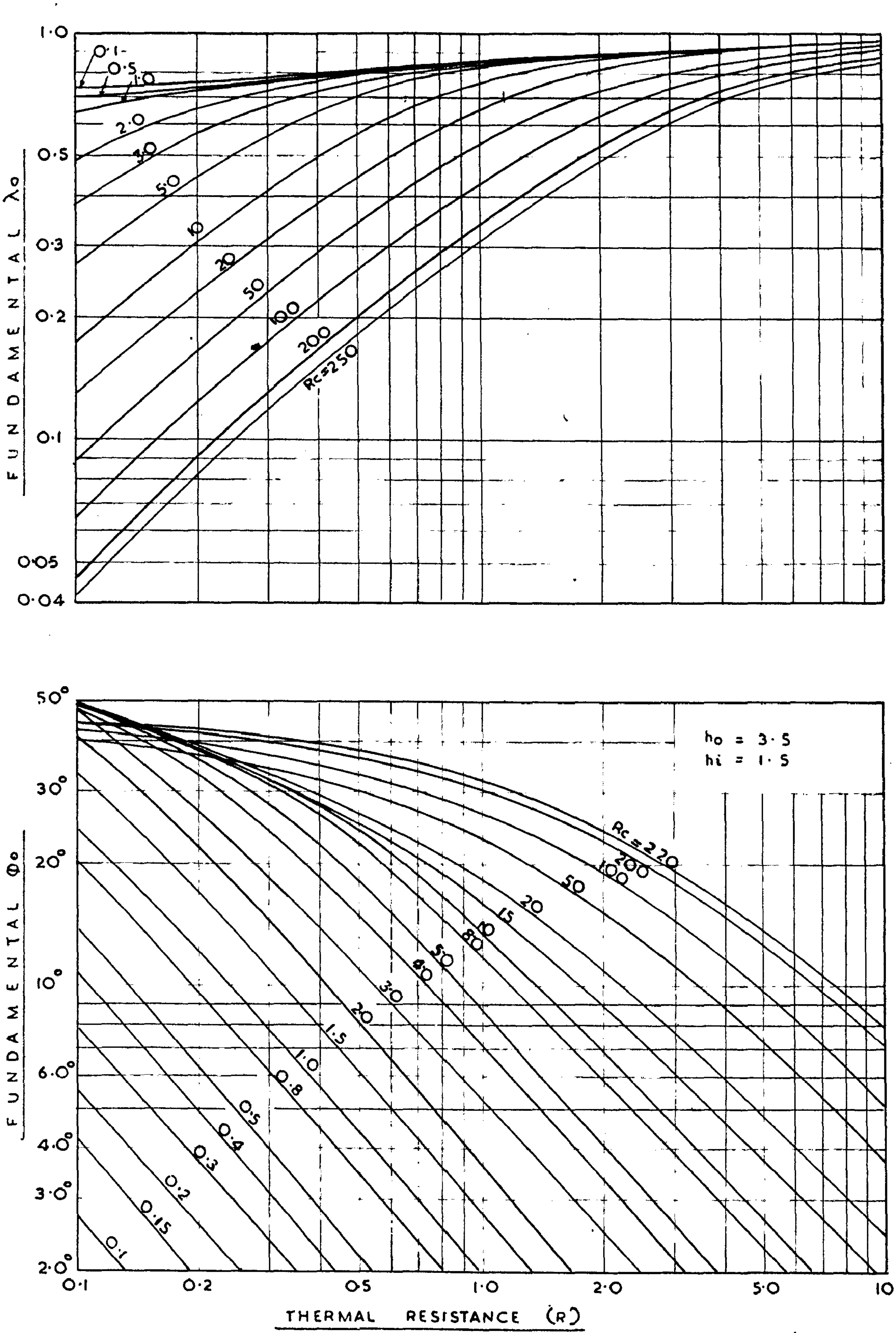

FIG. 6·9 R Vs EXTERNAL DRIVING POINT-FUNCTION ($\lambda_0 \angle -\varphi_0$)
FOR RC VALUES 0·1 TO 250

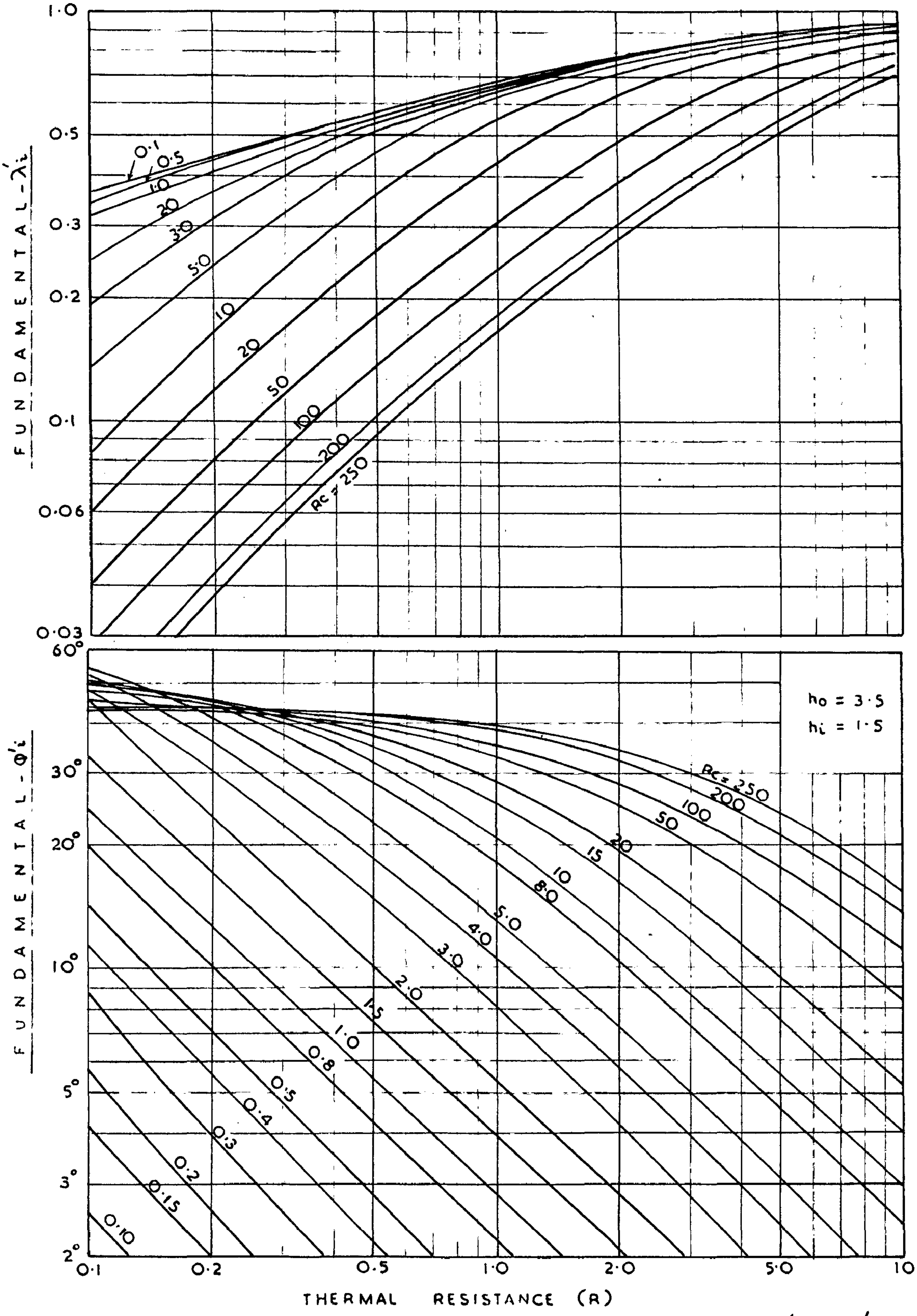

FIG. 6·10. R Vs INTERNAL DRIVING POINT FUNCTION ($\lambda_i' \angle -\Phi_i'$) FOR RC VALUES 0·1 TO 250

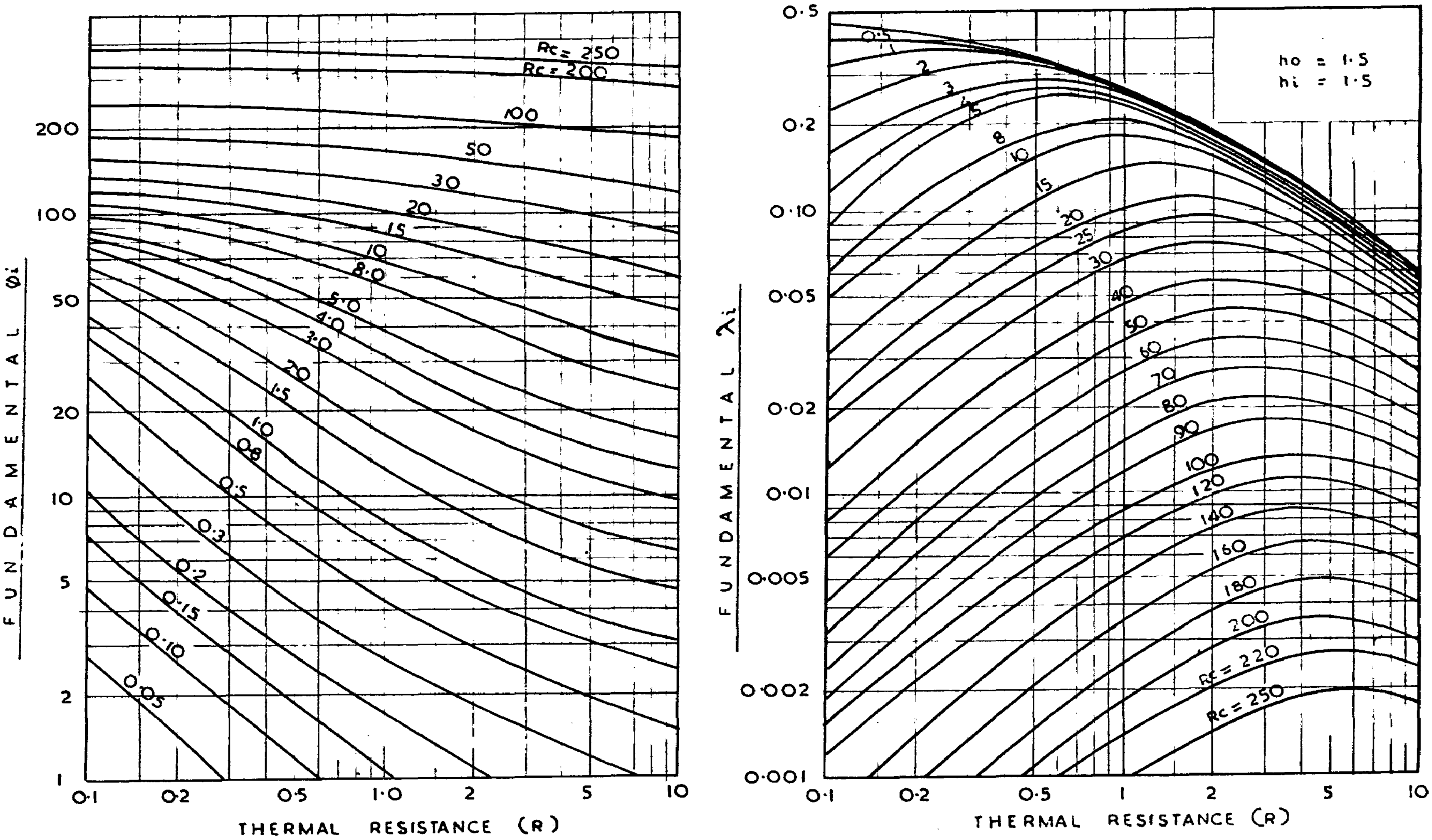

FIG. 6·11. R Vs TRANSFER FUNCTION ($\lambda_i \angle -\phi_i$) FOR RC VALUES 0·1 TO 250

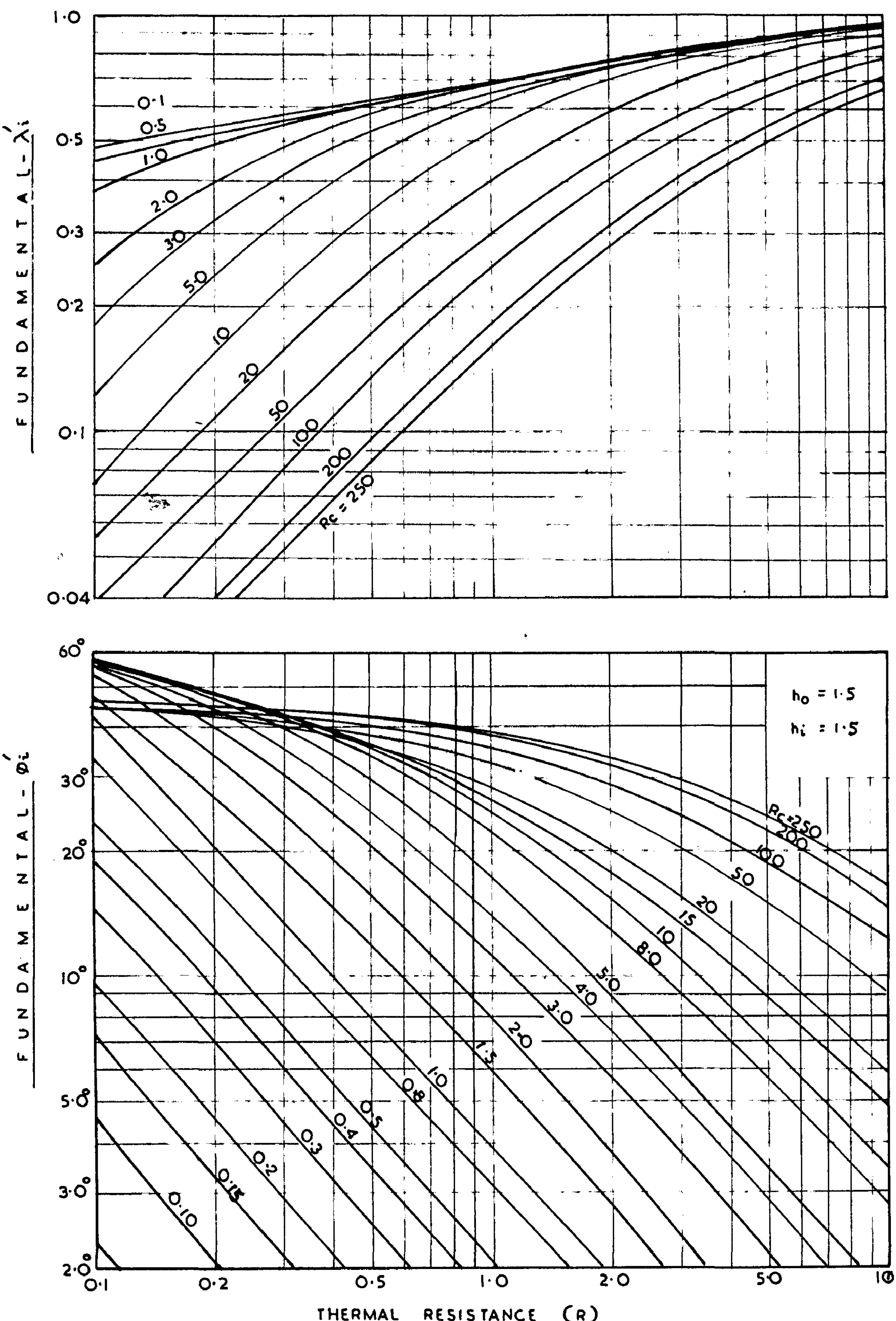

FIG. 6.12. R Vs INTERNAL DRIVING POINT FUNCTION ($\lambda_i' \angle \phi_i'$) FOR R VALUES 0.1 TO 250

of known K, ρ, s values and a given thickness (L) whether used as an external or internal element can directly be obtained.

Though these charts are for the fundamental (thermal functions) the higher harmonics can also be obtained from them. The characteristics for the n th harmonic (period 24/n hours) can be obtained from the charts by using a value of RC of n times the actual value for the same R.

The use of these charts is explained below by an illustrative example. Suppose we are interested to find the thermal transfer and driving point functions for a material with K = 8.0 properties of

$\rho = 120$ $s = 0.20$ and $L = 10''$ inches.

First of all the thermal resistance R and thermal capacity C are to be determined.

$$R = L/K = 10.0/8.0 = 1.25$$

$$C = L\rho s = 10/12 \times 120 \times 0.2 = 20$$

$$\therefore \; RC = 1.25 \times 20 = 25$$

For these values of R and RC, the transfer and driving point functions read from the charts, for the fundamental and three higher harmonics, are given in Table (6.1).

These charts are mostly self explanatory. However, the following broad inferences can be made

TABLE 6.1

THERMAL SYSTEM FUNCTIONS OBTAINED FROM THE CHARTS FOR RC = 25 AND R = 1.25
(illustrated example)

Harmonic	External Driving point Function		Transfer Fucntion		Internal Driving point Function	
	Modulus λ_o	Arg in deg $-\phi_o$	Modulus λ_i	Arg in deg $-\phi_i$	Modulus λ_i'	Arg in deg. $-\phi_i'$
Fundamental	0.67	17	0.14	100	0.46	26
Second	0.60	20	0.07	151	0.36	30
Third	0.55	22	0.03	194	0.32	32
Fourth	0.50	24	0.02	220	0.28	33

from them.

1. $\lambda i \angle \phi i$

1) For a given value of 'R', λi will decrease and ϕi increases, with the increasing of MC.

2) Materials with very low MC, behave as if they are purely resistive.

3) For a given MC, λi is low for very low values of R and increases, with the increase of R, reaching a maximum and decreases with a further increase of R.

4) The occurance of maximum is shifted towards higher values of R with the increase of 'MC'.

5) For a given MC, ϕi will decrease with the increase of R and for a given R it increases with the increase of MC.

2. $\lambda o \angle -\phi o$

1) The magnitude of λo increases, with the increase of R, for a given MC, while it decreases with the increase of MC for a given R.

2) For large values of R all the curves for different values of MC, tend to converge.

3) ϕo decreases, with the increase of R, for a given MC, while it increases with the increase of MC for a given R.

3. $\lambda'_i \angle -\phi'_i$

The variation of λ'_i and ϕ'_i with R and KC are similar to that of λ_o and ϕ_o. The value of λ'_i is lower than λ_o, while ϕ'_i are higher than ϕ_o, for a given KC and R.

6.10 Effect of Surface Heat Transfer Coefficients on Thermal System Functions

It is an accepted procedure to assume the surface heat transfer coefficients (h_o and h_i) as constant in the computations of periodic heat flow. In the above studies the outside and inside surface heat transfer coefficients were assumed to be constant of values 3.5 and 1.5 Btu/sq.ft./Hr/^oF, respectively. However, in practice these are not strictly constant and sometimes vary within wide limits, especially the outside surface coefficient (h_o). Hence for more precise computations it is required to know quantitatively the effect of the variations of 'h_o' and 'h_i' on these thermal system functions. Johnson (74) has analysed this problem mathematically taking $\lambda_i \angle -\phi_i$, as a function of three dimension less moduli. However, he did not study the effect of these surface heat transfer coefficients on the driving point functions. These have now been investigated for all the three sets of thermal system functions, as a function of

R (values ranging from 0.1 to 20) and RC (values ranging from 0.1 to 200) for a range of surface coefficients of practical importance (varying from 0.5 to 10). As these form a large number of family of curves only a few typical curves have been presented here. These include two values of RC viz., 1.0, and 20 for values of R varying from 0.1 to 20. In one set 'h_o' was kept constant at 3.5 and 'h_i' varied (0.5, 1.5 and 5.0) and in another set 'h_i' was fixed as 1.5 and 'h_o' varied (1.0, 3.5 and 10). The results of these studies are presented graphically in Figs. (6.13 through 6.21). Though these sets of curves clearly bring out the effect of surface resistance and on thermal functions, the broad conclusions drawn are summarised below.

1) The influence of surface heat transfer coefficients, on the thermal system functions depends upon the RC and R values of a given building element. Sections with small RC and R are affected to a greater extent than those of with large RC and R. For different building sections having the same RC, but of different Rs the effect of h_o and h_i will be different. Their influence on thermal system functions, is not significant for sections with large 'R'.

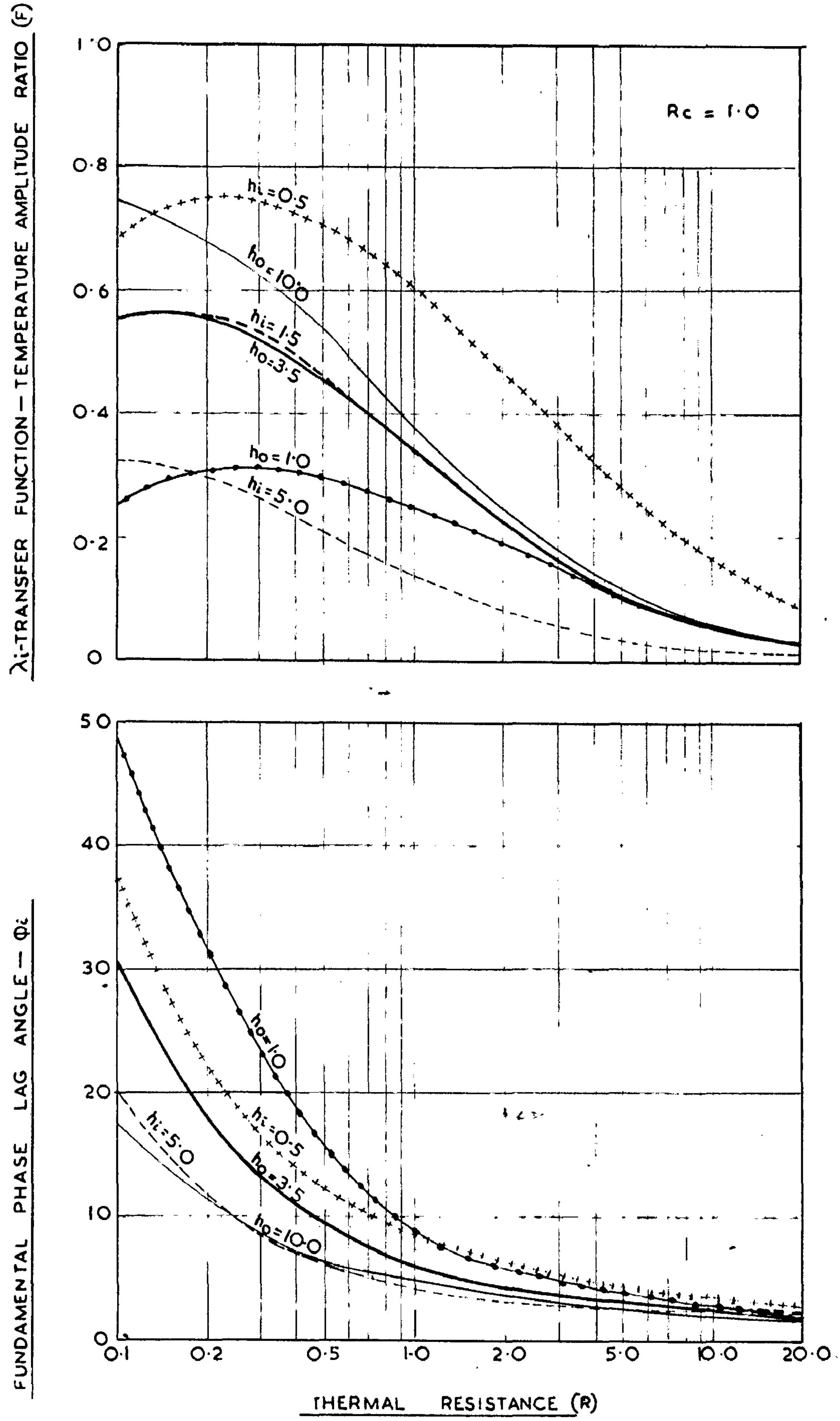

FIG. 6·13 EFFECT OF h_o AND h_i ON λ_i AND Φ_i FOR HOMOGENEOUS SECTIONS WITH LOW TIME CONSTANT

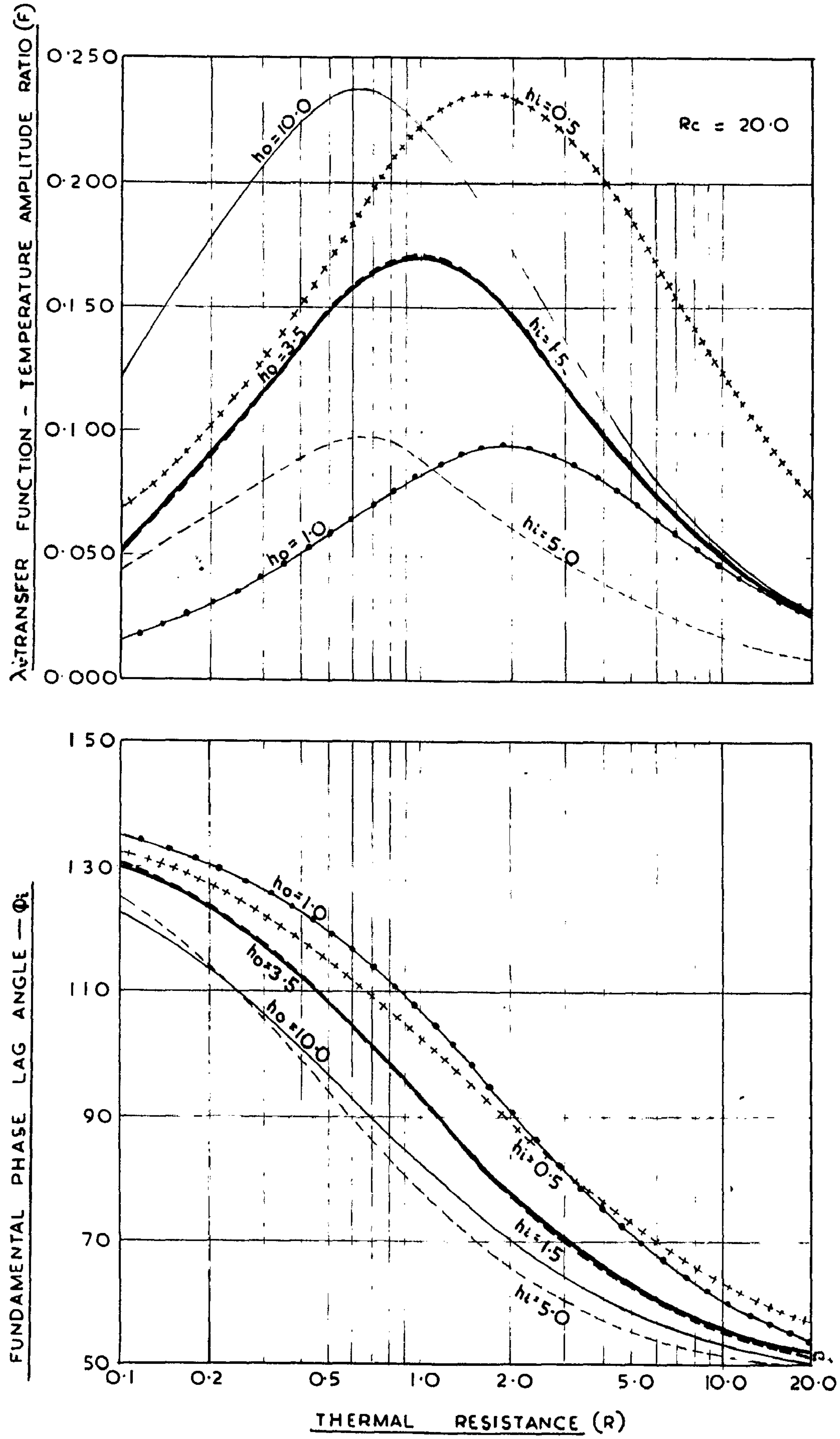

FIG.6·14 EFFECT OF ho AND hi ON λi AND φi FOR HOMOGENEOUS SECTIONS WITH MEDIUM TIME CONSTANT

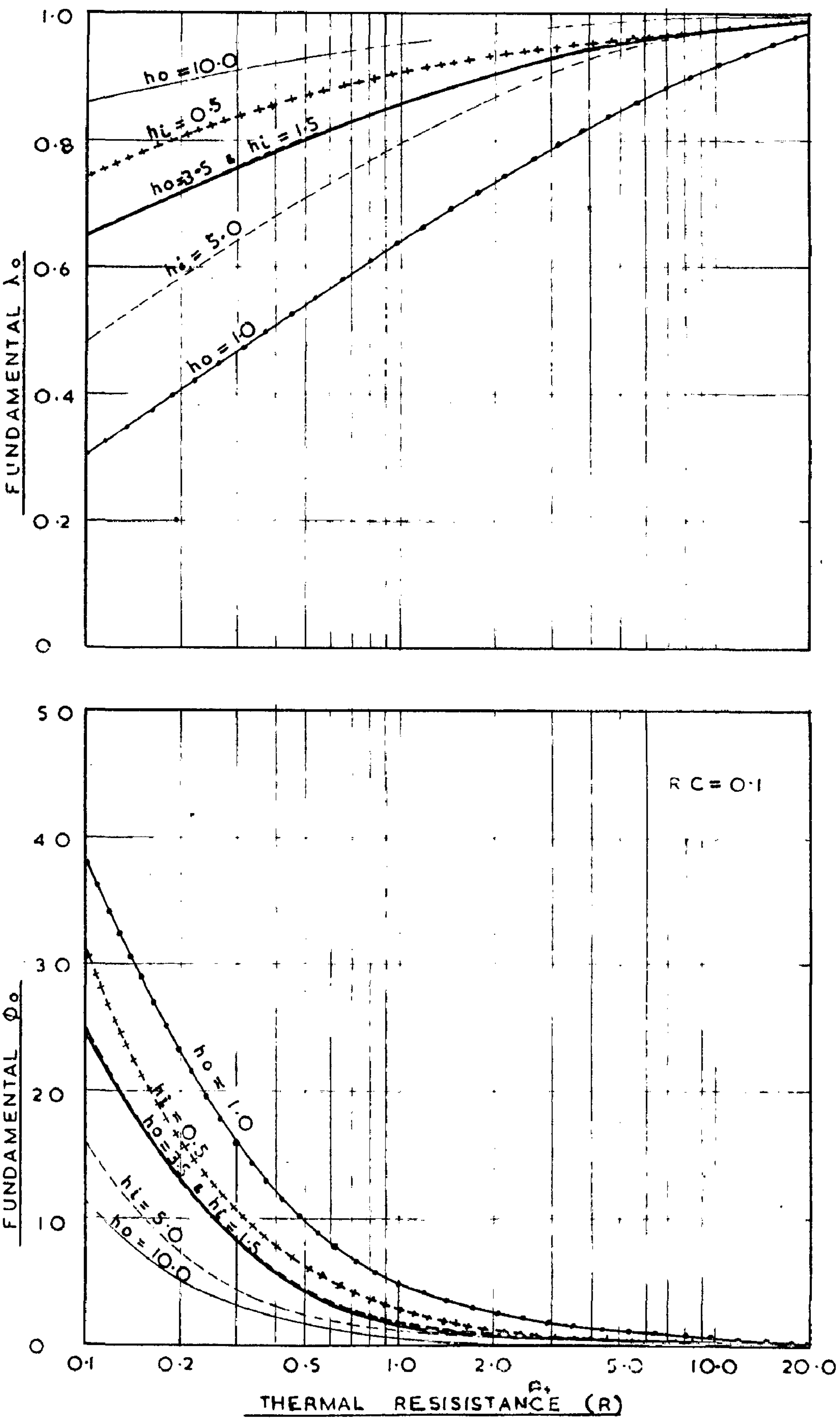

FIG.6·15 EFFECT OF h_o AND h_i ON λ_o AND ϕ_o FOR HOMOGENEOUS SECTIONS WITH LOW TIME CONSTANT

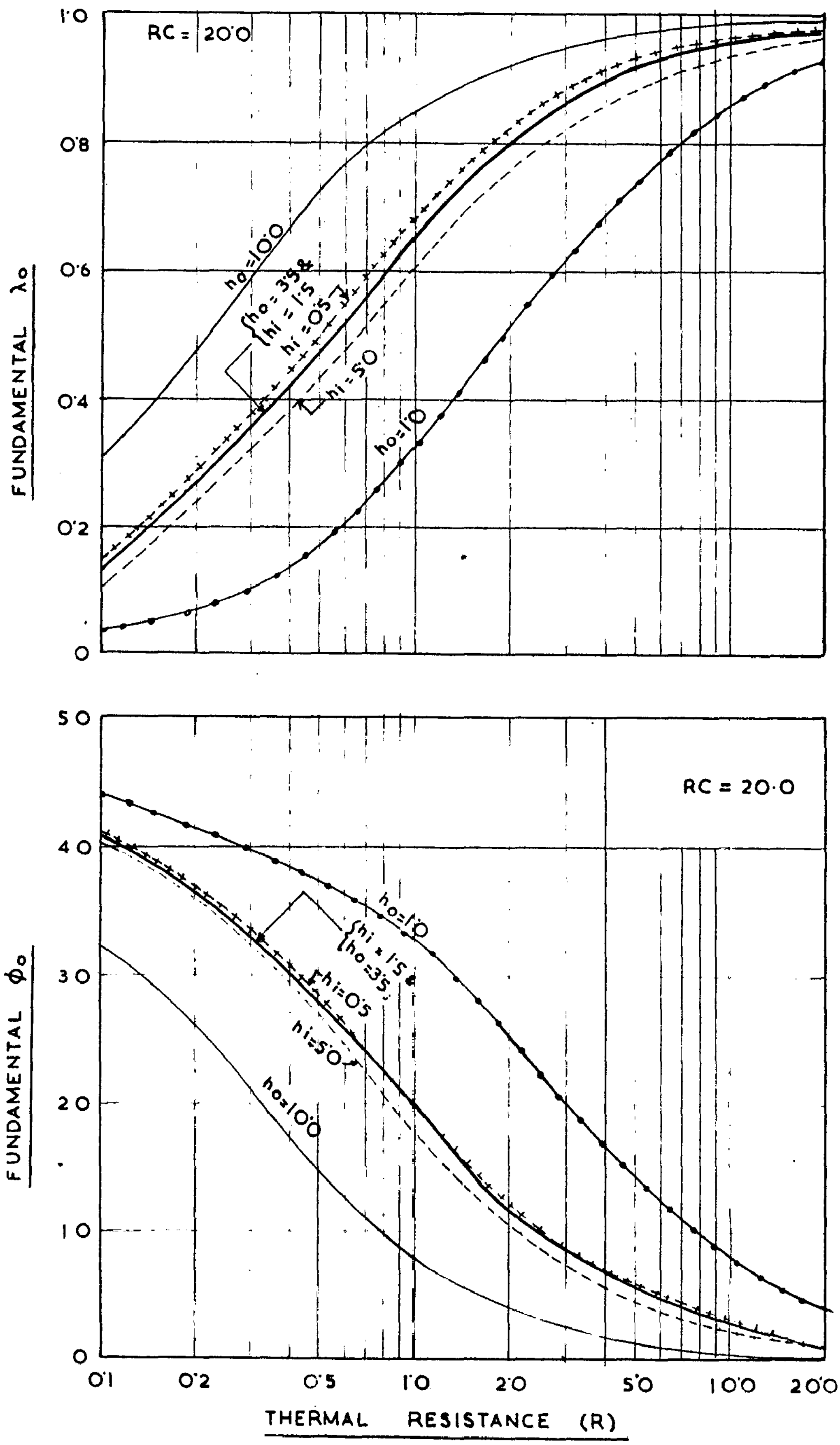

FIG. 6·16. EFFECT OF h_o AND h_i ON λ_o AND ϕ_o FOR HOMOGENEOUS SECTIONS WITH MEDIUM TIME CONSTANT

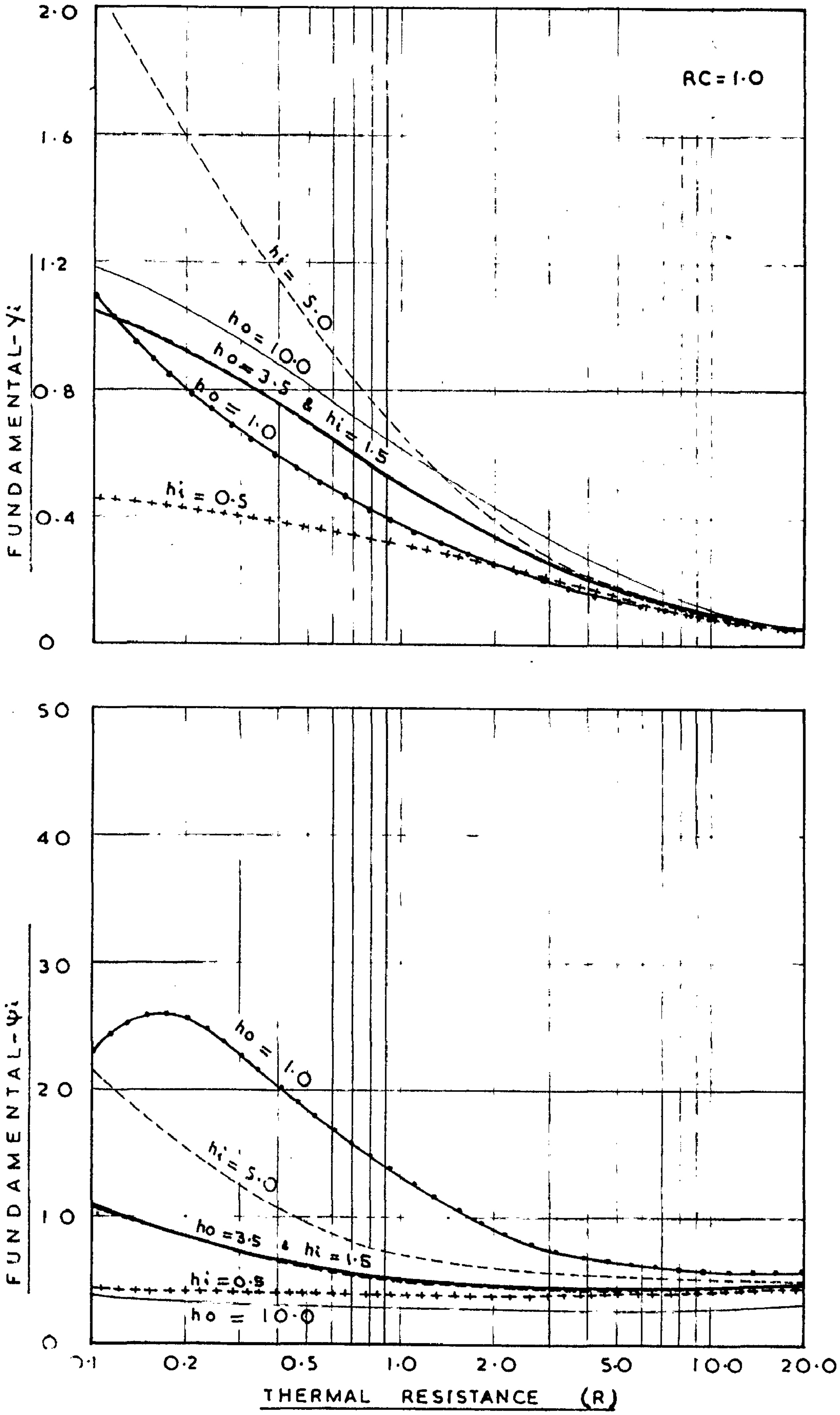

FIG.6·17 EFFECT OF h_o AND h_i ON Y_i' AND ψ_i' FOR HOMOGENEOUS SECTIONS WITH LOW TIME CONSTANT

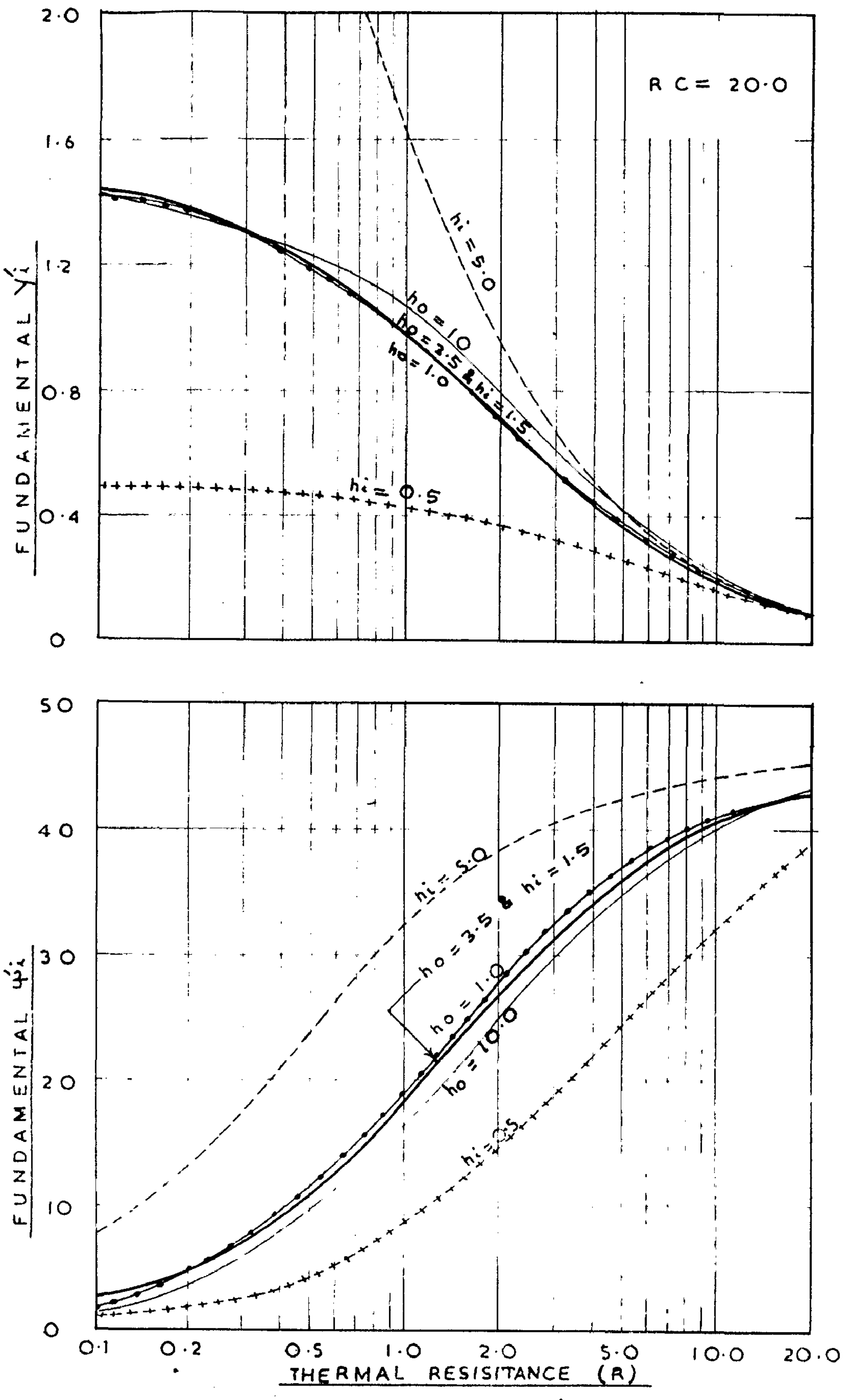

FIG.6·18 EFFECT OF h_o AND h_i ON Y_i' AND ψ_i' FOR HOMOGENEOUS SECTIONS WITH MEDIUM TIME CONSTANT

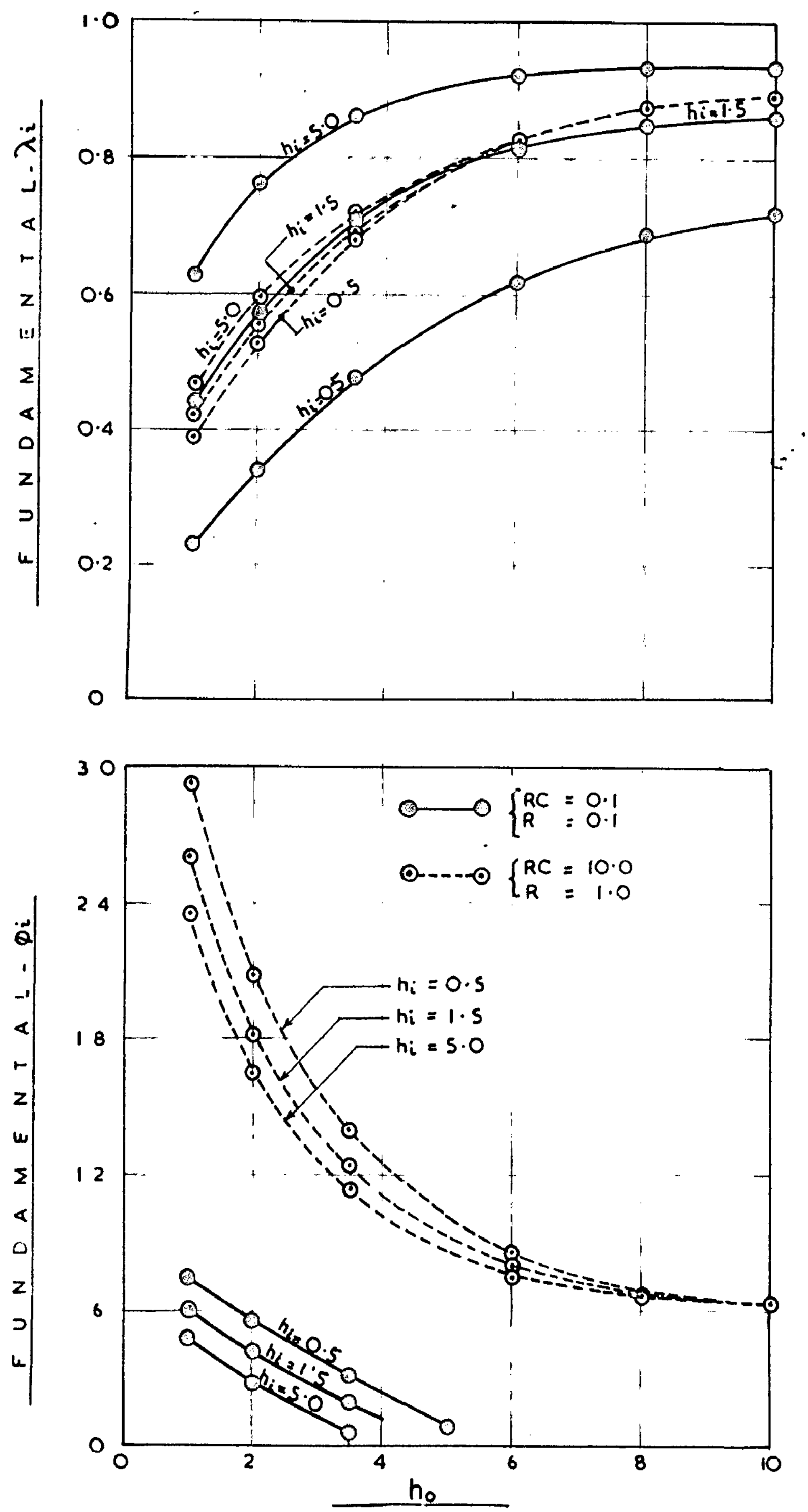

FIG.6·19 EFFECT OF h_o AND h_i ON λ_i AND ϕ_i FOR THIN AND THICK SECTIONS OF DENSE MATERIALS

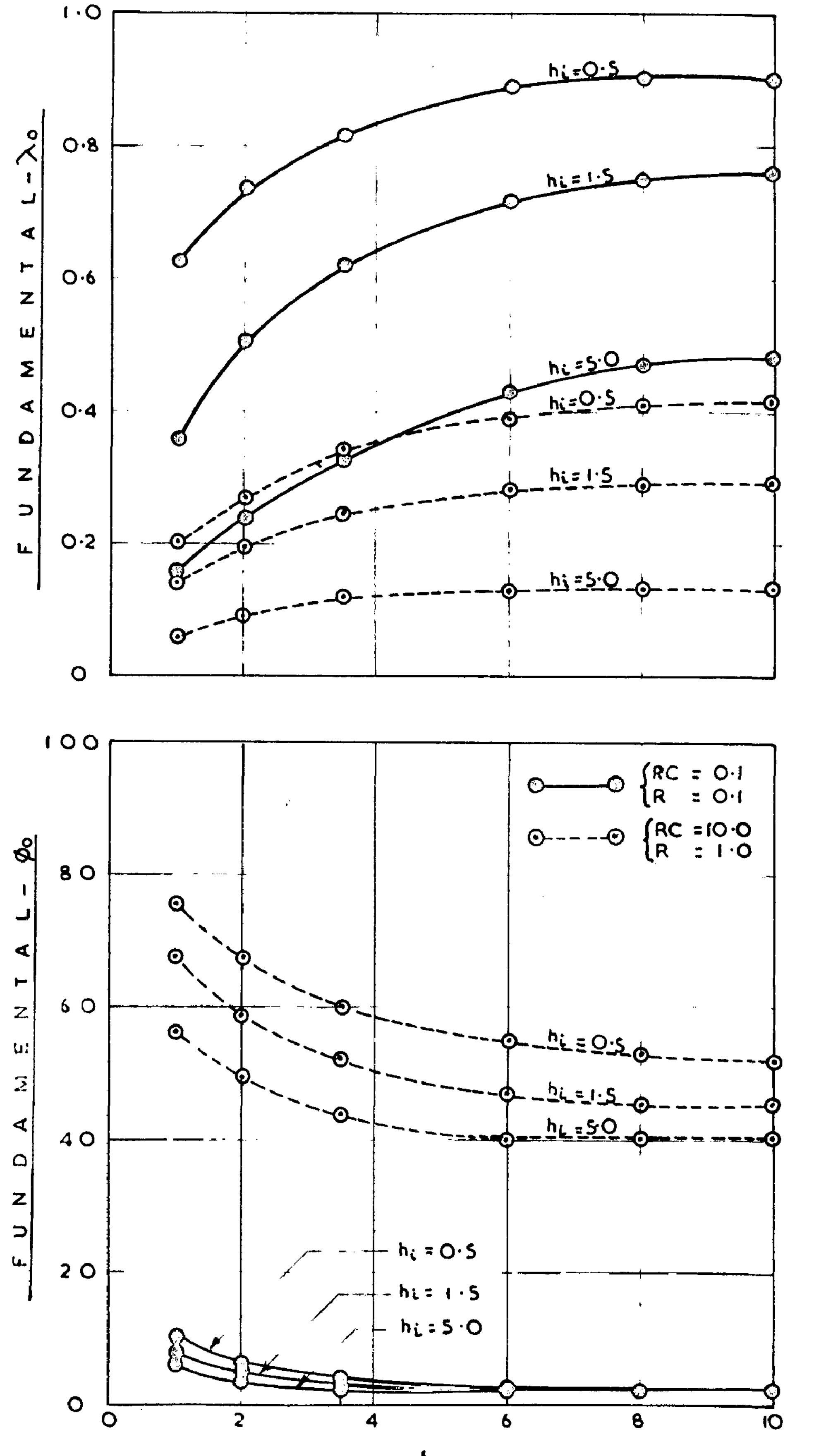

FIG.6.20 EFFECT OF h_o AND h_i ON λ_o AND ϕ_o FOR THIN AND THICK SECTIONS OF DENSE MATERIALS

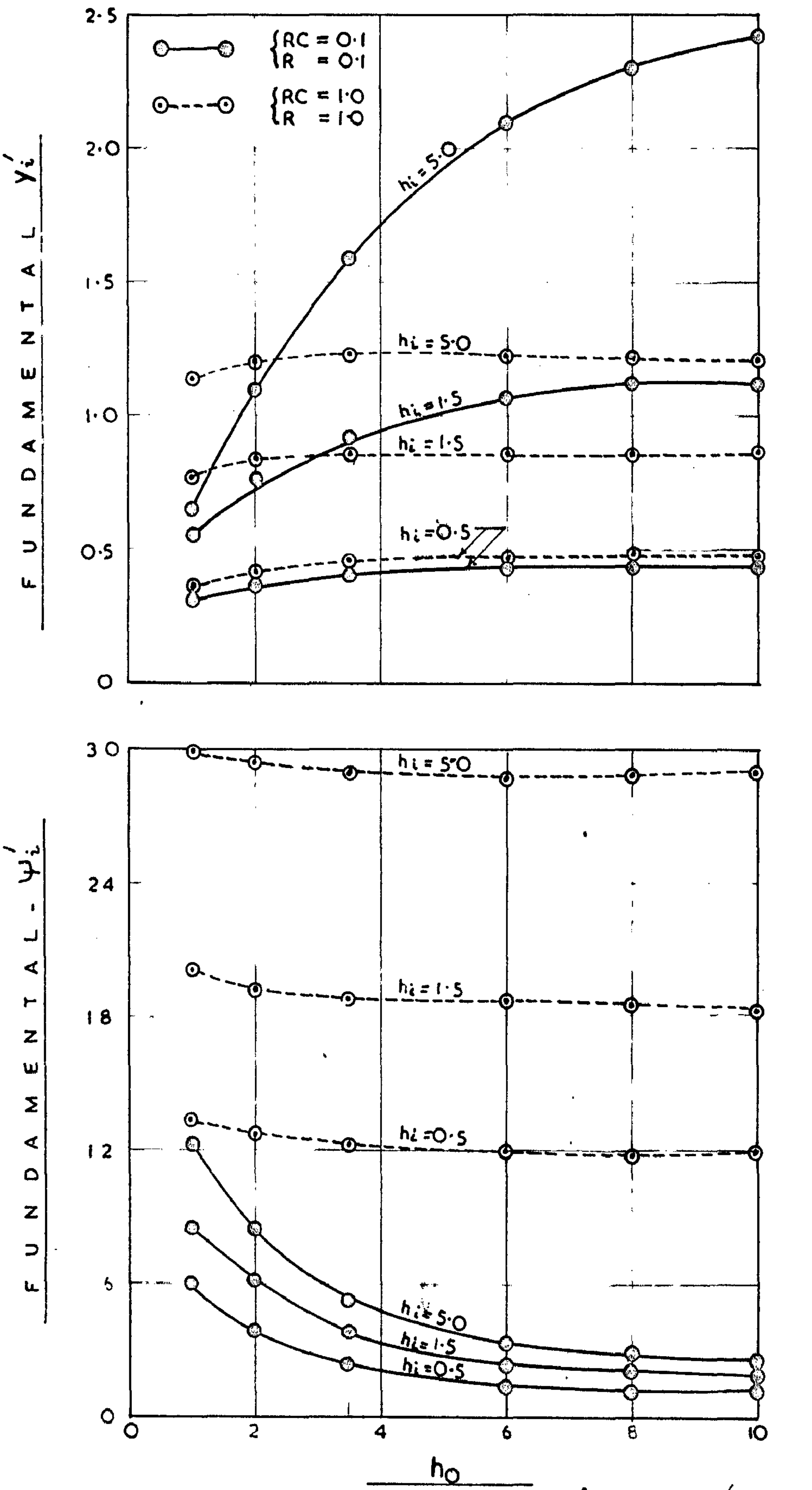

FIG.6·21 EFFECT OF h_o AND h_i ON γ_i' AND ψ_i' FOR THIN AND THICK SECTIONS OF DENSE MATERIALS

2) Except for thin sections (which have small RC as well as R) the influence of the variation of 'h_o' on $Y_i' \angle \Psi_i'$ and of 'h_i' on $\lambda_o \angle \Phi_o$ is not significant. $\lambda_o \angle \Phi_o$ are influenced greatly by 'h_o' while $Y_i' \angle \Psi_i'$ are influenced 'h_i' considerably.

3) For thin sections increase of h_o increases λ_o and Y_i' and decreases Φ_o and Ψ_i', whereas the increase of 'h_i' decreases λ_o, Φ_o and Ψ_i' and increases Y_i'.

4) For any given value of RC (small or large) both 'h_o' and 'h_i' have considerable effect on the transfer functions ($\lambda_i \angle \Phi_i$). Increase of 'h_o' increases λ_i and decreases Φ_i, whereas increase of 'h_i' decreases λ_i as well as Φ_i.

5) For building sections with large R and even with small RC, viz., insulating materials, 'h_o' and 'h_i' have no significant effect on thermal system functions.

6) For a building section with a given RC and a given 'h_o' and 'h_i', λ_i will be maximum for a particular resistance. For either an increase or decrease of the resistance from this optimum λ_i will decrease. This optimum resistance depends upon the RC value.

For higher values of RC, this R will also be higher. For a given C, the occurance of maximum of λ_i shifts towards the lower resistance with the increase of 'h_o' as well as 'h_i'.

C H A P T E R 7

THERMAL SYSTEM (TRANSFER AND DRIVING POINT) FUNCTIONS OF COMPOSITE CONSTRUCTIONS

CHAPTER 7

THERMAL SYSTEM (TRANSFER AND DRIVING POINT) FUNCTIONS OF COMPOSITE CONSTRUCTIONS

7.1 Introduction

In the previous chapter (6) thermal functions for homogeneous constructions were dealt with. However, structural elements used in most of the present day buildings are composite (multi-layered). These composite constructions may consist of two or more layers of homogeneous materials in perfect thermal contact. There can also be a large number of combinations of layers made of different types of materials and thicknesses. In order to predict the thermal behaviour of such structural elements, the thermal functions of a wide range of composite constructions that are commonly met with in building practice are required.

The type and thickness of each layer and the order of arrangement affect the thermal behaviour of composite elements under periodic heat flow conditions. Hence to make the most efficient use of the new as well as conventional materials, individually or in combination, the influence of the type and location of the individual layers, on the overall thermal functions is to be known.

Analytical methods developed by Mackey and Wright (75) are complex even for homogeneous materials and become much more so for composite constructions. Other mathematical methods also developed by Ukhlover (26) Marmet (37), no doubt, lessen the mathematical burdent, but still are unwieldy. The matrix method (24) is more convenient, but when the number of layers is more than two, manual computation becomes impractical and a digital computer will be required, especially when the decrement factors of individual layers are also required to be determined. In contrast, the Electrical Analogue method requires only a few more measurements of the temperature amplitudes and phase lag angles at junction points of different layers. A typical composite construction and its equivalent network representation is shown in Fig. (7.1). The junction points at which temperature and phase measurements are made are indicated therein. For the representation of the composite element on the electrical network, the number of lumps employed for each layer were chosen according to the recommendations made in Chapter 4. The procedure, for the determination of the thermal transfer and driving point functions, is the same as that followed for homogeneous materials (described in Chapter 3).

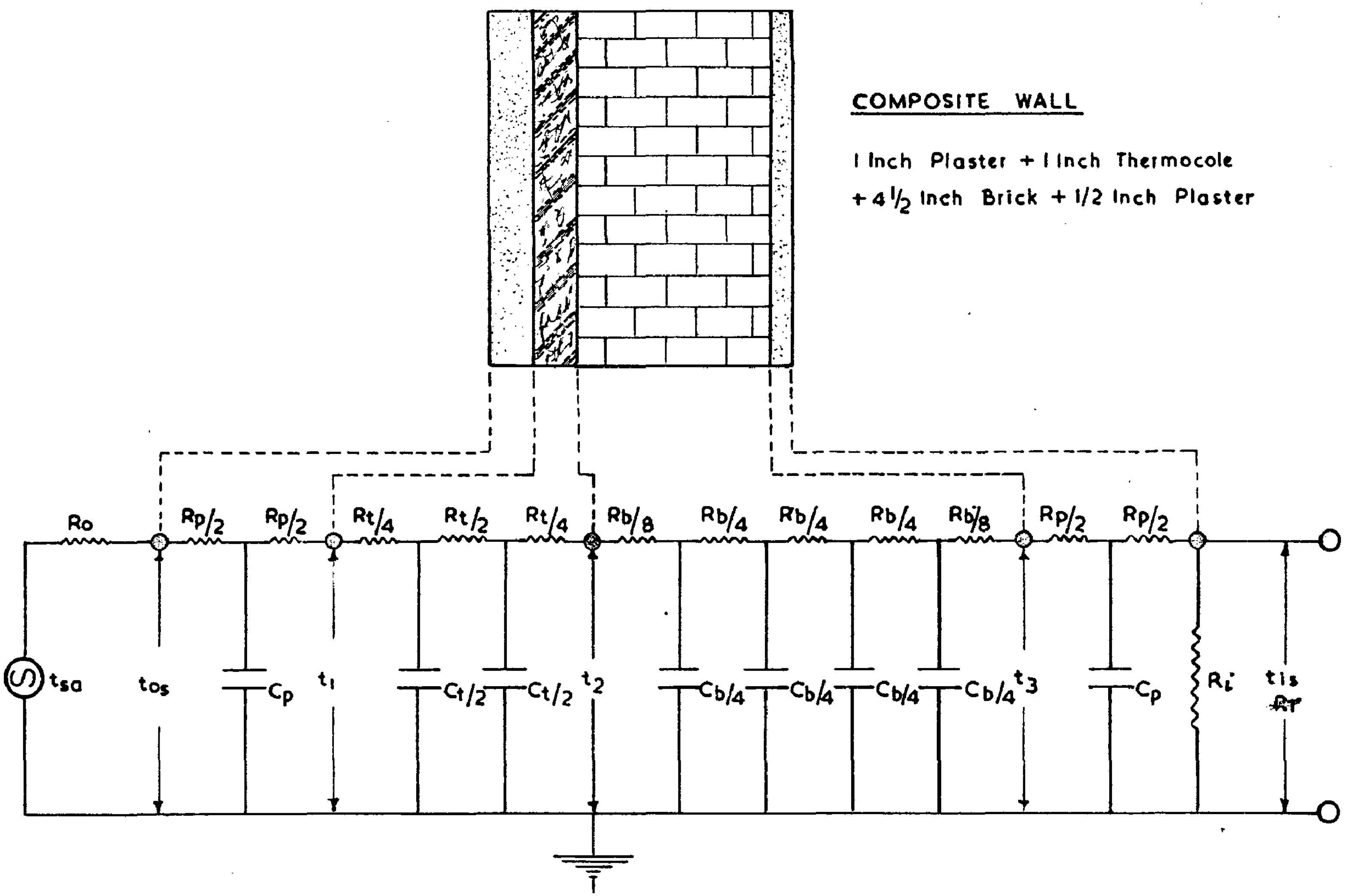

ANALOGUE REPRESENTATION OF A COMPOSITE WALL

FIG. 7·1

The thermal decrement factors of individual layers were obtained from the measurements of amplitude across them. For example for a four layer composite element (shown in Fig. 7.1) the decrement factor of the individual layers may be written as

$$\vec{\lambda}_0 = \frac{\vec{t}_{os}}{t_{oa}} \qquad \vec{\lambda}_1 = \frac{\vec{t}_1}{t_{os}}$$

$$\vec{\lambda}_2 = \frac{\vec{t}_2}{t_1} \qquad \vec{\lambda}_3 = \frac{\vec{t}_3}{t_2}$$

$$\vec{\lambda}_4 = \frac{\vec{t}_{is}}{t_3}$$

The over all decrement factor (i.e. transfer function) of the whole building element is then obtained by the product of all the decrement factors of individual layers. Hence $\lambda_i \angle{-\phi_i}$ is given as

$$\lambda_i\angle{-\phi_i} = (\lambda_o\angle{-\phi_o})(\lambda_1\angle{-\phi_1})(\lambda_2\angle{-\phi_2})(\lambda_3\angle{-\phi_3})(\lambda_4\angle{-\phi_3}) \quad ..(1)$$

From the principles of vector multiplication, we get

$$\lambda_i = \lambda_o \times \lambda_1 \times \lambda_2 \times \lambda_3 \times \lambda_4 \quad ..(2)$$

and $$\phi_i = \phi_o + \phi_1 + \phi_2 + \phi_3 + \phi_4 \quad ..(3)$$

The overall transfer and driving point functions for a large number of composite constructions were determined for fundamental and three higher harmonics, analogically. These alongwith 'U' values are given in Appendix (IV) Tables (1 to 6) with illustrative diagrams. For the sake of convenience the above data is arranged in different groups in accordance with their functional use in a building.

It is well known that surface heat transfer coefficients vary with the inclination of the surface (i.e. vertical and horizontal surfaces will have different values). Since no precise data on these variations is available, it is the common practice to treat them as equal for most building calculations. With this simplifying assumption, the data (in Appendix IV), for a given construction used as a wall, may be used, without undue error either for roof or for walls.

The surface heat transfer coefficients used in the determination of the thermal functions are :

i) For external building elements

h_o = 3.5 Btu/sq.ft./Hr/°F

h_i = 1.5 " " " "

and ii) For internal structural elements

h_o = 1.5 Btu/sq.ft./Hr/°F

h_i = 1.5 " " " "

For the ground floor h_i is taken as 1.5 and the other surface (at a depth of 20 inches) is assumed to be at a constant temperature. This assumption is based on experimental evidence (60).

For the calculation of thermal resistance (R) and thermal capacity (C) of individual layers, the average values of the physical properties of the materials listed in Table 1 of Appendix III were used. An examination of the thermal function data given in Appendix IV brings out the following points.

7.2 $\lambda_o \angle -\phi_o$ — External Driving Point Function

λo and ϕo mainly depend upon the type of the material and thickness of the upper most layer. If this layer is thick the preceding layers have no influence on them. When dense materials having large thermal absorption coefficient 'p' ($\sqrt{\frac{\omega C}{R}}$ for the top layer, λo will be less and ϕo will be high while the reverse is true for light weight insulating materials (with small 'p').

With the increase of thickness of the top layer, λo decreases and ϕo increases (slightly), for dense materials, while λo increases and ϕo decreases for insulating materials. For higher frequencies, λo decreases and ϕo increases, and this is more for dense materials than for light weight materials used as a top layer. The variations of λo and ϕo are not large for different dense materials as top layer (fundamental λ_o varied from 0.6 to 0.75 and ϕ_o varied from 10 to 30°) while the variation between dense and insulating materials is quite large (fundamental λ_o varied from 0.6 to 0.95 and ϕ_o varied from 1° to 30°). If the insulating layer forms the top layer, the phase lag angles will be very low (1° or less), whereas, if even a thin layer of a dense material like a plaster (which is usually be the case) is placed above it, ϕ_o increases upto 12 to 15°, while there is no appreciable change in λ_o. Intermediate floors and partition walls etc. where the surface heat transfer coefficients are equal (i.e., $h_o = h_i$) are of dense materials, λ_o and ϕ_o vary within narrow limits (fundamental λ_o varied from 0.4° to 0.45° and ϕ_o varied from 25° to 30°).

7.3 $\lambda_i' \angle -\phi_i'$ - Internal Driving Point Function

The magnitude of λ_i' and ϕ_i' is mainly determined by the inner most layer (as the heat flow direction is from inside to outside). These are influenced by the type of material and thickness of the inside layer in the same manner as the top layer affects λ_o and ϕ_o. λ_i' is always lower than the corresponding λ_o and ϕ_i' is greater than the corresponding ϕ_o. For most of the conventional types of structural elements (Bricks, stones, concrete etc.) λ'_i varied within narrow limits, i.e., 0.42 to 0.52 for fundamental. With insulating layers on the inner side this varied from 0.7 to 0.84, depending upon the type of the insulating material and its thickness.

For partitions and intermediate floors $\lambda'_i \angle{-\phi'_i}$ will be equal to $\lambda_o \angle{-\phi_o}$ as both surfaces are interior ones and have equal surface coefficients (i.e., $h_o = h_i$).

7.4 <u>$\lambda_i \angle{-\phi_i}$ - Transfer Function</u>

As, λ_i and ϕ_i give the overall decrement factor and phase lag of the entire composite element, these will depend upon the nature of all the layers. It is further noted that these quantities (λ_i and ϕ_i) are affected, not only by the type of the materials and thickness of the individual layers, but also on the arrangement of these layers (i.e., the order of the layers viewed in the direction of heat flow).

For the composite constructions studied, the fundamental λ_i varied from 0.3 to 0.6 for conventional types (i.e., combinations of brick, concrete, stone, etc. of different thicknesses) and ϕ_i varied from 50^{o} to 220^{o}. With the inclusion of insulating layers λi decrease considerably (as low as 0.009) even for smaller over all thickness.

A study of all the factors, that affect λi and ϕi and the decrement factors of individual layers, will provide an insight of the mechanism of heat flow through composite constructions under periodic variations. These were studied and the results are given in Tables (7.1 through 7.6). A discussion, of the above results, follows in the next few pages.

7.5 Effect of the Location of the Insulating Layer on its Decrement Factor and on the Overall Thermal Functions

In this, a study of the effect of location of a highly insulating material (Thermocole) as outer, middle and inner layer and also on either side, in combination with a dense material (concrete) has been made. The decrement factors of the insulating layers and, the concrete layer are given in Table (7.1), along with the transfer and driving point functions.

It is seen from the table, that distributing the insulating layers on both sides of a dense material gives the lowest λi and higher phase lag (ϕi). But in this case $\lambda' i$ will be quite high.

EFFECT OF THE LOCATION OF INSULATING LAYER ON THERMAL SYSTEM FUNCTIONS
(Fundamental)

$h_o = 3.5$
$h_i = 1.5$

Sl. No.	Type of Construction		External Driving point Function	Decrement Factors of Layers: Top layer	Middle layer	Bottom layer	Overall Transfer function	Internal Driving point function
1.	3" thermocole + 4" dense concrete	λ Mod.	0.839	0.059	...	0.549	0.031	0.544
		-φ Arg.	1°	45°	...	24°	69°	39°
2.	4" dense concrete + 2" thermocole	λ Mod.	0.735	0.918	...	0.036	0.044	0.935
		-φ Arg.	24°	29°	...	1°	54°	1°
3.	1" thermocole + 4" dense concrete + 1" thermocole	λ Mod.	0.918	0.099	0.346	0.117	0.009	0.830
		-φ Arg.	1°	61°	29°	1°	90°	1°
4.	2" dense concrete + 2" thermocole + 2" dense concrete	λ Mod.	0.921	0.971	0.032	0.726	0.041	0.753
		-φ Arg.	16°	8°	35°	6°	65°	32°

The next best arrangement is obtained by placing all the insulation on the external side, where both λi and $\lambda' i$ are sufficiently low. The least advantageous way of utilising an insulating layer is to use it as an inside layer, if the main task is to prevent the entry of external heat, into the enclosure (for hot climates). On the other hand, if the main problem is to maintain higher indoor air temperatures and prevention of heat losses (for cold climates) placing the insulating layer on the inner side will be most advantageous.

If the insulating material is backed by a dense material the decrement factor (λ) of the insulating layer, decreases slightly, whereas the phase lag angle increases considerably. When the dense material is backed by an insulating layer the decrement factor (λ) of the dense material increases considerably, but the phase lag angle increases only slightly. For various possible arrangements, the greatest damping occurs when layers with small 'p' (insulating materials) alternate with layers of large 'p' (dense materials). In a two layer structure, when a layer with large 'p' is placed inside the transfer and internal driving point functions will be lower, though the external surface temperatures will be much higher, than for the reverse order.

7.6 Effect of the Back Layer on the Decrement Factor of an Insulating Upper Layer

In the above study it was found that placing insulation on the external side will provide maximum advantage. The decrement factor of the insulating layer depends upon the type of layer on which it is placed. The effect of the backing layer on the decrement factor of the insulating layer was studied. For this purpose a 2 inch thick Thermocole was taken as the outside layer and the following were used as backing layers :-

1. Thin Asbestos cement sheet.
2. Dense materials - concrete and brick.
3. Insulating materials - foamed concrete and celotex board.

The results are shown in Table (7.2). These indicate that the decrement factor and phase lag across a top insulating layer are considerably affected by the type and thickness of the backing layer. With backing materials, are of dense type (large p value) the decrement factor of the insulating layer decreases and phase lag increases to a large extent. On the other hand with materials having small p value, λ increases considerably but not the phase lag (ϕ).

7.7 Effect of the Bounding layers on the Enclosed Air Space of Double Wall Constructions

Cavity wall and sandwitch panel constructions

TABLE 7.3

EFFECT OF THE BACKING LAYER ON THE DECREMENT FACTOR OF THE TOP INSULATING LAYER AND THE THERMAL SYSTEM FUNCTIONS (Fundament)

$h_o = 3.5$
$h_i = 1.5$

Sl. No.	Type of Construction		External Driving point Function	Decrement Factors of Layers: Front Layer	Decrement Factors of Layers: Back Layer	Overall Transfer Function	Internal Driving point function
1.	2" thermocole	λ Mod.	0.976	0.065	...	0.065	0.040
		−φ Arg.	1°	1°	...	1°	1°
2.	3" thermocole + 2" dense concrete	λ Mod.	0.973	0.062	0.725	0.047	0.744
		−φ Arg.	1°	35°	6°	41°	32°
3.	2" thermocole + 4" dense concrete	λ Mod.	0.959	0.058	0.549	0.031	0.544
		−φ Arg.	1°	45°	24°	69°	39°
4.	2" thermocole + 4½" brick	λ Mod.	0.944	0.060	0.441	0.024	0.523
		−φ Arg.	1°	46°	28°	74°	30°
5.	2" thermocole + 4" foamed concrete	λ Mod.	0.976	0.259	0.101	0.025	0.844
		−φ Arg.	1°	33°	39°	72°	8°
6.	2" thermocole + ¼" A.C. sheet	λ Mod.	0.975	0.063	0.919	0.060	0.961
		−φ Arg.	1°	5°	1°	5°	3°

which enclose air spaces are coming into use in building practice of this country. In order to determine the effect of the bounding layers on the damping across the air space bounded by different types of layers, the decrement factors and thermal functions were determined with different bounding layers. These are given in Table (7.3). It can be seen that the decrement factor and phase lag across an air space are affected to a considerable extent by the inner layer only but not by the outer one. If the inner layer is a thin sheet like, glass pane, galvonised iron sheet, and plywood sheet, practically no phase lag is introduced across the air space. If the backing layer is of a dense material like brick or concrete; sufficiently large phase lag angles (of the order of 20^o to 25^o) are introduced. If the insulating materials form the backing layer, the decrement factor across the air space is increased (λ_{air} is increased) and only small phase lag angle (5^o or so) results.

The air space affects the decrement factor of the front bounding layer adversely (i.e., λ increases) but increases its phase lag (by 10 to 12^o).

7.8 Effect of the Order of Layers on the Thermal Functions

It was pointed out earlier that the

TABLE 7.3

EFFECT OF BOUNDING LAYERS ON THE DECREMENT FACTOR OF THE ENCLOSED AIR SPACE AND THE THERMAL SYSTEM FUNCTIONS (Fundamental)

$h_o = 3.5$
$h_i = 1.5$

S. No.	Type of Construction		External Driving point Function	Decrement Factors of Layers: Front Layer	Air Space	Back Layer	Overall Transfer Function	Internal Driving point Function
1.	1/8" glass + 2" air space + 1/8" glass	λ Mod. $-\phi$ Arg.	0.835 1°	0.836 1°	0.478 1°	0.971 1°	0.382 2°	0.613 1°
2.	½" plywood + 2" air space + ½" plywood	λ Mod. $-\phi$ Arg.	0.890 2°	0.795 4°	0.581 5°	0.636 3°	0.263 14°	0.705 5°
3.	½" A.C. sheet + 2" air space + ½" celotex board	λ Mod. $-\phi$ Arg.	0.921 2°	0.974 1°	0.767 1°	0.321 1°	0.215 5°	0.830 1°
4.	1½" dense concrete + 2" air space + 1½" dense concrete	λ Mod. $-\phi$ Arg.	0.740 14°	0.910 7°	0.556 24°	0.852 4°	0.293 49°	0.483 29°
5.	3" brick + 2" air space + 3" brick	λ Mod. $-\phi$ Arg.	0.776 10°	0.710 31°	0.545 22°	0.578 13°	0.175 76°	0.635 22°
6.	4½" brick + 2" air space + 4½" brick	λ Mod. $-\phi$ Arg.	0.703 15°	0.569 40°	0.542 25°	0.482 28°	0.093 108°	0.506 27°
7.	2" reed board + 2" air space + 2" reed board	λ Mod. $-\phi$ Arg.	0.833 2°	0.513 27°	0.881 5°	0.099 15°	0.043 49°	0.934 4°
8.	9" brick + 2" air space + ½" plywood	λ Mod. $-\phi$ Arg.	0.719 14°	0.281 91°	0.531 5°	0.633 3°	0.073 112°	0.686 9°

arrangement of the layers and their order (in the direction of heat flow) influence the overall thermal behaviour of the structural element. This effect was studied. The results, given in Table (7.4), clearly illustrate this effect on the transfer and driving point functions. If, insulating layers are also included the maximum damping occurs when the dense materials are used on the inner side. The decrement factors of the dense materials effect adversely when these are used as the outer layers.

7.9 Effect of the Direction of Heat Flow (Outside to Inside or Inside to Outside)

It is also interesting to know for a given composite construction, if the direction of the heat flow is reversed, how the decrement factors of individual layers and the over all thermal functions are affected. This has been studied for a half a dozen types of constructions and the results are given in Table (7.5). It is apparent that with the reversal of the heat flow directions (i.e., from inside to outside) for any given construction, the overall transfer function will be reduced by a ratio of h_o / h_i and the phase angle is not altered just as in the case of homogeneous elements. λ'_i is lower than the corresponding λ_o while ϕ'_i is higher than ϕ_o. The backing layers have considerable influence on the

TABLE 7.4

EFFECT OF THE ORDER OF LAYERS ON THE THERMAL SYSTEM FUNCTIONS (Fundamental)

$h_o = 3.5$
$h_i = 1.5$

	S. No.	Type of Construction		External Driving point Function	Transfer Function	Internal Driving point Function
A.	1.	½" plaster + 4½" brick + 1" F.C. + ½" plaster	λ Mod. -φ Arg.	0.778 17°	0.159 75°	0.722 13°
	2.	½" plaster + 4½" brick + 2" F.C. ½" plaster	λ Mod. -φ Arg.	0.756 31°	0.089 94°	0.776 15°
	3.	½" plaster + 4½" brick + 4" F.C. + ½" plaster	λ Mod. -φ Arg.	0.763 22°	0.047 120°	0.822 22°
	4.	½" plaster + 4½" brick + 1" T.C. + 1" plaster	λ Mod. -φ Arg.	0.734 24°	0.055 87°	0.923 18°
	5.	½" plaster + 4" dense Conc. + 2" F.C. ½" p	λ Mod. -φ Arg.	0.770 36°	0.113 33°	0.782 14°
	6.	½" plaster + 2" dense Conc. + 2" F.C. + ½" p	λ Mod. -φ Arg.	0.812 30°	0.136 60°	0.718 14°
B.		Reverse Order				
	1.	½" plaster + 1" F.C. + 4½" brick + ½" plaster	λ Mod. -φ Arg.	0.900 16°	0.112 84°	0.576 30°
	2.	½" plaster + 2" F.C. + 4½" brick + ½" plaster	λ Mod. -φ Arg.	0.934 12°	0.073 100°	0.622 23°
	3.	½" plaster + 4" F.C. + 4½" brick + ½" plaster	λ Mod. -φ Arg.	0.950 7°	0.034 128°	0.533 27°
	4.	1" plaster + 1" T.C. + 4½" brick + ½" plaster	λ Mod. -φ Arg.	0.934 10°	0.048 90°	0.570 24°
	5.	½" plaster + 2" F.C. + 4" dense conc. + ½" p	λ Mod. -φ Arg.	0.912 14°	0.086 94°	0.573 36°
	6.	½" plaster + 2" F.C. + 2" dense conc. + ½" p	λ Mod. -φ Arg.	0.916 7°	0.119 68°	0.573 32°

F.C. = Foamed concrete T.C. = Thermocole p = plaster

TABLE 7.5

EFFECT OF THE DIRECTION OF HEAT FLOW ON THE THERMAL SYSTEM FUNCTIONS (Fundamental)

$h_o = 3.5$
$h_i = 1.5$

S. No.	Type of Construction		Heat flow from outside to inside: Ext. Driving point function	Heat flow from outside to inside: Transfer function	Heat flow from inside to outside: Int. Driv. point function	Heat flow from inside to outside: Reverse Transfer function
1.	½" p + 9" brick + ½" p	λ Mod. -φ Arg.	0.744 17°	0.128 113°	0.500 26°	0.053 113°
2.	½" p + 4½" brick + 4" F.C. + ½" p	λ Mod. -φ Arg.	0.737 23°	0.047 120°	0.323 24°	0.020 120°
3.	½" p + 4" D.C. + 2" F.C. + ½" p	λ Mod. -φ Arg.	0.770 36°	0.113 36°	0.782 14°	0.048 86°
4.	1" p + 1" T.C. + 4½" brick + ½" p	λ Mod. -φ Arg.	0.934 10°	0.048 90°	0.570 34°	0.021 90°
5.	1½" F.C. + 2" jux board + 4½" brick + ½" p	λ Mod. -φ Arg.	0.934 15°	0.039 106°	0.511 24°	0.018 106°
6.	6" sandstone + 9" brick + ½" p	λ Mod. -φ Arg.	0.634 18°	0.047 170°	0.439 23°	0.020 170°
7.	3" lime conc. + 4" R.C.C. + ½" p	λ Mod. -φ Arg.	0.733 13°	0.200 78°	0.423 31°	0.036 78°
8.	2½" bricktile + 3" lime conc. + 4½" brick + ½" p	λ Mod. -φ Arg.	0.644 20°	0.037 124°	0.430 27°	0.037 124°

p = plaster F.C. = Foamed concrete D.C. = Dense concrete
T.C. = Thermocole R.C.C. = Reinforced cement concrete

decrement factors of the individual layers while front layers have no influence (viewed in the direction of heat flow). The decrement factor of the same layer is not same for either directions of heat flow. As a rule, the decrement factors for the same layer is lower, when the heat flows from inside to outside, than for the condition, of heat flow from outside to inside, if all the layers are of dense materials. If the insulating layers are also present the decrement factor of the layer located in front (viewed in the direction of heat flow) will have higher values.

7.10 Damping Across Individual Layers as Affected by Their Location

It was noted earlier that a given layer will have different damping properties depending upon its position with respect to other layers. In order to obtain a better understanding of the behaviour of different types of layers, as affected by their location, the decrement factors were determined for a few types of materials, with different locations. These are given in Table (7.6). It is clear from the above data, that the inner most layer or a combination of two or more layers (in the same order) is not affected by the layers placed above them (for heat flow from outside to inside). On the other hand, the inner layers affect the decrement factors of the upper layer

TABLE 7.6

DECREMENT FACTOR OF INDIVIDUAL LAYERS AS AFFECTED BY THEIR LOCATION
(Fundamental)

$h_o = 3.5$
$h_i = 1.5$

Sl. No.	Type of Construction		External Driving point function	Decrement Factor of Layers: 1st layer	2nd layer	3rd layer	4th layer	Transfer function
A.	BRICK							
1.	4½" brick	λ Mod. −φ Arg.	0.756 14°	0.447 28°	... ...	... ...	... ...	0.330 42°
2.	4½" brick + ½" plaster	λ Mod. −φ Arg.	0.756 12°	0.445 35°	0.942 1°	... ...	... ...	0.316 47°
3.	½" p + 4" F.C. + 4½" B.+ ½" p	λ Mod. −φ Arg.	0.950 7°	0.980 1°	0.098 86°	0.445 35°	0.938 1°	0.034 123°
4.	1" p + 1" T.C. + 4½" B. + ½" p	λ Mod. −φ Arg.	0.934 10°	0.983 2°	0.125 42°	0.443 35°	0.940 1°	0.048 90°
5.	½" p + 4½" B. + 4" F.C. + ½" p	λ Mod. −φ Arg.	0.766 22°	0.943 4°	0.650 45°	0.103 45°	0.938 1°	0.047 120°
6.	½" p + 4½" B. + 1" T.C. + 1" p	λ Mod. −φ Arg.	0.734 24°	0.915 8°	0.739 35°	0.125 16°	0.884 1°	0.055 87°
B.	CONCRETE							
1.	4" D.C. +	λ Mod. −φ Arg.	0.730 17°	0.552 23°	... ...	... ...	... ...	0.403 40°
2.	4" D.C. + ½" p	λ Mod. −φ Arg.	0.732 13°	0.545 30°	0.943 1°	... ...	... ...	0.376 43°
3.	½" p + 4" D.C. + ½" p	λ Mod. −φ Arg.	0.732 13°	0.960 4°	0.544 32°	0.942 1°	... ...	0.360 54°
4.	½" p + 2" F.C. + 4" D.C. + ½" p	λ Mod. −φ Arg.	0.912 14°	0.933 1°	0.186 53°	0.545 30°	0.940 1°	0.086 94°
5.	½" p + 4" D.C. + 2" F.C. + ½" p	λ Mod. −φ Arg.	0.770 26°	0.961 5°	0.798 29°	0.205 23°	0.938 1°	0.113 36°
6.	4" D.C. + 2" T.C.	λ Mod. −φ Arg.	0.735 24°	0.918 29°	0.066 1°	0... ...	... ...	0.044 54°
C.	FOAMED CONCRETE							
1.	2" F.C.	λ Mod. −φ Arg.	0.911 3°	0.216 12°	... ...	... ...	... ...	0.197 15°
2.	2" F.C.+ ½" p	λ Mod. −φ Arg.	0.911 3°	0.210 26°	0.941 1°	... ...	... ...	0.180 29°
3.	½" p + 2" F.C. + ½" p	λ Mod. −φ Arg.	0.911 7°	0.930 1°	0.210 26°	0.943 1°	... ...	0.177 34°
4.	½" p + 2" D.C. + 2" F.C. + ½" p	λ Mod. −φ Arg.	0.812 20°	0.964 2°	0.881 12°	0.210 26°	0.943 1°	0.136 60°
5.	½" p + 2" F.C. + 2" D.C. + ½" p	λ Mod. −φ Arg.	0.916 7°	0.935 1°	0.197 48°	0.712 12°	0.940 1°	0.119 63°
D.	PLYWOOD							
1.	½" p.w.	λ Mod. −φ Arg.	0.780 2°	0.622 3°	... ...	... ...	... ...	0.435 5°
2.	½" AC sheet + 1" I.B.+ ½" p.w.	λ Mod. −φ Arg.	0.932 3°	0.933 1°	0.375 12°	0.622 3°	... ...	0.207 19°
3.	[illegible]	λ Mod. −φ Arg.	0.[illegible] [illegible]	0.703 4°	0.531 5°	0.[illegible] 3°	0.257 ...	0.[illegible]7 [illegible]
4.	[illegible]	λ Mod. −φ Arg.	0.[illegible] 3°	[illegible] [illegible]	0.178 12°	0.[illegible] 3°	... ...	0.[illegible] [illegible]

p = plaster p.w. = plywood D.C. = dense concrete F.C. = foamed concrete A.C. = Asbestos cement
T.C. = [illegible]cole B = brick I.B. = Insulation board

to a considerable extent.

For example, a 4½ in. brick wall alone has a decrement factor (λ) of 0.447 and phase lag angle of 28°. When it is plastered inside (½ inch), λ is decreased to 0.445 and ϕ is increased to 35°. These values did not change when additional plaster or other layers are placed on the external side. But when additional insulation layers are placed on the inner side the λ for the brick section is increased to 0.739 and ϕ is increased to 41°. Other materials also behaved similarly.

7.11 Equivalent Homogeneous Construction of Composite Structures

Though the transfer and driving point function data given in Appendix (IV) covers most of the commonly used composite constructions, there can be many more combinations possible. Any new specific case will have to be studied afresh. Moreover, the physical properties of the materials used in these studies are average values only. The variations in their properties should also be accounted for. This may be simplified by determining the equivalent homogeneous construction, which has the same decrement factor (λ i) and phase lag (ϕ i) that of the composite construction. The two thermal properties necessary to determine the equivalent homogeneous construction are

i) equivalent thermal resistance R (eq)

and ii) equivalent thermal capacitance C (eq)

The equivalent resistance is obtained simply by adding all the resistances of the individual layers i.e., $\sum_{n=1}^{n=n} R$. Mackey and Wright (75) have given an empirical relation for the determination of the equivalent (kρs)(eq) for periodic heat flow conditions. Stewart (76) pointed out that it is difficult to establish limits for the empirical equations derived by Mackey and Wright. Bruckmayer (77) had also derived equations for equivalent capacity brick wall, based on Krischers equations (78) for free cooling of structures (transient response). Hofbauer (79) has derived equations for half value time for multilayered constructions and related it with Bruckmayer's equivalent capacity brick wall. The equivalent (RC) eq and hence the equivalent (C) eq can be obtained from these equations.

The greatest advantage of these equivalent homogeneous R_{eq} and C_{eq} is that the same set of charts of thermal functions prepared for homogeneous constructions, given in Chapter 6, can be utilised for obtaining these functions for any composite constructions, whatever be the number, type and order of the layers.

Skhlover (26) questioned the validity of these empirical relations and doubted the possibility of having an equivalent homogeneous construction which will under all circumstances, have the same damping and phase shift.

Although these methods yield approximate values, they are worth the effort as they enable a quick estimation of all the thermal functions and provide general solutions, provided the methods adopted for the calculation of the equivalent RC_{eq} are reliable.

Mackey and Wright have checked the validity of their empirical relations by comparing the decrement factors for λi and ϕi only with the analytical solutions. As the periodic heat flow characteristics of a building element are described by a set of three thermal functions, the validity of the equivalent homogeneous computational methods, should also be checked for the driving point functions. This check has been made for 10 types of composite constructions covering layers made of conventional and insulating materials. The equivalent R and RC for these constructions were calculated both by Mackey and Wright and Bruckmayers equations. The thermal functions were read from the respective charts (given in Chapter 6). These were compared with the corresponding functions determined by the analogue method. As a further check these thermal functions were computed by Matrix method also. In the matrix method the overall transmission matrix is obtained by the matrix multiplication of the transfer matrices of the individual layers, in the order of heat flow direction. The transfer functions and the driving point functions were determined with the equations given in Appendix (ii). The results obtained by the above four methods are compared in Table (7.7). From the table it can be seen that the analogue and Matrix values agree closely, as expected. However, results obtained by Mackey and Wright equations are only approximate and are useful only with layers of dense materials. The deviations become too large especially in phase lag angles when insulating layers are present and the method becomes unreliable. Bruckmayers (77) equations also do not hold good for composite constructions which include insulating materials. From these studies it is apparent that as pointed out by Shklover (23) it is not always possible to obtain an equivalent homogeneous construction, which gives the same thermal system functions, of a composite building element under all circumstances.

TABLE 7.7

COMPARISON OF THE THERMAL SYSTEM FUNCTIONS OBTAINED BY EQUIVALENT HOMOGENEOUS, ANALOGUE AND MATRIX METHODS
(Fundamental)

$h_o = 3.5$
$h_i = 1.5$

S. No.	Type of Construction	Thermal system function	Mackey and Wright Formula Modulus	Mackey and Wright Formula Arg. in deg	Bruckmayer Formula Modulus	Bruckmayer Formula Arg. in deg	Analogue Method Modulus	Analogue Method Arg. in deg	Matrix Method Modulus	Matrix Method Arg. in deg.
1.	½" p + 9" B + ½" p		0.740	16	0.710	16	0.744	17	0.733	13
			0.123	103	0.125	108	0.123	113	0.133	110
			0.530	21	0.420	35	0.509	23	0.522	23
2.	3" B. + 2" air space + 3" B		0.805	11	0.810	11	0.773	10	0.781	12
			0.170	63	0.165	73	0.175	73	0.179	75
			0.625	19	0.600	10	0.635	22	0.644	20
3.	6" sand stone + 9" brick + ½" plaster		0.720	16	0.690	16	0.634	18	0.642	16
			0.050	150	0.036	176	0.047	170	0.045	166
			0.490	24	0.460	25	0.489	23	0.468	27
4.	3" L.C. + 4" R.B. + ½" p		0.740	15	0.740	15	0.733	13	0.719	13
			0.175	84	0.170	84	0.182	78	0.184	70
			0.535	24	0.520	24	0.489	28	0.500	23
5.	½" p + 8" e.s.c. + ½" p		0.850	8	0.820	8	0.839	11	0.865	11
			0.031	118	0.059	125	0.035	115	0.034	114
			0.670	16	0.700	16	0.639	23	0.670	21
6.	½" p + 4½" B. + 4" F.C. + ½" p		0.870	7	0.910	6	0.763	22	0.736	20
			0.027	155	0.055	93	0.047	127	0.040	132
			0.740	15	0.800	11	0.822	22	0.812	20
7.	1" p + 1" T.C. + 4½" B. + ½" p		0.850	7	0.840	8	0.934	10	0.933	9
			0.037	137	0.018	180	0.043	90	0.046	87
			0.763	13	0.390	16	0.670	34	0.533	32
8.	2" T.C. + 4" D.C.		0.930	5	0.890	7	0.939	1	0.959	1
			0.013	150	0.005	236	0.031	69	0.034	63
			0.795	11	0.760	13	0.544	39	0.540	39
9.	2" D.C. + 2" T.C. + 2" D.C.		0.950	4	0.920	5	0.921	16	0.913	15
			0.023	112	0.015	180	0.043	65	0.041	60
			0.830	8	0.820	10	0.753	32	0.750	31
10.	½" AC sheet + 1" m.w. + ½" p.w.		0.900	3	0.900	3	0.944	2	0.948	2
			0.187	14	0.136	22	0.193	21	0.193	23
			0.810	4	0.790	8	0.834	8	0.854	9

p = plaster p.w. = plywood D.C. = Dense concrete L.C. = Lime concrete R.B. = Reinforced brick
e.s.c. = Expanded slag concrete F.C. = foamed concrete B. = brick m.w. = mineral wool
T.C. = Thermocole A.C. = Asbestos cement.

CHAPTER 8

A METHOD FOR THE PREDICTION OF INDOOR AIR TEMPERATURES OF ENCLOSURES

CHAPTER 8

A METHOD FOR THE PREDICTION OF INDOOR AIR TEMPERATURE OF ENCLOSURES

8.1 Introduction

Chapters 6 and 7 deal with the transfer and driving point functions of a large number of common building elements (homogeneous and composite) which provide a quick means of comparing their thermal efficiencies. Criteria for the choice of a building component mostly consists of (i) Low 'U' values, (ii) Low transfer function (λi) value, and (iii) Low internal driving point transfer function ($\lambda' i$). Such a choice will result in lower cooling loads for air conditioning and better thermal behaviour of unconditioned buildings. For a quantitative estimation, of the indoor air temperature, where due allowance has to be made for fluctuations of climate and variations in design a computational method using the above data is required.

Mathematical methods have been developed by Muncey (25) Shklover (26) and Harmott (27). Muncey has shown that the mathematical treatment of van Gorcum (20) could be extended to a complete building. Shklover and Harmott, by applying the symbolic calculus techniques have developed methods for the estimation of indoor air temperatures of unconditioned buildings. But these computational procedures are quite involved and time consuming. Electrical analogue techniques have also been employed (48, 80) for the determination of indoor air temperatures. In these methods, the room with all its structural components, was simulated on the analogue model, coupled with proper radiative and convective resistances at the inner surfaces. The network with all the inputs provided by specially designed function generators at various boundaries becomes complex experimentally and economically. One such network arrangement is illustrated in Fig. (8.1). Another disadvantage of this method is that any specific variation in any one factor had to be represented on the analogue and studied separately. Since one comes across, quite a large number of individual variations of climate and design, such a method of analogue representation is not feasible to attain generalised solutions and some simpler and more flexible methods are to be aimed at.

A computational method utilising the (pre-tabulated) analogue transfer and driving point functions is given here. As buildings are subjected to periodic temperature and solar radiation, the indoor air temperature variations of enclosures are also

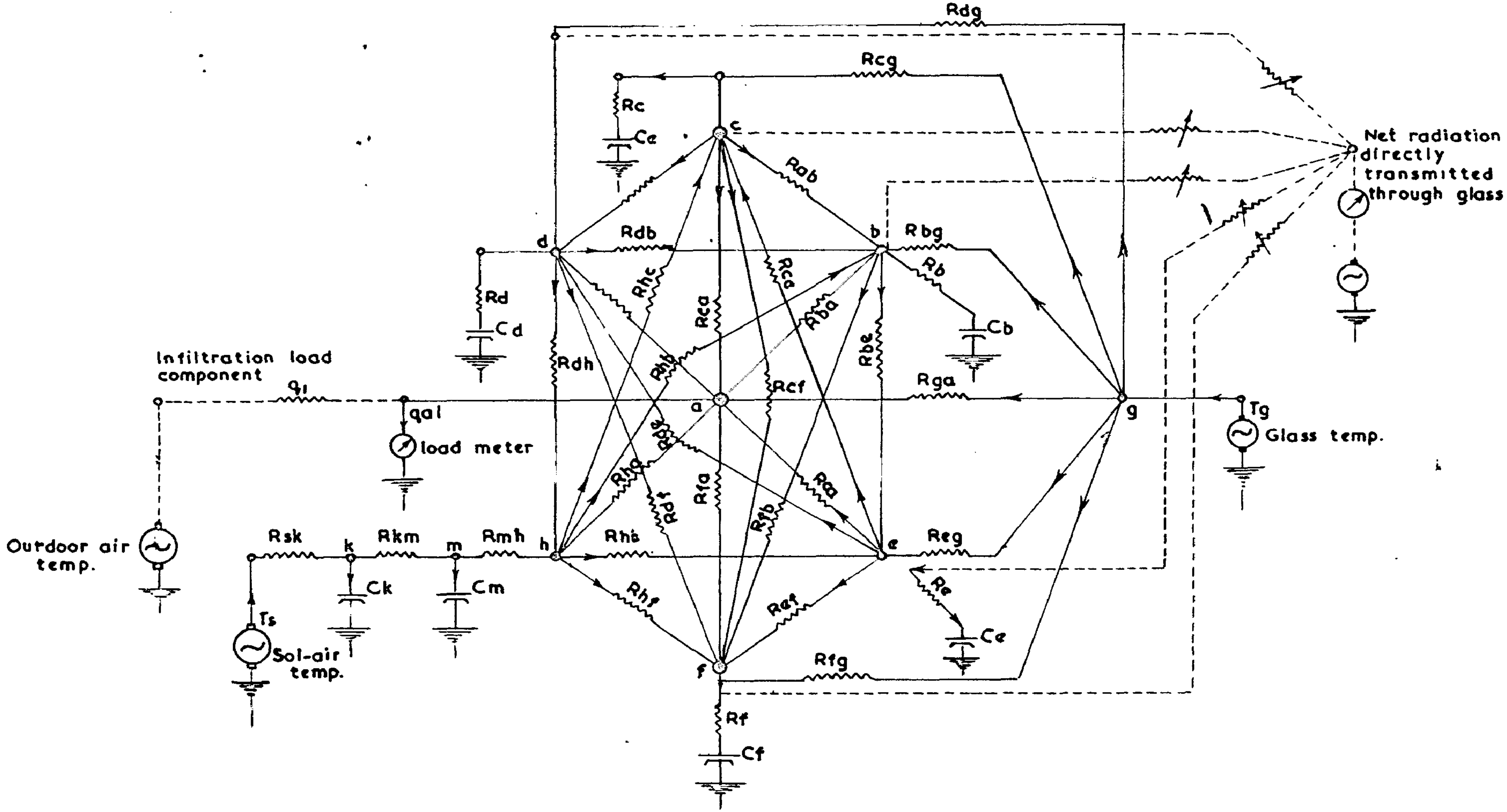

THERMAL CIRCUIT FOR A ROOM

FIG. 8·1

periodic. These can be represented by Fourier series.

$$t_{ia}(\mathcal{T}) = t_{ia}(\text{mean}) + \sum_{n=0}^{\infty} t_{ia\,n} \, \text{Cos}(\omega_n t - \xi_n) \quad (1)$$

Determination of $t_{ia}(\mathcal{T})$ consists of two parts viz., (i) determination of the steady state temperature (t_{ia} (mean)) and (ii) the determination of the harmonic components.

8.2 <u>Determination of the Mean Indoor Air Temperature</u>

The steady state heat flow (Q mean) through any building component 'k' due to the temperature differences between the mean sol-air temperature (t_{sa}(mean)) and the mean indoor air temperature (t_{ia}(mean)) is calculated from the equation (2)

$$Q_k(\text{mean}) = U_k \, A_k \left\{ t_{sa\,k}(\text{mean}) - t_{ia}(\text{mean}) \right\} \quad ..(2)$$

where U_k is the steady state over all thermal transmission coefficient of the building element in Btu/sq.ft./Hr/$^{\circ}$F. A_k is the area of the exposed surface of the building element in sq.ft. The total steady state heat flow into the interior of a building, through all exterior bounding surfaces is obtained by the summation of all the individual quantities and is expressed by

$$Q(\text{mean})_{Total} = \sum Q_k \text{ mean} = \sum U_k A_k \left\{ t_{sa\ k}(\text{mean}) - t_{ia}(\text{mean}) \right\} \quad .. (3)$$

In order to satisfy the steady state heat balance conditions of the enclosure, the net heat gains of the enclosure should be zero i.e., the total heat gains of the enclosure should be equal to the total heat losses from it. If heat gains through ventilation and internal sources are also present, their steady state components are to be added to the total heat gains of the enclosure. Then the equation (3) becomes

$$Q(\text{mean}) = U_k A_k \left\{ t_{sa\ k}(\text{mean}) - t_{ia}(\text{mean}) \right\} + Q_s(\text{mean}) + Q_v(\text{mean}) \quad .. (4)$$

According to the conditions for heat balance the Q (mean) is to be equated to zero. Then we get

$$U_k A_k \left\{ t_{sa\ k}(\text{mean}) - t_{ia}(\text{mean}) \right\} + Q_s(\text{mean}) + Q_v(\text{mean}) = 0 \quad .. (5)$$

This gives the mean indoor air temperature as

$$t_{ia}(\text{mean}) = \frac{U_k A_k \left\{ t_{sa\ k}(\text{mean}) \right\} + Q_s(\text{mean}) + Q_v(\text{mean})}{U_k A_k} \quad .. (6)$$

8.3 Determination of the Harmonic Components of Indoor Air Temperature Variation

The next step is to determine the fundamental and higher harmonics of the indoor air temperature variations, which result from the harmonic heat flow through all the bounding elements. This can be solved in two steps, viz., (i) calculation of the heat flux entering the enclosure through each element due to the sol-air temperature variations of the exposed surfaces and (ii) calculation of the amount of heat flux absorbed by each internal surface due to indoor air temperature harmonic variation with unit amplitude, for the fundamental and higher harmonics.

i) The sinusoidal heat flux transmitted into the enclosed space through any exposed element k can be calculated, if the transfer admittance function Y_{ik} is known, by the equation

$$\vec{Q}_{n_k}(\tau) = \vec{t}_{sa\,nk} \quad A_{n_k}\,\vec{Y}_{in_k} \qquad \ldots (7)$$

where t_{sank} is the n th harmonic component of the sol-air temperature of the element k.

Y_{ink} is the transfer admittance of the n th harmonic for the same element k.

A_k is the exposed surface area of the element k.

$\overrightarrow{t_{sank}}$ and $\overrightarrow{Y_{ink}}$ are vectorial quantities which are expressed in polar co-ordinate form by

$$t_{sank} \angle \gamma_n \;,\; Y_{ink} \angle -\psi_{ink} \qquad \text{respectively.}$$

The total amount of heat flux entered into the enclosed space through all the exposed elements, for any harmonic, is obtained by summation of all the individual quantities of heat flux i.e.,

$$\overrightarrow{Q_n}(\tau) = \sum \overrightarrow{Q_{nk}}(\tau) = \sum \overrightarrow{t_{sank}}\ A_k\ \overrightarrow{Y_{ink}} \qquad ..(8)$$

Sol-air temperature variations will be different for different components of a building (i.e. roof, walls, door, windows etc.) even though the outside air temperature is the same. Hence their harmonic components will also have different amplitudes and phases. The summation of the heat flux quantities in equation (8) are to be carried out as complex additions. If any internal periodic heat source or heat flow due to ventilation are present, the harmonic components of their heat flux are to be added to the corresponding harmonic heat flux entering through all the exposed elements to obtain the over all heat flux entering the enclosure. This may be written as

$$\overrightarrow{Q_n}(\tau) = \sum \overrightarrow{Q_{nk}}(\tau) + \overrightarrow{Q_{ns}}(\tau) + \overrightarrow{Q_{nv}}(\tau) \qquad ..(9)$$

11) This heat flux received in the room,

will produce a temperature variation of the indoor air. Let the corresponding harmonic variation of the indoor air temperature be $\overrightarrow{t_{ian}}$. This harmonic temperature variation of the indoor air, will in turn induce harmonic heat flux in all the interior surfaces, including the partitions, furniture etc. The quantity of heat flux absorbed, at the inside surface by any building element k can be calculated if the internal driving point admittance function $\overleftarrow{Y'_{ink}}$ is known. The equation relating these quantities is given by

$$\overleftarrow{Q'_{nk}}(\tau) = \overleftarrow{t_{ian}} \quad A_k \quad \overleftarrow{Y'_{ik}} \qquad ..(10)$$

The total heat flux absorbed by all the interior surfaces of the enclosure is then obtained by summation of the individual quantities. This is expressed as

$$\overleftarrow{Q'_n}(\tau) = \sum \overleftarrow{t_{ian}} \quad A_k \quad \overleftarrow{Y'_{ink}} \qquad ..(11)$$

Since all the interior surfaces are in contact with the same air, the driving temperature t_{ian} will be same for all surfaces, and the equation (11) can be written as

$$\overleftarrow{Q'_n}(\tau) = \overleftarrow{t_{ian}} \sum A_k \quad \overleftarrow{Y'_{ink}} \qquad ..(12)$$

As the condition for heat balance should also be satisfied for each harmonic, the total amount of heat flux transmitted into the enclosure and that emitted by the internal periodic source, should be equal to the total heat flux absorbed by all the interior surfaces. This means

$$Q_n(\tau) = Q'_n(\tau)$$

i.e., $$\sum t_{oank} A_k Y_{ink} + Q_{ns} + Q_{nv} = t_{ian} \sum A_k Y'_{ink} \quad ..(13)$$

Then t_{ian} is obtained as

$$t_{ian} = \frac{\sum t_{oank} A_k Y_{ink} + Q_{ns} + Q_{nv}}{\sum A_k Y'_{ink}} \quad (14)$$

Thus for obtaining t_{ian}, transfer admittance functions and internal driving point admittance functions are required. These can be obtained from the transfer and driving point functions (amplitude decrement and phase lag angles of temperatures) by the following relations

$$\overrightarrow{Y_i} = h_i \overrightarrow{\lambda_i} \quad .. (15)$$

$$\overleftarrow{Y'_i} = h_i (1 - \overleftarrow{\lambda'_i}) \quad .. (16)$$

By combining the steady state temperature and the harmonic components, the Fourier equation for the periodic indoor air temperatures of any enclosure can be obtained as

$$t_{ia}(\tau) = t_{ia}(\text{mean}) + \sum t_{ian} \cos(\omega_n t - \xi_n) \quad .(17)$$

This method gives the indoor air temperature variations in terms of the thermal system functions, 'U' values and the sol-air temperatures. Any changes in the building components can be incorporated in the calculations taking its corresponding 'U' value and thermal system function, while changes in climatic and other factors like orientation, surface treatments etc. can also be incorporated by corresponding changes in sol-air temperature. In this method the radiation exchanges between the interior surfaces are not separately considered. The surface coefficients were taken as the resultant of radiative and convective transfer coefficients and the heat is directly transferred to the room air, from the interior surfaces.

8.4 Verification of the Method

To check the reliability of this method, the predicted temperatures were compared with the model measurements of Muncey (25). Muncey had used two models (i) a masonry one with heavy structural elements like brick, and (ii) a timber one with light structural parts. These models were subjected to the same external air temperature variation. The inside air temperatures were measured and computed by Matrix method. The physical properties of the materials of the model are given in Table (8.1). The 'U' values and the thermal transfer and driving point functions of the materials used determined by the analogue are

TABLE 8.1

PHYSICAL PROPERTIES OF THE MATERIALS USED IN THE MODELS

S. No.	Material	K	ρ	s
.	Brick	8.0	120	0.20
.	Concrete	10.0	150	0.20
.	Timber	1.0	50	0.30
.	Plywood	1.0	50	0.30
.	Mineral Wool	0.25	12	0.20
.	Cane Fibre Board	0.40	30	0.30
.	Glass	7.3	155	0.19

K = Thermal conductivity in Btu.in/Ft^2.Hr.^{o}F

ρ = Density in Lb/Ft^3

s = Specific heat in Btu/Lb.^{o}F

given in Table (3.2 and 3.3) for the two models respectively. As all the six sides were exposed to the same air temperature cycle, the mean inside air temperature of the models will be equal to the mean outside air temperature.

i.e., $t_{ia}(\text{mean}) = t_{oa}(\text{mean})$

The heat flux entering the model through each exterior element due to external temperature variations, for the fundamental and three higher harmonics were calculated from the equation (5) and given in column 'A' of tables (3.4 and 3.5). The heat flux absorbed by each internal surface per unit amplitude variation of internal air temperature for the fundamental and three higher harmonics were also calculated from the equation (9) and given in columns 'B' of the same tables (3.4 and 3.5). The summation of all items, in column 'A' will give the total heat flux entering the model

i.e., $\sum t_{oank} A_k Y_{ink} = Q_n$

and the summation of all the items in column 'B' will give the total heat flux absorbed by all interior surfaces of the model for unit amplitude harmonic variation of inside air temperature

i.e., $\sum A_k Y'_{ink} = \overleftarrow{Q'_n}$

If the resultant indoor air temperature variation had an amplitude t_{ian} then the total heat flux absorbed

TABLE 8.2

THERMAL FUNCTIONS AND 'U' VALUES OF THE COMPONENTS OF THE MASONRY MODEL

$h_o = 2.5$
$h_i = 1.4$

S. No.	Component	U value	Harmonic	Transfer Function: Modulus λ_i	Transfer Function: Arg $-\varphi_i$ in deg.	Internal Driving point Function: Modulus λ_i	Internal Driving point Function: Arg. $-\varphi_i'$ in deg.
1.	2" brick wall	0.735	F	0.056	132	0.122	40
			H_2	0.018	162	0.091	38
			H_3	0.008	200	0.076	36
			H_4	0.005	218	0.069	34
2.	2" concrete roof	0.760	F	0.046	130	0.100	44
			H_2	0.016	164	0.075	40
			H_3	0.007	208	0.062	40
			H_4	0.004	228	0.053	38
3.	1" timber floor	0.473	F	0.038	124	0.333	30
			H_2	0.034	134	0.230	32
			H_3	0.014	204	0.240	32
			H_4	0.007	226	0.213	30
4.	2" brick partition wall	0.595	F	..	..	0.123	40
			H_2	..	..	0.100	38
			H_3	..	..	0.030	36
			H_4	..	..	0.072	34
5.	1/16" glass window	0.800	F	0.598	18	0.333	20
			H_2	0.522	34	0.300	36
			H_3	0.434	44	0.253	46
			H_4	0.336	62	0.218	54

TABLE 8.3

THERMAL FUNCTIONS AND 'U' VALUES OF THE COMPONENTS OF THE TIMBER MODEL

h_o = 2.5
h_i = 1.4

S. No.	Component	U value	Harmonic	Transfer Function Modulus λ_i	Transfer Function Arg-ϕ_i in deg.	Internal Driving point Function Modulus λ'_i	Internal Driving point Function Arg -ϕ'_i in deg.
1.	1/8" plywood + 1" mineral wool + 1/3" plywood walls	0.186	F	0.062	120	0.600	36
			H_2	0.022	168	0.422	44
			H_3	0.009	234	0.322	48
			H_4	0.004	264	0.274	50
2.	2" Cane fibre board roof	0.277	F	0.065	120	0.511	22
			H_2	0.025	162	0.422	24
			H_3	0.014	224	0.378	24
			H_4	0.011	248	0.356	24
3.	1/3" plywood floor	0.877	F	0.534	20	0.339	16
			H_2	0.464	32	0.356	28
			H_3	0.422	42	0.312	34
			H_4	0.356	50	0.230	40
4.	1½" timber frame	0.424	F	0.066	140	0.366	30
			H_2	0.021	196	0.312	30
			H_3	0.007	224	0.272	23
			H_4	0.004	246	0.244	26
5.	1/16" Glass window	0.900	F	0.600	18	0.334	20
			H_2	0.522	34	0.300	36
			H_3	0.433	44	0.256	46
			H_4	0.367	52	0.218	54

TABLE 6.4

[illegible] HEAT FLUXES RECEIVED AND ABSORBED BY THE MASONRY MODEL AND THE [illegible] [illegible] AIR TEMPERATURES

S. No.	Construction	Fundamental A	Fundamental B	2nd Harmonic A	2nd Harmonic B	3rd Harmonic A	3rd Harmonic B	4th Harmonic A	4th Harmonic B
		$Fxh_1 \times \overrightarrow{\lambda_i}$	$Fxh_1 x(1- \overleftarrow{\lambda_i})$	$Fxh_1 \times \overrightarrow{\lambda_i}$	$Fxh_1 x(1- \overleftarrow{\lambda_i})$	$Fxh_1 \times \overrightarrow{\lambda_i}$	$Fxh_1 x(1- \overleftarrow{\lambda_i})$	$Fxh_1 x \overrightarrow{\lambda_i}$	$Fxh_1 x(1- \overleftarrow{\lambda_i})$
1.	2" brickwall 9.3 sq.ft.	-0.085-j0.54	11.77+j1.00	-0.23-j0.03	12.10+j0.75	-0.024+j0.035	12.20+j0.59	-0.047+j0.037	12.24+j0.53
2.	1" timber floor 7.1 sq.ft.	-0.400-j0.720	7.09+j1.66	-0.32-j0.09	7.59+j1.50	-0.125+j0.063	7.93+j1.30	-0.046+j0.037	8.16+j1.0
3.	2" concrete roof 7.1 sq.ft.	-0.230-j0.310	9.23+j0.70	-0.15-j0.05	9.37+j0.48	-0.033+j0.024	9.43+j0.40	-0.020+j0.030	9.53+j0.33
4.	1/10" glass window 1.7 sq.ft.	1.350-j0.65	1.65+j0.27	1.02-j0.70	1.90+j0.43	0.75 -j0.70	1.95+j0.45	0.40 -j0.69	2.00+j0.42
5.	2" brick wall (partition) 4.0 sq.ft.	...	5.05+j0.47	...	5.17+j0.34	...	5.20+j0.20	...	5.27+j0.23
	Total Heat Flow :	0.125-j2.02	34.79+j4.09	0.32-j0.92	33.03+j3.51	0.47-j0.59	30.77+j2.04	0.37 -j0.82	37.20+j2.40
		2.02 $\angle$-93°30'	35.0 $\angle$7°	0.975 $\angle$-70°49'	33.22 $\angle$5°30'	0.76 $\angle$-51°	30.90 $\angle$4°30'	0.94 $\angle$-63°30'	37.24 $\angle$3°49'
	Temperature amplitude and phase	0.057 $\angle$-93°30'		0.027 $\angle$-73°18'		0.021 $\angle$-55°33'		0.024 $\angle$-63°12'	

TABLE 6.5

HARMONIC HEAT FLUXES RECEIVED AND ABSORBED BY THE TIMBER MODEL AND THE RESULTANT INSIDE AIR TEMPERATURES

$h_o = 2.5$
$h_i = 1.4$

SI. No.	Construction	Fundamental A $F \times h_i \times \vec{\lambda}_i$	Fundamental B $F \times h_i \times (1 - \overleftarrow{\lambda'_i})$	2nd Harmonic A $F \times h_i \times \vec{\lambda}_i$	2nd Harmonic B $F \times h_i \times (1 - \overleftarrow{\lambda'_i})$	3rd Harmonic A $F \times h_i \times \vec{\lambda}_i$	3rd Harmonic B $F \times h_i \times (1 - \overleftarrow{\lambda'_i})$	4th Harmonic A $F \times h_i \times \vec{\lambda}_i$	4th Harmonic B $F \times h_i \times (1 - \overleftarrow{\lambda'_i})$
1.	1/8" plywood + 1" mineral wool + 1/8" plywood walls 5.9 sq.ft.	-0.28-j0.44	4.30+j2.80	-0.175-j0.04	6.80+j2.40	-0.048+j0.03	6.45+j2.05	-0.034+j0.003	6.80+j1.8
2.	1/8" plywood floor 7.6 sq.ft.	5.20-j1.80	6.70+j1.20	4.30-j2.70	7.30+j1.80	3.30-j3.00	7.80+j1.85	3.40 -j2.80	8.35+j1.80
3.	1" cane fibre board roof 7.6 sq.ft.	-0.34-j0.60	5.60+j2.00	-0.24-j0.03	6.50+j1.80	-0.105+j0.105	7.00+j1.60	-0.004+j0.01	8.50+j0.80
4.	1½" timber frame 3.4 sq.ft.	-0.24-j0.20	3.30+j0.88	-0.023+j0.023	3.60+j0.75	-0.021+j0.021	3.65+j0.60	-0.003+j0.017	3.70+j0.50
5.	1/16" glass window 1.7 sq.ft.	1.35-j0.45	1.67+j0.37	1.03 -j0.70	1.82+j0.43	0.75 -j0.70	1.97+j0.45	0.40 -j0.69	2.10+j0.42
Total Heat Flow :		5.72-j3.59	21.57+j7.22	4.51 -j3.49	24.82+j7.18	3.88 -j3.52	26.97+j6.55	2.86 -j3.50	30.45+j5.12
		6.63 ∠-32°12'	22.73 ∠18°30'	5.70 ∠-35°43'	25.82 ∠16°12'	5.25 ∠-42°18'	27.8 ∠13°42'	4.51 ∠-52°56'	30.9 ∠9°30'
Temperature amplitude and phase.		0.29 ∠-50°42'		0.22 ∠-62°		0.19 ∠-83°		0.146 ∠-60°30'	

will be

$$t_{ian} \sum A_k \quad Y'_{ink}$$

To satisfy the heat balance equation the sums of column 'A' and the product of t_{ia} and the sum of the column 'B' should be equal for each harmonic.

Then $\vec{Q}_n = \overleftarrow{t_{ian}} \, \overleftarrow{Q'_n}$

where $\vec{Q}_n = Q_n \angle -\theta'_n$. and $Q'_n = Q'_n \angle -\theta''_n$

This gives $t_{ian} = \dfrac{Q_n}{Q'_n}$

The term Q_n/Q'_n will give the amplitude of the harmonic temperature variation and $-(\theta'_n - \theta''_n)$ gives the phase lag. By dividing the total of column 'A' by the total of column 'B' for each harmonic, the amplitude and phase of the indoor air temperature variation are obtained. The amplitudes and phases for the fundamental and higher harmonics, obtained by the above procedure are also given in Tables (8.4 and 8.5). The Fourier equations of the inside air temperatures for the models are obtained as

i) Masonry Model

$$\begin{aligned} t_{ia}(\tau) = 24.05 &+ 1.14 \, \mathrm{Cos}(1\omega t - 115^\circ) \\ &+ 0.06 \, \mathrm{Cos}(2\omega t - 100^\circ) \\ &+ 0.09 \, \mathrm{Cos}(3\omega t - 210^\circ) \\ &+ 0.02 \, \mathrm{Cos}(4\omega t - 215^\circ) \end{aligned} \quad ..(18)$$

ii) Timber Model

$$\begin{aligned} t_{ia}(\tau) = 24.05 &+ 5.8 \, \mathrm{Cos}(\omega t - 72^\circ) \\ &+ 0.40 \, \mathrm{Cos}(2\omega t - 85^\circ) \\ &+ 0.66 \, \mathrm{Cos}(3\omega t - 220^\circ) \\ &+ 0.20 \, \mathrm{Cos}(4\omega t - 218^\circ) \end{aligned} \quad ..(19)$$

By synthesising the above Fourier equations, the time temperature variations of the indoor temperatures were obtained and are compared with the measured and Matrix calculated values (Muncey) in Figs. (8.2 and 8.3) for Masonry and Timber Models respectively. The analogue predicted results found to be in close agreement with the Matrix calculated values than the measured ones, as expected. The deviations from the measured temperatures are due to the assumptions made in theory and are less significant, than what they appear to be, in view of the fact that the thermal properties of the materials could vary between wide limits. The main advantage of this method is the flexibility and ease of computation. The effect of almost any factor can be evaluated with a little additional effort. This is possible because it utilises a set of thermal system functions, which have been tabulated for a large number of commonly used structural elements and these transfer functions are not affected by the external climatic variations, as these are dependent only on the frequency of the wave form, but not on the amplitude. By adopting this procedure there is no need to represent the building as a whole on the analogue model and hence the experimental part also is very much simplified and less expensive. This method is particularly suited for generalised design problems, where a quantitative knowledge of the improvement in the thermal efficiency versus economic factors, as affected by design variations, is of great practical importance.

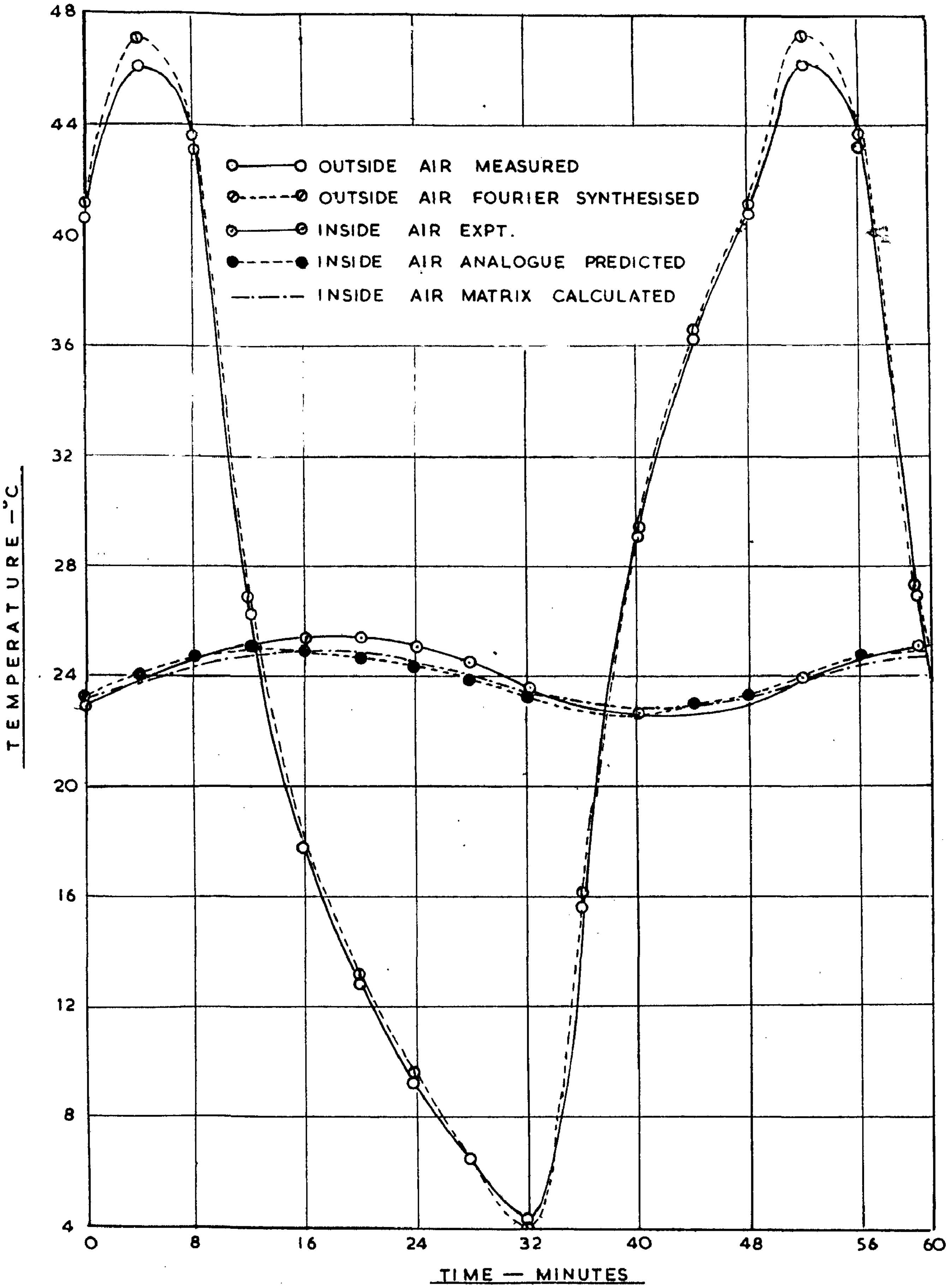

COMPARISION OF INSIDE AIR TEMPERATURES OF MASONRY MODEL

FIG. 8·2

C H A P T E R 9

APPLICATION OF THE THERMAL SYSTEM FUNCTION DATA TO DESIGN PROBLEMS

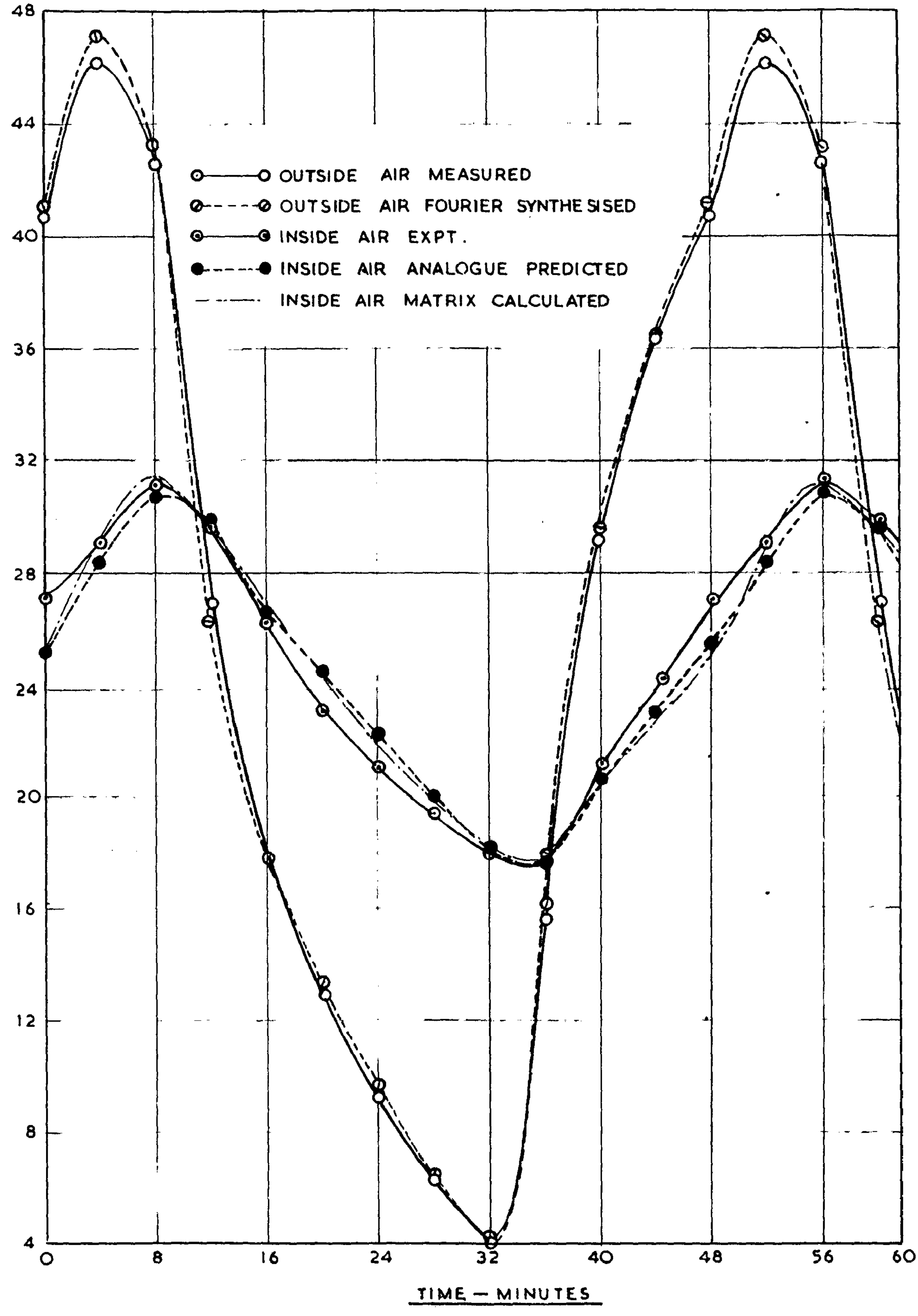

COMPARISION OF INSIDE AIR TEMPERATURES OF TIMBER MODEL

FIG. 8·3

C H A P T E R 8

APPLICATION OF THE THERMAL SYSTEM FUNCTION DATA TO DESIGN PROBLEMS

CHAPTER 9

APPLICATIONS OF THE THERMAL SYSTEM FUNCTION DATA TO DESIGN PROBLEMS

9.1 Introduction

In the last Chapter (8) it has been shown that the analogically obtained, thermal system function data, for individual elements, can directly be applied for the prediction of indoor air temperatures with reasonable accuracy. The transfer and driving point function data also provide a quick and realistic estimates of cooling loads of the fabrics for air-conditioned buildings, taking the internal masses also into account.

The method described is highly flexible. The effects of many factors, such as, the type of materials and their combinations, design features, orientation surface colour treatments, regional and seasonal climatic variations, partitions, insulation and shading of roof, walls, windows and ventilation etc. on thermal efficiency, for both conditioned and unconditioned buildings can be evaluated with minimum effort.

A few typical applications of the transfer and driving point function data in solving the above mentioned problems are illustrated in this chapter.

9.2 Effect of Orientation on Indoor Air Temperatures

For evaluating the effect of orientation on the indoor air temperature variation a room of dimensions 30' x 20' x 12' has been considered (Fig.9.1(a). Physical properties and constants are given in Table 9.1. The doors and windows are also considered to be made of a construction which has the same U value and transfer and driving point functions as that of the walls. The surface absorption coefficient of wall exterior surfaces are taken as 0.5 while for the roof as 0.1. Roof being flat the sol-air temperatures of the roof will not be affected by orientation. Two orientations one with long walls facing East-West and another with long walls facing South-North have been considered. The example has been worked out for a place situated on a latitude of 29°N and for a typical summer day (May 16th). For these conditions, the sol-air temperatures were calculated. The sol-air temperature curves obtained for roof, and walls are shown in Fig. (9.2). These were harmonically analysed and their Fourier equations are in Table (9.2).

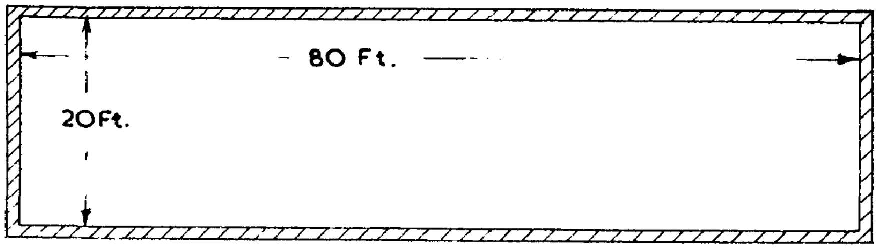

1. WALLS — 1/2" Plaster + 9" Brick + 1/2" Plaster
2. ROOF — 3" Lime Concrete + 4" R.C.C. + 1/2" Plaster
3. FLOOR — 1½" D.C. + 3" L.C. + 6" H.C. + 20" Soil.
4 HEIGHT — 12 FT.

ROOM CONSIDERED FOR THE ILLUSTRATIVE EXAMPLES FOR ORIENTATION

FIG. 9·1 (a)

C.-FOAMED CONC.
C.-DENSE CONC.
C.-THERMOCOLE
C.-HARD CORE
C.-LIME CONC.
B -REINFORCED BRICK.

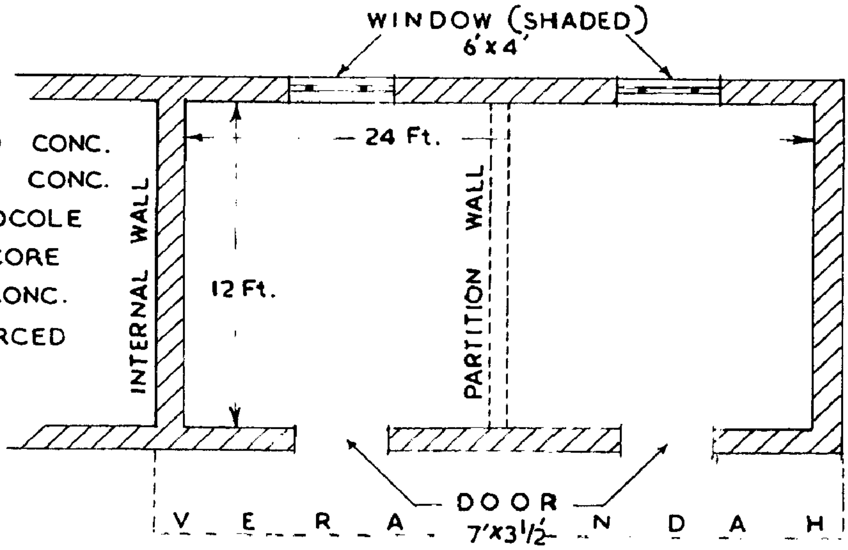

WINDOWS — 1/8" Glass

DOORS — 1½" Teak wood.

1. WALLS — 1/2" Plaster + 9" Brick + 1/2" Plaster
2. ROOF — (i) 3" Lime Concrete + 4" R.C.C. + 1/2" Plaster
   (ii) 1/2" Plaster + 2" F.C. + 4" R.C.C. + 1/2" Plaster
   (iii) 1" Plaster + 1" T.C. + 4½" R.B. + 1/2" Plaster
3. FLOOR — 1/2" D.C. + 3" L.C. + 6" H.C. + 20" Soil
4. HEIGHT — 10 Ft.

ROOM CONSIDERED FOR OTHER ILLUSTRATIVE EXAMPLES

FIG. 9·1 (b)

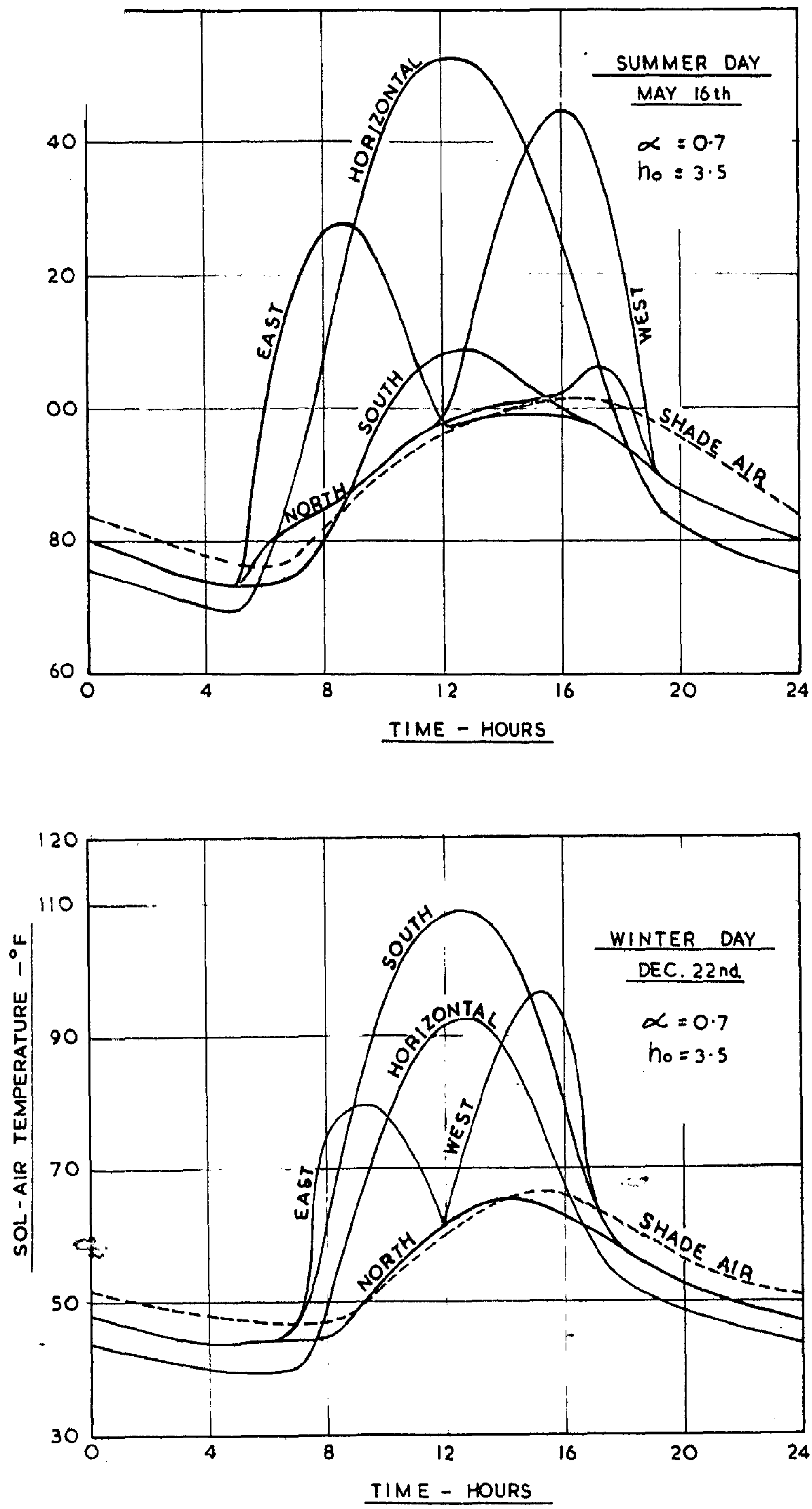

SOL-AIR TEMPERATURES OF DIFFERENTLY ORIENTED SURFACES (LAT-29°N)

FIG. 9·2

TABLE 9.1

PHYSICAL PROPERTIES OF THE MATERIALS TAKEN IN THE EXAMPLES

S. No.	Material	K	ρ	s
1.	Brick	6.0	100	0.21
2.	Plaster	12.0	120	0.32
3.	Teakwood	1.2	40	0.39
4.	Thermocole	0.20	1	0.32
5.	Dense Concrete	8.0	120	0.21
6.	Foamed Concrete	0.75	30	0.25
7.	Lime Concrete	6.0	106	0.20
8.	Hard Core	7.0	110	0.20
9.	Soil	8.0	110	0.20
10.	Glass	6.6	160	0.16

K = Thermal conductivity in Btu.in/Ft^2.Hr.^{o}F

ρ = Density in Lb/Ft^3

s = Specific heat in Btu/Lb.^{o}F

TABLE 9.1

PHYSICAL PROPERTIES OF THE MATERIALS TAKEN IN THE [illegible]

S. No.	Material	K	ρ	s
1.	Brick	6.0	100	0.21
2.	Plaster	12.0	120	0.32
3.	Teakwood	1.2	40	0.39
4.	Thermocole	0.20	1	0.32
5.	Dense Concrete	8.0	120	0.21
6.	Foamed Concrete	0.75	30	0.25
7.	Lime Concrete	6.0	106	0.20
8.	Hard Core	7.0	110	0.20
9.	Soil	8.0	110	0.20
10.	Glass	6.6	160	0.16

K = Thermal conductivity in Btu.in/Ft^2.Hr.^oF

ρ = Density in Lb/Ft^3

s = Specific heat in Btu/Lb.^oF

TABLE 9.2

OUTDOOR AIR AND SOL-AIR TEMPERATURE FOURIER EQUATIONS $\alpha = 0.7$

$h_0 = 3.5$

A. SUMMER DAY (MAY 16TH)

1. Flat Roof	104.7 + 40.1 Cos (15 t - 194°) + 13.9 Cos (30 t - 3°) + 1.7 Cos (45 t - 57°) + 2.2 Cos (60 t - 345°)
2. East Wall	95.1 + 17.6 Cos (15 t - 176°) + 10.6 Cos (30 t - 255°) + 0.4 Cos (45 t - 14°) + 3.3 Cos (60 t - 54°)
3. West Wall	95.1 + 29.8 Cos (15 t - 234°) + 12.2 Cos (30 t - 103°) + 10.8 Cos (45 t - 43°) + 10.5 Cos (60 t - 169°)
4. South Wall	83.8 + 14.6 Cos (15 t - 203°) + 5.3 Cos (30 t - 9°) + 2.0 Cos (45 t - 135°) + 0.6 Cos (60 t - 273°)
5. North Wall	88.4 + 14.8 Cos (15 t - 229°) + 0.0 Cos (30 t - 115°) + 2.8 Cos (45 t - 39°) + 1.5 Cos (60 t - 337°)
6. Shade Air Temperature	80.0 + 10.1 Cos (15 t - 249°) + 1.5 Cos (30 t - 1°) + 1.7 Cos (45 t - 60°) + 0.0 Cos (60 t - 235°)

B. WINTER DAY (DEC. 22ND)

1. Flat Roof	57.2 + 22.3 Cos (15 t - 109°) + 11.8 Cos (30 t - 13°) + 3.3 Cos (45 t - 170°) + 0.3 Cos (60 t - 170°)
2. East Wall	53.8 + 12.5 Cos (15 t - 160°) + 4.7 Cos (30 t - 305°) + 5.0 Cos (45 t - 83°) + 4.1 Cos (60 t - 189°)
3. West Wall	50.8 + 17.7 Cos (15 t - 230°) + 10.4 Cos (30 t - 77°) + 6.5 Cos (45 t - 302°) + 5.4 Cos (60 t - 183°)
4. South Wall	66.6 + 30.4 Cos (15 t - 190°) + 13.9 Cos (30 t - 13°) + 2.3 Cos (45 t - 6°) + 1.8 Cos (60 t - 353°)
5. Shade Air Temperature	56.4 + 11.4 Cos (15 t - 232°) + 1.7 Cos (30 t - 46°) + 0.3 Cos (45 t - 190°) + 0.5 Cos (60 t - 347°)
6. North Wall	52.7 + 9.9 Cos (15 t - 229°) + 3.5 Cos (30 t - 53°) + 0.7 Cos (45 t - 193°) + 0.5 Cos (60 t - 277°)

C. FLAT ROOF - SUMMER DAY (MAY 16TH) $h_0 = 3.5$

1. $\alpha = 0.1$	83.2 + 13.6 Cos (15 t - 219°) + 6.8 Cos (30 t - 5°) + 1.3 Cos (45 t - 31°) + 0.8 Cos (60 t - 223°)
2. $\alpha = 0.3$	89.1 + 21.9 Cos (15 t - 337°) + 6.9 Cos (30 t - 5°) + 1.5 Cos (45 t - 75°) + 1.3 Cos (60 t - 207°)
3. $\alpha = 0.5$	95.8 + 30.3 Cos (15 t - 193°) + 7.2 Cos (30 t - 60°) + 1.6 Cos (45 t - 65°) + 4.0 Cos (60 t - 157°)
4. $\alpha = 0.9$	109.4 + 49.7 Cos (15 t - 191°) + 17.4 Cos (30 t - 2°) + 2.9 Cos (45 t - 55°) + 4.6 Cos (60 t - 7°)

The outside and inside surface coefficients are taken as 3.5 and 1.5 Btu/sq.ft./Hr/°F respectively. The 'U' values and the transfer and driving point admittance functions for the walls, roof and floor are given in Table (9.3). The steady state and harmonic heat flow rates, through each building element into the room and the heat absorption at the inside surfaces of all the bounding elements of the room, and the mean room air temperature and the amplitudes of the harmonic components, were determined by the procedure as outlined in Chapter (8). The Fourier representation of the indoor air temperatures for the two orientations are given below :

South Orientation

$$t_{ia}(\tau) = 83.6 + 2.45\ \mathrm{Cos}(15\omega t + 23^{\circ}) + 0.25\ \mathrm{Cos}(30\omega t + 197^{\circ}) + 0.07\ \mathrm{Cos}(45\omega t + 190^{\circ}) + 0.03\ \mathrm{Cos}(60\omega t + 330^{\circ})$$

West Orientation

$$t_{ia}(\tau) = 83.4 + 2.3\ \mathrm{Cos}(15\omega t + 27^{\circ}) + 0.2\ \mathrm{Cos}(30\omega t + 210^{\circ}) + 0.16\ \mathrm{Cos}(45\omega t + 118^{\circ}) + 0.05\ \mathrm{Cos}(60\omega t + 333^{\circ})$$

The hourly indoor air temperature variations obtained are shown in Fig. (0.3). This example clearly demonstrates the advantage of facing the long walls in South-North (orientation). The advantage of this orientation will be more marked, for buildings, with

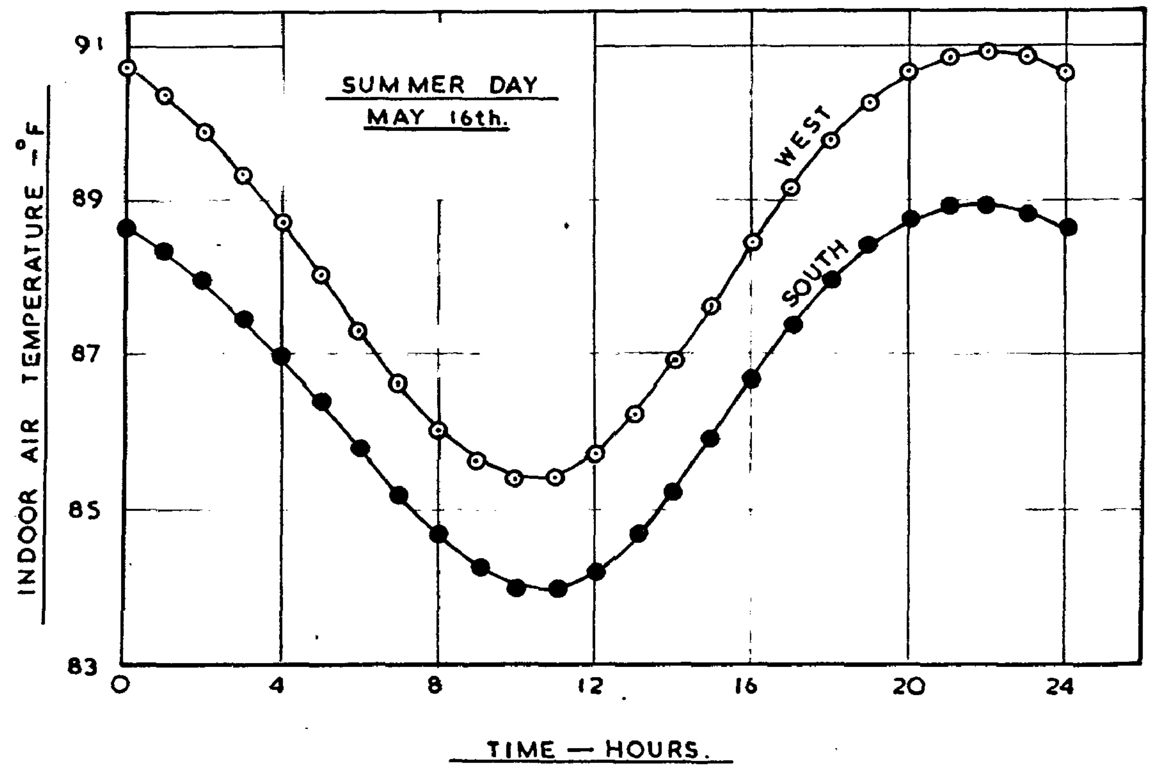

FIG. 9·3. EFFECT OF ORIENTATION ON INDOOR AIR TEMPERATURES

$h_o = 3.5$

$h_1 = 1.5$

S. No.	...co	4th Harmonic: Transfer admittance function: Modulus y_i	Arg. in deg. $-\psi_i$	Internal driving point admittance function
1.				
a)	0.248	0.066	160	1.219+j0.233
b)	0.240	0.030	160	1.020+j0.201
c)	0.285	0.014	202	1.165+j0.279
2.	0.284	0.026	228	1.104+j0.273
3.	0.244	...	..	1.169+j0.226
4.	0.316	0.010	254	1.164+j0.301
5.	0.179	0.393	40	0.016+j0.185
6.	0.027	1.035	5	1.034+j0.032
7.	0.320	...	..	1.150+j0.303

TABLE 9.3

TRANSFER AND DRIVING POINT ADMITTANCE FUNCTIONS OF THE CONSTRUCTIONS USED IN THE EXAMPLES
(Fundamental)

$h_o = 9.5$

$h_i = 1.5$

S. No.	Construction	U value	Fundamental: Transfer admittance function: Modulus Y_i	Fundamental: Transfer admittance function: Arg. in deg $-\psi_i$	Fundamental: Internal Driving point admittance function	2nd Harmonic: Transfer admittance function: Modulus Y_i	2nd Harmonic: Transfer admittance function: Arg. in deg $-\psi_i$	2nd Harmonic: Internal driving point admittance function	3rd Harmonic: Transfer admittance function: Modulus Y_i	3rd Harmonic: Transfer admittance function: Arg. in deg $-\psi_i$	3rd Harmonic: Internal driving point admittance function	4th Harmonic: Transfer admittance function: Modulus Y_i	4th Harmonic: Transfer admittance function: Arg. in deg. $-\psi_i$	4th Harmonic: Internal driving point admittance function
1.	ROOFS													
a)	3" lime concrete + 4" R.C.C. + ½" plaster	0.602	0.300	78	0.867+j0.325	0.160	116	1.116+j0.279	0.100	140	1.184+j0.248	0.066	160	1.218+j0.233
b)	½" plaster + 3" foamed concrete + 4" R.C.C. + ½" plaster	0.283	0.117	80	0.723+j0.376	0.069	104	0.921+j0.323	0.046	123	0.975+j0.280	0.030	160	1.020+j0.301
c)	½" plaster + 1" thermocole + 4½" R.B. + ½" plaster	0.247	0.063	83	0.856+j0.447	0.063	110	0.950+j0.333	0.021	164	1.110+j0.336	0.014	202	1.155+j0.279
2.	WALLS													
	½" plaster + 9" brick + ½" plaster	0.323	0.104	103	0.916+j0.462	0.037	152	1.064+j0.333	0.046	200	1.137+j0.304	0.023	828	1.164+j0.273
3.	FLOOR													
	1½" concrete + 3" lime concrete + 6" hardcore + 20" soil	0.200	...	..	0.863+j0.318	...	..	1.032+j0.273	0..	..	1.112+j0.244	...	..	1.169+j0.225
4.	[illegible]													
	½" plaster + [illegible] brick + ½" plaster	0.345	0.117	123	0.864+j0.337	0.044	174	1.032+j0.340	0.020	234	1.111+j0.316	0.010	284	1.164+j0.301
5.	DOORS													
	1½" teakwood	0.502	0.490	13	0.516+j0.033	0.466	24	0.539+j0.080	0.434	32	0.595+j0.170	0.368	40	0.616+j0.185
6.	WINDOWS													
	1/8" glass	1.025	1.035	..	1.034+j0.016	1.035	3	1.034+j0.021	1.036	4	1.030+j0.037	1.035	5	1.034+j0.032
7.	PARTITION WALL													
	½" plaster + 9" brick + ½" plaster	0.345	...	..	0.809+j0.420	...	..	1.031+j0.248	...	..	1.080+j0.330	...	..	1.153+j0.303

R.B = Reinforced Brick   R.C.C. Reinforced Cement Concrete.

sloping roofs than with flat ones especially for a large length to breadth ratio.

9.3 Effect of Seasonal Variations on Indoor Air Temperatures

For evaluating the thermal behaviour of any building in different seasons, at any particular geographical location, a single room structure, shown in Fig. (9.1(b) was considered. The physical properties of the materials are given in Table (9.1). The 'U' values and the transfer functions and driving point admittance of the structural elements are given in Table (9.3). A typical summer day (May 16th) and a winter day (Dec. 22nd) have been taken. The orientation is fixed as South. The windows were considered to be completely shaded from the sun and no direct solar radiation penetrates into the room. The surface absorption coefficient (1) of the roof was taken as 0.7 and of the walls as 0.5. The sol-air temperatures for the roof, walls, doors and windows have been computed from the climatological data and their Fourier equations are given in Table (9.3).

The steady state and harmonic heat flow into the room through all external facing structural elements and the harmonic heat absorption at the internal surface for unit amplitude variation of indoor harmonic temperature variations, and the mean indoor air temperature and harmonic variations have been determined for both the days. Their Fourier equations are given below.

Summer Day (May 16th)

$$t_{iu}(\tau) = 93.8 + 4.3\ \mathrm{Cos}(15\ t + 57^{o}) + 0.55\ \mathrm{Cos}(30\ t + 233^{o}) + 0.05\ \mathrm{Cos}(45\ t + 180^{o}) + 0.03\ \mathrm{Cos}(60\ t + 146^{o})$$

Winter Day (Dec. 22nd)

$$t_{iu}(\tau) = 55.2 + 3.9\ \mathrm{Cos}(15\ t + 69^{o}) + 0.40\ \mathrm{Cos}(30\ t + 105^{o}) + 0.03\ \mathrm{Cos}(45\ t + 63^{o}) + 0.00\ \mathrm{Cos}(60\ t + 120^{o})$$

The hourly indoor air temperatures as obtained from the equations are shown in Fig. (9.4).

9.4 Effect of Surface Treatments on Indoor Air Temperatures

It is interesting to know the influence of surface colour of a building element exposed to the solar radiation on indoor air temperatures. Such a study will provide an indication of the effectiveness of different surface treatments in improving the indoor thermal conditions. For this purpose the same single room structure Fig. (9.1 (b) was considered for a typical summer day and south orientation. Four surface absorption coefficients viz., 0.1 0.5, 0.7 and 0.9, for roof only were considered. The solair temperature wave

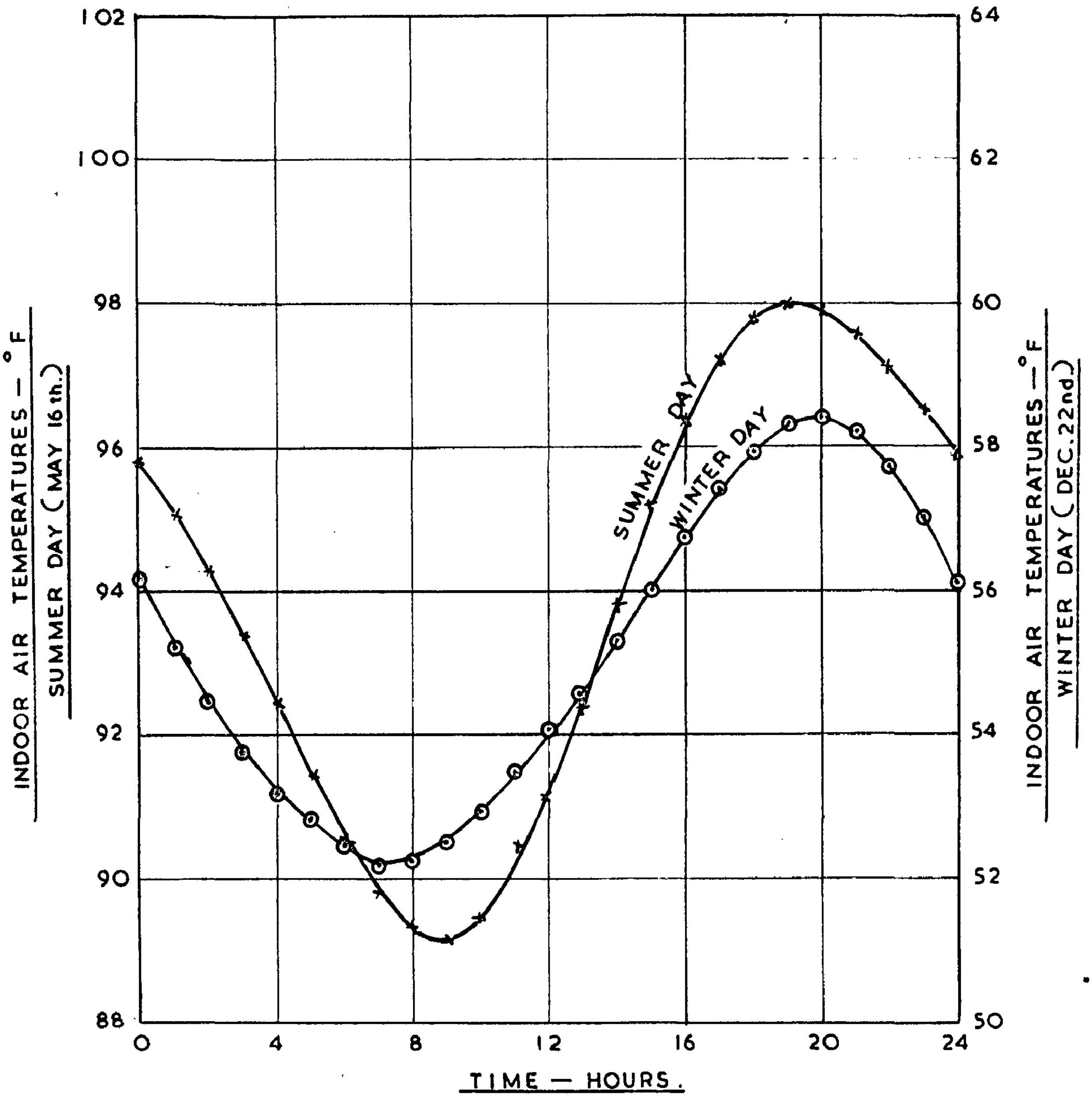

SEASONAL VARIATIONS OF INDOOR AIR TEMPERATURES

FIG. 9·4

forms of the roof with these four surface absorption coefficients are shown in Fig. (9.5). Here heat flow through all other building elements except the roof are, the same as that of the summer day, in the previous example (2). The fourier equations of the indoor air temperatures obtained for these four variations of ,
are given below.

For $\alpha = 0.1$;

$$t_{ia}(\tau) = 87.2 + 2.6\ \mathrm{Cos}(15\ t + 40^{\circ}) + 0.32\ \mathrm{Cos}(30\ t + 242^{\circ}) + 0.04\ \mathrm{Cos}(45\ t + 188^{\circ}) + 0.02\ \mathrm{Cos}(60\ t + 78^{\circ})$$

For $\alpha = 0.5$

$$t_{ia}(\tau) = 91.1 + 3.7\ \mathrm{Cos}(15\ t + 51^{\circ}) + 0.23\ \mathrm{Cos}(30\ t + 200^{\circ}) + 0.05\ \mathrm{Cos}(45\ t + 188^{\circ}) + 0.07\ \mathrm{Cos}(60\ t + 53^{\circ})$$

For $\alpha = 0.7$

$$t_{ia}(\tau) = 93.8 + 4.3\ \mathrm{Cos}(15\ t + 57^{\circ}) + 0.55\ \mathrm{Cos}(30\ t + 235^{\circ}) + 0.05\ \mathrm{Cos}(45\ t + 190^{\circ}) + 0.03\ \mathrm{Cos}(60\ t + 146^{\circ})$$

For $\alpha = 0.9$

$$t_{ia}(\tau) = 94.9 + 5.0\ \mathrm{Cos}(15\ t + 59^{\circ}) + 0.67\ \mathrm{Cos}(30\ t + 235^{\circ}) + 0.06\ \mathrm{Cos}(45\ t + 187^{\circ}) + 0.07\ \mathrm{Cos}(60\ t + 155^{\circ})$$

The hourly indoor air temperature variations are calculated and compared in Fig. (9.6).

It is clear from this study that highly reflective surface finishes have a marked influence in

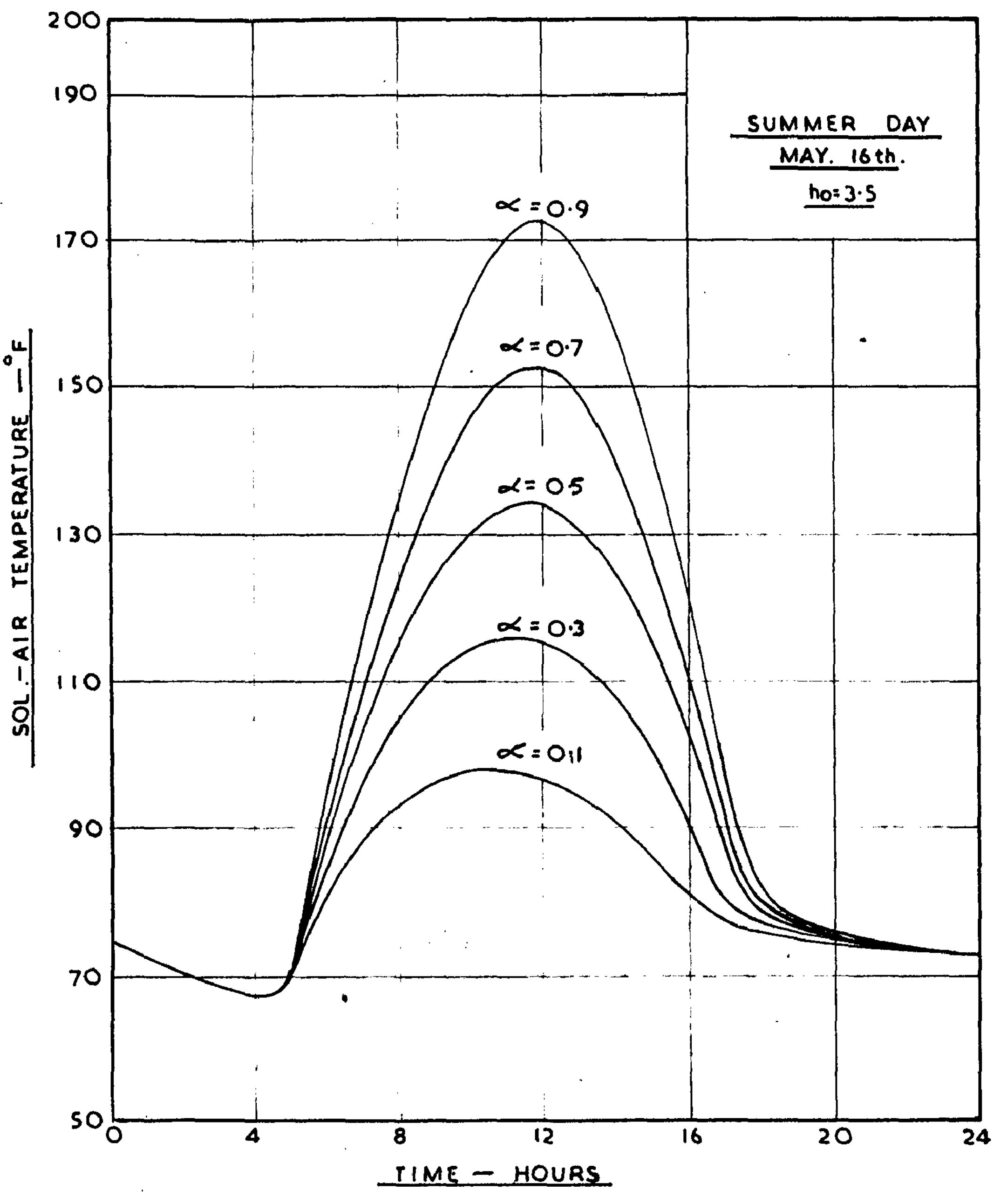

EFFECT OF SURFACE ABSORPTION COEFFICIENT ON SOL-AIR TEMPERATURE OF A FLAT ROOF

FIG. 9·5

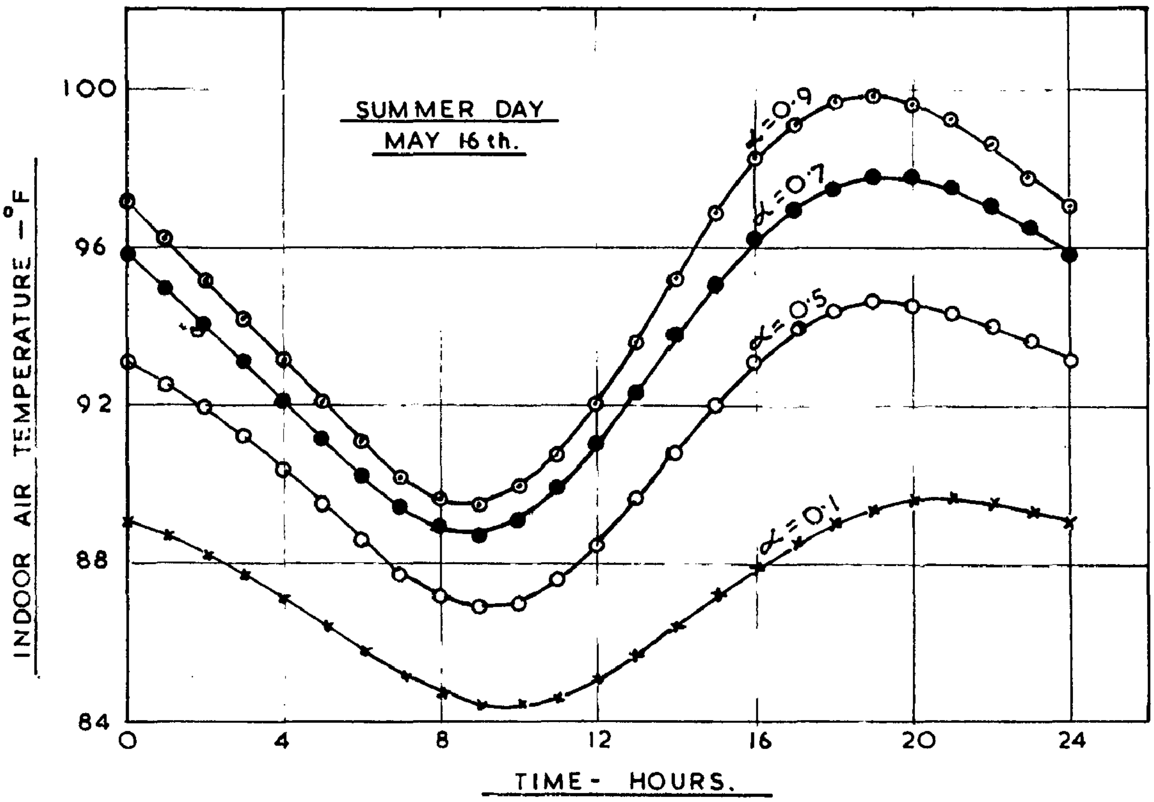

EFFECT OF SURFACE TREATMENT ON INDOOR AIR TEMPERATURES

FIG. 9·6

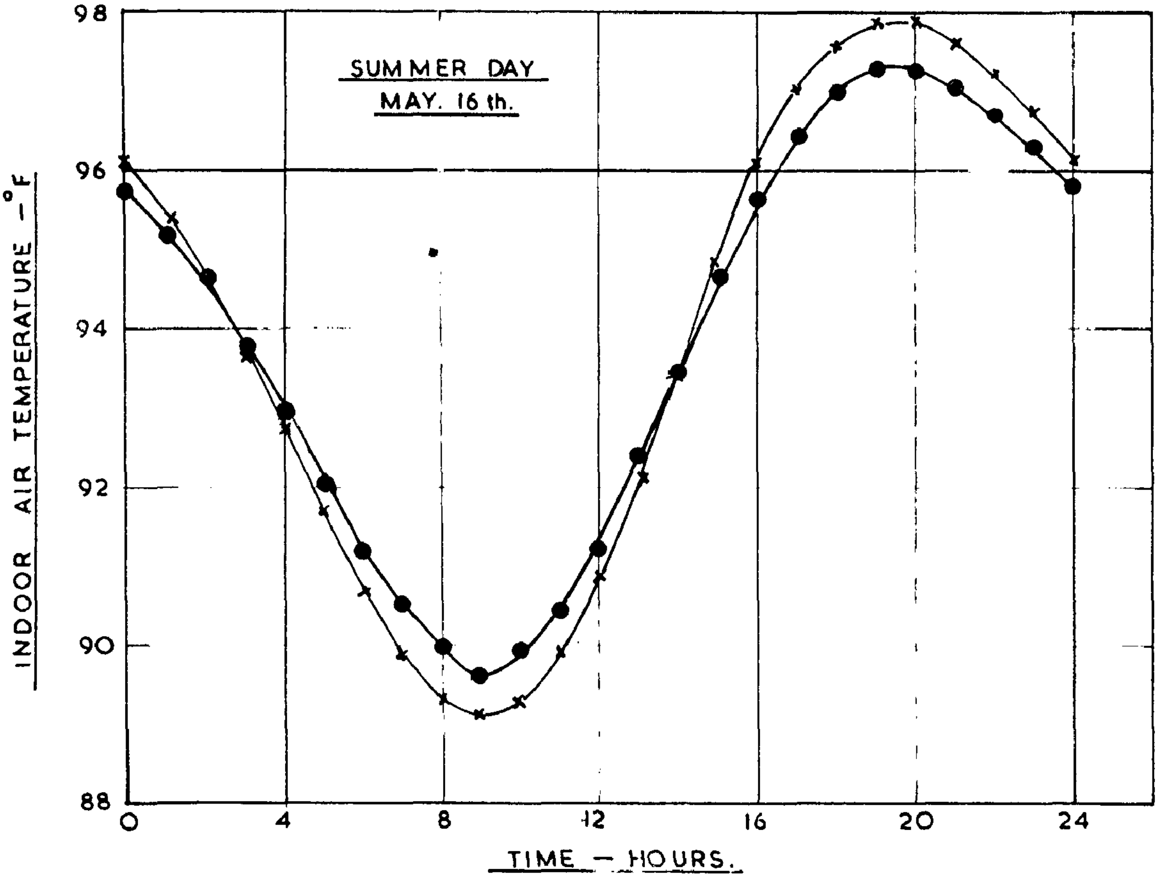

EFFECT OF INTERNAL MASS ON INDOOR AIR TEMPERATURES

FIG. 9·7

reducing the indoor air temperatures. The differences between two extreme cases $\alpha = 0.9$ and 0.1 was nearly 10°F, which is a very significant reduction. The major part of the reduction is affected in the steady state level (7.7°F).

9.5 Effect of Internal Mass on Indoor Air Temperature

Internal masses like partitions and furniture, have thermal capacity and hence a part of the heat that enters into the room is absorbed by them to modify the indoor air temperature. The magnitude of the reduction in indoor air temperature will depend upon the internal driving point admittance function and area of those internal masses. As an illustrative example, the same single room structure taken in earlier examples (Fig. 9.1(b) has been considered with the inclusion of a partition wall of 9" brick with 1/2" plaster on either side as shown by dotted lines in the same figure. This being an internal wall the surface coefficients on either side can be taken to be the same. The driving point and transfer admittance functions of the partition wall with this surface coefficients will be different from that of the external bounding wall though of same construction. There will be no change in the mean indoor air temperature with and without the partition, while the amplitudes of harmonic components will be reduced. These have been determined and the corresponding Fourier equation of the indoor air temperature is given below.

$$t_{ia}(\tau) = 93.8 + 3.62\ \mathrm{Cos}(15\ t + 56^{\circ}) + 0.46\ \mathrm{Cos}(30\ t + 236^{\circ}) + 0.04\ \mathrm{Cos}(45\ t + 190^{\circ}) + 0.03\ \mathrm{Cos}(60\ t + 146^{\circ})$$

The hourly indoor air temperatures obtained with and without the partition are compared in Fig. (9.7). These indicate that the reduction in temperatures due to the addition of a partition (internal mass) is not very significant in small buildings. This may reach a significant value for large buildings with many internal walls and larger surface areas.

9.6 Effect of the Type of Roof on Indoor Air Temperature

In order to find the effect of the type of roof, on the indoor air temperatures of unconditioned buildings, two types of insulated roofs were considered and compared with the normal roof taken in the previous examples, for the same room under similar conditions. The two roofs considered are (i) 1/2" plaster + 2" Foamed concrete + 4½" Reinforced brick work + 1/2" plaster, and (ii) 1" plaster + 1" thermocole + 4½" Reinforced brick work + 1/2" plaster.

The physical properties of the materials and the 'U' values and transfer driving point functions are given in Tables (9.1. and 9.4) respectively. The heat flow through the roof entering the room and the rate of heat flux absorption at the internal surfaces of these roof will be different while the rest will be same as in the case of normal roof. The resultant indoor air temperatures are obtained, and their Fourier equations are given below.

Type A

$$t_{ia}(\tau) = 81.7 + 3.8 \cos(15t + 43^{\circ}) + 0.3 \cos(30t + 253^{\circ}) + 0.04 \cos(45t + 200^{\circ}) + 0.03 \cos(60t + 190^{\circ})$$

Type B

$$t_{ia}(\tau) = 80.7 + 3.2 \cos(15t + 52^{\circ}) + 0.22 \cos(30t + 258^{\circ}) + 0.03 \cos(45t + 216^{\circ}) + 0.03 \cos(60t + 113^{\circ})$$

The hourly indoor air temperatures for these three roof types are obtained and compared in Fig. (9.8). Insulating the building components, especially the roof will improve the indoor thermal conditions, to considerable extent, but not as effective as surface treatments.

9.7 Effect of Ventilation on Indoor Air Temperatures

It is known, that the indoor air temperature of a room, will not only depend upon the heat flux received through the building fabrics, but also on ventilation rate. Because of the temperature differences

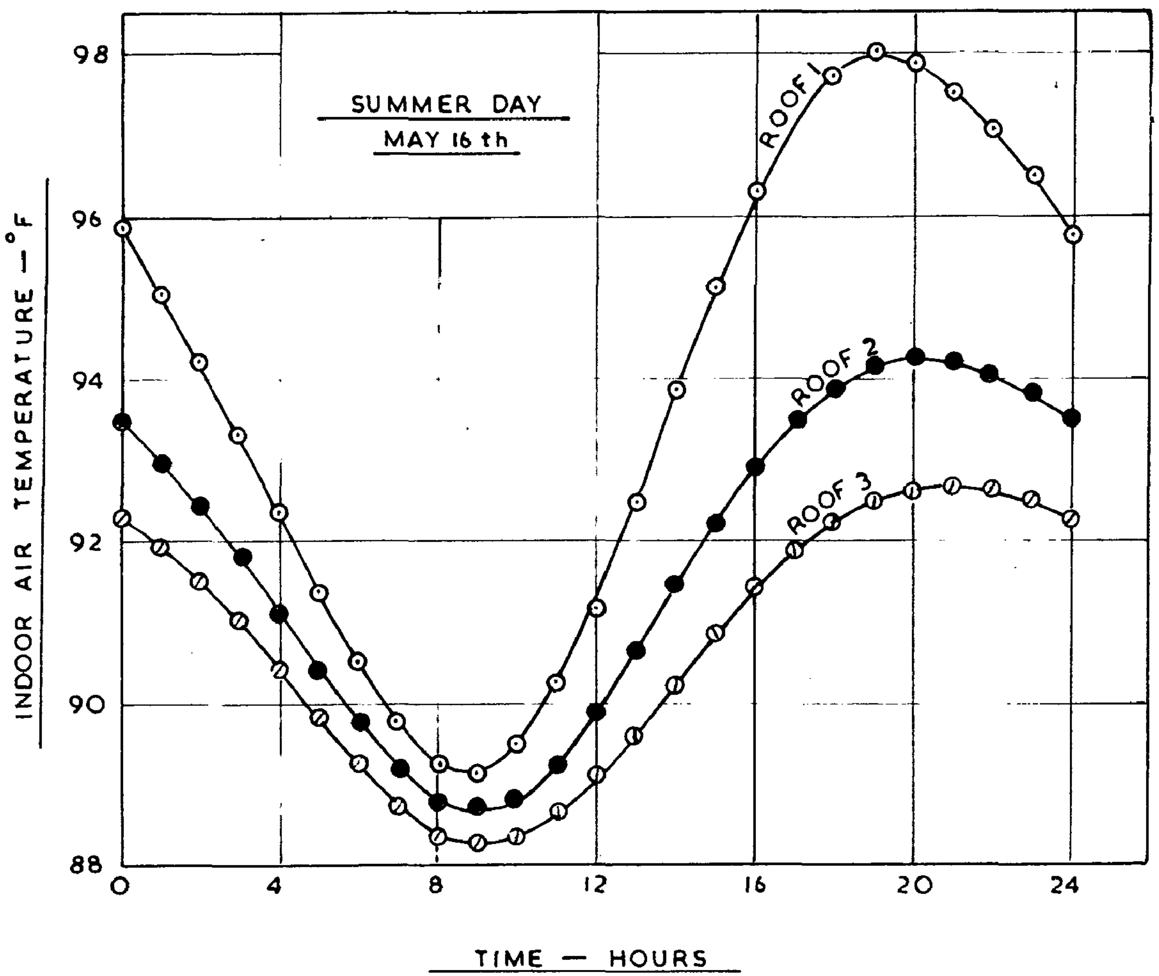

FIG. 9·8. EFFECT OF ROOF ON INDOOR AIR TEMPERATURES

TABLE 9.4

THERMAL SYSTEM FUNCTIONS OF THE ROOFS USED IN THE EXAMPLES

S. No.	Roof Construction	U value	Harmonic	External Driving point function: Modulus λ_o	External Driving point function: Arg in deg $-\phi_o$	Transfer Function: Modulus λ_i	Transfer Function: Arg in deg $-\phi_i$	Internal Driving point Function: Modulus λ_i'	Internal Driving point Function: Arg in deg $-\phi_i'$	Reverse Transfer Function: Modulus λ_o'	Reverse Transfer Function: Arg in deg. $-\phi_o'$
1.	3" lime concrete + 4" R.C.C. + ½" plaster	0.502	F	0.733	13	0.200	78	0.422	31	0.086	73
			H_2	0.649	17	0.111	116	0.316	36	0.047	115
			H_3	0.600	19	0.067	140	0.268	38	0.029	140
			H_4	0.567	21	0.044	160	0.244	40	0.019	160
2.	½" plaster + 3" foamed concrete + 4" R.C.C. + ½" plaster	0.238	F	0.912	14	0.078	80	0.573	36	0.034	80
			H_2	0.893	17	0.041	104	0.433	41	0.018	103
			H_3	0.856	21	0.030	126	0.378	43	0.013	123
			H_4	0.818	26	0.020	160	0.351	44	0.009	160
3.	1" plaster + 1" thermocole + 4½"R. brick + ½" plaster	0.147	F	0.934	11	0.037	88	0.507	34	0.016	88
			H_2	0.844	20	0.024	110	0.378	36	0.010	110
			H_3	0.782	28	0.014	154	0.322	38	0.006	154
			H_4	0.734	35	0.009	202	0.286	39	0.004	202

that exist between the indoor and outdoor air heat is either supplied to or extracted from, the room, by the process of ventilation. The exact quantity of heat transfer by the ventilation process depends upon the volume of the room and the rate of ventilation (number of air changes per hour).

In order to illustrate the effect of ventilation on the indoor air temperature, the same single room structure taken in earlier examples (Fig. 9.1(b) has been considered. The steady state and the harmonic components of the heat flux received in the room by ventilation, have been calculated, for an assumed ventilation rate of 4 volume changes per hour. The indoor air temperature harmonic variations are determined as outlined in Chapter (8). The Fourier equations of the indoor air temperatures obtained for the conditions of, with and without ventilation are given below.

1. <u>With Ventilation</u>

$$
\begin{aligned}
t_{ia}(\tau) = 82.1 &+ 7.13 \operatorname{Cos}(15\,t + 70^{\circ}) \\
&+ 0.52 \operatorname{Cos}(30\,t + 260^{\circ}) \\
&+ 0.25 \operatorname{Cos}(45\,t + 275^{\circ}) \\
&+ 0.12 \operatorname{Cos}(60\,t + 123^{\circ})
\end{aligned}
$$

2. <u>Without Ventilation</u>

$$
\begin{aligned}
t_{ia}(\tau) = 83.6 &+ 4.0\ \operatorname{Cos}(15\,t + 70^{\circ}) \\
&+ 0.65 \operatorname{Cos}(30\,t + 233^{\circ}) \\
&+ 0.05 \operatorname{Cos}(45\,t + 190^{\circ}) \\
&+ 0.03 \operatorname{Cos}(60\,t + 146^{\circ})
\end{aligned}
$$

The hourly indoor air temperature variations are also calculated and compared in Fig. (9.9). It can be seen from this, that the ventilation,will tend to reduce the temperature differences between the indoor and outdoor air, and also the time lag in the occurence of their maxima.

9.8 Estimation of Fabric Cooling Loads for Air-Conditioning

Most of the methods employed for the estimation of fabric cooling loads do not take the internal masses into account. These are approximate methods and sizeable errors are likely to occur. The thermal circuit techniques (81) which do take those internal masses into account are complex and involve considerable labour. The transfer function approach will simplify the computations to a minimum. The application of transfer functions for these cooling load calculations, is explained below. For a given building, under any known climatic conditions, the amount of heat flux entering the building through all the external bounding surfaces can be obtained as illustrated in the previous examples. Let us suppose that the room air is to be maintained constant at a temperature 75°F; we have to calculate the amount of heat that is to be extracted from the room. The steady state part of the cooling load is obtained by

$$\sum U_k A_k \left\{ t_{sak}(\text{mean}) - 75^\circ \right\}$$

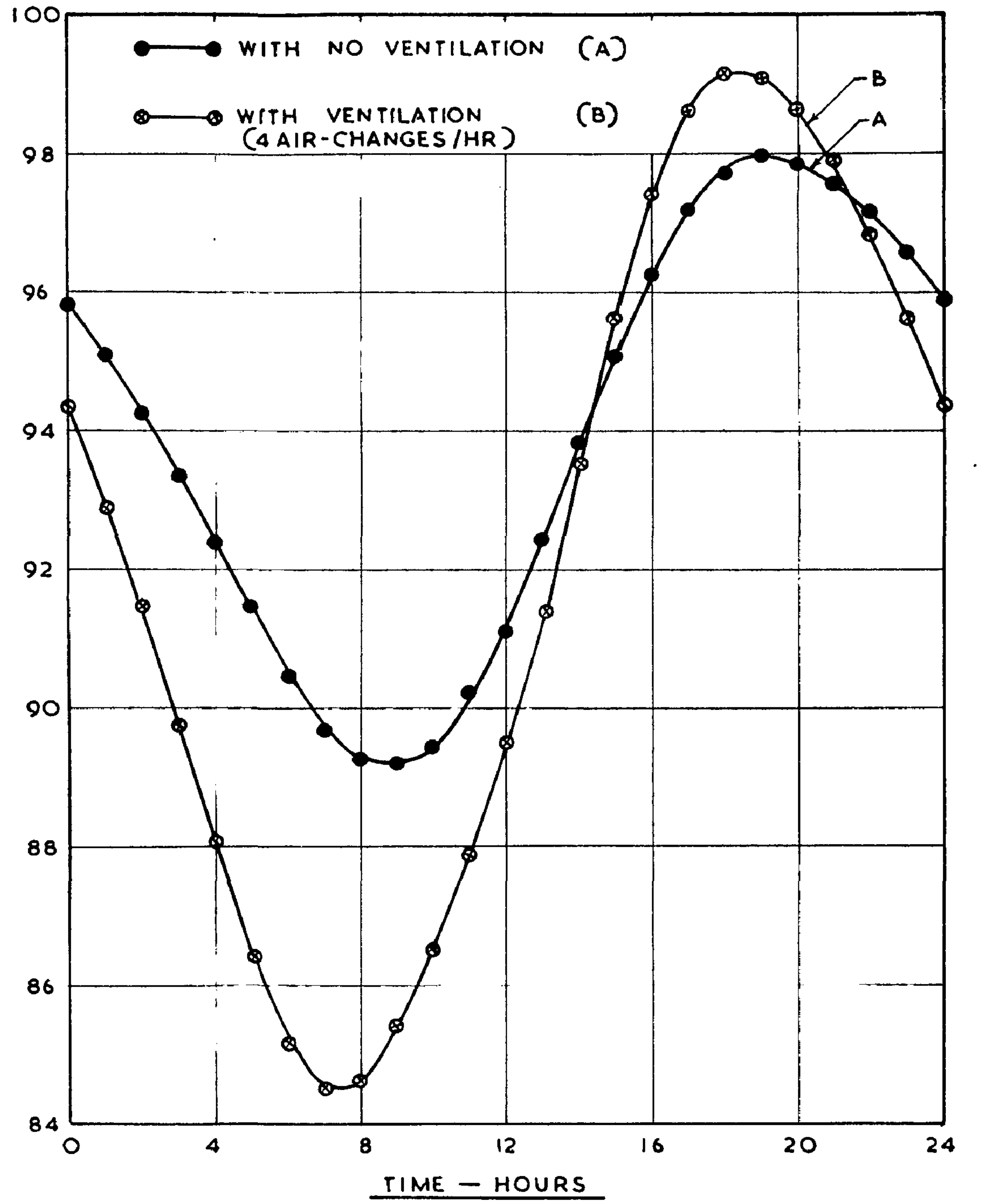

ECT OF VENTILATION ON INDOOR AIR TEMPERATURES

FIG. 9·9

The total amount of the harmonic heat flux entering the room through all exposed building elements can be computed with transfer admittance function $\overrightarrow{Y_1'}$ in the same way, as done for non air conditioned buildings. All the amount of heat flux entering will not appear as the cooling load to the air-conditioning plant. The floor and the interior masses like partitions and furniture, will absorb a certain amount of the heat flux. Thus the cooling load transferred to the plant is the heat entering the enclosure less that absorbed by the internal masses. The quantity of heat flux absorbed by these internal elements can be obtained from the internal driving point admittance function $\overleftarrow{Y_1'}$.

As an illustration, the same room taken in the previous examples for unconditioned buildings, (Fig. 9.1(b) with internal partition wall is considered here. The quantities of heat flow into the room, (steady state as well as harmonic components) and the quantity of heat flux absorbed by the floor and partition wall and the balance of the heat quantity to be extracted by the plant to maintain the indoor air temperature constant at 75°F are calculated. The Fourier equations for the cooling load with and without considering the internal masses are given below.

1. <u>Without taking the internal masses into account</u>

$$
\begin{aligned}
Q(\tau) = 8836 &+ 5390 \cos(15t + 79^\circ) \\
&+ 788 \cos(30t + 252^\circ) \\
&+ 76 \cos(45t + 203^\circ) \\
&+ 50 \cos(60t + 153^\circ)
\end{aligned}
$$

2. Internal masses taken into account

$$q(T) = 8336 + 3245 \cos(15t + 79^\circ) + 455 \cos(30t + 252^\circ) + 46 \cos(45t + 202^\circ) + 29 \cos(60t + 161^\circ)$$

The hourly variations of cooling load with and without for a condition, considering the internal masses are shown in Fig. (9.10).

Increase of internal masses will make this difference proportionately more. This method of approach gives more realistic picture of fabric cooling loads of buildings for air conditioning estimations.

9.9. Estimation of Outside Surface Temperatures

The above examples deal with the applications of only two thermal system functions namely, i) the transfer admittance function, and ii) internal driving point admittance function. The use of third function i.e., external driving point function (t_{os}/t_{sa}) is explained here. It was mentioned earlier that outside surface temperatures of building elements are not usually available. These have to be determined by actual measurement. Different building elements attain different (outside) surface temperatures when exposed to same weather conditions. A knowledge of these external surface temperatures, is a prerequisite for computing the thermal stresses induced in the structural elements and the expansions and contractions that are likely to take place during diurnal and seasonal variations. The external driving point functions will provide the external surface temperatures attained by different constructions under different climatic exposures. As an illustrative example, the same case of (9.6) has been considered here. The $\vec{\lambda}_o$ for the three types of roofs for the fundamental and three higher harmonics are given in Table (9.4). The Fourier equations of the external surface temperatures obtained for the three types of roofs for the corresponding sol-air temperature are given below.

Uninsulated roof

$$\begin{aligned} t_{os}(\tau) = 103.3 &+ 30.4 \cos(15t - 207^\circ) \\ &+ 9.1 \cos(30t - 20^\circ) \\ &+ 1.0 \cos(45t - 74^\circ) \\ &+ 1.2 \cos(60t - 6^\circ) \\ &+ 0.37 \cos(15t - 21^\circ) \end{aligned}$$

Insulated type roof A

$$\begin{aligned} t_{os}(\tau) = 103.0 &+ 33.5 \cos(15t - 203^\circ) \\ &+ 12.4 \cos(30t - 20^\circ) \\ &+ 1.4 \cos(45t - 73^\circ) \\ &+ 1.8 \cos(60t - 11^\circ) \\ &+ 0.00 \cos(15t - 31^\circ) \end{aligned}$$

Insulated type roof B

$$\begin{aligned} t_{os}(\tau) = 104.1 &+ 37.4 \cos(15t - 210^\circ) \\ &+ 11.7 \cos(30t - 20^\circ) \\ &+ 1.3 \cos(45t - 33^\circ) \\ &+ 1.6 \cos(60t - 20^\circ) \\ &+ 0.33 \cos(15t - 45^\circ) \end{aligned}$$

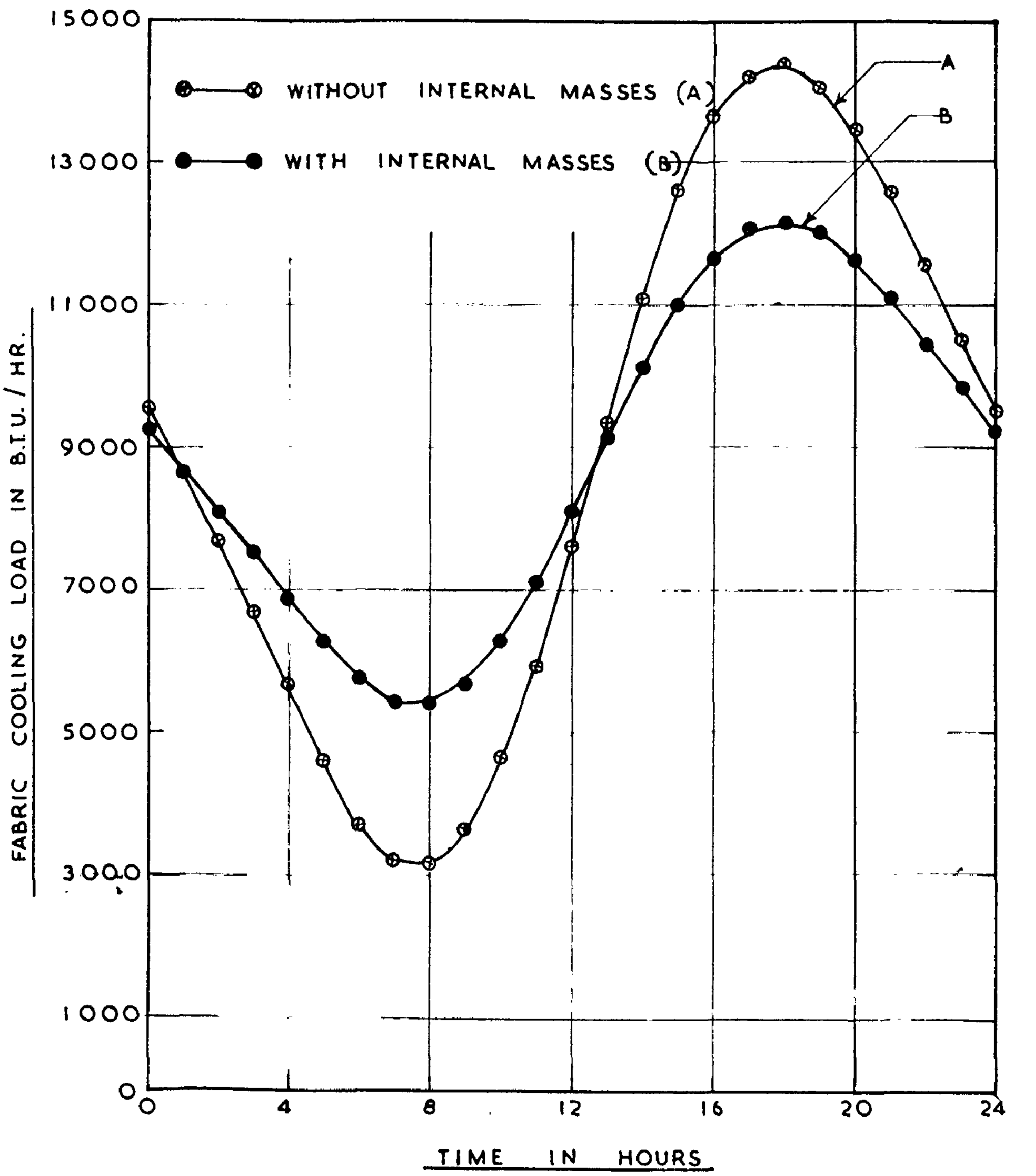

EFFECT OF INTERNAL MASSES ON FABRIC COOLING LOAD

FIG. 9·10

the expansions and contractions that are likely to take place during diurnal and seasonal variations. The external driving point functions will provide the external surface temperatures attained by different constructions under different climatic exposures. As an illustrative example, the same case of (9.6) has been considered here. The $\vec{\lambda}_o$ for the three types of roofs for the fundamental and three higher harmonics are given in Table (9.4). The Fourier equations of the external surface temperatures obtained for the three types of roofs for the corresponding sol-air temperature are given below.

<u>Uninsulated roof</u>

$$
\begin{aligned}
t_{os}(\tau) = 103.3 &+ 30.4 \ \mathrm{Cos}\ (15\,t - 207^\circ) \\
&+ 9.1 \ \mathrm{Cos}\ (30\,t - 20^\circ) \\
&+ 1.0 \ \mathrm{Cos}\ (45\,t - 74^\circ) \\
&+ 1.2 \ \mathrm{Cos}\ (60\,t - 6^\circ) \\
&+ 0.37 \ \mathrm{Cos}\ (15\,t - 21^\circ)
\end{aligned}
$$

<u>Insulated type roof A</u>

$$
\begin{aligned}
t_{os}(\tau) = 103.9 &+ 33.5 \ \mathrm{Cos}\ (15\,t - 203^\circ) \\
&+ 12.4 \ \mathrm{Cos}\ (30\,t - 20^\circ) \\
&+ 1.4 \ \mathrm{Cos}\ (45\,t - 76^\circ) \\
&+ 1.8 \ \mathrm{Cos}\ (60\,t - 11^\circ) \\
&+ 0.00 \ \mathrm{Cos}\ (15\,t - 31^\circ)
\end{aligned}
$$

<u>Insulated type roof B</u>

$$
\begin{aligned}
t_{os}(\tau) = 104.1 &+ 37.4 \ \mathrm{Cos}\ (15\,t - 210^\circ) \\
&+ 11.7 \ \mathrm{Cos}\ (30\,t - 23^\circ) \\
&+ 1.3 \ \mathrm{Cos}\ (45\,t - 83^\circ) \\
&+ 1.6 \ \mathrm{Cos}\ (60\,t - 20^\circ) \\
&+ 0.33 \ \mathrm{Cos}\ (15\,t - 45^\circ)
\end{aligned}
$$

The hourly temperature variations were calculated from these equations and compared in Fig. (9.11). The insulated type roofs will attain higher temperatures than the uninsulated ones, when the insulating layer is on the top.

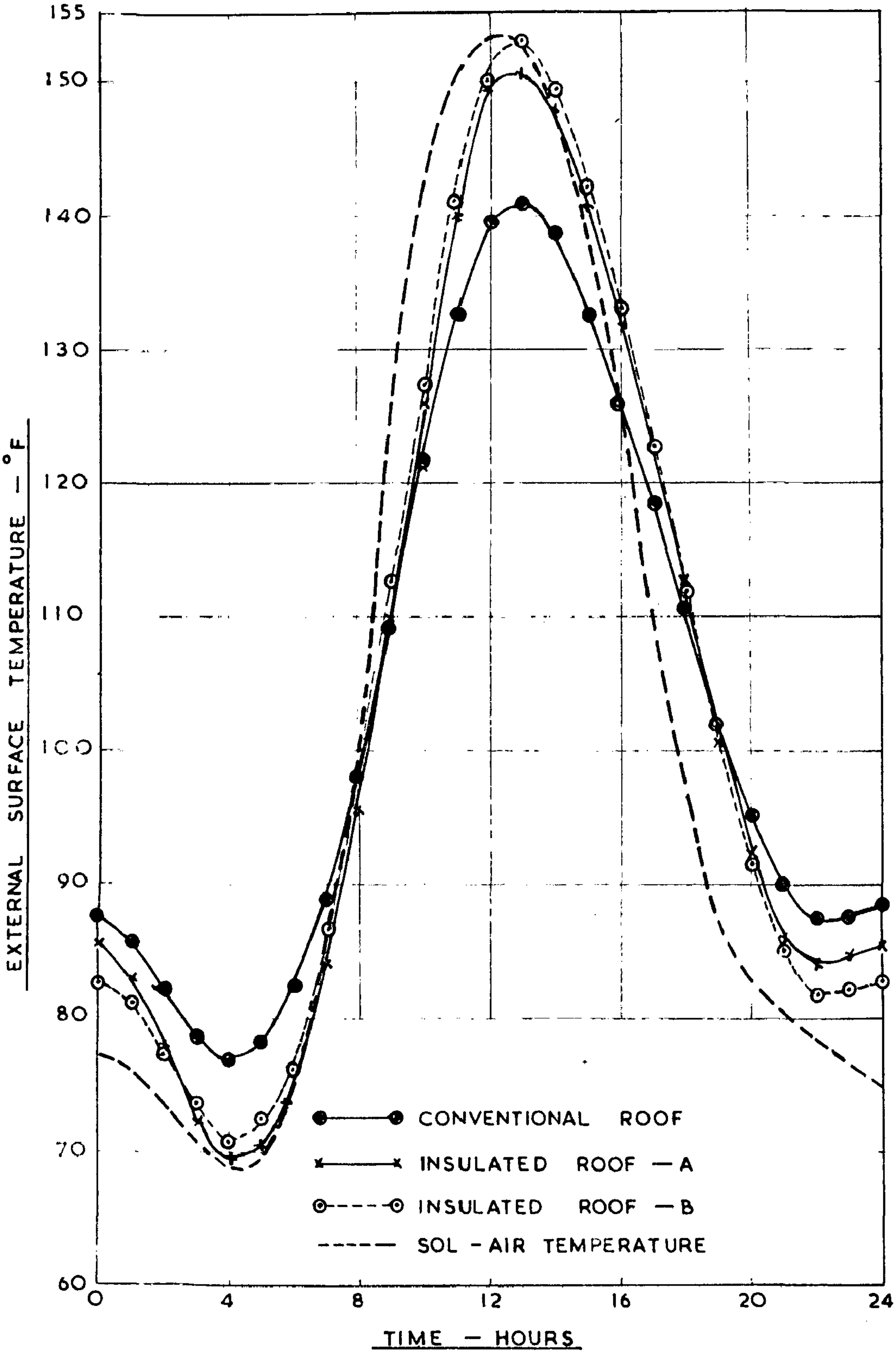

EXTERNAL SURFACE TEMPERATURES OF DIFFERENT TYPES OF ROOFS

FIG. 9·11

C O N C L U S I O N S

CONCLUSIONS

In this thesis an adequate quantitative data, on the transient thermal characteristics of building sections, and a simple and flexible computational procedure, which will enable a designer to calculate the heat transfer and temperatures of enclosures, under given conditions, are established.

An analysis of the electrical analogue studies made on the transient thermal behaviour of building elements, with special reference to a) the effect of surface heat transfer coefficients, b) the effect of different combinations of layers of various materials and c) lumped network representation of the building section, lead to the following conclusions :-

1. The steady state sinusoidal approach adopted here separates the effects of the climatic factors from the thermal characteristics of building elements, so that each could be studied independently and then combined to get the thermal behaviour of the fabric under any climatic conditions.

2. A knowledge of transfer function only, is not sufficient to specify the transient thermal behaviour of any building element completely and two more thermal system

functions viz., i) external driving point function and ii) internal driving point function are also required. With these three system functions the surface temperatures and heat fluxes of the outer and inner surfaces can easily be obtained for any boundary condition.

3. a) The influence surface heat transfer coefficients on the thermal system functions depends upon both RC and R of a given building section.

b) The external and internal surface heat transfer coefficients influence their respective driving point functions for sections with large RC and R. For thin sections (with small RC and R) however, both surface coefficients affect both driving point functions.

c) The transfer functions of any building section are affected by both the surface coefficients considerably.

4. a) In hot climates, placing the insulation on the exposed side is more advantageous than placing it inside.

b) For various possible arrangements, the greatest damping occurs when insulating layers alternate with layers of dense materials.

c) Backing layers have considerable influence on the decrement factors of the front layers while the converse is not true.

d) If the heat flow direction is reversed (i.e. from inside to outside) the overall decrement factor will be reduced by the ratio of the outside to inside surface heat transfer coefficients (h_o/h_i) while the phase lag is not altered.

e) The decrement factor of the individual layers in a composite section will not be the same when the direction of heat flow is reversed.

f) It is not always possible to obtain an equivalent homogeneous, constructions, which will have the same thermal system functions of heat of a composite construction.

5. The number of lumps of T network required for an adequate representation of a building section, is proportional to the square root of the thermal time constant (RC) of the section.

6. This thesis has several practical uses. For instance :

a) Reference data on transient thermal characteristics of building components commonly used in India, given in Appendices III and IV, enables to make the right choice of the materials for a given situation.

b) The data given on external driving point functions provides a basis for the easy computation of outside surface temperatures attained by building components under different climatic exposures.

7. With the aid of the data on the matrix coefficients of the distributed and lumped systems (Appendix I) it is possible to evaluate the errors due to lumping on any of the thermal quantities of interest (surface temperatures, heat fluxes, or the thermal system functions) for any homogeneous layer.

8. Moreover as the method, put forth for the computation of indoor air temperatures of enclosures, utilises pretabulated data on thermal system functions and 'U' values, almost all types of conditions that may be encountered in practice can be analysed by means of the graphs and tables given here, without constructing an analogue for each case. Thus the method suggested here offers a number of advantages over the analytical or field measurement techniques.

A P P E N D I C E S

I TO IV

APPENDIX I

TRANSFER MATRICES OF DISTRIBUTED AND LUMPED NETWORKS (FOR SINUSOIDAL TEMPERATURE VARIATIONS)

Distributed System

$$\begin{bmatrix} A_D & B_D \\ C_D & D_D \end{bmatrix} = \begin{bmatrix} \cosh (1+j)\theta & \dfrac{R \sinh (1+j)\theta}{(1+j)\theta} \\ \dfrac{(1+j)\theta \sinh (1+j)\theta}{R} & \cosh (1+j)\theta \end{bmatrix}$$

where $= \sqrt{\dfrac{\omega C R}{2}}$

$= \dfrac{2\pi}{P}$

P = Period of the thermal cycle.

C = Total thermal capacity ($l \rho s$)

R = Total thermal resistance (l/K)

l = Thickness in Ft.

K = Thermal conductivity of the material in Btu/Ft./Hr/°F

ρ = Density in Lb/Cu.Ft.

s = Specific heat in Btu/Lb/°F

$$\cosh (1+j)\theta = \left\{ \left(1 - \frac{\theta^4}{6} + \frac{\theta^8}{2520} \cdots \right) + j\left(\theta^2 - \frac{\theta^6}{90} + \cdots \right) \right\}$$

$$\frac{\sinh (1+j)\theta}{(1+j)\theta} = \left\{ \left(1 - \frac{\theta^4}{30} + \frac{\theta^8}{22680} \cdots \right) + j\left(\frac{\theta^2}{3} - \frac{\theta^6}{630} \cdots \right) \right\}$$

and

$$(1+j)\theta \sinh (1+j)\theta = 2 \left\{ \left(-\frac{\theta^4}{3} + \frac{\theta^8}{630} + \cdots \right) + j\left(\theta^2 - \frac{\theta^6}{30} \cdots \right) \right\}$$

T - Network

The transfer matrices for one lump and N - lumped circuits (Figs. 1 & 2 respectively) are given by :-

One Lump Circuit

$$\begin{bmatrix} A_T & B_T \\ C_T & D_T \end{bmatrix} = \begin{bmatrix} \left(1 + \frac{\dot{\gamma}\omega CR}{2}\right) & R\left(1 + \frac{\dot{\gamma}\omega CR}{4}\right) \\ \dot{\gamma}\omega C & \left(1 + \frac{\dot{\gamma}\omega CR}{2}\right) \end{bmatrix}$$

N Lumped Circuit

$$\begin{bmatrix} A_T & B_T \\ C_T & D_T \end{bmatrix} = \begin{bmatrix} \left(1 + \frac{\dot{\gamma}\omega CR}{2N^2}\right) & \frac{R}{N}\left(1 + \frac{\dot{\gamma}\omega CR}{4N^2}\right) \\ \frac{\dot{\gamma}\omega C}{N} & \left(1 + \frac{\dot{\gamma}\omega CR}{2N^2}\right) \end{bmatrix}^N$$

where C = Total thermal capacitance of the building element.

R = Total thermal resistance of the building element.

T - NET WORK

I - LUMP CIRCUIT

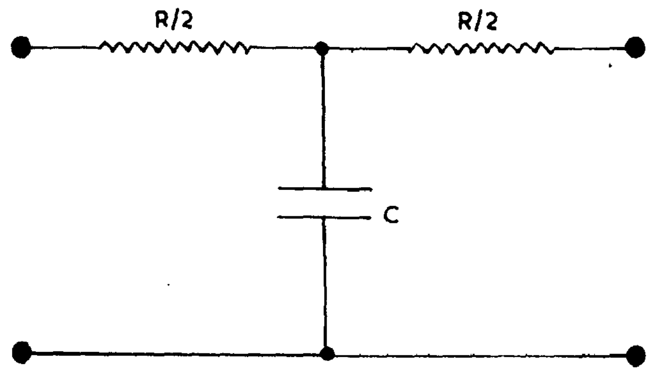

FIG. 1.

N - LUMPED CIRCUIT

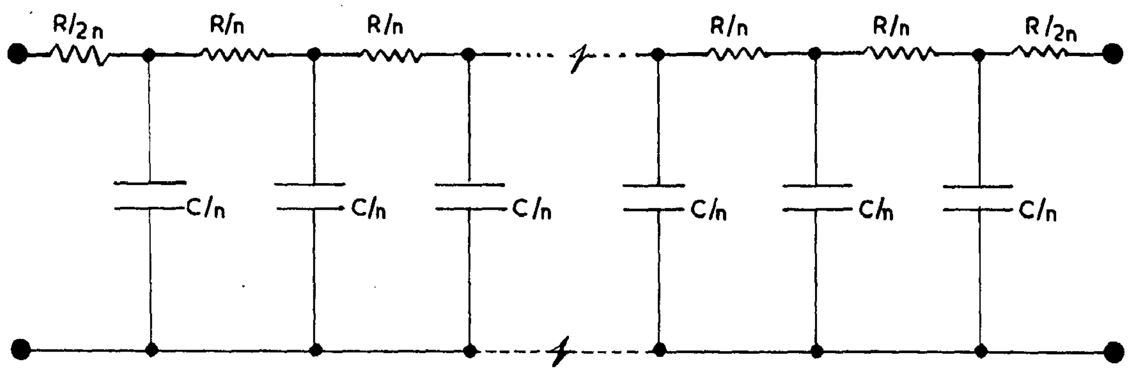

FIG. 2.

π - Network

The transfer matrices for one lump and N lumped circuits (Figs. 3 & 4 respectively) are given by :-

One Lump Circuit

$$\begin{bmatrix} A_\pi & B_\pi \\ C_\pi & D_\pi \end{bmatrix} = \begin{bmatrix} \left(1 + \frac{j\omega CR}{2}\right) & R \\ j\omega C\left(1 + \frac{j\omega CR}{4}\right) & \left(1 + \frac{j\omega CR}{2}\right) \end{bmatrix}$$

N Lumped Circuit

$$\begin{bmatrix} A_\pi & B_\pi \\ C_\pi & D_\pi \end{bmatrix} = \begin{bmatrix} \left(1 + \frac{j\omega CR}{2N^2}\right) & \frac{R}{N} \\ \frac{j\omega C}{N}\left(1 + \frac{j\omega CR}{4N^2}\right) & \left(1 + \frac{j\omega CR}{2N^2}\right) \end{bmatrix}^N$$

Where C = Total thermal capacitance of the building element.

R = Total thermal resistance of the building element.

Π- NET WORK

I - LUMP CIRCUIT

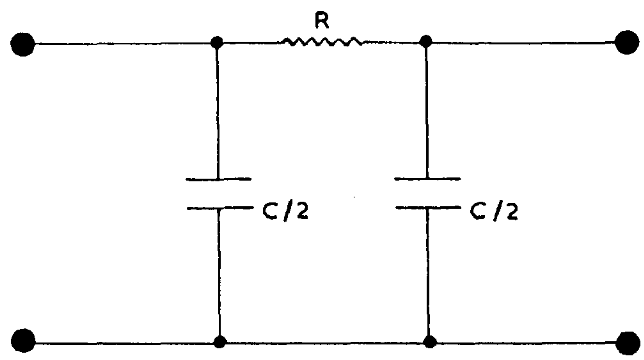

FIG. 3.

N- LUMPED CIRCUIT

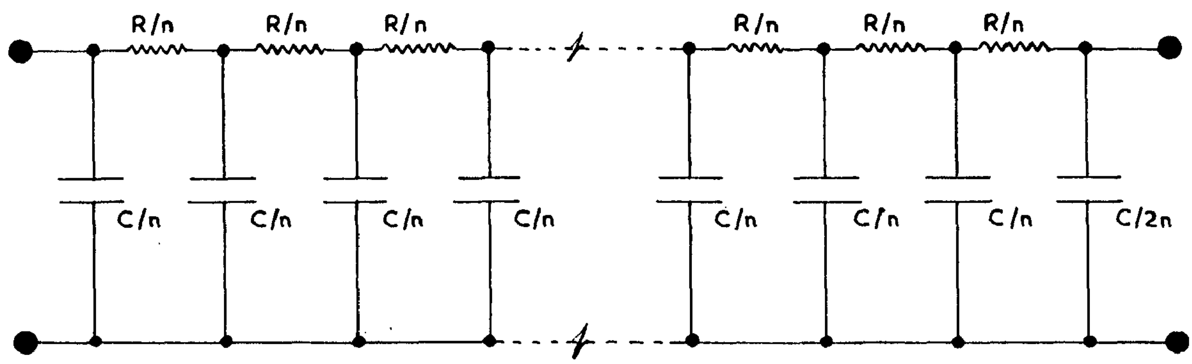

FIG.4

L - Network

The transfer matrices for one lump and N lumped circuits (Figs. 5 & 6 respectively) are given by :-

One Lump Circuit

$$\begin{bmatrix} A_L & B_L \\ C_L & D_L \end{bmatrix} = \begin{bmatrix} (1 + \gamma\omega CR) & R \\ \gamma\omega C & 1 \end{bmatrix}$$

N Lumped Circuit

$$\begin{bmatrix} A_L & B_L \\ C_L & D_L \end{bmatrix} = \begin{bmatrix} \left(1 + \frac{\gamma\omega CR}{N^2}\right) & \frac{R}{N} \\ \frac{\gamma\omega C}{N} & 1 \end{bmatrix}^N$$

where C = Total thermal capacitance of the building element.

R = Total thermal resistance of the building element.

L - NET WORK

I - LUMP CIRCUIT

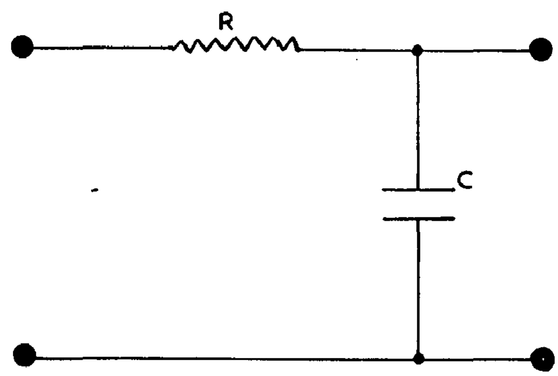

FIG. 5.

N - LUMPED CIRCUIT

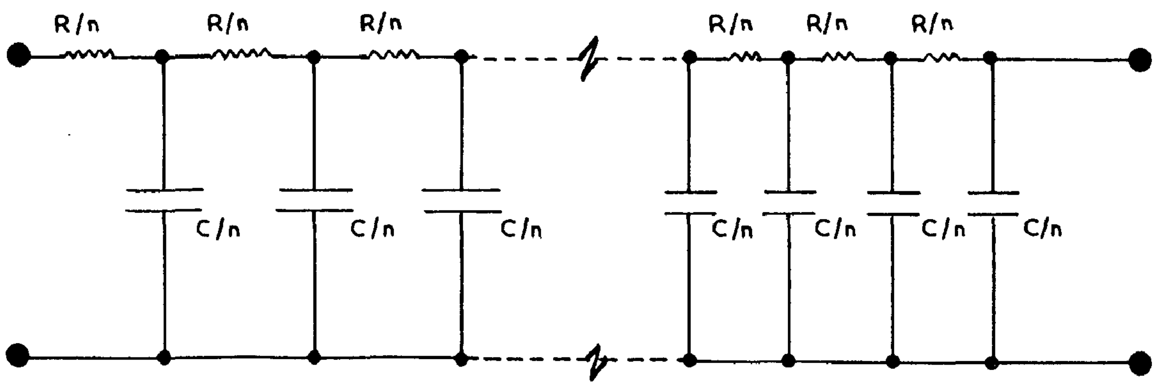

FIG. 6.

TRANSFER MATRIX COEFFICIENTS OF DISTRIBUTED AND LUMPED (T, π & L)

CIRCUITS OF HOMOGENEOUS BUILDING ELEMENTS

(FOR SINUSOIDAL TEMPERATURE VARIATIONS)

(a) MATRIX COEFFICIENT- A

Thermal time-constant RC	Distributed: Modulus	Distributed: Argument in degrees	No. of Lumps	Lumped T & π circuits: Modulus	Lumped T & π circuits: Argument in degrees	Lumped L - circuit: Modulus	Lumped L - circuit: Argument in degrees
0.1	1.0001	0.69	1	1.0000	0.8	1.0000	1.6
			2	1.0000	0.8	1.0000	1.1
			4	1.0000	0.8	1.0000	0.9
			6	1.0000	0.8	1.0000	0.8
			8	1.0000	0.8	1.0000	0.8
0.5	1.0015	3.87	1	1.0030	3.7	1.0030	7.5
			2	1.0018	3.7	1.0030	5.6
			4	1.0015	3.7	1.0023	4.7
			6	1.0016	3.7	1.0020	4.4
			8	1.0018	3.7	1.0020	4.2
1.0	1.0053	7.40	1	1.0304	7.5	1.0240	14.7
			2	1.0035	7.5	1.0150	11.0
			4	1.0030	7.5	1.0093	9.3
			6	1.0053	7.5	1.0030	8.7
			8	1.0053	7.5	1.0070	8.5
5.0	1.1350	35.12	1	1.1940	33.2	1.6470	52.6
			2	1.1503	34.7	1.3270	47.7
			4	1.1335	35.0	1.2124	42.1
			6	1.1371	35.0	1.1320	39.0
			8	1.1360	35.0	1.1620	38.8
10.0	1.4349	60.63	1	1.6471	52.6	2.2030	69.1
			2	1.5237	59.0	2.0450	73.8
			4	1.4832	60.3	1.7117	69.5
			6	1.4775	60.7	1.6230	67.1
			8	1.4730	60.7	1.5300	65.9
20.0	2.4331	93.05	1	2.5035	89.1	5.3300	70.3
			2	2.5319	93.9	3.9010	102.7
			4	2.4833	91.5	3.0355	100.1
			6	2.4476	93.3	2.8030	99.0
			8	2.4530	93.6	2.7200	93.1
50.0	6.4393	143.60	1	6.6312	81.3	13.1230	83.4
			2	7.5319	129.6	13.5030	124.7
			4	7.0334	140.1	9.6323	150.1
			6	6.7100	144.6	8.3150	153.0
			8	6.5520	143.3	7.7359	152.5
			10	6.5500	143.4	7.4440	152.3
100.0	13.2074	203.23	1	13.1210	85.6	28.2300	87.2
			2	21.2350	147.4	43.3100	154.0
			4	22.5270	191.3	31.9420	204.1
			6	20.3100	199.5	20.0500	211.0
			8	16.7300	200.6	21.7000	213.4
			10	16.4500	203.7	23.2400	215.2
200.0	68.3333	293.21	1	53.8000	87.3	53.3700	88.0
			2	88.6200	132.8	174.5000	132.0
			4	133.9700	240.9	217.2350	233.2
			6	107.2000	274.0	163.6000	252.2
			8	97.5200	232.4	134.1300	204.2
			10	63.5300	223.4	107.3320	203.3

(b) MATRIX COEFFICIENT - D x 1/A

Thermal time-constant RC	Distributed Modulus	Distributed Argument in degrees	No. of Lumps	Lumped T - Circuit Modulus	Lumped T - Circuit Argument in degrees	Lumped π & L - Circuits Modulus	Lumped π & L - Circuits Argument in degrees
0.1	1.0000	0.33	1	1.0000	0.4	1.0000	0.3
			2	1.0000	0.2	1.0000	0.2
			4	1.0000	0.2	1.0000	0.2
			6	1.0000	0.2	1.0000	0.3
			8	1.0000	0.2	1.0000	0.2
0.5	1.0001	1.20	1	1.0005	1.9	1.0000	0.0
			2	1.0001	1.4	1.0000	0.9
			4	1.0001	1.3	1.0000	1.2
			6	1.0001	1.3	1.0001	1.1
			8	1.0001	1.3	1.0001	1.0
1.0	1.0004	2.47	1	1.0020	3.7	1.0000	0.9
			2	1.0003	2.8	1.0005	1.9
			4	1.0005	2.6	1.0004	2.4
			6	1.0004	2.5	1.0003	2.4
			8	1.0004	2.5	1.0002	2.4
5.0	1.0095	12.43	1	1.0521	18.1	1.0000	0.0
			2	1.0163	14.0	1.0124	9.3
			4	1.0112	12.8	1.0105	11.7
			6	1.0103	12.3	1.0100	12.1
			8	1.0023	12.6	1.0100	12.5
10.0	1.0371	21.43	1	1.1909	33.2	1.0000	0.0
			2	1.0331	27.4	1.0521	18.1
			4	1.0437	25.3	1.0423	22.0
			6	1.0403	23.0	1.0402	24.0
			8	1.0390	24.8	1.0397	24.5
20.0	1.2463	47.31	1	1.3033	53.6	1.0000	0.0
			2	1.2575	51.3	1.1910	33.3
			4	1.1699	43.6	1.1650	44.0
			6	1.1557	43.0	1.1559	45.0
			8	1.1511	47.8	1.1450	43.8
50.0	1.7330	101.53	1	3.4220	73.0	1.0000	0.0
			2	2.4770	91.9	1.9175	53.3
			4	1.8477	97.7	1.8024	80.1
			6	1.8317	101.5	1.8425	83.4
			8	1.8224	101.0	1.8150	[illegible]
			10	1.8190	100.6	1.8024	[illegible]
100.0	3.5203	161.30	1	6.6210	81.3	1.0000	0.0
			2	6.6315	131.6	3.3723	73.0
			4	4.6030	157.4	4.2307	125.3
			6	4.0351	160.7	3.9290	150.3
			8	3.8397	161.6	3.3533	155.3
			10	3.8140	163.1	3.7723	150.0
200.0	11.3712	247.21	1	13.1200	85.6	1.0000	0.0
			2	21.6550	151.3	6.6213	81.0
			4	19.4775	221.5	15.0720	122.2
			6	15.8153	233.6	14.5700	210.0
			8	13.3530	243.2	13.2450	231.3
			10	12.5230	244.8	12.4910	237.0

(c) MATRIX COEFFICIENT - C x R

Thermal time-constant RC	Distributed Modulus	Distributed Argument in degrees	No. of Lumps	Lumped T & L Circuits Modulus	Lumped T & L Circuits Argument in degrees	Lumped π - Circuit Modulus	Lumped π - Circuit Argument in degrees
0.1	0.0242	90.23	1	0.0262	90.0	0.0232	90.4
			2	0.0232	90.2	0.0232	90.3
			4	0.0272	90.2	0.0232	90.2
			6	0.0234	90.2	0.0232	90.2
			8	0.0234	90.3	0.0232	90.2
0.5	0.1283	93.20	1	0.1309	90.0	0.1303	91.9
			2	0.1414	91.0	0.1303	91.4
			4	0.1337	91.1	0.1303	91.4
			6	0.1313	91.1	0.1303	91.3
			8	0.1312	91.1	0.1303	91.3
1.0	0.2593	93.47	1	0.2310	90.0	0.2823	93.8
			2	0.2314	91.9	0.2819	92.8
			4	0.2390	92.3	0.2818	92.6
			6	0.2340	92.4	0.2818	92.6
			8	0.2340	92.4	0.2818	92.4
5.0	1.3247	103.43	1	1.3090	90.0	1.3774	103.1
			2	1.4194	99.3	1.3300	104.0
			4	1.3232	101.7	1.3233	102.8
			6	1.3222	102.1	1.3228	102.3
			8	1.3210	102.3	1.3231	102.5
10.0	2.6053	114.43	1	2.6180	90.0	3.1239	122.2
			2	2.7543	103.1	2.7913	120.0
			4	2.7293	113.0	2.7322	115.4
			6	2.7232	113.9	2.7223	114.9
			8	2.7193	114.3	2.7203	114.8
20.0	6.0140	137.61	1	5.2330	90.0	8.7159	143.1
			2	6.2533	113.2	6.5341	143.3
			4	6.1044	133.8	6.1253	133.6
			6	6.0304	135.9	6.0415	133.0
			8	6.0248	133.6	6.0236	137.3
50.0	30.2312	191.23	1	13.0800	90.0	44.7210	163.0
			2	25.1000	148.6	32.4350	187.9
			4	24.8300	180.1	26.4970	191.7
			6	24.1740	187.4	24.2400	191.3
			8	23.6330	188.5	23.9210	191.0
			10	23.6900	189.4	25.3240	190.3
100.0	98.1313	251.20	1	26.1800	90.0	173.3200	171.3
			2	89.5760	163.9	171.7300	231.6
			4	111.2240	225.9	120.2100	257.5
			6	104.6230	240.3	105.9700	259.7
			8	100.8000	244.9	101.2800	251.6
			10	93.9100	243.1	101.4400	243.2
200.0	591.5133	337.21	1	52.3300	90.0	693.1500	175.7
			2	346.4200	171.3	831.1000	214.8
			4	739.2200	272.2	1017.3000	311.6
			6	732.6000	309.3	763.3000	323.4
			8	653.4200	321.4	714.9100	330.2
			10	651.8300	323.7	648.2200	334.1

(d) MATRIX COEFFICIENT - B

Thermal time-constant RC	Distributed Modulus	Distributed Argument in degrees	No. of Lumps	Lumped L - Circuit Modulus	Lumped L - Circuit Argument in degrees
0.1	1.0001	0.69	1	1.0000	0.0
			2	1.0000	1.5
			4	1.0000	0.4
			6	1.0000	0.6
			8	1.0000	0.6
0.5	1.0015	3.37	1	1.0000	0.0
			2	1.0003	7.5
			4	1.0010	2.8
			6	1.0010	3.1
			8	1.0010	3.3
1.0	1.0053	7.40	1	1.0020	0.0
			2	1.0024	14.7
			4	1.0023	5.4
			6	1.0040	6.2
			8	1.0040	6.5
5.0	1.1350	36.13	1	1.0000	0.0
			2	1.6470	52.6
			4	1.1001	25.9
			6	1.1220	23.7
			8	1.1230	31.1
10.0	1.4343	60.53	1	1.0000	0.0
			2	2.8030	69.1
			4	1.3033	43.4
			6	1.3530	53.0
			8	1.3750	55.1
20.0	2.4831	83.05	1	1.0000	0.0
			2	6.3200	70.3
			4	1.5324	73.5
			6	2.1610	82.8
			8	2.1820	85.4
50.0	6.4839	144.99	1	1.0000	0.0
			2	13.1200	86.6
			4	4.0333	113.3
			6	5.3720	120.1
			8	5.8130	136.2
			10	5.7340	123.0
100.0	13.3074	203.83	1	1.0000	0.0
			2	23.2000	87.8
			4	13.5377	153.3
			6	14.8300	173.8
			8	15.4300	187.0
			10	16.3300	183.2
200.0	32.0033	282.81	1	1.0000	0.0
			2	32.3700	83.9
			4	55.7135	183.3
			6	64.0300	210.4
			8	69.4300	253.9
			10	71.1000	283.7

N.B. :- For distributed, T and   circuits the matrix coefficients A and D are equal.

APPENDIX II

DERIVATION OF THE THERMAL SYSTEM FUNCTIONS OF BUILDING ELEMENTS BY MATRIX ANALYSIS

Von Gorcum (23) and Pipes (24) have shown that a homogeneous building element is analogous to a two element (R & C) four terminal passive network (quadripole) and it is possible to use all the mathematical techniques employed in electrical circuit analyses in the study of linear heat conduction problems.

Analogous to the passive network system functions we have a set of thermal system functions, which will specify completely the transient behaviour of a building element. The system function is defined as a function representing the ratio of the Laplace transformations of response variable to excitation variable. In the formation of this ratio it is assumed that all the initial conditions within the system are zero.

There are two types of system functions of interest, namely (i) the transfer functions and (ii) the driving point functions. Each of these may have the dimensions of impedance, admittance, in addition to the dimensionless quantities. For a driving point function the input and output (excitation and response) are measured at the same pair of terminals, while for a transfer function the input and output are measured at two different pairs of terminals.

The transfer functions are given as :-

i) $\frac{t_i}{t_o}$ = temperature ratio.

ii) $\frac{q_i}{q_o}$ = heat flux ratio.

iii) $\frac{q_i}{t_o}$ = transfer admittance.

iv) $\frac{t_i}{q_o}$ = transfer impedance.

The driving point functions are given as :-

i) $\frac{t_o}{q_o}$ = external driving point impedance.

ii) $\frac{q_o}{t_o}$ = external driving point admittance.

iii) $\frac{t_i}{q_i}$ = internal driving point impedance.

iv) $\frac{q_i}{t_i}$ = internal driving point admittance.

The ratios of the input to output are called the reciprocal system functions. All these functions are not independent and only three functions (one transfer and two driving point) are sufficient to characterise a building element. The rest of the functions can be obtained from these three as they are interrelated.

The two linear equations that relate the input and output temperatures and heat fluxes (analogous to the quadripole) are given by :-

$$t_o = A\,t_i + B\,q_i \qquad \ldots (1)$$

$$q_o = C\,t_i + D\,q_i \qquad \ldots (2)$$

where A, B, C and D are the general circuit parameters. A and D are dimensionless numbers, B and C have dimensions of impedance and admittance respectively. These general circuit parameters are the reciprocal system functions and are given by :-

$$A = \left.\frac{t_o}{t_i}\right|_{q_i = 0} \quad \text{i.e., open circuit output.}$$

$$B = \left.\frac{t_o}{q_i}\right|_{t_i = 0} \quad \text{i.e., short circuit output.}$$

$$C = \left.\frac{q_o}{t_i}\right|_{q_i = 0} \quad \text{i.e., open circuit output.}$$

$$D = \left.\frac{q_o}{q_i}\right|_{t_i = 0} \quad \text{i.e., short circuit output.}$$

For a sinusoidal excitation all these parameters will be complex quantities.

The above equations (1) and (2) may also be expressed in the matrix form as :-

$$\begin{bmatrix} t_o \\ q_o \end{bmatrix} = \begin{bmatrix} A & B \\ C & D \end{bmatrix} \begin{bmatrix} t_i \\ q_i \end{bmatrix} \qquad \ldots (3)$$

Where $\begin{bmatrix} A & B \\ C & D \end{bmatrix}$ is the transfer matrix of the building element.

The determinant of the above matrix is equal to unity as the building element is considered as a passive network. i.e., $(AD - BC) = 1$

For a symmetrical network $A = D$

In addition to the above matrix equation (3) there are two other useful forms of matrices, relating the input and output quantities of a network namely the impedance matrix and the admittance matrix. The corresponding matrix equations are given by :-

$$\begin{bmatrix} t_o \\ t_1 \end{bmatrix} = \begin{bmatrix} Z_{11} & Z_{12} \\ Z_{21} & Z_{22} \end{bmatrix} \begin{bmatrix} q_o \\ q_1 \end{bmatrix} \quad \ldots (4)$$

and

$$\begin{bmatrix} q_o \\ q_1 \end{bmatrix} = \begin{bmatrix} Y_{11} & Y_{12} \\ Y_{21} & Y_{22} \end{bmatrix} \begin{bmatrix} t_o \\ t_1 \end{bmatrix} \quad \ldots (5)$$

The relationship between the coefficients of the transfer matrix and the Z's and Y's of the impedance and admittance matrices may be simply derived as :-

$$Z_{11} = \frac{A}{C} \qquad Z_{12} = -\frac{1}{C}$$

$$Z_{21} = \frac{1}{C} \qquad Z_{22} = -\frac{D}{C}$$

and $Y_{11} = \frac{D}{B}$ $\qquad Y_{12} = -\frac{1}{B}$

$Y_{21} = \frac{1}{B}$ $\qquad Y_{22} = -\frac{A}{B}$

The overall transfer matrices and the system functions of a network will not only depend upon the general circuit parameters but also on the nature of the termination. The heat transfer between the ambient air and the building element, takes place through the surface film conductances (h_o and h_i). The reciprocals of these surface conductances ($1/h_o$ and $1/h_i$) may be considered as analogous to the source impedance and load respectively in electrical circuits.

The overall thermal system functions, for building elements in terms of general circuit parameters and the surface heat transfer coefficients, for boundary conditions of practical importance, are derived below :-

i) External surface subjected to temperature variations (sinusoidal) while the heat flow from the inside surface is prevented. This condition is illustrated by Fig. 1. The corresponding matrix equation is given by :-

$$\begin{bmatrix} t_{os} \\ q_{os} \end{bmatrix} = \begin{bmatrix} A & B \\ C & D \end{bmatrix} \begin{bmatrix} t_{is} \\ 0 \end{bmatrix} \qquad \ldots (6)$$

This gives $t_{os} = A\, t_{is}$

$q_{os} = C\, t_{is}$

Transfer Function

$$\vec{\lambda_i} = \lambda_i \angle{-\varphi_i} = \frac{t_{is}}{t_{os}} = \frac{1}{A} \qquad ..(7)$$

Driving Point Admittance Function

$$\vec{Y_o} = Y_o \angle{\psi_o} = \frac{q_{os}}{t_{os}} = \frac{C\ t_{is}}{t_{os}} = \frac{C}{A} \qquad ..(8)$$

ii) External Surface Temperature Variation with a Constant Indoor Air Temperature. (Fig. 2).

This condition is expressed by the Matrix equation

$$\begin{bmatrix} t_{os} \\ q_{os} \end{bmatrix} = \begin{bmatrix} A & B \\ C & D \end{bmatrix} \overset{t_{is}}{\vdots} \begin{bmatrix} 1 & 1/h_i \\ 0 & 1 \end{bmatrix} \begin{bmatrix} 0 \\ q_{ia} \end{bmatrix} = \begin{bmatrix} A & B \\ C & D \end{bmatrix} \begin{bmatrix} t_{is} \\ q_{is} \end{bmatrix} \qquad ..(9)$$

where $t_{is} = q_{ia}/h_i$

$$q_{is} = q_{ia} = t_{is} \times h_i$$

Then we get

$$t_{os} = t_{is}\ (A + B\ h_i)$$

$$q_{os} = t_{is}\ (C + D\ h_i)$$

Transfer Function is given by :-

$$\vec{\lambda_i} = \lambda_i \angle{-\varphi_i} = \frac{t_{is}}{t_{os}} = \frac{1}{(A + B\ h_i)} \qquad ..(10)$$

Transfer admittance function is given by

$$\vec{Y_i} = Y_i \angle{-\psi_i} = \frac{q_{is}}{t_{os}} = \frac{t_{is} \times h_i}{t_{os}} = \frac{h_i}{(A + B\ h_i)} = \vec{\lambda_i} h_i \qquad ..(11)$$

Driving point admittance function is given by :-

$$\vec{Y_o} = Y_o \angle \psi_o = \frac{q_{os}}{t_{os}} = \frac{t_{is}\ (C + D\ h_i)}{t_{os}} = \frac{(C + D\ h_i)}{(A + B\ h_i)} \quad ..(12)$$

iii) Sol-Air temperature input with a constant indoor air temperature. (Fig. 3).

For this condition the matrix equation takes the form

$$\begin{bmatrix} t_{sa} \\ q_{sa} \end{bmatrix} = \begin{bmatrix} 1 & 1/h_o \\ 0 & 1 \end{bmatrix} \overset{t_{os}}{\vdots} \begin{bmatrix} A & B \\ C & D \end{bmatrix} \overset{t_{is}}{\vdots} \begin{bmatrix} 1 & 1/h_i \\ 0 & 1 \end{bmatrix} \begin{bmatrix} 0 \\ q_{ia} \end{bmatrix} \quad ..(13)$$

$$= \begin{bmatrix} 1 & 1/h_o \\ 0 & 1 \end{bmatrix} \begin{bmatrix} t_{os} \\ q_{os} \end{bmatrix}$$

where $\begin{matrix} t_{os} \\ q_{os} \end{matrix} = \begin{matrix} t_{is}\ (A + B\ h_i) \\ t_{is}\ (C + D\ h_i) \end{matrix}$

Therefore $t_{sa} = t_{is}\ (A + B\ h_i + C/h_o + D\ h_i/h_o)$

$q_{sa} = t_{is}\ (C + D\ h_i)$

The transfer function is obtained as :-

$$\vec{\lambda_i} = \lambda_i \angle -\varphi_i = \frac{t_{is}}{t_{sa}} = \frac{1}{(A + B\ h_i + C/h_o + D\ h_i/h_o)} \quad ..(14)$$

Transfer admittance function is obtained as :-

$$\vec{Y_i} = Y_i \angle -\psi_i = \frac{q_{is}}{t_{sa}} = \frac{t_{is} \times h_i}{t_{sa}} = \frac{h_i}{(A + B\ h_i + C/h_o + D\ h_i/h_o)}$$

Driving point admittance function is given by :-

$$\vec{Y}_o = Y_o \angle \psi_o = \frac{q_{os}}{t_{sa}} = \frac{t_{is}\,(C + D\,h_i)}{t_{sa}} = \vec{\lambda}_i (C + D\,h_i)$$

Driving point function is given by :-

$$\vec{\lambda}_o = \lambda_o \angle -\varphi_o = \frac{t_{os}}{t_{sa}} = \frac{t_{is}\,(A + B\,h_i)}{t_{sa}} = \vec{\lambda}_i (A + B\,h_i)$$

iv) Indoor air temperature is variable and external air temperature is constant (heat flow direction is reversed) (Fig. 4).

The matrix equation for this condition is given by:-

$$\begin{bmatrix} t_{ia} \\ -q_{ia} \end{bmatrix} = \begin{bmatrix} 1 & 1/h_i \\ 0 & 1 \end{bmatrix} \overset{t_{is}}{\vdots} \begin{bmatrix} D & B \\ C & A \end{bmatrix} \overset{t_{os}}{\vdots} \begin{bmatrix} 1 & 1/h_o \\ 0 & 1 \end{bmatrix} \begin{bmatrix} 0 \\ -q_{oa} \end{bmatrix} \quad ..(15)$$

Then we get

$$t_{os} = -q_{oa}/h_o$$

$$-q_{os} = -q_{oa} = t_{os} \times h_o$$

and

$$\begin{bmatrix} t_{ia} \\ -q_{ia} \end{bmatrix} = \begin{bmatrix} 1 & 1/h_i \\ 0 & 1 \end{bmatrix} \begin{bmatrix} t_{is} \\ -q_{is} \end{bmatrix}$$

where

$$t_{is} = t_{os}\,(D + B\,h_o)$$

$$-q_{is} = t_{os}\,(C + A\,h_o) \quad \cdots (16)$$

Therefore

$$t_{ia} = t_{os}\,(D + B\,h_o + C/h_i + A\,h_o/h_i)$$

$$-q_{ia} = t_{os}\,(C + A\,h_o)$$

The transfer function is obtained as :-

$$\overleftarrow{\lambda'_o} = \lambda'_o \angle{-\varphi'_o} = \frac{t_{os}}{t_{ia}} = \frac{1}{h_o/h_i\ (A + B\ h_i + C/h_o + D\ h_i/h_o)}$$

Transfer admittance function will be

$$\overleftarrow{Y'_o} = Y'_o \angle{-\psi'_o} = \frac{-q_{os}}{t_{ia}} = \frac{t_{os} \times h_o}{t_{ia}} = \frac{h_i}{(A + B\ h_i + C/h_o + D\ h_i/h_o}$$

Driving point admittance function is obtained as

$$\overleftarrow{Y'_i} = Y'_i \angle{\psi'_i} = \frac{-q_{is}}{t_{ia}} = \frac{t_{os}\ (C + A\ h_o)}{t_{ia}} = \lambda'_o(C + A\ h_o)$$

and the driving point function will be

$$\overleftarrow{\lambda'_i} = \lambda'_i \angle{-\varphi'_i} = \frac{t_{is}}{t_{ia}} = \frac{t_{os}\ (D + B\ h_o)}{t_{ia}} = \lambda'_o(D + B\ h_o)$$

v) Variable air temperature both sides (external and internal) (Fig. 5).

The matrix equation for this condition is given by

$$\begin{bmatrix} t_{oa} \\ q_{oa} \end{bmatrix} = \begin{bmatrix} 1 & 1/h_o \\ 0 & 1 \end{bmatrix} \overset{t_{os}}{\vdots} \begin{bmatrix} A & B \\ C & D \end{bmatrix} \overset{t_{is}}{\vdots} \begin{bmatrix} 1 & 1/h_i \\ 0 & 1 \end{bmatrix} \begin{bmatrix} t_{ia} \\ q_{ia} \end{bmatrix} \quad \ldots (17)$$

Then

$$t_{is} = t_{ia} + q_{ia}/h_i$$

$$q_{is} = q_{ia} \quad \ldots (18)$$

and

$$t_{os} = t_{ia}\ A + q_{ia}/h_i\ (A + B\ h_i)$$

$$q_{os} = t_{ia}\ C + q_{ia}/h_i\ (C + D\ h_i) \quad \ldots (19)$$

In the above equations q_{1a} is an unknown quantity and has to be expressed in terms of known parameters. This can be obtained from the matrix equation given below :-

$$\begin{bmatrix} t_{oa} \\ q_{oa} \end{bmatrix} = \begin{bmatrix} \frac{1}{h_o}\left(C + A\, h_o\right) & \frac{1}{h_1}\left(A + B\, h_1 + \frac{C}{h_o} + D\, \frac{h_1}{h_o}\right) \\ C & \frac{1}{h_1}\left(C + D\, h_1\right) \end{bmatrix} \begin{bmatrix} t_{1a} \\ q_{1a} \end{bmatrix}$$

This gives t_{oa} and q_{oa} as

$$t_{oa} = \frac{t_{1a}}{h_o}\left(C + A\, h_o\right) + \frac{q_{1a}}{h_1}\left(A + B\, h_1 + \frac{C}{h_o} + \frac{D\, h_1}{h_o}\right)$$

$$q_{oa} = t_{1a}\, C + \frac{q_{1a}}{h_1}\left(C + D\, h_1\right)$$

From the above equation we get

$$q_{1a} = \frac{t_{oa} - \frac{t_{1a}}{h_o}\left(C + A\, h_o\right)}{\frac{1}{h_1}\left(A + D\, h_1 + \frac{C}{h_o} + D\, \frac{h_1}{h_o}\right)}$$

Substituting this value of q_{1a} in the equation (18) and (19) by rearranging the terms we get

$$t_{1o} = t_{oa} \times \overrightarrow{\lambda_i} + t_{1a} \times \overleftarrow{\lambda'_i}$$

$$q_{1o} = t_{oa} \times \overrightarrow{Y_1} - t_{1a} \times \overleftarrow{Y'_1}$$

$$t_{oo} = t_{oa} \times \overrightarrow{\lambda_o} + t_{1a} \times \overleftarrow{\lambda'_o}$$

$$q_{oo} = t_{oa} \times \overrightarrow{Y_o} - t_{1a} \times \overleftarrow{Y'_o}$$

This condition of both sides subjected to variable air temperature can be considered as the super position of cases (iii) and (iv) (i.e., outside air temperature is variable with inside constant and vice-versa). By applying the principle of super position (which is permissible for linear circuits) we obtain the above results for the surface temperatures and heat fluxes in a much simpler way.

vi.) The air temperature on both sides is variable with the same amplitude and phase (this applies for partition walls) (Fig. 6).

For this special case the matrix equation becomes

$$\begin{bmatrix} t_{1a} \\ q_{1a} \end{bmatrix} = \begin{bmatrix} 1 & 1/h_1 \\ 0 & 1 \end{bmatrix} \begin{bmatrix} A & B \\ C & D \end{bmatrix} \begin{bmatrix} 1 & 1/h_1 \\ 0 & 1 \end{bmatrix} \begin{bmatrix} t_{1a} \\ -q_{1a} \end{bmatrix}$$

In this case we are interested in finding out the q_{1a} i.e., the heat flux entering into the partition from either side. This is obtained as :-

$$q_{1a} = t_{1a} (\overleftarrow{Y_1'} - \overrightarrow{Y_1})$$

The total quantity of heat flux entering the partition i.e., from both sides will be equal to $2\ q_{1a}$. If the building section is symmetrical with respectito the central plane, the heat flow at that plane of symmetry will be zero.

The inter relationship between the thermal system functions are easily established from the above derivations as given below :-

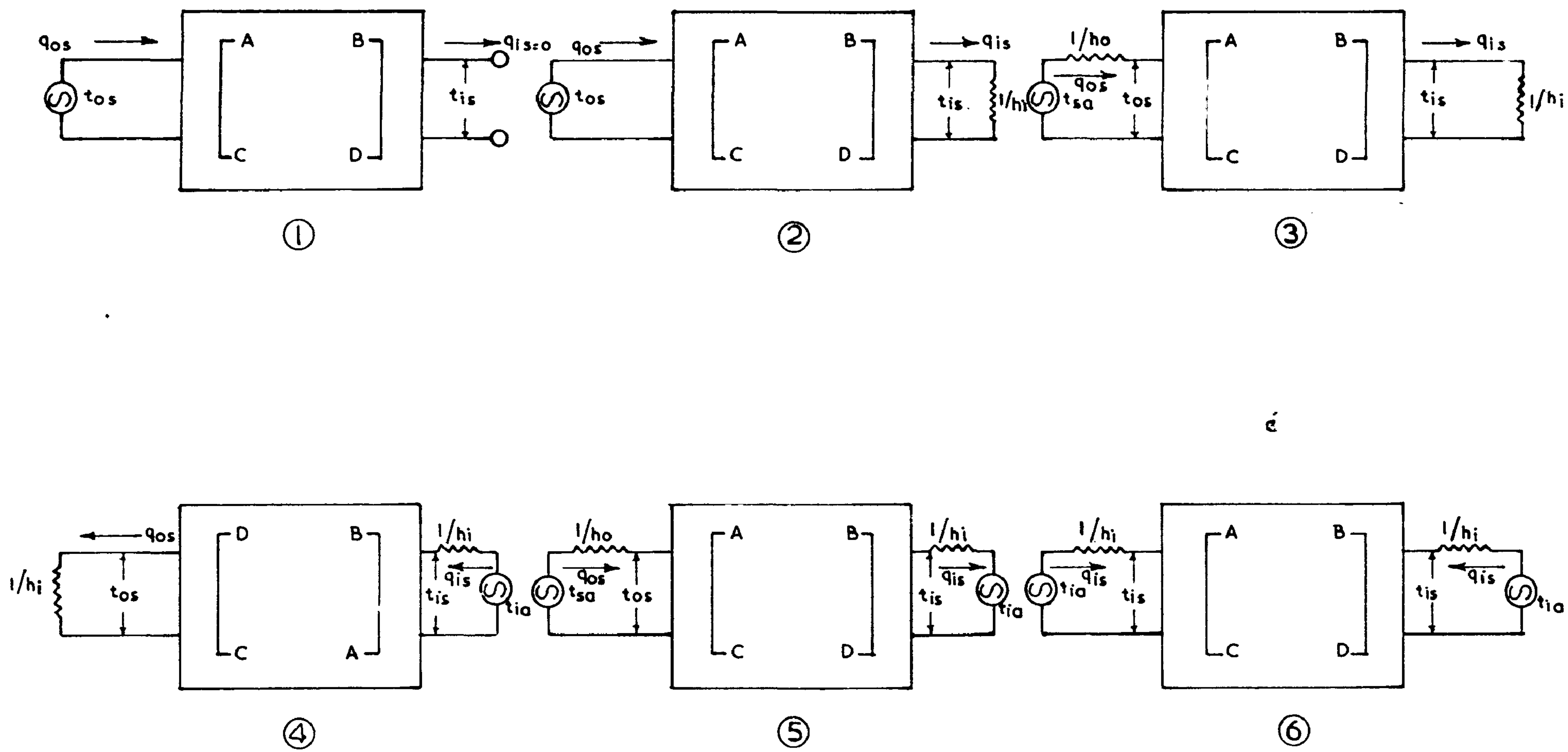

FIGS. 1 TO 6. DIAGRAMATIC REPRESENTATION OF DIFFERENT BOUNDARY CONDITIONS

Transfer Functions

1. $\lambda_i \angle -\varphi_i = \left(\frac{t_{is}}{t_{sa}}\right) \qquad t_{ia} = 0$

2. $\lambda'_o \angle -\varphi'_o = \left(\frac{t_{os}}{t_{ia}}\right) \qquad t_{sa} = 0$

$$\lambda'_o \angle -\varphi'_o = \frac{}{h_o} \lambda_i \angle -\varphi_i$$

Transfer Admittance Functions

1. $Y_i \angle -\psi_i = \left(\frac{q_{is}}{t_{sa}}\right) \qquad t_{ia} = 0$

$$Y_i \angle -\psi_i = h_i \times \lambda_i \angle -\varphi_i$$

2. $Y'_o \angle -\psi'_o = \left(\frac{q_{os}}{t_{ia}}\right) \qquad t_{sa} = 0$

$$Y'_o \angle -\psi'_o = Y_i \angle -\psi_i$$

Driving Point Functions

1. $\lambda_o \angle -\varphi_o = \left(\frac{t_{os}}{t_{sa}}\right) \qquad t_{ia} = 0$

2. $\lambda'_i \angle -\varphi'_i = \left(\frac{t_{is}}{t_{ia}}\right) \qquad t_{sa} = 0$

Driving Point Admittance Functions

1. $Y_o \angle \psi_o = \left(\frac{q_{os}}{t_{sa}}\right) \qquad t_{ia} = 0$

$$Y_o \angle \psi_o = h_o (1 - \lambda_o \angle -\varphi_o)$$

2. $Y'_i \angle \psi'_i = \left(\frac{q_{is}}{t_{ia}}\right) \qquad t_{sa} = 0$

The above relationships between the surface temperatures and heat fluxes and the thermal system functions (in terms of general circuit parameters and surface heat transfer coefficients) will hold good not only for homogeneous building elements but also for composite (multi layered) building sections. In the case of multi layered sections the transfer matrix coefficients (general circuit parameters A, B, C and D) are obtained by the matrix multiplication of the transfer matrices of the individual layers. The overall transfer matrix of a composite building element is then given by

$$\begin{bmatrix} A & B \\ C & D \end{bmatrix} = \begin{bmatrix} A_1 & B_1 \\ C_1 & D_1 \end{bmatrix} \begin{bmatrix} A_2 & B_2 \\ C_2 & D_2 \end{bmatrix} \begin{bmatrix} A_n & B_n \\ C_n & D_n \end{bmatrix}$$

A P P E N D I X   III

TABLE I

THERMAL AND PHYSICAL CONSTANTS OF VARIOUS BUILDING MATERIALS

Sl. No.	Material	Thermal conductivity K Btu/in/Ft.^{2}Hr.^{o}F	Density ρ Lb/Ft.^{3}	Sp. Heat s Btu/Lb.^{o}F	b	z_g	α	γ	δ
1.a)	Dense Concrete	8.0	120	0.21	2.097	0.477	0.025	3.147	2.823
b)	"	10.0	130	0.21	2.440	0.410	0.031	2.931	3.033
c)	"	12.0	140	0.21	2.774	0.361	0.034	2.775	3.201
d)	"	13.0	150	0.21	2.939	0.335	0.034	2.760	3.218
e)	"	10.8	132	0.22	3.030	0.325	0.030	2.972	2.595
2.	Light weight Concretes								
a)	Expanded slag	2.0	65	0.21	0.771	1.297	0.012	4.633	1.920
b)	Cinder	5.0	95	0.21	1.475	0.678	0.021	3.541	2.508
c)	Expanded clay	2.8	90	0.21	1.074	0.935	0.012	4.614	1.929
d)	Expanded Vermiculite	1.1	50	0.20	0.490	2.041	0.009	5.350	1.631
e)	Saw dust	2.6	73	0.23	1.055	0.943	0.110	4.879	1.821
f)	Coal ash (i)	2.0	60	0.21	0.741	1.349	0.013	4.451	1.997
g)	Coal ash (ii)	2.5	60	0.21	0.957	1.045	0.012	4.563	1.933
3.	Foamed Concretes								
a)	"	0.75	30	0.25	0.350	2.854	0.008	5.613	1.536
b)	"	1.45	50	0.25	0.629	1.590	0.010	5.209	1.706
c)	"	2.30	70	0.25	0.917	1.090	0.011	4.994	1.775
d)	"	3.60	90	0.25	1.310	0.763	0.013	4.433	1.977
4.	Bricks								
a)	"	6.0	100	0.21	1.653	0.603	0.023	3.317	2.677
b)	"	6.4	117	0.20	1.469	0.635	0.034	2.757	3.245
c)	"	8.0	120	0.21	2.097	0.477	0.025	3.147	2.824
d)	"	10.0	130	0.21	2.440	0.410	0.031	2.931	3.033
5.	Stones								
a)	Granite	25.0	170	0.20	4.303	0.232	0.031	3.033	4.330
b)	Sand stone	9.0	140	0.18	3.177	0.459	0.030	2.933	3.050
c)	Lime stone	11.0	150	0.22	2.814	0.355	0.023	3.071	2.329
d)	Slate	12.5	170	0.20	3.046	0.190	0.031	2.924	1.750
6.	Wood								
a)	Teak	1.3	40	0.39	0.639	1.535	0.003	6.333	1.350
b)	Sheesham	1.0	35	0.39	0.545	1.835	0.003	6.550	1.353
c)	Oak	1.25	42	0.57	0.809	1.223	0.004	7.733	1.144
7.	A.C. Sheet	2.0	95	0.20	0.753	1.323	0.009	5.470	1.233
8.	G.I. Sheet	420.0	470	0.12	22.740	0.044	0.620	0.650	13.375
9.	Glass Sheet	6.6	160	0.16	1.920	0.521	0.021	3.494	3.541
10.	Sun Dried Bricks	8.9	124	0.20	2.193	0.454	0.030	2.970	2.980

TABLE I (Cont'd..)

Sl. No.	Material	K	ρ	s	p	Z_c	a	γ	δ
11.	Soil (Compacted)	3.0	110	0.20	1.953	0.513	0.031	2.930	3.032
12.	Lime Concrete	6.1	103	0.20	1.674	0.599	0.024	3.320	2.630
13.	Terrazotile	12.0	140	0.20	2.759	0.332	0.035	2.707	3.216
14.	Mangalore Tile	5.8	120	0.17	1.607	0.621	0.024	3.327	2.668
15.	Plasters								
a)	Sand Cement	12.0	120	0.22	2.629	0.380	0.038	2.630	3.372
b)	Lime Cement	8.0	110	0.22	2.055	0.487	0.027	3.084	2.880
c)	Gypsum	3.5	70	0.23	1.103	0.901	0.018	3.302	2.336
d)	Stucco	12.6	110	0.22	2.579	0.358	0.043	2.457	3.616
e)	Mud plaster(Phuska)	4.84	90	0.35	1.921	0.521	0.011	4.733	1.833
16.	Foamed Glass	0.40	10	0.18	0.125	8.000	0.010	3.760	2.358
17.	Foamed Plastic	0.23	8	0.32	0.125	8.000	0.009	5.357	1.353
18.	Thermocole	0.20	1	0.32	0.083	27.930	0.053	2.216	4.134
19.	Insulation Boards								
a)	Celotex	0.34	14	0.28	0.170	5.839	0.007	6.012	1.477
b)	Gypsum Fibre	1.45	53	0.26	0.690	1.449	0.003	5.374	1.555
c)	Wood Fibre	0.23	16	0.34	0.207	4.331	0.006	6.920	1.237
d)	Rock wool (with a binder)	0.34	17	0.24	0.246	5.747	0.007	6.140	1.446
e)	Hair Felt	0.23	11	0.33	0.103	7.143	0.006	6.852	1.300
20.	Loose Fills								
a)	Vermiculite (i)	0.64	9	0.20	0.147	6.803	0.024	3.273	2.710
b)	-do- (ii)	0.33	6	0.20	0.093	10.750	0.022	3.495	2.543
c)	Slag wool	0.30	6	0.20	0.088	11.300	0.021	3.647	2.500
d)	Asbestos wool	1.10	30	0.20	0.380	2.632	0.015	4.141	2.142
e)	Mineral wool	0.48	13	0.18	0.178	5.618	0.013	4.437	2.011
21.	Boards								
a)	Reed Board	0.40	11	0.22	0.185	5.405	0.003	5.557	1.600
b)	Jacks Board	0.34	14	0.23	0.172	5.814	0.007	6.140	1.445
c)	Wood chip board (Rosin bounded)	0.89	49	0.32	0.554	1.803	0.005	7.440	1.195
d)	Synthetic wood	0.81	10	0.45	0.384	2.604	0.003	5.730	1.554
e)	Bamboo Mating	1.61	31	0.60	0.811	1.233	0.007	6.048	1.433
f)	Plywood	1.21	37	0.60	0.770	1.299	0.005	7.645	1.163

TABLE 2

THERMAL SYSTEM (TRANSFER AND DRIVING POINT) FUNCTION DATA FOR HOMOGENEOUS BUILDING ELEMENTS

(FOR SINUSOIDAL TEMPERATURE VARIATIONS)

Inside and Outside surface heat transfer coefficients $h_i = 1.5$, $h_o = 3.5$

S.No.	Building Element	Thickness in inches	U Value	Harmonic	External Driving point Function λ_o	$-\phi_o$ in degrees	Transfer Function λ_t	$-\phi_t$ in degrees	Internal Driving point Function λ_i	$-\phi_i$ in degrees
		2	0.833	F	0.752	10	0.548	17	0.440	10
				H_2	0.693	17	0.490	33	0.400	19
				H_3	0.623	22	0.464	42	0.330	23
				H_4	0.553	23	0.401	54	0.320	31
		4	0.633	F	0.730	17	0.338	40	0.480	18
				H_2	0.616	24	0.301	68	0.390	29
				H_3	0.533	26	0.225	82	0.330	33
				H_4	0.450	23	0.170	100	0.315	35
1.	Concrete K = 8.0 = 120 s = 0.21	6	0.537	F	0.693	18	0.224	62	0.470	21
				H_2	0.592	22	0.154	100	0.370	30
				H_3	0.533	25	0.101	123	0.330	33
				H_4	0.450	23	0.075	141	0.290	31
		8	0.513	F	0.634	18	0.201	82	0.430	23
				H_2	0.604	21	0.112	125	0.330	30
				H_3	0.548	24	0.062	160	0.320	30
				H_4	0.420	23	0.037	180	0.230	24
		2	0.740	F	0.733	8	0.432	16	0.500	8
				H_2	0.711	15	0.472	30	0.470	15
				H_3	0.637	20	0.426	42	0.430	22
				H_4	0.611	23	0.375	54	0.393	27
		4	0.570	F	0.747	12	0.360	33	0.530	16
				H_2	0.673	18	0.300	65	0.462	24
				H_3	0.611	21	0.200	85	0.420	29
				H_4	0.547	22	0.049	105	0.373	29
2.	Cinder Concrete K = 5.0 = 95 s = 0.21	6	0.434	F	0.733	14	0.237	60	0.530	19
				H_2	0.637	18	0.137	102	0.445	23
				H_3	0.611	19	0.101	124	0.405	29
				H_4	0.573	21	0.070	150	0.335	31
		8	0.392	F	0.733	13	0.149	83	0.530	23
				H_2	0.637	17	0.035	136	0.440	23
				H_3	0.311	19	0.050	168	0.380	23
				H_4	0.547	21	0.029	200	0.330	31
		2	0.612	F	0.822	4	0.352	15	0.630	5
				H_2	0.800	8	0.323	23	0.620	10
				H_3	0.737	11	0.293	40	0.597	15
				H_4	0.733	13	0.255	50	0.573	18
		4	0.339	F	0.844	7	0.200	39	0.720	11
				H_2	0.800	10	0.150	70	0.630	17
				H_3	0.755	12	0.112	90	0.550	20
				H_4	0.733	13	0.093	103	0.533	22
3.	Coal ash Concrete K = 2.0 = 60 s = 0.21	6	0.253	F	0.844	7	0.113	69	0.725	14
				H_2	0.800	10	0.033	110	0.640	16
				H_3	0.755	12	0.040	144	0.590	21
				H_4	0.733	13	0.033	163	0.550	22
		8	0.202	F	0.844	7	0.073	93	0.740	13
				H_2	0.800	10	0.033	150	0.640	17
				H_3	0.755	11	0.020	195	0.630	20
				H_4	0.711	12	0.011	223	0.630	22

TABLE 8 (Cont'd.)

$h_o = 3.5$
$h_i = 1.5$

S.No.	Building Element	Thickness in inches	U Value	Harmonic	External Driving point Function λ_o	$-\phi_o$ in degrees	Transfer Function λ_i	$-\phi_i$ in degrees	Internal Driving point Function λ_i'	$-\phi_i'$ in degrees
4.	Expanded Slag Concrete K = 2.0 = 65 s = 0.21	2	0.612	F	0.833	5	0.352	16	0.640	6
				H_2	0.812	9	0.320	30	0.620	11
				H_3	0.778	13	0.301	43	0.580	15
				H_4	0.733	14	0.237	54	0.550	18
		4	0.330	F	0.837	7	0.202	40	0.720	11
				H_2	0.800	11	0.150	75	0.640	18
				H_3	0.753	13	0.112	100	0.580	21
				H_4	0.722	14	0.080	117	0.550	23
		6	0.239	F	0.837	8	0.112	74	0.720	14
				H_2	0.800	11	0.075	122	0.640	18
				H_3	0.733	13	0.045	155	0.580	21
				H_4	0.732	14	0.030	175	0.550	22
		8	0.202	F	0.844	8	0.075	104	0.720	24
				H_2	0.739	11	0.035	162	0.640	18
				H_3	0.756	12	0.018	204	0.580	21
				H_4	0.711	14	0.003	234	0.550	22
5.	Expanded Clay Agg. Concrete K = 3.3 = 80 s = 0.21	2	0.500	F	0.800	7	0.413	20	0.580	3
				H_2	0.773	12	0.373	33	0.530	15
				H_3	0.722	16	0.337	50	0.500	20
				H_4	0.670	18	0.233	61	0.470	21
		4	0.413	F	0.822	10	0.250	46	0.650	14
				H_2	0.753	14	0.175	82	0.550	22
				H_3	0.680	16	0.125	103	0.480	25
				H_4	0.633	17	0.038	123	0.450	27
		6	0.321	F	0.811	10	0.135	80	0.640	10
				H_2	0.744	13	0.038	123	0.520	20
				H_3	0.700	15	0.050	158	0.450	24
				H_4	0.657	16	0.030	133	0.455	23
		8	0.231	F	0.739	10	0.035	103	0.640	10
				H_2	0.722	13	0.023	168	0.600	20
				H_3	0.637	15	0.018	214	0.470	24
				H_4	0.633	16	0.010	246	0.440	25
6.	Expanded Vermiculite Concrete K = 1.1 = 60 s = 0.20	2	0.353	F	0.837	3	0.237	17	0.711	4
				H_2	0.844	7	0.225	32	0.718	8
				H_3	0.822	8	0.200	45	0.685	12
				H_4	0.800	10	0.173	53	0.330	15
		4	0.220	F	0.873	5	0.125	43	0.700	8
				H_2	0.844	8	0.103	81	0.740	13
				H_3	0.812	9	0.075	103	0.710	16
				H_4	0.778	10	0.057	123	0.670	13
		6	0.157	F	0.973	5	0.072	80	0.800	10
				H_2	0.844	8	0.040	134	0.740	14
				H_3	0.813	9	0.022	165	0.700	13
				H_4	0.773	10	0.012	205	0.650	13
		8	0.123	F	0.800	5	0.040	120	0.810	11
				H_2	0.873	8	0.013	180	0.740	14
				H_3	0.844	9	0.007	223	0.600	16
				H_4	0.811	10	0.003	234	0.630	17

TABLE 3 (Cont'd.)

$h_o = 3.5$

$h_i = 1.5$

No.	Building Element	Thickness in inches	U value	Harmonic	Internal Driving Point Function λ_o	$-\phi_o$ in degrees	Transfer Function λ_i	ϕ_i in degrees	Internal Driving Point Function λ'_i	$-\phi'_i$ in degrees
7.	Sawdust Concrete	2	0.535	F	0.800	6	0.384	19	0.595	8
	k = 2.3			H_2	0.753	11	0.334	35	0.530	16
	ρ = 70			H_3	0.711	15	0.314	49	0.510	21
	c = 0.23			H_4	0.637	16	0.254	60	0.430	25
		4	0.404	F	0.811	9	0.230	50	0.630	15
				H_2	0.733	13	0.150	83	0.530	33
				H_3	0.673	15	0.101	108	0.500	35
				H_4	0.644	15	0.030	123	0.460	36
		6	0.309	F	0.800	10	0.125	82	0.640	18
				H_2	0.733	12	0.075	124	0.530	22
				H_3	0.630	14	0.042	163	0.480	24
				H_4	0.644	15	0.023	194	0.450	23
		8	0.250	F	0.800	9	0.031	116	0.640	18
				H_2	0.733	13	0.034	184	0.550	22
				H_3	0.609	14	0.016	216	0.475	25
				H_4	0.653	15	0.003	256	0.445	23
8.	Foamed Concrete	1	0.453	F	0.353	2	0.323	7	0.700	2
	k = 0.75			H_2	0.853	4	0.303	13	0.700	3
	ρ = 30			H_3	0.844	5	0.223	18	0.695	4
	s = 0.25			H_4	0.840	6	0.230	23	0.650	5
		2	0.277	F	0.911	3	0.200	17	0.800	3
				H_2	0.911	5	0.173	30	0.763	6
				H_3	0.889	7	0.135	42	0.730	9
				H_4	0.837	8	0.151	54	0.750	11
		4	0.169	F	0.911	4	0.101	43	0.850	6
				H_2	0.911	7	0.075	73	0.750	10
				H_3	0.873	8	0.053	103	0.730	12
				H_4	0.853	9	0.040	123	0.740	14
		6	0.112	F	0.932	4	0.050	80	0.840	7
				H_2	0.930	6	0.033	133	0.800	11
				H_3	0.873	8	0.016	164	0.733	12
				H_4	0.856	9	0.010	204	0.740	14
9.	Brick	4.5	0.580	F	0.756	14	0.330	42	0.620	15
	k = 6.0			H_2	0.653	20	0.230	69	0.450	27
	ρ = 130			H_3	0.573	22	0.123	95	0.330	31
	c = 0.21			H_4	0.533	23	0.150	112	0.330	33
		9	0.403	F	0.723	15	0.150	53	0.500	24
				H_2	0.644	19	0.073	144	0.416	27
				H_3	0.533	21	0.042	178	0.335	30
				H_4	0.544	22	0.023	203	0.320	33
		13.5	0.312	F	0.714	14	0.030	142	0.500	21
				H_2	0.633	18	0.031	216	0.412	27
				H_3	0.573	20	0.003	253	0.370	29
				H_4	0.533	21	0.003	312	0.337	31
		18	0.254	F	0.711	14	0.021	191	0.515	23
				H_2	0.633	17	0.005	273	0.420	27
				H_3	0.578	13	◦	◦	0.350	31
				H_4	0.633	19	◦	◦	0.310	33

TABLE 2 (Cont'd.)

$h_o = 3.5$
$h_i = 1.5$

S.No.	Building Element	Thickness in inches	U value	Harmonic	External Driving point Function λ_o	$-\phi_o$ in degrees	Transfer Function λ_i	$-\phi_i$ in degrees	Internal Driving point Function λ'_i	$-\phi'_i$ in degrees
		4	0.633	F	0.637	15	0.433	36	0.460	19
				H_2	0.533	23	0.315	65	0.380	20
				H_3	0.457	23	0.250	82	0.303	35
				H_4	0.422	27	0.200	93	0.280	33
10.	Sand Stone	8	0.543	F	0.632	18	0.240	78	0.460	27
				H_2	0.533	22	0.133	122	0.370	30
				H_3	0.489	24	0.033	152	0.310	33
				H_4	0.444	23	0.043	173	0.275	34
	K = 9.0 = 140 s = 0.18	12	0.433	F	0.611	17	0.120	125	0.430	27
				H_2	0.533	22	0.054	177	0.350	30
				H_3	0.473	23	0.023	224	0.300	32
				H_4	0.433	23	0.013	254	0.275	33
		16	0.355	F	0.633	17	0.052	180	0.440	27
				H_2	0.553	21	0.016	238	0.345	30
				H_3	0.500	22	0.005	283	0.305	32
				H_4	0.457	24	°	°	0.270	34
		0	0.599	F	0.635	18	0.170	95	0.430	27
				H_2	0.590	21	0.037	125	0.350	31
				H_3	0.520	23	0.048	160	0.320	33
				H_4	0.480	25	0.031	135	0.260	34
11.	Sun Dried Brick K = 0.9 = 123 s = 0.20	13.5	0.405	F	0.680	17	0.080	130	0.420	26
				H_2	0.570	20	0.031	180	0.370	30
				H_3	0.520	23	0.012	245	0.320	32
				H_4	0.475	24	0.007	265	0.230	34
		18	0.333	F	0.630	17	0.033	180	0.425	23
				H_2	0.570	21	0.010	230	0.350	30
				H_3	0.510	23	0.003	320	0.295	33
				H_4			°	°		
12.	Lime Concrete K = 6.1 = [illegible] s = 0.20	3	0.633	F	0.770	9	0.430	25	0.520	13
				H_2	0.620	10	0.330	45	0.445	20
				H_3	0.610	22	0.310	60	0.330	23
				H_4	0.630	24	0.330	77	0.325	33
13.	Soil (Rammed earth)	10	0.450	F	0.630	17	0.150	93	0.440	25
				H_2	0.620	19	0.075	140	0.380	29
				H_3	0.530	21	0.033	180	0.335	31
				H_4	0.510	23	0.025	220	0.310	32
	K = 0.0 = 110 s = 0.20	20	0.291	F	0.700	15	0.027	195	0.480	24
				H_2	0.611	19	0.003	260	0.390	27
				H_3			°	°		
				H_4			°	°		
14.	Terracotile K = 13 = 120 s = 0.20	1	0.931	F	0.730	5	0.640	7	0.370	5
				H_2	0.730	10	0.310	15	0.330	10
				H_3	0.680	15	0.575	19	0.340	15
				H_4	0.660	30	0.550	27	0.310	20
15.	A.C. Sheet K = 2.0 = 00 s = 0.20	1/4	0.985	F	0.711	°	0.620	2	0.300	1
				H_2	0.711	4	0.620	6	0.350	2
				H_3	0.630	5	0.618	8	0.350	3
				H_4	0.633	7	0.603	12	0.233	4

TABLE 8 (Cont'd.)

$H_o = 3.5$

$h_i = 1.5$

S.No.	Building Element	Thickness in inches	U value	Harmonic	External Driving point Function λ_o	External Driving point Function $-\phi_o$ in degrees	Transfer Function λ_i	Transfer Function $-\phi_i$ in degrees	Internal Driving point Function λ'_i	Internal Driving point Function $-\phi'_i$ in degrees
		1	0.531	F	0.833	3	0.370	8	0.620	3
				H_2	0.832	6	0.353	16	0.605	6
				H_3	0.800	9	0.342	23	0.584	9
				H_4	0.778	10	0.318	31	0.575	11
16.	Rockwood	2	0.333	F	0.837	5	0.244	25	0.720	6
				H_2	0.833	9	0.207	41	0.680	11
				H_3	0.739	11	0.182	60	0.630	15
	K = 1.2			H_4	0.763	11	0.159	74	0.600	19
	= 40	4	0.204	F	0.667	7	0.118	64	0.680	10
	s = 0.39			H_2	0.822	9	0.073	103	0.680	17
				H_3	0.778	11	0.050	133	0.620	19
				H_4	0.744	11	0.032	160	0.580	21
		2	0.201	F	0.900	2	0.180	15	0.800	4
				H_2	0.900	4	0.175	29	0.780	7
				H_3	0.880	5	0.165	42	0.720	10
17.	Synthetic wood			H_4	0.860	7	0.150	53	0.700	12
	K = 0.31	4	0.109	F	0.930	3	0.095	46	0.840	7
	= 19			H_2	0.900	6	0.075	80	0.770	11
				H_3	0.880	7	0.053	125	0.730	13
	s = 0.45			H_4	0.850	7	0.043	140	0.680	15
		1/4	0.833	F	0.750	1	0.575	2	0.440	1
18.	Plywood			H_2	0.750	2	0.570	4	0.440	2
				H_3	0.750	3	0.570	5	0.430	4
	K = 1.2			H_4	0.740	4	0.570	7	0.430	4
	= 37	1/3	0.750	F	0.730	2	0.485	5	0.500	2
				H_2	0.730	4	0.435	8	0.520	5
	s = 0.60			H_3	0.730	6	0.480	12	0.510	7
				H_4	0.730	8	0.475	17	0.490	[illegible]
19.	Hard board	1/4	0.880	F	0.740	2	0.550	3	0.480	2
				H_2	0.740	3	0.550	6	0.470	4
	K = 0.92			H_3	0.740	4	0.530	11	0.470	5
				H_4	0.740	6	0.520	15	0.435	7
	= 63	1/2	0.671	F	0.805	3	0.450	9	0.550	4
				H_2	0.800	6	0.430	13	0.550	7
	s = 0.33			H_3	0.735	8	0.410	21	0.530	11
				H_4	0.750	11	0.405	27	0.520	14
20.	Wood fibre board	1	0.333	F	0.911	1	0.137	8	0.320	1
	K = 0.23			H_2	0.911	1	0.132	13	0.315	2
	= 16			H_3	0.911	1	0.175	19	0.310	4
	s = 0.34			H_4	0.911	1	0.171	23	0.303	6
		2	0.163	F	0.910	1	0.103	10	0.330	[illegible]
				H_2	0.900	3	0.093	33	0.320	[illegible]
				H_3	0.839	3	0.032	49	0.840	[illegible]
				H_4	0.839	4	0.071	60	0.835	[illegible]
21.	Mineral wool	1	0.333	F	0.900	1	0;225	2	0.730	[illegible]
	K = 0.43			H_2	0.900	1	0.225	4	0.720	[illegible]
	= 13			H_3	0.900	1	0.235	6	0.770	[illegible]
	s = 0.13			H_4	0.900	1	0.225	9	0.770	[illegible]
		2	0.197	F	0.930	1	0.135	7	0.860	[illegible]
				H_2	0.930	1	0.130	15	0.860	[illegible]
				H_3	0.930	2	0.123	20	0.820	[illegible]
				H_4	0.930	3	0.120	23	0.820	[illegible]

TABLE 2 (Cont'd.)

$h_o = 3.5$

$h_i = 1.5$

S.No.	Building Element	Thickness in inches	U value	Harmonic	External Driving point Function λ_o	$-\phi_o$ in degrees	Transfer Function λ_i	$-\phi_i$ in degrees	Internal Driving point Function λ'_i	$-\phi'_i$ in degrees
		1	0.290	F	0.911	1	0.205	3	0.800	1
				H_2	0.911	1	0.205	4	0.800	1
				H_3	0.911	1	0.205	5	0.800	1
				H_4	0.911	1	0.205	6	0.800	2
22.	Foamed Glass	2	0.163	F	0.933	1	0.120	7	0.890	1
				H_2	0.933	1	0.120	10	0.800	2
				H_3	0.933	1	0.116	16	0.835	3
	K = 0.4			H_4	0.933	2	0.114	22	0.830	4
	= 13	4	0.093	F	0.944	1	0.062	20	0.940	2
				H_2	0.944	1	0.059	36	0.940	4
	s = 0.18			H_3	0.944	2	0.052	50	0.935	5
				H_4	0.944	3	0.047	66	0.930	6
		1	0.220	F	0.933	1	0.160	4	0.850	1
				H_2	0.933	1	0.160	6	0.850	1
				H_3	0.933	1	0.160	9	0.850	2
				H_4	0.933	1	0.153	11	0.850	3
23.	Foamed Plastic	2	0.125	F	0.944	1	0.039	10	0.930	1
				H_2	0.944	1	0.034	19	0.920	3
				H_3	0.944	2	0.032	26	0.925	3
	K = 0.23			H_4	0.944	3	0.078	35	0.920	3
	= 3	4	0.055	F	0.944	1	0.041	33	0.950	3
				H_2	0.944	2	0.034	48	0.940	4
	s = 0.32			H_3	0.944	3	0.027	72	0.930	5
				H_4	0.944	4	0.022	96	0.920	6
		1	0.163	F	0.940	1	0.115	1	0.890	1
				H_2	0.940	1	0.115	1	0.890	1
				H_3	0.940	1	0.115	1	0.890	1
				H_4	0.940	1	0.115	2	0.890	1
24.	Thermocole	2	0.082	F	0.970	1	0.033	1	0.940	1
				H_2	0.970	1	0.033	3	0.940	1
				H_3	0.970	1	0.033	4	0.940	1
	K = 0.20			H_4	0.970	1	0.033	6	0.940	1
	= 1	4	0.049	F	0.930	1	0.034	5	0.930	1
				H_2	0.930	1	0.034	11	0.930	1
	s = 0.32			H_3	0.930	1	0.033	17	0.930	1
				H_4	0.930	1	0.032	22	0.930	1
25.	Wood Board	1	0.239	F	0.900	1	0.200	3	0.810	1
				H_2	0.900	1	0.200	6	0.810	2
				H_3	0.900	1	0.190	9	0.800	2
	K = 0.40			H_4	0.900	2	0.185	14	0.730	3
	= 11	2	0.153	F	0.940	1	0.120	11	0.800	2
				H_2	0.940	1	0.105	21	0.855	3
	s = 0.33			H_3	0.940	3	0.100	33	0.850	5
				H_4	0.940	3	0.095	43	0.850	7
26.	Celotex Board	1/2	0.413	F	0.873	1	0.290	3	0.730	1
				H_2	0.873	1	0.290	5	0.730	1
				H_3	0.873	1	0.290	6	0.730	2
	K = 0.24			H_4	0.873	1	0.290	7	0.730	3
	= 14	1	0.257	F	0.911	1	0.175	6	0.830	1
				H_2	0.911	1	0.175	10	0.820	2
	s = 0.23			H_3	0.910	1	0.173	15	0.810	3
				H_4	0.903	1	0.171	19	0.800	4

° Not measureable.

– Minus sign indicates lag angle.

APPENDIX IV

THERMAL SYSTEM (TRANSFER AND DRIVING POINT) FUNCTION DATA FOR COMPOSITE BUILDING ELEMENTS

(FOR SINUSOIDAL TEMPERATURE VARIATION)

In building practice a large number of composite constructions (made up of two or more layers of homogeneous materials of different thicknesses) are met with. The traditional building materials like brick, stone, timber, concrete etc. still form the basic core in these constructions. Of late, a large variety of lightweight concretes, insulating boards, sandwitch, panel constructions etc. have come into use and their use in combination with the conventional materials in a variety of ways, are becoming popular.

In this Appendix the thermal system functions for a number of composite constructions (both traditional and modern) that are employed in the present day building practice are given along with the steady state thermal transmission coefficients (U - values).

For the sake of convenience these data are divided into different sections, according to their functional use viz., walls, roofs, floors, doors and windows.

TABLE 1

[illegible]

$h_o = 3.5$
$h_i = 1.5$

S.No.	Wall Section	U value	Harmonic	External Driving Point Function: λ_o	External Driving Point Function: $-\phi_o$ in degrees	Transfer Function: λ_i	Transfer Function: $-\phi_i$ in degrees	Internal Driving Point Function: λ'_i	Internal Driving Point Function: $-\phi'_i$ in degrees
1.	1/2" plaster + 4½" brick + 1/2" plaster	0.630	F	0.763	10	0.263?	48	0.537?	21
			H_2	0.453?	19	0.222	73	0.337	23
			H_3	0.539	24	0.160	104	0.329	31
			H_4	0.641	27	0.116	122	0.300	33
2.	1/2" plaster + 9" brick + 1/2" plaster	0.395?	F	0.744	17	0.123	113	0.500?	33
			H_2	0.644	23	0.063	163	0.333?	30
			H_3	0.573	23	0.031	200	0.313?	32
			H_4	0.634	23	0.017	220	0.305?	34
3.	1/2" plaster + 13½" brick + 1/2" plaster	0.305?	F	0.724	15	0.052?	160	0.499?	25
			H_2	0.644	22	0.013	228	0.373	30
			H_3	0.593?	36	0.004?	276	0.311	33
			H_4	0.634	27	0.003	320	0.282	35
4.	1/2" plaster + 4½" brick + 1" foamed concrete + 1/2" plaster	0.331	F	0.778	17	0.159	75	0.722	13
			H_2	0.644	21	0.050?	103?	0.656?	20
			H_3	0.673	23	0.052	132	0.630	23
			H_4	0.634	23	0.040	153	0.563	31
5.	1/2" plaster + 4½" brick + 2" foamed concrete + 1/2" plaster	0.325?	F	0.753	21	0.059	94	0.773	16
			H_2	0.644	26	0.056	134	0.716	23
			H_3	0.620	27	0.031	162	0.633?	30
			H_4	0.634	24	0.018	203	0.532?	23
6.	1/2" plaster + 4½" brick + 4" foamed concrete + 1/2" plaster	0.141	F	0.733	22	0.047	137	0.822	22
			H_2	0.644	27	0.023	201	0.713	27
			H_3	0.673	29	0.014	243	0.629	35
			H_4	0.633?	31	0.207?	270	0.537	30
7.	1/2" plaster + 1" foamed concrete + 4½" brick + 1/2" plaster	0.320	F	0.800?	16	0.112	94	0.516	20
			H_2	0.559?	20	0.063	112	0.333	20
			H_3	0.453?	24	0.040	133	0.327	31
			H_4	0.332?	23	0.027	142	0.303?	32
8.	1/2" plaster + 2" foamed concrete + 4½" brick + 1/2" plaster	0.325?	F	[illegible]	12	0.073	100	0.538?	27
			H_2	0.011	13	0.037	133	0.330?	30
			H_3	[illegible]	23?	0.021	166	0.323?	32
			H_4	0.344?	23	0.013	212	0.311	33
9.	3/4" plaster + 1" wood board + 4½" brick + 1/2" plaster	0.253?	F	[illegible]	8	0.074	90	0.511	22
			H_2	[illegible]	15	0.053	123	0.373	24
			H_3	0.241?	21	0.019	152	0.221?	23
			H_4	[illegible]	23	0.009	170	0.300	37

WALL SECTIONS

½" p + 4½" brick + ½" p

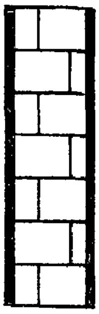

(1)

½" p + 9" brick + ½" p

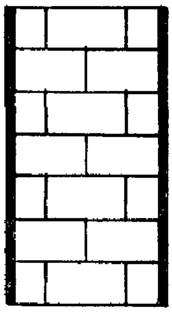

(2)

½" p + 13½" brick + ½" p

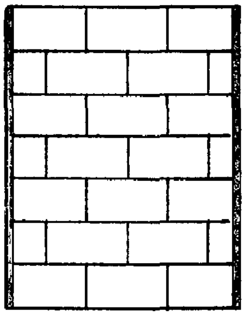

(3)

½" p + 4½" brick + 1" F.C. + ½" p

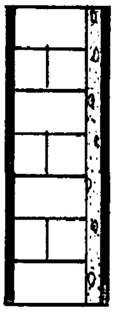

(4)

½" p + 4½" brick + 2" F.C. + ½" p

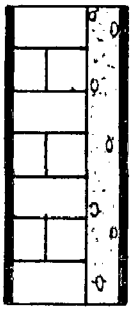

(5)

½" p + 4½" brick + 4" F.C. + ½" p

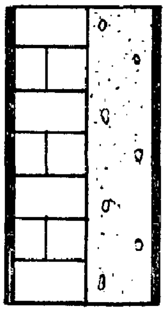

(6)

½" p + 1" F.C.+ 4½" brick + ½" p

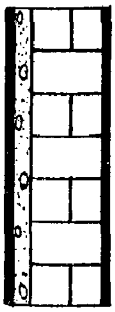

(7)

½" p + 2" F.C. + 4½" brick + ½" p

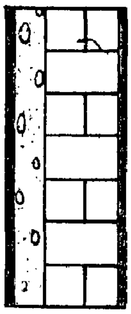

(8)

½" p + 1" r.b. + 4½" brick + ½" p

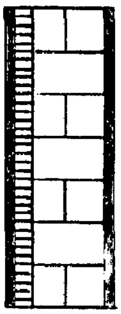

(9)

p = plaster F.C. = Foamed concrete
r.b. = reed board

TABLE 3 (Cont'd.)

$h_o = 3.5$

$h_i = 1.5$

Wall No.	Wall Section	U value	Harmonic	External Driving Point Function λ_o	$-\phi_o$ in degrees	Transfer Function λ_i	$-\phi_i$ in degrees	Internal Driving Point Function λ'_i	$-\phi'_i$ in degrees
10.	1/2" plaster + 3" foamed concrete + 1/2" plaster	0.123	F	0.911	7	0.122	40	0.822	16
			H_2	0.873	14	0.102	67	0.733	23
			H_3	0.827	19	0.038	102	0.644	33
			H_4	0.738	23	0.049	130	0.573	33
11.	3/4" plaster + 3" wood board + 3/4" plaster	0.104	F	0.844	7	0.094	40	0.812	18
			H_2	0.822	15	0.073	69	0.713	31
			H_3	0.774	22	0.030	92	0.622	40
			H_4	0.720	25	0.047	112	0.533	44
12.	3/4" plaster + 4" wood board + 3/4" plaster	0.090	F	0.934	8	0.049	63	0.893	18
			H_2	0.912	10	0.031	109	0.711	32
			H_3	0.844	24	0.019	144	0.600	40
			H_4	0.733	23	0.012	162	0.611	45
13.	1/2" plaster + 2" foamed concrete + 2" dense concrete + 1/2" plaster	0.259	F	0.916	7	0.119	68	0.573	32
			H_2	0.893	13	0.032	92	0.400	40
			H_3	0.863	19	0.052	103	0.311	42
			H_4	0.813	23	0.063	132	0.232	44
14.	1/2" plaster + 2" foamed concrete + 4" dense concrete + 1/2" plaster	0.233	F	0.912	14	0.023	64	0.573	33
			H_2	0.823	17	0.041	104	0.423	41
			H_3	0.853	21	0.030	123	0.373	43
			H_4	0.818	23	0.020	160	0.351	45
15.	1/2" plaster + 2 " dense concrete + 2" foamed concrete + 1/2" plaster	0.259	F	0.312	20	0.133	60	0.718	14
			H_2	0.632	23	0.094	63	0.653	24
			H_3	0.520	22	0.032	125	0.639	30
			H_4	0.429	34	0.044	140	0.533	35
16.	1/2" plaster + 4" dense concrete + 2" foamed concrete + 1/2" plaster	0.233	F	0.770	23	0.113	83	0.732	14
			H_2	0.610	30	0.057	104	0.722	24
			H_3	0.530	32	0.024	123	0.344	31
			H_4	0.450	34	0.201	130	0.573	33
17.	1½" dense concrete + 2" jem board + 4½" brick + 1/2" plaster	0.130	F	0.924	15	0.050	103	0.511	24
			H_2	0.849	27	0.017	123	0.373	23
			H_3	0.733	35	0.009	170	0.337	33
			H_4	0.644	40	0.005	230	0.309	40
18.	1/2" plaster + 4½" brick + 2" air space + 4½" brick + 1/2" plaster	0.205	F	0.744	19	0.038	123	0.437	30
			H_2	0.623	24	0.034	170	0.340	33
			H_3	0.530	27	0.015	224	0.300	33
			H_4	0.516	20	0.003	253	0.283	39

WALL SECTIONS

½" p + 3" F.C. + ½" p

(10)

¾" p + 2" r.b. + ¾" p

(11)

¾" p + 4" r.b. + ¾" p

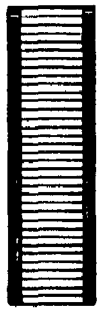

(12)

½" p + 2" F.C. + 2" D.C. + ½" p

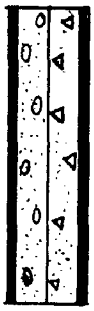

(13)

½" p + 2" F.C. + 4" D.C. + ½" p

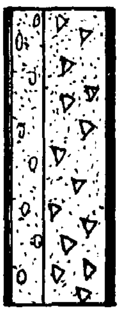

(14)

½" p + 2" D.C. + 2" F.C. + ½" p

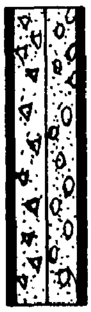

(15)

½" p + 4" D.C. + 2" F.C. + ½" p

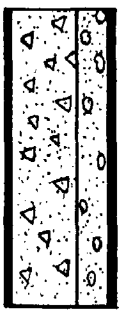

(16)

1½" conc. + 2" jax board + 4½" brick + ½" p

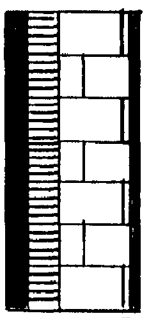

(17)

½" p + 4½" brick + 2" airspace + 4½" brick + ½" p

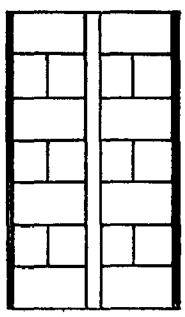

(18)

F.C. = Foamed concrete r.b. = reed board
D.C. = Dense concrete p = plaster

TABLE 3 (Cont'd.)

h_o = 3.5

h_i = 1.6

S.No.	Wall section	U value	Harmonic	External Driving Point Function λ_o	$-\phi_o$ in degrees	Transfer Function λ_i	$-\phi_i$ in degrees	Internal Driving Point Function λ_i	$-\phi_i$ in degrees
19.	1" plaster + 1" thermocole + 4½" brick + 1/2" plaster	0.147	F	0.884	19	0.043	80	0.570	24
			H_2	0.911	20	0.024	110	0.378	33
			H_3	0.844	23	0.014	154	0.322	33
			H_4	0.733	35	0.009	202	0.283	39
20.	1/2" plaster + 4½" brick + 1" thermocole + 1/2" plaster	0.147	F	0.734	24	0.055	87	0.822	18
			H_2	0.600	28	0.035	102	0.601	32
			H_3	0.534	30	0.022	138	0.537	38
			H_4	0.420	32	0.012	191	0.471	42
21.	16" rubble masonry + 3/4" plaster	0.373	F	0.649	18	0.059	150	0.418	20
			H_2	0.586	22	0.015	220	0.333	30
			H_3	0.512	24	0.006	275	0.223	32
			H_4	0.433	27	0.003	305	0.271	34
22.	3/4" plaster + 16" rubble masonry + 3/4" plaster	0.304	F	0.641	18	0.043	185	0.423	27
			H_2	0.563	23	0.012	224	0.353	32
			H_3	0.493	23	0.004	230	0.311	35
			H_4	0.483	27	0.002	314	0.278	37
23.	18" rubble masonry + 3/4" plaster	0.282	F	0.644	18	0.025	169	0.409	30
			H_2	0.571	22	0.006	272	0.329	32
			H_3	0.511	24	0.003	316	0.300	34
			H_4	0.475	25	0.001	°	0.237	35
24.	1½" marble + 9" brick + 1/2" plaster	0.323	F	0.636	22	0.052	132	0.383	24
			H_2	0.523	32	0.052	162	0.373	33
			H_3	0.440	37	0.023	220	0.322	32
			H_4	0.300	40	0.010	230	0.200	33
25.	2" marble + 9" brick + 1/2" plaster	0.339	F	0.503	24	0.022	140	0.439	32
			H_2	0.423	33	0.024	163	0.332	34
			H_3	0.410	40	0.013	235	0.324	38
			H_4	0.332	43	0.006	230	0.304	40
26.	3" sand stone + 13½" brick + 1/2" plaster	0.300	F	0.644	17	0.027	131	0.454	27
			H_2	0.531	21	0.020	239	0.403	31
			H_3	0.432	20	0.006	204	0.233	35
			H_4	0.451	24	0.001	240	0.331	30
27.	6" sand stone + 9" brick + 1/2" plaster	0.317	F	0.684	18	0.047	170	0.420	30
			H_2	0.547	21	0.014	230	0.339	34
			H_3	0.429	24	0.003	208	0.329	33
			H_4	0.444	23	0.003	340	0.300	38

WALL SECTIONS

1" p + 1" T.C. + 4½" brick + ½" p

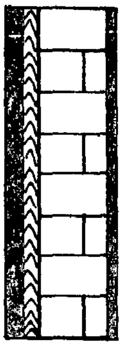

(19)

½" p + 4½" brick + 1" T.C. + ½" p

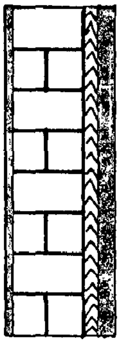

(20)

15" R.M. + ¾" p

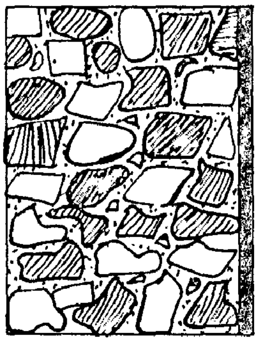

(21)

¾" p + 15" R.M. + ¾" p

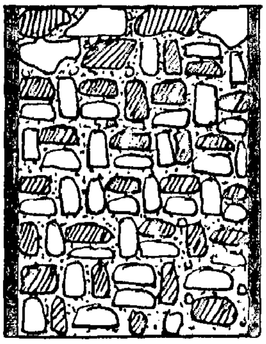

(22)

18" R.M. + ¾" p

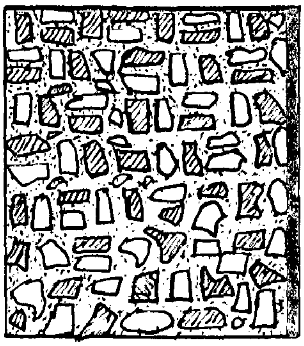

(23)

1½" stone + 9" brick + ½" p

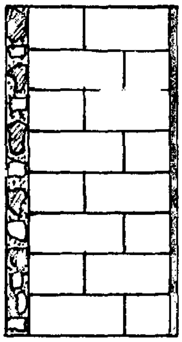

(24)

3" stone + 9" brick + ½" p

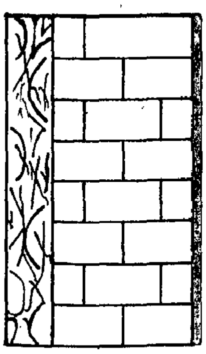

(25)

3" stone + 13½" brick + ½" p

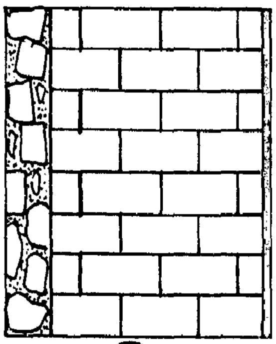

(26)

6" stone + 9" brick + ½" p

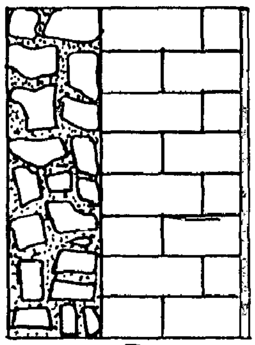

(27)

p = plaster   T.C. = Thermocole   R.M. = Rubble Masonry

TABLE 3 (Cont'd.)

$h_o = 3.5$

$h_i = 1.5$

W.No.	Wall Section	U value	Harmonic	Internal Driving Point Function λ_o	Internal Driving Point Function $-\phi_o$ in degrees	Transfer Function λ_i	Transfer Function $-\phi_i$ in degrees	Internal Driving Point Function λ'_i	Internal Driving Point Function $-\phi'_i$ in degrees
28.	6" sand stone + 13½" brick + 1/2" plaster	0.283	F	0.627	20	0.018	220	0.437	28
			H_2	0.647	22	0.005	273	0.373	34
			H_3	0.490	24	0.002	318	0.333	30
			H_4	0.444	27	0.001	0	0.331	41
29.	1" bricktile + 9" brick + 1/2" plaster	0.323	F	0.489	18	0.110	118	0.437	31
			H_2	0.600	22	0.052	162	0.332	35
			H_3	0.559	24	0.031	203	0.329	37
			H_4	0.489	25	0.019	259	0.304	39
30.	2" bricktile + 9" brick + 1/2" plaster	0.372	F	0.637	20	0.084	132	0.480	20
			H_2	0.553	24	0.040	194	0.373	24
			H_3	0.450	23	0.020	223	0.322	23
			H_4	0.444	23	0.010	273	0.300	41
31.	1" bricktile + 13½" brick + 1/2" plaster	0.300	F	0.633	15	0.059	163	0.403	23
			H_2	0.573	20	0.016	223	0.411	32
			H_3	0.522	23	0.003	285	0.350	31
			H_4	0.473	25	0.003	310	0.331	37
32.	2" bricktile + 13½" brick + 1/2" plaster	0.391	F	0.644	20	0.049	178	0.500	27
			H_2	0.563	25	0.010	246	0.413	32
			H_3	0.409	28	0.004	300	0.322	34
			H_4	0.444	30	0.002	325	0.333	37
33.	3" brick + 2" air space + 3" brick	0.334	F	0.773	10	0.175	73	0.625	28
			H_2	0.663	16	0.023	120	0.389	30
			H_3	0.533	22	0.036	146	0.313	35
			H_4	0.533	24	0.023	163	0.273	30
34.	1/2" plaster + 3" brick + 3" air space + 3" brick + 1/2" plaster	0.369	F	0.774	12	0.153	85	0.580	29
			H_2	0.624	20	0.032	123	0.413	30
			H_3	0.573	23	0.042	162	0.333	40
			H_4	0.523	30	0.027	173	0.300	43
35.	8" hollow concrete block	0.531	F	[illegible]	23	0.233	73	0.424	28
			H_2	0.310	33	0.133	117	0.373	32
			H_3	0.530	33	0.091	144	0.222	34
			H_4	0.523	33	0.065	164	0.203	37
36.	8" hollow concrete block + 1/2" plaster	0.599	F	0.600	20	0.210	82	0.455	33
			H_2	[illegible]	24	0.116	123	0.324	35
			H_3	0.630	33	0.071	154	0.304	41
			H_4	0.531	40	0.047	170	0.373	43

WALL SECTIONS

6" stone + 13½" brick + ½" p

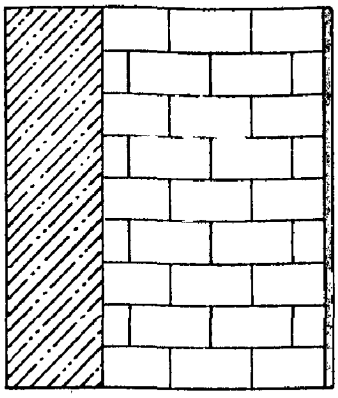

28

1" B.T. + 9" brick + ½" p

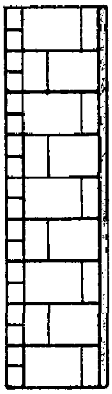

29

2" B.T. + 9" brick + ½" p

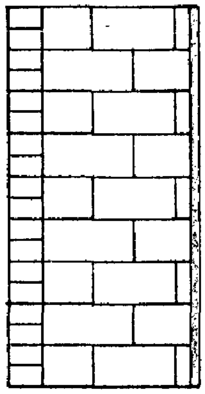

30

1" B.T. + 13½" brick + ½" p

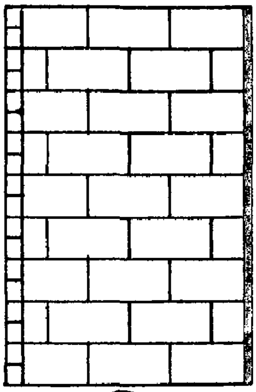

31

2" B.T. + 13½" brick + ½" p

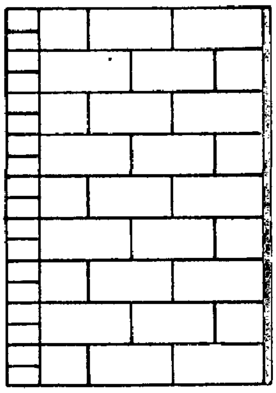

32

3" brick + 2" air space + 3" brick

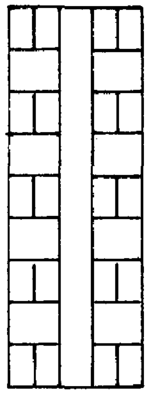

33

½" p + 3" brick + 2" airspace +3" br. ½" p

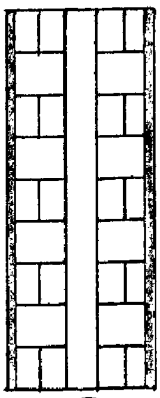

34

8" H.Block

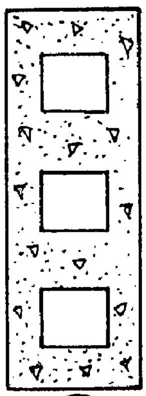

35

8" H. Block + ½" p

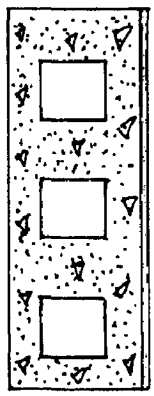

36

p = plaster B.T. = Bricktile br. = brick
H. Block = Hollow block

TABLE 1 (Cont'd.)

$h_o = 3.6$

$h_i = 1.5$

S.No.	Wall Section	U value	Harmonic	External Driving Point Function λ_o	External Driving Point Function $-\phi_o$ in degrees	Transfer Function λ_i	Transfer Function $-\phi_i$ in degrees	Internal Driving Point Function λ'_i	Internal Driving Point Function $-\phi'_i$ in degrees
37.	1/2" plaster + 8" cinder concrete hollow block + 1/2" plaster	0.373	F	0.733	17	0.160	88	0.534	23
			H_2	0.637	24	0.032	133	0.413	23
			H_3	0.630	29	0.047	172	0.324	40
			H_4	0.650	34	0.031	210	0.304	42
38.	9" brick + 1/2" plaster	0.403	F	0.783	13	0.140	100	0.511	27
			H_2	0.637	17	0.033	148	0.404	31
			H_3	0.604	19	0.034	193	0.324	34
			H_4	0.647	21	0.020	220	0.311	30
39.	8" gypsum hollow block	0.300	F	0.844	12	0.167	75	0.653	22
			H_2	0.723	15	0.100	116	0.530	23
			H_3	0.720	18	0.034	145	0.500	20
			H_4	0.624	20	0.042	153	0.453	20
40.	1/8" wood chip board + 4½" gypsum hollow block + 1/8" wood chip board	0.413	F	0.973	6	0.239	32	0.729	12
			H_2	0.844	12	0.240	50	0.630	13
			H_3	0.830	15	0.207	60	0.600	22
			H_4	0.773	17	0.173	72	0.563	24
41.	4" synthetic wood panel	0.169	F	0.953	4	0.100	57	0.944	11
			H_2	0.911	7	0.070	80	0.732	15
			H_3	0.834	9	0.052	110	0.730	15
			H_4	0.832	11	0.035	130	0.691	17
42.	1½" concrete + 2" air space + 1½" concrete	0.491	F	0.720	14	0.333	49	0.537	10
			H_2	0.639	18	0.220	64	0.430	20
			H_3	0.634	22	0.130	88	0.450	33
			H_4	0.623	24	0.123	104	0.350	40
43.	3/4" plaster + 1/2" wood board + 4" air space + 1/2" wood board + 3/4" plaster	0.231	F	0.964	9	0.153	32	0.800	13
			H_2	0.910	13	0.134	50	0.703	30
			H_3	0.833	20	0.100	73	0.640	30
			H_4	0.810	22	0.053	92	0.533	44
44.	3/4" mud plaster + 1" bamboo matting + 3/4" mud plaster	0.547	F	0.724	15	0.340	31	0.531	30
			H_2	0.703	18	0.304	52	0.511	37
			H_3	0.673	21	0.250	72	0.473	52
			H_4	0.632	24	0.207	85	0.420	53
45.	3/4" mud plaster + 9" sun dried brick + 3/4" mud plaster	0.451	F	0.644	17	0.142	104	0.424	37
			H_2	0.530	21	0.033	146	0.333	29
			H_3	0.514	24	0.042	175	0.311	31
			H_4	0.437	23	0.023	203	0.253	32

WALL SECTIONS

½" p + 8" H.block + ½" p

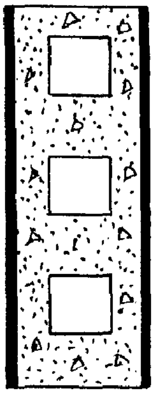

(37)

9" brick + ½" p

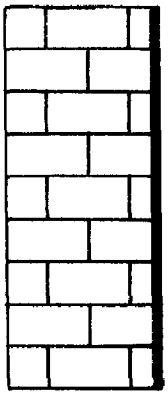

(38)

8" H.G. block

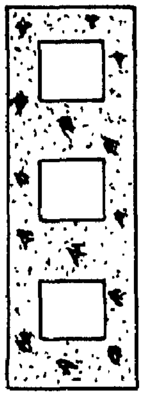

(39)

1/8" W.B. + 4½" H.G.block +1/8"W.B.

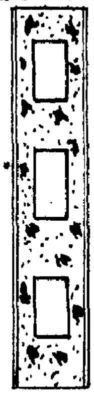

(40)

4" Syntheticwood panel

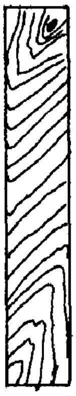

(41)

1½" conc. + 2" air apace + 1½" conc.

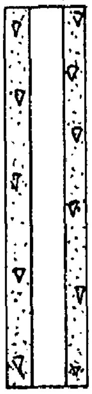

(42)

3/4" p + ½" r.b.+ 4" airspace + ½" r.b. + ¾" p

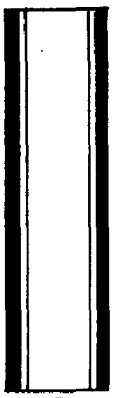

(43)

3" m.p. + 1" b.b. + ¾" m.p.

(44)

¾" m.p. + 9" S.B. + ¾" m.p.

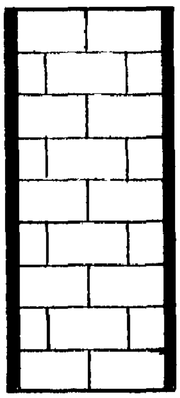

(45)

p = plaster H.block = Hollow block H.G. = Hollow gypsum
r.b. = reed board m.p. = mud plaster b.b. = bamboo board

TABLE 1 (Cont'd.)

$h_o = 3.5$

$h_i = 1.5$

S.No.	Wall Section	U value	Harmonic	External Driving point Function λ_o	External Driving point Function $-\phi_o$ in degrees	Transfer Function λ_i	Transfer Function $-\phi_i$ in degrees	Internal Driving point Function λ'_i	Internal Driving point Function $-\phi'_i$ in degrees
46.	3" mud plaster + 13½" sun dried brick + 3/4" mud plaster	0.237	F	0.644	13	0.070	140	0.422	30
			H_2	0.630	22	0.031	200	0.344	33
			H_3	0.511	25	0.016	250	0.301	34
			H_4	0.437	27	0.003	235	0.232	36
47.	9" brick + 3/4" air space + 1/2" plywood	0.200	F	0.719	14	0.073	112	0.623	9
			H_2	0.622	22	0.032	163	0.644	13
			H_3	0.622	23	0.016	215	0.622	16
			H_4	0.620	23	0.009	245	0.607	18
48.	1/2" plaster + 4" expanded slag concrete + 1/2" plaster	0.320	F	0.889	10	0.191	60	0.711	21
			H_2	0.822	17	0.133	100	0.578	20
			H_3	0.764	21	0.039	128	0.489	35
			H_4	0.712	24	0.031	150	0.433	30
49.	1/2" plaster + 8" expanded slag concrete + 1/2" plaster	0.180	F	0.839	11	0.035	115	0.639	20
			H_2	0.822	17	0.031	190	0.574	31
			H_3	0.753	21	0.018	233	0.493	33
			H_4	0.712	24	0.012	274	0.423	40
50.	1/2" plaster + 4" cinder concrete + 1/2" plaster	0.544	F	0.778	16	0.323	50	0.544	25
			H_2	0.633	19	0.220	80	0.422	24
			H_3	0.621	22	0.164	100	0.333	30
			H_4	0.637	25	0.113	123	0.300	41
51.	1/2" plaster + 8" cinder concrete + 1/2" plaster	0.379	F	0.730	16	0.144	104	0.533	28
			H_2	0.682	21	0.033	152	0.400	33
			H_3	0.610	24	0.030	193	0.333	41
			H_4	0.578	27	0.031	220	0.200	49
52.	1/2" plaster + 4" foamed concrete + 4½" brick + 1/2" plaster	0.141	F	0.063	7	0.024	116	0.533	27
			H_2	0.834	13	0.013	200	0.422	20
			H_3	0.880	18	0.005	213	0.337	21
			H_4	0.844	21	0.003	230	0.309	30
53.	4½" brick + 2" air space + 4½" brick		F	0.703	15	0.023	103	0.503	27
54.	2" wood board + 2" air space + 3" wood board		F	0.933	3	0.043	49	0.934	4

WALL SECTIONS

3" m.p. + 13½" S.B. + ¾" m.p.

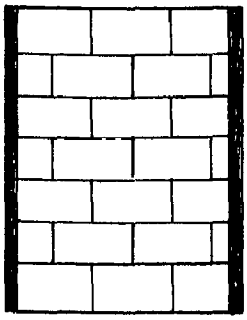

(46)

½" p + 9" brick + ¾" airspace + ½" p.w.

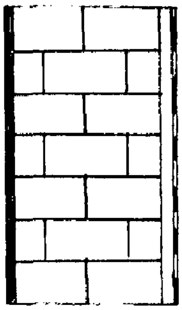

(47).

½" p + 4" e.s.c.+ ½" p

(48)

½" p + 8" e.s.c.+ ½" p

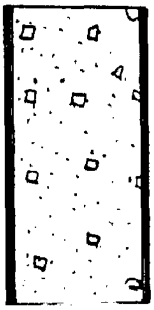

(49)

½" p + 4" c.c. + ½" p

(50)

½" p + 3" c.c. + ½" p

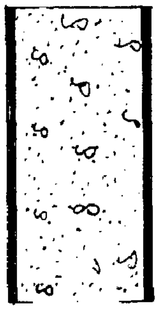

(51)

½" p + 4" F.C. + 4½" brick + ½" p

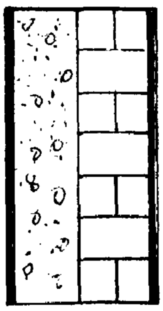

(52)

4½" brick + 2" air space + 4½" brick

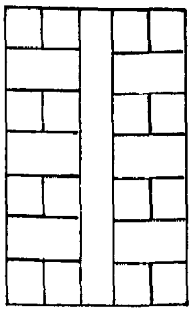

(53)

2" r.b. + 2" air space + 2" r.b.

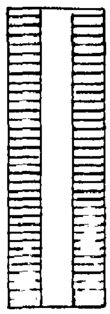

(54)

p = plaster, r.b. = reed board m.p. mud plaster
S.B = sun dried brick p.w. = plywood c.c. = cinder conc.
e.s.c. = expanded slag concrete. F.C. = Foamed concrete

TABLE 8

[illegible]

$h_o = 3.5$

$h_i = 1.5$

S.No.	Roof Section	U Value	Harmonic	External Driving point Function λ_o	$-\phi_o$ in degrees	Transfer Function λ_i	$-\phi_i$ in degrees	Internal Driving point Function λ'_i	$-\phi'_i$ in degrees
1.	3" lime concrete + 4" R.C.C. + 1/2" plaster	0.583	F	0.733	13	0.200	78	0.422	31
			H_2	0.640	17	0.111	116	0.316	35
			H_3	0.600	19	0.057	140	0.283	33
			H_4	0.537	31	0.044	160	0.244	40
2.	3" lime concrete + 4½" R.B. + 1/2" plaster	0.443	F	0.733	13	0.182	73	0.459	23
			H_2	0.633	17	0.093	118	0.353	33
			H_3	0.600	19	0.057	144	0.300	37
			H_4	0.563	21	0.040	163	0.271	40
3.	3" lime concrete + 6" R.B. + 1/2" plaster	0.410	F	0.733	13	0.133	92	0.456	29
			H_2	0.633	15	0.032	133	0.333	33
			H_3	0.600	19	0.034	193	0.289	38
			H_4	0.553	20	0.024	210	0.253	41
4.	3" lime concrete + 7½" R.B. + 1/2" plaster	0.339	F	0.733	14	0.110	116	0.437	42
			H_2	0.654	18	0.043	162	0.333	37
			H_3	0.600	20	0.022	212	0.300	40
			H_4	0.554	22	0.016	244	0.237	42
5.	3" lime concrete + 2" sand stone slab	0.583	F	0.744	12	0.239	45	0.511	13
			H_2	0.644	16	0.200	76	0.400	20
			H_3	0.588	18	0.138	92	0.344	22
			H_4	0.561	20	0.100	110	0.311	24
6.	1" sand stone + 3" lime concrete + 2" sand stone	0.531	F	0.722	15	0.249	60	0.500	19
			H_2	0.622	19	0.153	90	0.400	22
			H_3	0.533	22	0.100	112	0.351	24
			H_4	0.500	24	0.039	128	0.316	25
7.	3" brick flats + 3" mud phuska + 4" R.C.C. + 1/2" plaster	0.400	F	0.711	15	0.100	104	0.411	23
			H_2	0.644	18	0.043	144	0.311	30
			H_3	0.589	20	0.021	203	0.270	35
			H_4	0.555	22	0.011	232	0.250	37
8.	Tarfelt + 4" foamed concrete + 3" R.C.C. + 1/2" plaster	0.3150	F	0.933	3	0.044	130	0.400	33
			H_2	0.911	5	0.030	142	0.344	35
			H_3	0.889	7	0.012	210	0.290	37
			H_4	0.837	0	0.004	240	0.253	30
9.	2½" brick tile + 3" lime concrete + 3" mud phuska + 6" R.B. + 1/2" plaster.	0.317	F	0.344	19	0.042	153	0.473	25
			H_2	0.546	22	0.012	240	0.373	30
			H_3	0.473	24	0.004	230	0.339	32
			H_4	0.422	23	0.002	316	0.300	34

ROOF SECTIONS

3" L.C. + 4" RCC + ½" p

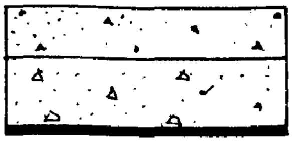

(1)

3" L.C. + 4½" R.B. + ½" p

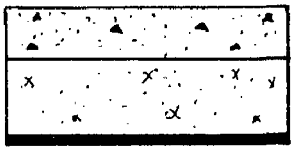

(2)

3" L.C. + 6" R.B. + ½" p

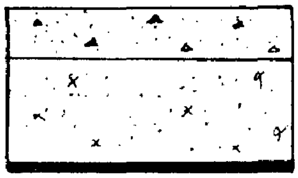

(3)

3" L.C. + 7½" R.B. + ½" p

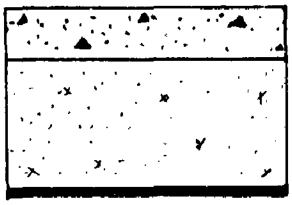

(4)

3" L.C. + 2" s.s.

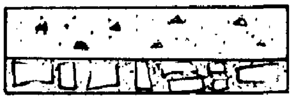

(5)

1" s.s. + 3" L.C. + 2" s.s.

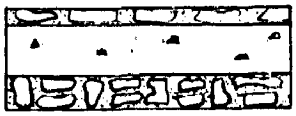

(6)

2" b.f. + 3" M.P. + 4" RCC + ½" p

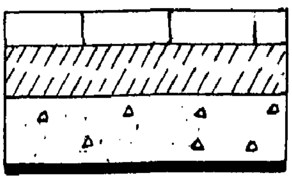

(7)

4" F.C. + 3" RCC + ½" p

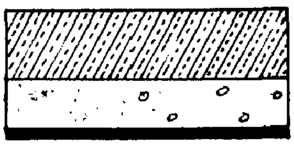

(8)

2½" b.t. + 3" L.C. + 2" M.P. + 6" R.B. + ½" p

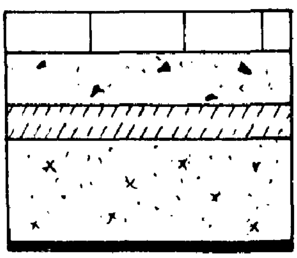

(9)

L.C. = Lime concrete RCC = Reinforced cement concrete
R.B. = Reinforced brick s.s. = sand stone M.P. Mudphusk
F.C. = Foamed concrete b.t. = bricktile p = plaster
b.f. = brickflat

TABLE 8 (Cont'd.)

$h_o = 3.5$

$h_i = 1.6$

S.No.	Roof section	U value	Harmonic	External Driving point Function λ_o	$-\phi_o$ in degrees	Transfer Function λ_i	$-\phi_i$ in degrees	Internal Driving point Function λ_i'	$-\phi_i'$ in degrees
10.	3" lime concrete + 4" mud phuska + 4" R.B. + ½" plaster	0.383	F	0.739	13	0.031	144	0.434	24
			H_2	0.663	17	0.017	224	0.339	29
			H_3	0.603	19	0.003	238	0.329	32
			H_4	0.539	21	0.003	300	0.300	34
11.	3½" brick tile + 3" lime concrete + 4½" R.B. + 1/2" plaster	0.403	F	0.644	20	0.037	124	0.489	27
			H_2	0.544	24	0.031	183	0.378	32
			H_3	0.473	23	0.014	236	0.311	34
			H_4	0.422	28	0.009	270	0.239	35
12.	1/2" plaster + 2" foamed concrete + 2" R.C.C. + 1/2" plaster	0.283	F	0.839	6	0.112	64	0.553	30
			H_2	0.837	11	0.737	83	0.378	34
			H_3	0.822	15	0.042	120	0.300	33
			H_4	0.753	18	0.029	133	0.260	40
13.	4½" brick + 3" lime concrete + 4" R.C.C. + 1/2" plaster	0.233	F	0.711	16	0.073	124	0.423	24
			H_2	0.633	18	0.023	200	0.339	28
			H_3	0.578	21	0.013	236	0.300	31
			H_4	0.533	24	0.005	238	0.271	33
14.	1/2" slate + 4" air space + 1/4" plywood	0.513	F	0.844	6	0.322	11	0.644	4
			H_2	0.832	11	0.316	19	0.633	7
			H_3	0.810	14	0.310	27	0.622	10
			H_4	0.773	18	0.303	35	0.613	13
15.	1/2" wood shingles + 4" air space + 1/4" plywood	0.429	F	0.873	3	0.239	11	0.700	4
			H_2	0.839	6	0.224	18	0.639	8
			H_3	0.853	8	0.280	25	0.624	12
			H_4	0.844	10	0.271	33	0.637	15
16.	1/4" A.C. sheet + 4" air space + 1/4" ply wood	0.600	F	0.849	2	0.311	7	0.653	3
			H_2	0.844	4	0.310	12	0.649	6
			H_3	0.838	6	0.303	17	0.644	9
			H_4	0.820	8	0.300	22	0.633	13
17.	3/4" Mangalore tile	0.593	F	0.790	5	0.509	14	0.504	10
			H_2	0.782	9	0.500	18	0.500	13
			H_3	0.773	14	0.491	20	0.463	15
			H_4	0.763	18	0.473	24	0.450	17
18.	3/4" Mangalore tile + 4" air space + 1/4" plywood	0.491	F	0.844	4	0.323	16	0.634	4
			H_2	0.822	8	0.318	21	0.623	7
			H_3	0.800	12	0.309	23	0.622	10
			H_4	0.773	16	0.283	32	0.610	13

ROOF SECTIONS

3" L.C. + 4" M.P. + 4½" R.B. + ½" p 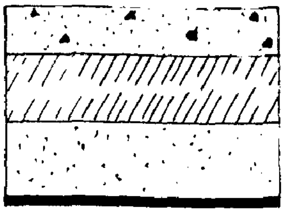 (10)	2½" b.t. + 3" L.C. + 4½" R.B. + ½" p  (11)	½" p + 2" F.C. + 2" R.C.C. + ½" p 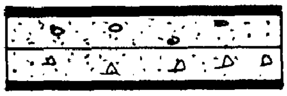 (12)
4½" brick + 3" L.C. + 4" R.C.C. + ½" p 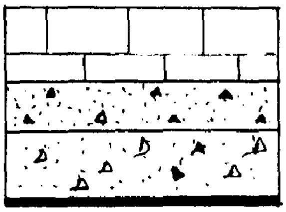 (13)	½" slate + 4" air space + ¼" p.w. 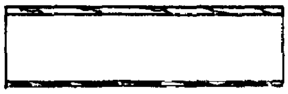 (14)	[illegible]" w.s. + 4" air space + ¼" p.w. 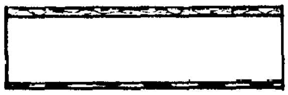 (15)
AC sheet + 4" air space + ¼" p.w. 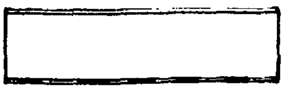 (16)	¾" Mangalore tile 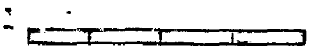 (17)	¾" m.t. + 4" air space + ¼" p.w. 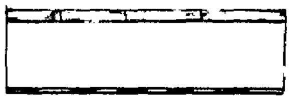 (18)

L.C. = Lime concrete M.P. = Mud phuska b.t.=bricktile
R.B. = Reinforced brick R.C.C.= Reinforced cement conc.
w.s. = wood shingle p.w. = plywood m.t. = Mangalore tile

TABLE 2 (Cont'd.)

$h_o = 3.5$

$h_i = 1.5$

S.No.	Roof Section	U value	Harmonic	External Driving point Function λ_o	$-\phi_o$ in degrees	Transfer Function λ_i	$-\phi_i$ in degrees	Internal Driving point Function λ_i'	$-\phi_i'$ in degrees
19.	G.I. sheet + 3" air space + 1" mineral wool + 1/4" plywood	0.223	F	0.922	1	0.167	8	0.822	4
			H_2	0.910	1	0.164	10	0.811	9
			H_3	0.914	2	0.153	23	0.739	13
			H_4	0.911	3	0.147	33	0.753	17
20.	G.I. sheet + 2" air space + 2" mineral wool + 1/4" plywood	0.163	F	0.933	1	0.107	23	0.837	6
			H_2	0.916	1	0.100	45	0.844	11
			H_3	0.889	2	0.039	64	0.811	16
			H_4	0.844	4	0.076	80	0.737	19
21.	1/4" A.C. sheet + 3" air space + 1/2 Celotex board	0.303	F	0.931	2	0.215	5	0.830	1
			H_2	0.910	4	0.203	12	0.759	3
			H_3	0.900	6	0.202	16	0.732	4
			H_4	0.899	8	0.200	20	0.753	5
22.	1/4" A.C. sheet + 3" air space + 1" mineral wool + 1/4" plywood	0.246	F	0.916	2	0.167	16	0.822	4
			H_2	0.911	4	0.164	24	0.811	9
			H_3	0.903	6	0.153	33	0.739	13
			H_4	0.900	8	0.147	42	0.753	17
23.	1/4" A.C. sheet + 3" air space + 1" Thermocole + 1/4" plywood	0.143	F	0.953	2	0.053	15	0.900	4
			H_2	0.943	4	0.090	21	0.839	9
			H_3	0.943	6	0.030	23	0.837	13
			H_4	0.938	8	0.034	35	0.844	16
24.	3" Thermocole + 4" Dense concrete	0.033	F	0.939	1	0.031	69	0.844	30
25.	4" Dense concrete + 3" Thermocole	0.033	F	0.735	24	0.032	64	0.835	1
26.	1" Thermocole + 4" Dense concrete + 1" Thermocole	0.033	F	0.940	1	0.009	50	0.839	1
27.	2" Dense concrete + 2" Thermocole + 2" Dense concrete	0.089	F	0.921	10	0.043	65	0.753	32

R.B. = Reinforced Brick, R.C.C. = Reinforced Cement Concrete, A.C. = Asbestos Cement,

G.I. = Galvanised Iron.

ROOF SECTIONS

G.I.sheet + 3" air space + 1" m.w. + $\frac{1}{4}$" p.w.

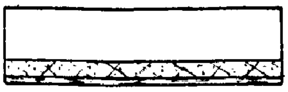

(19)

G.I.sheet + 3" air space + 2" m.w. + $\frac{1}{4}$" p.w.

(20)

A.C.sheet + 2" air space + $\frac{1}{2}$" c.b.

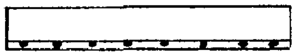

(21)

A.C.sheet + 3" air space + 1" m.w. + $\frac{1}{4}$" p.w.

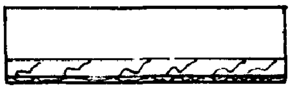

(22)

A.C.sheet + 3" air space + 1" T.C. + $\frac{1}{4}$" p.w.

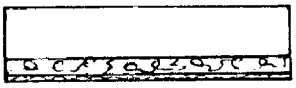

(23)

2" T.C. + 4" D.C.

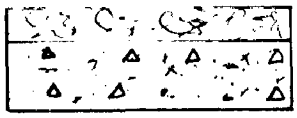

(24)

4" D.C. + 2" T.C.

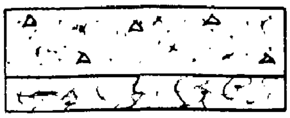

(25)

1" T.C. + 4" D.C. + 1" T.C.

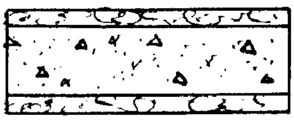

(26)

2" D.C. + 2" T.C. + 2" D.C.

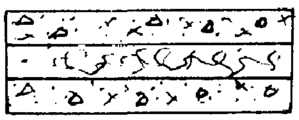

(27)

m.w. = mineral wool p.w. = plywood c.b. = celotex board
D.C. = Dense concrete T.C. = Thermocole

TABLE 3

THERMAL MATRIX FUNCTIONS FOR DOORS AND WINDOWS

$h_o = 3.5$

$h_i = 1.5$

Sl. No.	Doors or windows	U value	Harmonic	External Driving point Function λ_o	External Driving point Function $-\phi_o$ in degrees	Transfer Function λ_i	Transfer Function $-\phi_i$ in degrees	Internal Driving point Function λ'_i	Internal Driving point Function $-\phi'_i$ in degrees
1.	1½" Teakwood	0.502	F	0.833	3	0.333	13	0.655	4
			H_2	0.820	6	0.311	24	0.644	8
			H_3	0.800	7	0.229	32	0.622	11
			H_4	0.773	8	0.232	40	0.593	12
2.	1½" Teakwood	0.453	F	0.830	4	0.239	17	0.639	5
			H_2	0.819	7	0.237	30	0.632	8
			H_3	0.791	8	0.223	40	0.622	11
			H_4	0.737	9	0.200	48	0.600	12
3.	1½" Teakwood	0.416	F	0.820	5	0.253	23	0.689	6
			H_2	0.810	7	0.218	38	0.637	9
			H_3	0.773	8	0.182	48	0.622	11
			H_4	0.763	10	0.153	64	0.600	12
4.	1/2" Plywood + 2" air space + 1/2" plywood.	0.395	F	0.920	2	0.257	14	0.705	5
			H_2	0.941	6	0.249	23	0.691	12
			H_3	0.922	10	0.231	33	0.671	17
			H_4	0.900	13	0.210	50	0.633	21
5.	1/2" Hard board + 2" air space + 1/2" hard board.	0.359	F	0.870	4	0.244	22	0.744	8
			H_2	0.834	8	0.200	36	0.689	17
			H_3	0.830	12	0.163	57	0.623	21
			H_4	0.723	14	0.133	69	0.520	25
6.	1/2" Plywood + 1" Thermocole + 1/2" plywood.	0.247	F	0.922	3	0.023	24	0.900	8
			H_2	0.910	7	0.037	37	0.853	15
			H_3	0.839	10	0.077	52	0.739	21
			H_4	0.857	12	0.037	64	0.722	23
7.	1/2" Hard board + 1" Thermocole + 1/2" hardboard.	0.143	F	0.913	5	0.039	30	0.873	11
			H_2	0.900	10	0.073	55	0.739	18
			H_3	0.857	14	0.033	74	0.680	24
			H_4	0.800	17	0.044	87	0.600	30
8.	1/2" Plywood + 1" mineral wool + 1/2" plywood.	0.331	F	0.839	4	0.167	20	0.832	7
			H_2	0.873	8	0.158	36	0.732	12
			H_3	0.844	11	0.133	50	0.722	18
			H_4	0.832	14	0.122	64	0.637	22
9.	1/2" Hardboard + 1" mineral wool + 1/2" hardboard.	0.244	F	0.900	6	0.153	30	0.811	11
			H_2	0.857	10	0.133	53	0.723	18
			H_3	0.810	14	0.124	74	0.644	24
			H_4	0.733	18	0.077	89	0.573	28
10.	1/8" Glass	1.023	F	0.711	1	0.699	1	0.311	1
			H_2	0.711	1	0.689	2	0.311	1
			H_3	0.711	1	0.689	4	0.311	1
			H_4	0.711	1	0.659	5	0.311	1
11.	1/8" Glass + 1" air space + 1/8" glass.	0.574	F	0.825	1	0.332	2	0.613	[illegible]
			H_2	0.824	1	0.330	4	0.623	[illegible]
			H_3	0.822	2	0.373	6	0.613	[illegible]
			H_4	0.829	4	0.373	9	0.611	[illegible]

DOOR & WINDOW SECTIONS

$1\frac{1}{4}$" Teakwood  (1)	$1\frac{1}{2}$" Teakwood  (2)	$1\frac{3}{4}$" Teakwood  (3)
$\frac{1}{2}$" p.w. + 1" air space + $\frac{1}{2}$" p.w.  (4)	$\frac{1}{2}$" h.b. + 1" air space + $\frac{1}{2}$" h.b.  (5)	$\frac{1}{2}$" p.w. + 1" T.C. + $\frac{1}{2}$" p.w.  (6)
$\frac{1}{2}$" h.b. + 1" T.C. + $\frac{1}{2}$" h.b.  (7)	$\frac{1}{2}$" p.w. + 1/8" m.w. + $\frac{1}{2}$" p.w.  (8)	$\frac{1}{2}$" h.b. + 1" m.w. + $\frac{1}{2}$" h.b.  (9)

p.w. = plywood h.b. = hardboard T.C. = Thermocole
m.w. = mineral wool

TABLE 4

$D_o = 1.5$

$D_i = 1.5$

THERMAL SYSTEM FUNCTIONS FOR INTERMEDIATE FLOORS

Sl. No.	Intermediate Floor Section	U Value	Harmonic	External Driving Point Function λ_o	$-\phi_o$ in degrees	Transfer Function λ_i	$-\phi_i$ in degrees	Internal Driving Point Function λ'_i	$-\phi'_i$ in degrees
1.	1½" Concrete + 4" R.C.C. + 1/2" plaster	0.480	F	0.422	23	0.167	70	0.422	30
			H_2	0.324	31	0.039	66	0.333	32
			H_3	0.239	32	0.057	112	0.300	33
			H_4	0.232	34	0.033	130	0.271	35
2.	1½" concrete + 3" lime concrete + 4" R.C.C. + 1/2" plaster.	0.337	F	0.443	23	0.030	83	0.416	29
			H_2	0.343	23	0.033	132	0.320	31
			H_3	0.301	30	0.013	140	0.300	32
			H_4	0.270	32	0.009	172	0.278	34
3.	1½" concrete + 3" lime concrete + 4½" R.B. + 1/2" plaster.	0.353	F	0.444	27	0.032	122	0.438	23
			H_2	0.345	30	0.034	168	0.333	33
			H_3	0.300	32	0.017	212	0.311	36
			H_4	0.273	33	0.009	240	0.287	33
4.	1½" concrete + 3" lime concrete + 6" R.B. + 1/2" plaster.	0.325	F	0.445	27	0.034	123	0.437	27
			H_2	0.345	30	0.024	172	0.333	33
			H_3	0.300	31	0.011	223	0.311	37
			H_4	0.278	33	0.004	253	0.279	39
5.	1½" concrete + 3" lime concrete + 7½" R.B. + 1/2" plaster.	0.233	F	0.444	23	0.243	130	0.437	23
			H_2	0.347	29	0.016	203	0.339	33
			H_3	0.300	31	0.007	248	0.311	33
			H_4	0.274	32	0.003	283	0.281	33
6.	1½" Concrete + 6" R.B. + 1/2" plaster.	0.481	F	0.445	27	0.120	84	0.437	36
			H_2	0.347	30	0.068	130	0.339	33
			H_3	0.300	32	0.031	156	0.311	37
			H_4	0.273	33	0.019	196	0.279	39
7.	1½" Concrete + 7½" R.B. + 1/2" plaster.	0.422	F	0.444	23	0.063	100	0.437	23
			H_2	0.344	30	0.037	140	0.336	33
			H_3	0.300	31	0.018	163	0.310	33
			H_4	0.277	33	0.010	220	0.281	31
8.	1" Terrazotile + 1/2" plaster + 4" R.C.C. + 1/2" plaster.	0.080	F	0.401	30	0.169	60	0.432	30
			H_2	0.311	32	0.323	220	0.333	30
			H_3	0.232	33	0.053	103	0.300	30
			H_4	0.233	34	0.040	124	0.273	35
9.	1" Kotah stone + 1/2" plaster + 4" R.C.C. + 1/2" plaster.	0.493	F	0.422	27	0.167	63	0.432	30
			H_2	0.311	30	0.093	83	0.350	32
			H_3	0.278	31	0.053	113	0.300	32
			H_4	0.256	32	0.040	132	0.274	33
10.	1/4" Mosaic + 1½" cinder concrete + 4" R.C.C. + 1/2" plaster.	0.475	F	0.402	23	0.165	63	0.413	30
			H_2	0.311	30	0.050	83	0.322	31
			H_3	0.239	31	0.053	110	0.300	32
			H_4	0.253	32	0.033	132	0.273	34
11.	1" wooden block + 1/3" bitumen + 1/2" plaster + 4" R.C.C. + 1/2" plaster.	0.231	F	0.600	10	0.111	82	0.432	30
			H_2	0.587	11	0.030	114	0.316	32
			H_3	0.533	12	0.033	133	0.300	33
			H_4	0.511	13	0.027	162	0.276	35

TABLE 5

THERMAL SYSTEM FUNCTIONS FOR PARTITION WALLS

$h_o = 1.5$
$h_i = 1.5$

Sl. No.	Partition Wall Section	U value	Harmonic	Transfer Function λ_i	Transfer Function $-\phi_i$ in degrees	Internal Driving point Function λ'_i	Internal Driving point Function $-\phi'_i$ in degrees
1.	1/2" Plaster + 4½" Brick + 1/2" plaster	0.432	F	0.204	56	0.511	30
			H_2	0.122	84	0.337	32
			H_3	0.076	103	0.329	24
			H_4	0.054	130	0.300	33
2.	1/2" Plaster + 9" Brick + 1/2" Plaster	0.243	F	0.073	116	0.499	30
			H_2	0.029	162	0.382	24
			H_3	0.013	214	0.333	33
			H_4	0.009	238	0.303	40
3.	1/2" Plaster + 3" foamed concrete + 1/2" plaster.	0.135	F	0.107	42	0.822	21
			H_2	0.073	80	0.781	23
			H_3	0.051	116	0.750	24
			H_4	0.033	140	0.700	30
4.	3/4" Plaster + 2" wood board + 3/4" plaster.	0.155	F	0.033	36	0.733	18
			H_2	0.034	64	0.624	24
			H_3	0.044	86	0.573	29
			H_4	0.031	104	0.500	26
5.	1/2" Plaster + 8" cinder hollow block + 1/2" plaster.	0.331	F	0.114	100	0.533	21
			H_2	0.056	139	0.444	27
			H_3	0.029	174	0.373	32
			H_4	0.016	210	0.333	33
6.	4" Synthetic wood panel	0.159	F	0.020	56	0.856	6
			H_2	0.036	84	0.812	9
			H_3	0.047	103	0.737	12
			H_4	0.036	123	0.733	13
7.	3"/8" Mud plaster + 1" bamboo matting + 3/4" mud plaster.	0.453	F	0.273	30	0.622	17
			H_2	0.213	56	0.523	22
			H_3	0.166	73	0.453	23
			H_4	0.131	93	0.400	20
8.	1/2" Hard board + 4" air space + 1/2" hardboard.	0.316	F	0.191	30	0.728	10
			H_2	0.162	52	0.637	13
			H_3	0.124	72	0.600	21
			H_4	0.100	86	0.524	35

TABLE 6

THERMAL FUNCTIONS (INTERNAL DRIVING POINT) FOR FLOOR SECTIONS

$h_i = 1.5$

No.	Floor section	U value	Harmonic	Internal Driving point Function λ'_i	$-\phi'_i$ in degrees
.	1½" Concrete + 3" lime concrete + 6" Hard core + 20" soil.	0.212	F H_2 H_3 H_4	0.444 0.344 0.300 0.237	27 32 33 34
.	1½" Concrete + 6" Hardcore + 20" soil.	0.237	F H_2 H_3 H_4	0.434 0.333 0.289 0.258	23 31 32 30
.	1" Terrazotile + 1/2" mortar + 6" Hardcore + 20" soil.	0.214	F H_2 H_3 H_4	0.433 0.329 0.283 0.240	23 31 33 37
.	1" Wood block + 3" cinder concrete + 6" Hardcore + 20" soil.	0.191	F H_2 H_3 H_4	0.600 0.569 0.544 0.520	9 11 12 13
.	1½" Sand stone + 6" Hardcore + 20" soil.	0.241	F H_2 H_3 H_4	0.395 0.300 0.244 0.201	31 35 33 39
.	1½" Sand stone + 3" lime concrete + 6" Hardcore + 20" soil.	0.215	F H_2 H_3 H_4	0.403 0.300 0.251 0.202	31 35 39 40
.	1" Kotah stone + 1/2" mortar + 3" lime concrete + 6" hard core + 20" soil.	0.214	F H_2 H_3 H_4	0.444 0.344 0.300 0.237	27 31 33 34
.	3" Brick + 3" lime concrete + 6" hardcore + 20" soil.	0.199	F H_2 H_3 H_4	0.437 0.377 0.323 0.290	23 23 27 28
.	4½" Brick + 3" lime concrete + 6" Hardcore + 20" soil.	0.190	F H_2 H_3 H_4	0.437 0.374 0.323 0.203	23 27 23 20
0.	3" Brick + 6" Hardcore + 20" soil.	0.221	F H_2 H_3 H_4	0.437 0.373 0.325 0.239	22 23 27 23
1.	4½" Brick + 6" Hardcore + 20" soil.	0.210	F H_2 H_3 H_4	0.437 0.373 0.323 0.329	23 27 23 29

R E F E R E N C E S

REFERENCES

1. Mackey, C.O. and Wright, L.T. "The Sol-Air Thermometer" Trans. ASHVE. Vol. 52, p 271, 1946.

2. Roux, A.J.A. "Periodic Heat Flow through Building Components - Heat exchange at the outside surface, with special reference to the application of Sol-Air Temperature. NBRI - South African CSIR - Series DR-8 Nov. 1950.

3. Hand, I.F. "Preliminary Measurements of Solar energy received on Vertical Surfaces" Trans. Amer. Geophysical Union. Vol. 28, 5, Oct. 1947.

4. Wilkes, G.B., Peterson, C.M.F. "Radiation and Convection from surfaces of various positions" Trans. ASHVE Vol. 44, p 513, 1938.

5. Hottel, H.C. and Mangelsdorf, H.G. "Heat Transmission by Radiation from Non-luminous gases" Trans. American Inst. of Chemical Engineers, Vol. 31, No. 3, Sept. 1935.

6. Beckett, H.E. "The reflecting powers of Rough Surfaces at Solar Wavelengths" Proceedings of the Physical Society, Vol. 43, p 227, 1931.

7. Holden, T.S. and Greenland, J.J. "The Coefficient of Solar absorptivity and Low temperature emissivity of various materials" A review, Commonwealth of Australia C.S.I.R.O. Division of Building Research Report No. R3, 1951.

8. Brunt, D. "Notes on Radiation in the Atmosphere" Quarterly Journal of Royal Meteorological Society, Vol. 58, p 389, 1932.

9. Brunt, D. "Radiation in the Atmosphere" Supplement to the Quarterly Journal of the Royal Meteorological Society, Vol. 66, 1940.

10. Dines, W.H. and Dines, L.H.G. "Monthly mean values of Radiation from various parts of the sky at Benson Oxfordshire" Memoirs of the Royal Meteorological Society, Vol. II, No. 11, 1927.

12. Hough[illegible] [illegible]nts of Heat
trans[illegible] [illegible]atural Weather
Condi[illegible] Vol. 34, p 397, 1933.

13. Houghten, F.C., Cutber[illegible] [illegible] Gutberlet, C.& C.P.
"Additional co[illegible]ficient of heat transfer as
measured under natural conditions" Trans.
ASHVE Vol. 35, p 161, 1929.

14. Rowley, F.B., Algren, A.B. and Blackshaw, J.L. "Effects
of air velocities on surface coefficients" Trans.
ASHVE Vol. 36, p 123, 1930.

15. Parmelee, G.V. and Huebscher, R.G. "Forced convection
heat transfer from flat surfaces" ASHVE Research
Bulletin Vol. 53, No. 3, Nov. 1947.

16. Colburn, A.P. "A method of correlating forced convection
heat transfer, and a comparision with fluid
friction" Trans. American Inst. Chem. Engrs.
Vol. 29, p 174 - 210, 1933.

17. Colburn, A.P. "Heat transfer by Natural and Forced
Convection" Bulletin of Purdue University,
Engineering Experiment Station, Series No. 84,
Jan. 1942.

18. Roux, A.J.A. "The effect of weather conditions on Heat
transfer through Building elements" Building
Research Congress 1951, Division 3, Part II, p 83.

19. Alford, J.S., Ryan, J.E. and Urban, F.O. "Effect of heat
storage and variation in indoor air temperature
and solar intensity on Heat transfer through
walls" Trans. ASHVE Vol. 45, p 369, 1939.

20. Mackey, C.O. and Wright, L.T. "Periodic heat flow -
homogeneous walls or roofs" Trans. ASHVE
Vol. 50, p 293, 1944.

21. Hawkins, G.A. and Agnew, J.T. "The solution of Transient
Heat conduction problems by Finite Differences"
Purdue University Engineering Experiment Station
Bulletin No. 99, March 1947.

22. Mackey, C.O. "The steady Periodic state" a Review of
some computational Methods" Building Research
Congress 1951, Division 3, Part II, p 60.

11. Rowley, F.B., Algren, A.B. and Blackshaw, J.L. "Surface conductances as affected by Air Velocity, Temperature and character of surface" Trans. ASHVE Vol. 36, p 429, 1930.

12. Houghten, F.C. and Gabel, S.G.P. "Coefficients of Heat transfer as measured under Natural Weather Conditions" Trans. ASHVE Vol. 34, p 397, 1928.

13. Houghten, F.C., Gutberlet, Carl and Gobel, S.G.P. "Additional coefficient of heat transfer as measured under natural conditions" Trans. ASHVE Vol. 35, p 161, 1929.

14. Rowley, F.B., Algren, A.B. and Blackshaw, J.L. "Effects of air velocities on surface coefficients" Trans. ASHVE Vol. 36, p 123, 1930.

15. Parmelee, G.V. and Huebscher, R.G. "Forced convection Heat transfer from flat surfaces" ASHVE Research Bulletin Vol. 53, No. 3, Nov. 1947.

16. Colburn, A.P. "A method of correlating forced convection heat transfer, and a comparision with fluid friction" Trans. American Inst. Chem. Engrs. Vol. 29, p 174 - 210, 1933.

17. Colburn, A.P. "Heat transfer by Natural and Forced Convection" Bulletin of Purdue University, Engineering Experiment Station, Series No. 84, Jan. 1942.

18. Loux, A.J.A. "The effect of weather conditions on Heat transfer through Building elements" Building Research Congress 1951, Division 3, Part II, p 33.

19. Alford, J.S., Ryan, J.E. and Urban, F.O. "Effect of heat storage and variation in indoor air temperature and solar Intensity on Heat transfer through walls" Trans. ASHVE Vol. 45, p 369, 1939.

20. Mackey, C.O. and Wright, L.T. "Periodic heat flow - homogeneous walls or roofs" Trans. ASHVE Vol. 50, p 293, 1944.

21. Hawkins, G.A. and Agnew, J.T. "The solution of Transient Heat conduction problems by Finite differences" Purdue University Engineering Experiment Station Bulletin No. 98, March 1947.

22. Mackey, C.O. "The steady Periodic state" a Review of some computational Methods" Building Research Congress 1951, Division 3, Part II, p 60.

23. Von, Gorcum, A.H. "Theoretical considerations on the conduction of fluctuating heat flow" Applied Scientific Research Vol. A2, Martinus Nijhoff, 1951.

24. Pipes, L.A. "Matrix analysis of heat transfer problems" Journal of the Franklin Institute, 1957, 263, 263, (3), 1957

25. Muncey, R.J. "The calculation of temperatures inside Buildings having variable external conditions" Australian Journal of Applied Science, 4(2), 189, 1953.

26. Shklover, A.M. "Method of calculating the heat transmission in Buildings" Inst. Build. Tech. Moscow 1945.

27. Marmet, P.E. "A study of sinusoidal thermal variations of walls and rooms by electrical analogy" Seventh International Congress of Heating, Ventilation and Air Conditioning, Sept. 1947.

28. Maeda, T. "Analytical method for obtaining weighting functions" 1947, Trans. Arch. Inst. Japan.

29. Fuju, S. "Analysis of Room temperatures by means of Weighting Functions" BRI Japan. Report No. 8, July, 1962.

30. Geisler, K.W. "The analysis of variable heating and cooling process" BRS library Communication No. L 643, 1962.

31. Paschkis, Victor. "Periodic Heat flow in Building Walls, Determined by electrical Analogy method" Trans. ASHVE Vol. 48, p 75, 1942.

32. Beuken, L. "Construction of an Electrical Analogy apparatus for the analysis of non-stationary heat flow" Econ. Tech. Tijdschr 19, No. 3, p 43, June, 1939.

33. Lawson, D.I. and Mcguire, J.H. "The solution on Transient heat flow problems by analogous electrical networks" Inst. Mech. Engr. proc.(A) Vol. 167, p 275, 1952.

34. Robertson, A.F. and GrossDaniel "An Electrical Analogue method for Transient heat flow analysis" Journal of Research of the National Bureau of Standards. Vol. 61, No. 2, Aug. 1958.

35. Nottage, H.B. and Parmelee, G.V. "Circuit analysis applied to load estimating" Trans. ASHAE, Vol. 60, p 59, 1954.

36. Liebmann, G. "A new Electrical Analogue method for the solution of transient heat conduction problems" ASME Transactions, 1956, Vol. 78, (3), p 655.

37. Buchberg, H. "Electric Analogue studies of single Walls" ASHAE Trans. Vol. 62, p 177, 1956.

38. Billington, N.S. "The use of Electrical Analogies in Heating Research" Building Research Congress Division 3, Part II, p 73, 1951.

39. Oppenheim, A.K. "Radiation analysis by the network method" ASME Trans. Vol. 78, p 725, 1956.

40. Stephenson, D.G. and Starke, C.D. "Design of a II network for heat flow analogue" Journal of Applied Mechanics, Vol. 26, (2), p 300, 1959.

41. Mitalas, G.P., Stephenson, D.G. and Baxter, D.C. "Use of an analogue computer for room air conditioning calculations" Proceeding Second Conference of the computing Data processing Society of Canada. Toronto, pp 175 - 192, June 1960.

42. Rogers, T.A. "Electronic Analog Computers and partial differential Equation solutions" University of California, Dept. of Eng. Los Angelo, Dec. 1952.

43. Willcox, T.N., Oergel, C.T., Reque, S.G., Toelaer, C.M. and Brisben, W.R. "Analogue Computer Analysis of Residential cooling loads" ASHVE Journal Section, Heating, Piping & Air Conditioning, p 149, Oct. 1954.

44. Rich, D.G. and Gable, G.K. "Electronic Analogue Computer Solution of combined Heat problems" Transactions ASHRAE Vol. 68, 1962.

45. Mitalas, G.P. and Stephenson, D.G. "Programme to Calculate Periodic Temperature and Heat flow in a Wall" D.B.R. Computer Programme No. 3, Ottawa, Dec. 1960.

46. Stephenson, D.G. "Methods of determining Non-steady state Heat flow through walls and roofs of buildings" J.I.H.V.E., Vol. 30, p 64 - 73, May, 1962.

47. Inderson, P.V. "A.A.C. negative resistances circuit and its use in Electrical Analogue" Electrical Engineering Division Symposium of Analogies in Engineering, 43rd Annual Convention, Institution of Engineers (India), May 21, 1963.

48. Burnand, G. "The study of the Thermal Behaviour of structures by Electrical Analogy" British Journal of Applied Physics, Vol. 3, p 50, Feb.1952.

49. Mackey, D.M. "A high speed electronic function generator" Nature, Vol. 159, p 406, March 22, 1947.

50. Ejinston, Edward, L. "Electronic phase angle meter" Electronics (15 May 1942), 60.

51. Au, Y.P. "Measuring Vector relationships" Electronics, 24 (July 1951), 134.

52. Florman, E.F. and Tait, A. "An electronic phasometer" Proc. I.R.E., p. 207, (Feb. 1940).

53. Au., Y.P. "Phase measured directly" by Coincident slicer, Electronics, p 99, (12 Sept. 1958).

54. Goodberg, James, A. "Measuring phase with transistor flip flops" Electronics, p 56, (22 Sept. 1961).

55. Paschkis, V. and Heisler, H.P. "The accuracy of measurement in lumped R-C cable circuits as used in the study of transient heat flow" Trans. AIEE, Vol. 63, p 165, (1944).

56. Klein, ..D.P., Tcuisudian, Y.S. and Eaton, J.H. "Limits of accuracy of electrical analogue circuits used in the solution of transient heat conduction problems" Annual meeting of the ASME, ASME paper No. 53-A-65, 30th Nov., 1952.

57. Clarke, L.S. "The effect of the number of sections on the accuracy of a particular RC electrical analogue" Australian Journal of Applied Sciences, Vol. 3, No. 2, p 119, June 1952.

58. Friedmann, N.E. "Truncation error in a semidiscrete analogy of the heat equation" J. Math. Phys., Vol. 35, No. 3, p 299, Oct. 1956.

59. Jaeger, J.C. "Introduction to the Laplace transformation" (C.S.I.R., Melbourne) Australia, p 60, Jan., 1946.

60. Carslaw, H.S. and Jaeger, J.C. "Conduction of heat in Solids" Oxford University press, 2nd Edition, 1959.

61. Mason, W.P. "Electromechanical Tranducer and Wave-filters" D.Van Nostrand Company Inc., New York, p 63, 1948.

62. Drake, W.D., Buchberg, H. and Loboll, D. "Transfer Admittance functions, for typical composite wall sections" Trans. ASHRAE, Vol. 65, p 523, 1959.

63. Stephenson, D.G. and Mitalas, G.P. "Lumping errors of Analogue circuits for Heat flow through a homogenous slab" ASME Part I Section A, p 23-33, 1961.

64. W.D., Murray and Fred Landis "The effect of space-wise lumping of the solution accuracy of the one dimensional diffusion equation" J. Applied Mech. Trans. of the ASME, p 629 - 636, Dec. 1962.

65. Raychaudhuri, B.C. "The behaviour of the film-heat transfer coefficient at the ceiling indoor air interface" Proc. of the Fifth Congress on Theoretical and Applied Mechanics, Roorkee, Dec., 1959.

66. Houghton, F.C., Blackshaw, J.L., Pugh, E.M. and McDermott, P "Heat transmission as influenced by Heat capacity and Solar Radiation" Trans. ASHVE, Vol. 38, p 231, 1932.

67. Roux, A.J.A. "Periodic heat flow through Building components - Heat transfer from the outside surface of homogeneous wall panels to the inside air under winter conditions" NBRI, South African C.S.I.R. Series DR-7, Nov. 1950.

68. Roux, A.J.A., Visser, J. and Minnaar, P.C. "Periodic heat flow through building components - Heat transfer through homogeneous walls from the outdoor climatic environment to the indoor air" NBRI, South African C.S.I.R. Series DR-9, Sept. 1951.

69. Raychaudhuri, B.C., Jain, S.P., Yadav, R.G. "Thermal Characteristics of Unconditioned Insulated Masonry Buildings in Hot Arid Regions" 3rd International Biometeorological Congress (I.B.B.) Pau (Southern France), Sept. 1963.

70. Weinberg, L. "Network Analysis and Synthesis" McGraw Hill Book Company Inc. New York, 1962.

71. Raychaudhuri, B.C. "Thermal performance of Lightweight structures in tropics" N.B.O. Journal, Oct.1961.

72. Billington, N.S. "Thermal Properties of Buildings" Cleaver Hume Press, London, p 63, 1952.

73. Danter, E. "Periodic heat flow characteristics of simple walls and roofs" J.I.H.V.E., July 1960.

74. Johnson, H.A. "Periodic heat flow transfer at the Inner surface of a Homogeneous wall" Trans. ASHVE Vol. 54, p 143 - 164, 1948.

75. Mackey, C.O. and Wright, L.T. "Equivalent Homogeneous Construction of composite walls and roofs" Trans. ASHVE Vol. 52, p 233, 1946.

76. Stewart "Sol-air Heat Gain through walls and roofs" Appendix B. Trans. ASHVE Vol. 54, p 379, 1948.

77. Bruckmayer, F. "The Equivalent Brickwall" BRS Library Communication No. 451.

78. Krischer and Rohnalter(?), K. "The heat transfer in damp porous substances of different structures" B.R.S. Library Communication No. 733.

79. Halfbower, G. "Thermal Capacity half value time and brickwall of equivalent capacity" B.R.S. Library Communication No. 410.

80. Muncey, R.W. "The design of a proposed Electrical Analogue for the calculation of Temperatures in Buildings" B.S.L. C.S.I.R. Australia, Melbourne, May, 1949.

81. Nottage, H.B. and Parmelee, G.V. "Circuit Analysis applied to load estimating Part II - Influence of transmitted sol-air radiation" Trans. ASHAE Vol. 61, p 125, 1955.

B I B L I O G R A P H Y

1. McAdams, W.H. "Heat Transmission" McGrawhill Book Co., New York, 2nd Ed., 1954.

2. Brown and Marco "Introduction to Heat Transfer" McGrawhill Book Co., New York, 1st Ed., 1942.

3. Carslaw, H.S. and Jaeger, J.C. "Conduction of heat in Solids" Oxford University Press, 2nd Ed., 1959.

4. Eckert, E.R.G. and Drake, R.M. "Heat and Mass Transfer" McGrawhill Book Co., N.Y., 1959.

5. Jakob, M and Hawkins, G.A. "Elements of heat transfer" John Wiley & Sons, N.Y., 3rd Ed. 1957.

6. Joseph Fourier "The Analytical theory of Heat" Dover Publications, N.Y., 1955.

7. Benjamin Gebhart "Heat Transfer" McGrawhill Book Co., N.Y., 1961.

8. Alan J. Chapman "Heat Transfer" MacMillan Co., N.Y., 1960.

9. Geiger Rudolf "Climate Near the Ground" Harvard University Press, 1959.

10. Groundwater, I.S. "Solar radiation in Air Conditioning" Crosby Lockwood & Sons Ltd., London, 1957.

11. Billington, N.S. "Thermal Properties of Building" Cleaver-Hume Press Ltd., London, 1952.

12. Dusinberre, G.M. "Numerical Analysis of heat flow" McGrawhill Book Co., N.Y., 1949.

13. Southwell, R.V. "Relaxation Methods in Theoretical Physics" Clarendon Press, Oxford, 195[illegible].

14. Householder, A.S. "Principles of Numerical Analysis" McGrawhill Book Co., N.Y., 1953.

15. Soroka, W.W. "Analogue methods in computation Simulation" McGraw Hill Book Co. Inc., 1954.

16. Korn and Korn "Electronic Analogue Computer" McGraw Hill Book Co., N.Y., 1952.

17. Karplus, W.J. "Analogue Simulation" McGrawhill Book Co., N.Y., 1958.

18. Guillemin, E.A. "Introductory Circuit Theory" John Wiley & Sons, Inc., New York, 1953.

19. Lepage - Seely "General Network Analysis" McGrawhill Book Co., N.Y., 1952.

20. King, R.W.P. "Transmission Line Theory" McGrawhill Book Co., N.Y., 1953.

21. Gardner and Barnes "Transients in Linear Systems" Vol. 1, John Wiley & Sons.

22. Lecorbeiller, P. "Matrix Analysis of Electrical Networks" Harvard University Press, Cambridge, 1950.

NOMENCLATURE

K	Thermal conductivity of the material in Btu/Ft./Hr.°F
ρ	Density of the material in Lb/Ft^3
s	Specific heat of the material in Btu/Lb.°F
a	Temperature conductivity (thermal diffusivity) of the material in Ft^2/Hr ($a = K/\rho s$)
p	Coefficient of thermal absorption of the material in $Btu/Hr.Ft^2.°F$ ($p = \sqrt{\omega K \rho s}$)
b	Specific coefficient of thermal absorption of the material in $Btu/Hr.Ft^2.°F$ ($b = \sqrt{K \rho s}$)
U	Coefficient of thermal transmission of the wall in $Btu/Hr.Ft^2.°F$
L	Thickness of a layer in Ft.
R	Thermal Resistance of a building section in $Hr.Ft^2.°F/Btu$. (L/K)
C	Thermal Capacity of a building section in $Btu/Ft^2.°F$ ($L \rho s$)
h	Coefficient of heat transfer from the surrounding medium (air) to the surface or from the surface to the air in $Btu/Hr.Ft^2.°F$.
t	Temperature variation (sinusoidal) in °F
P	Fundamental period (24 hours)
τ	Time in hours.
q	Variable thermal current (heat flux) in $Btu/Hr.Ft^2$
D	Thermal absorption capacity of a building section in $Btu/Hr.Ft^2$
γ	Propagation constant. $\sqrt{j\omega\rho s/K}$
θ	Dimensionless parameter characteristic of the building section ($\sqrt{j\omega CR}$)
j	$\sqrt{-1}$

δ	Wave length of the temperature wave in a material in Ft.
σ	Stephen Boltzman constant (0.1712×10^{-8} Btu/Ft^2.Hr.^{o}R^4)
T	Absolute temperature (^{o}F + 459.69)
ϵ	Emissivity of the surface.
α	Absorbtivity of the surface to solar radiation.
I_T	Intensity of incident solar radiation in Btu/Ft^2.Hr.
I_{LT}	Difference between low temperature radiation emitted and received by the surface in Btu/Ft^2.Hr
F	Area of the surface in Ft^2.
p_v	Vapour pressure in inches of mercury.
Z	Thermal impedance in Hr.Ft^2.^{o}F/Btu.
Z_c	Characteristic thermal impedance in Hr.Ft^2.^{o}F/Btu.
Y	Thermal admittance in Btu/Hr.Ft^2.^{o}F
N	Number of lumps
F	Fundamental frequency.
H_2	Second harmonic
H_3	Third harmonic
H_4	Fourth harmonic
R_o	Outside surface resistance ($1/h_o$) in Hr.Ft^2.^{o}F/Btu.
R_i	Inside surface resistance ($1/h_i$) in Hr.Ft^2.^{o}F/Btu.
A, B, C, D	Coefficients of transfer matrix for a building section.
λ_o	Modulus of the external driving point function $\left\{\frac{t_{os}}{t_{su}}\right\}$
ϕ_o	Argument of the external driving point function.
λ_i	Modulus of the transfer function (t_{is}/t_{su})
ϕ_i	Argument of the transfer function (

λ'_i	Modulus of the internal Driving point function $\left\{\frac{t_{1s}}{t_{1a}}\right\}$
ϕ'_i	Argument of the internal driving point function.
Y_o	Modulus of the external driving point admittance function (q_{os}/t_{sa}).
ψ_o	Argument of the external driving point admittance function.
Y_1	Modulus of the transfer admittance function (q_{1s}/t_{sa})
ψ_i	Argument of the transfer admittance function.
Y'_1	Modulus of the internal driving point admittance function (q_{1s}/t_{1a}).
ψ'_i	Argument of the internal driving point admittance function.

Subscripts

ia	internal air
sa	sol-air
oa	external air
os	external surface
is	internal surface
n	harmonic of the frequency